2014

Investigating the Role of the Synaptic Transcriptome in Ethanol-Responsive Behaviors

Megan A. O'Brien
Virginia Commonwealth University, obrienma@vcu.edu

Investigating the Role of the Synaptic Transcriptome in Ethanol-Responsive Behaviors

A dissertation submitted in partial fulfillment of the requirements for the degree of Doctor of Philosophy at Virginia Commonwealth University.

by

Megan Anne O'Brien
Bachelor of Science, University of Wisconsin - Eau Claire, 2006
Master of Science, Arcadia University, 2008

Director: Michael F. Miles, M.D., Ph.D.,
Professor, Departments of Pharmacology and Toxicology and Neurology

Virginia Commonwealth University
Richmond, Virginia
August, 2014

Acknowledgments

There are many people I would sincerely like to thank for their contributions, without which, none of this would have been possible. First and foremost, I must thank my family and friends, who to me are essentially family. I would like to thank my mother, Peggy Strum, for her unwavering love, support, and belief that I can do anything I set out to accomplish, even when I may have changed my mind. I would like to thank my father, Stewart Strum, for the constant pride he has for my academic endeavors. To my brother, Jim Strum, and sister, Shelly Strum, for always being there when I needed to take my mind off of the hard work. I would also like to thank my family and friends, who are essentially my adopted siblings: Sara Hagen, Catherine Mueller, Jesse Small, Andrea McKenna, Meghan Seymour, and Brandy Puls, A special thank you goes to my mother-in-law, Laura Reali, for coming to help out during the last push to finish my dissertation and to my uncle, Tony O'Brien, for being my personal proofreader. I also would like to thank, with the deepest appreciation, my husband, Dominic Reali. His calm to my panic, his go with the flow to my perfectionism, are what made this entire process possible. Without his truly unconditional support, I would not be where I am today.

I would also like to thank all members of the Miles Laboratory, past and present, for their scientific contributions to this work, especially Jennifer Wolstenholme, Nathanial Bruce, Paul Vorster, Aaron Wolen, Sean Farris, and Blair Costin. I would also like to

thank Angela Batman for making life in the lab a little bit better these past two years. An immense amount of gratitude also goes to my advisor, Dr. Michael Miles, for accepting me into his lab and believing in me more than I probably believed in myself at most times. I truly appreciate the guidance that I know has made me a better scientist.

I would like to thank the members of my dissertation committee, Dr. Jill Bettinger, Dr. John Bigbee, Dr. Richard Moran, and Dr. Linda Phillips for your direction and assistance along the way. Thank you, Dr. Bettinger, for always being available to give advice and for being an admirable role model. Additionally I would like to thank the chair, Dr. William Dewey, and program directors, past and present, Drs. Sawyer and Akbarali, for accepting me it to the Pharmacology and Toxicology doctoral program.

Finally, to my daughter, Noelle, who has brought new light and purpose to my life. You have made earning this degree mean something completely different than its original intention; you have made it mean more.

Table of Contents

Clarification of Contributions vi

List of Tables vii

List of Figures ix

List of Abbreviations. xii

Abstract xvi

Chapter 1 – Introduction. 1

Chapter 2 – Background and Significance

Role of mRNA trafficking and local protein synthesis in synaptic plasticity. 5

Utilization of the synaptoneurosome preparation in neurogenomic research . . . 10

Behavioral sensitization as a model of neuronal plasticity 12

Application of microarrays and RNA-Seq to ethanol-related behaviors 17

Role of BDNF in drug addiction 19

Bdnf$^{klox/klox}$ mouse as a model for altered synaptic transcript trafficking 28

Behavioral models for assessing phenotypic responses to ethanol 32

Chapter 3 – Characterization of the Synaptoneurosome Preparation

Introduction 38

Materials and Methods 39

Results 54

Discussion 74

Chapter 4 – Regulation of the Synaptic Transcriptome by Repeated Ethanol Administration

Introduction 81

Materials and Methods 83

Results. 89

Discussion 112

Chapter 5 – Role of Synaptically Targeted *Bdnf* mRNA in Ethanol-Responsive Behaviors

Introduction. 119

Materials and Methods 122

Results 129

Discussion 154

Chapter 6 – Viral Vector Rescue of *Bdnf*$^{klox/klox}$ Altered Ethanol Phenotypes

Introduction 162

Materials and Methods 164

Results 176

Discussion 185

Chapter 7 – Concluding Discussion and Future Directions 189

Literature Cited 201

Vita 237

Clarification of Contributions

Without the technical and scientific contributions of those listed below, the work reported herein would not have been possible. All other work included within this dissertation, aside from cited, is exclusively my own.

Chapter 3

Dr. John Bigbee performed and interpreted the TEM. Dr. Myrna Serrano prepared the cDNA library and ran RNA-Seq. Nihar Sheth and Steven Bradley devised and ran the RNA-Seq data analysis pipeline. Dr. Robert Williams (University of Tennessee) provided the B6 genomic sequence containing D2 SNPs.

Chapter 4

Nihar Sheth and Steven Bradley devised and ran the RNA-Seq data analysis pipeline.

Chapter 5

Dr. Kevin Jones (University of Colorado-Boulder) provided the breeding pairs for *Bdnf*$^{klox/klox}$ mice. Dr. Jolene Windle and the VCU Transgenic Mouse Core re-derived and managed the colony for the *Bdnf*$^{klox/klox}$ mice. Qing Tao and Julie (So Hyun) Park performed genotyping of *Bdnf*$^{klox/klox}$ colony. Dr. Pretal Muldoon performed the ethanol CPP behavioral analyses. Dr. Keith Shelton analyzed BEC samples. Justin Poklis analyzed BrEC samples.

Chapter 6

Dr. Baoji Xu (Georgetown University Medical Center) provided the pAAV-BDNF-A, pAAV-BDNF-A*B, and pAAV-GFP plasmids. AAV production was performed by the University of Carolina-Chapel Hill Vector Core. Dr. Angela Batman blinded the LORR experiments.

List of Tables

Chapter 1

There are no tables in Chapter 1

Chapter 2

There are no tables in Chapter 2

Chapter 3

Table 3.1 – Immunoblotting antibodies 45

Table 3.2 – Primer sequences used for quantitative, real-time PCR. 47

Table 3.3 – RNA-Seq Data Quality Assessment 51

Table 3.4 – Functional Enrichment Analysis, P2 Enriched Gene List 72

Table 3.5 – Functional Enrichment Analysis, S2 Enriched Gene List 73

Table 3.6 – Top 50 Enriched Genes for the P2 Fraction (RMA Expression Values) 75

Table 3.7 – Top 50 Enriched Genes for the S2 Fraction (RMA Expression Values) 76

Chapter 4

Table 4.1 – Ethanol-induced behavioral sensitization experimental design. 85

Table 4.2 – Functional Enrichment Analysis, P2 Significant Gene List (Initial Microarray Analysis, One-Factor ANOVA, q < 0.3). 94

Table 4.3 – Functional Enrichment Analysis, S2 Significant Gene List (Initial Microarray Analysis, One-Factor ANOVA, q < 0.3). 95

Table 4.4 – Ingenuity Pathway Analysis, P2 Significant Gene List (Initial Microarray Analysis, One-Factor ANOVA, q < 0.3) 96

Table 4.5 – Ingenuity Pathway Analysis, S2 Significant Gene List

(Initial Microarray Analysis, One-Factor ANOVA, q < 0.3). 97

Table 4.6 – Functional Enrichment Analysis, P2 Candidate Gene List (RNA-Seq, Cuffdiff, q < 0.2). 102

Table 4.7 – Functional Enrichment Analysis, S2 Significant Gene List (RNA-Seq, Cuffdiff, q < 0.2) 103

Table 4.8 – Validated P2 Fraction, Ethanol Treatment Candidate Genes from overlap of Microarray Limma and RNA-Seq Cuffdiff 110

Table 4.9 – Functional Enrichment Analysis, Validated P2 Fraction, Ethanol Treatment Candidate Genes from Overlap of Microarray Limma and RNA-Seq Cuffdiff 111

Chapter 5

There are no tables in Chapter 1

Chapter 6

Table 6.1 – Primer sequences used for *Bdnf* qRT-PCR 169

Supplemental Tables

Available by email request to Dr. Michael F. Miles at mfmiles@vcu.edu.

List of Figures

Chapter 1

There are no figures in Chapter 1

Chapter 2

Figure 2.1 – Exon/intron structure and alterative transcripts of rodent *Bdnf*. . . . 21

Figure 2 2 – Structural organization of prepro-BDNF 24

Figure 2.3 – Diagram of the *Bdnf*^{klox} allele. 29

Chapter 3

Figure 3.1 – Schematic depicting synaptoneurosome preparation. 41

Figure 3.2 – Representative electron micrographs from P2 and P1 fractions. 55

Figure 3.3 – DAPI staining of synaptoneurosome fractions. 56

Figure 3.4 – Comparison of synaptoneurosomal preparation centrifugation speeds by DAPI staining 58

Figure 3.5 – Immunoblotting of subcellular protein markers across synaptoneurosome fractions. 59

Figure 3.6 – qRT-PCR profile across synaptoneurosome fractions. 61

Figure 3.7 – Enrichment of small molecular weight RNAs in the P2 fraction. . . 64

Figure 3.8 – Distinct RNA populations between P2 and S2 fractions affect microarray sample preparation. 66

Figure 3.9 – Microarray normalization factor determination. 68

Figure 3.10 – Venn diagrams for P2 versus S2 fraction significant genes. 70

Figure 3.11 – Venn diagram depicting overlap between synapse related data sets 71

Chapter 4

Figure 4.1 – Repeated ethanol exposure induced behavioral sensitization in D2 mice 90

Figure 4.2 – qRT-PCR of S2 and P2 fractions from mice subjected to behavioral sensitization paradigm. 92

Figure 4.3 – Visual representation of gene expression patterns identified by PTM in the initial microarray analysis. 99

Figure 4.4 – RNA-Seq significant genes broken down by ethanol treatment and synaptoneurosome fraction 100

Figure 4.5 – RNA-Seq P2 candidate gene list functional association networks using GeneMANIA 105-106

Figure 4.6 – Overlap of genes regulated by ethanol in the synaptic transcriptome between microarray and RNA-Seq analyses 109

Chapter 5

Figure 5.1 – Pair-feeding maintains comparable body mass between *Bdnf*$^{klox/klox}$ mice and wildtype littermates 130

Figure 5.2 – Locomotor activity dose response curves. 132

Figure 5.3 – Locomotor activity time courses. 133

Figure 5.4 – Body mass of animals used for locomotor dose response. 135

Figure 5.5 – Correlation between mass and locomotor activity. 136

Figure 5.6 – LORR in non-pair-fed *Bdnf*$^{klox/klox}$ mice. 138

Figure 5.7 – LORR in pair-fed *Bdnf*$^{klox/klox}$ mice. 140

Figure 5.8 – Internal ethanol concentration of pair-fed *Bdnf*$^{klox/klox}$ mice at LORR Time 2. 141

Figure 5.9 – Correlation between body mass and latency and duration of LORR. 142

Figure 5.10 – Altered ethanol consumption in *Bdnf*$^{klox/klox}$ mice. 144

Figure 5.11 – Altered quinine and saccharin consumption in *Bdnf*$^{klox/klox}$ mice. 146

Figure 5.12 – Ethanol CPP in *Bdnf*$^{klox/klox}$ mice. 148

Figure 5.13 – Light-dark box (LDB) assay for anxiety-like behavior in *Bdnf*$^{klox/klox}$ mice. 150

Figure 5.14 – Ethanol metabolism time course for *Bdnf*$^{klox/klox}$ and wildtype mice. 152

Figure 5.15 – Correlation between body mass and BEC 153

Chapter 6

Figure 6.1 – Plasmid diagrams 165

Figure 6.2 – qRT-PCR of AAV transduced HT1080 cells 177

Figure 6.3 – *In vitro* expression of BDNF protein by AAV 179

Figure 6.4 – BDNF protein levels in the dorsal striatum of *Bdnf*$^{klox/klox}$ mice 181

Figure 6.5 – LORR in AAV injected mice 183

Figure 6.6 – Locomotor response to low dose ethanol in AAV injected mice 184

Chapter 7

Figure 7.1 – Ethanol behavioral sensitization across the BXD line. 195

List of Abbreviations

AC	adenylyl cyclase
AFT	acute functional tolerance
AUD	alcohol use disorder
B6	C57BL/6J
BCA	bicinchoninic acid
BDNF	brain-derived neurotrophic factor
BEC	blood ethanol concentration
BrEC	brain ethanol concentration
CDS	coding sequence
CNS	central nervous system
CPP	conditioned place preference
D2	DBA/2J
DA	dopamine
DAPI	4', 6-diamidino-2-phenylindole
DAT	dopamine active transporter
DNA	deoxyribonucleic acid

DTT	dithiothreitol
EC	entorhinal cortex
EDTA	ethylenediaminetetraacetic acid
ELISA	enzyme-linked immunosorbent assay
ER	endoplasmic reticulum
EtOH	ethanol
eQTL	expression quantitative trait loci
FDR	false discovery rate
FISH	fluorescent *in situ* hybridization
GC	gas chromatograph
GO	gene ontology
GRE	glucocorticoid responsive element
H4	histone 4
HPA	hypothalamic-pituitary-adrenal
i.p.	intraperitoneal
ICC	immunocytochemistry
IPA	ingenuity pathway analysis
LB	luria broth
LDH	lactate dehydrogenase
LDB	light-dark box
LDS	lithium dodecyl sulfate

H4	histone 4
KO	knockout
LDH	lactate dehydrogenase
LepR	leptin receptor
LNGFR	low-affinity nerve growth factor receptor
LORR	loss of righting reflex
LTP	long term potentiation
LTD	long term depression
mAB	monoclonal antibody
MBP	myelin basic protein
MOI	multiplicity of infection
mRNA	messenger RNA
NAc	nucleus accumbens
NMDA	n-methyl-d-aspartic acid
NT	neurotrophin factor
pAB	polyclonal antibody
PFC	prefrontal cortex
PDT	percent distance traveled
PNS	peripheral nervous system
PSD95	postsynaptic density protein 95
PTM	pavlidis template matching

PTS	percent time spent
QHCl	quinine hydrochloride
qRT-PCR	quantitative reverse transcription polymerase chain reaction
RBP	RNA binding protein
RI	recombinant inbred
RNA	ribonucleic acid
RNP	ribonucleoprotein
RQI	RNA quality index
SYT	synaptotagmin
TB	terrific broth
TBST	tris buffered saline with Tween 20
TEM	transmission electron microscopy
UTR	untranslated region
V_d	volume of distribution
VTA	ventral tegmental area
WH	whole homogenate

Abstract

INVESTIGATING THE ROLE OF THE SYNAPTIC TRANSCRIPTOME IN ETHANOL-RESPONSIVE BEHAVIORS

By Megan Anne O'Brien, M.S.

A dissertation submitted in partial fulfillment of the requirements for the degree of Doctor of Philosophy at Virginia Commonwealth University.

Virginia Commonwealth University, 2014.

Major Director, Michael F. Miles, M.D., Ph.D.,
Professor, Pharmacology and Toxicology and Neurology

Alcoholism is a complex neurological disorder characterized by loss of control in limiting intake, compulsion to seek and imbibe ethanol, and chronic craving and relapse. It is suggested that the characteristic behaviors associated with the escalation of drug use are caused by long-term molecular adaptations precipitated by the drug's continual

administration. These lasting activity-dependent changes that underlie addiction-associated behavior are thought, in part, to depend on new protein synthesis and remodeling at the synapses. It is well established that mRNA can be transported to neuronal distal processes, where it can undergo localized translation that is regulated in a spatially restricted manner in response to stimulation. Through two avenues of investigation, the research herein demonstrates that behavioral responses to ethanol result, at least in part, from alterations in the synaptic transcriptome which contribute to synaptic remodeling and plasticity. The synaptoneurosome preparation was utilized to enrich for RNAs trafficked to the synapse. Two complementary methods of genomic profiling, microarrays and RNA-Seq, were used to survey the synaptic transcriptome of DBA/2J mice subjected to ethanol-induced behavioral sensitization. A habituating expression profile, characteristic of glucocorticoid-responsive genes, was observed for a portion of synaptically targeted genes determined to be sensitive to repeated ethanol exposure. Other ethanol-responsive genes significantly enriched for at the synapse were related to biological functions such as protein folding and extra-cellular matrix components, suggesting a role for local regulation of synaptic functioning by ethanol. In a separate series of experiments, it was shown that altered trafficking of *Bdnf*, an ethanol-responsive gene, resulted in aberrant ethanol behavioral phenotypes. In particular, mice lacking dendritically targeted *Bdnf* mRNA exhibited enhanced sensitivity to low, activating doses and high, sedating doses of ethanol. Together these experiments suggest that ethanol has local regulatory effects at the synapse and lays the foundation for further investigations into the role of the synaptic transcriptome in ethanol-responsive behaviors. *Supported by NIAA grants R01AA014717, U01*

AA016667 and P20AA017828 to MFM, F31AA021035 to MAO, and NIDA T32DA007027 to WLD.

Chapter 1 – Introduction

Alcohol use disorder (AUD) is a medical condition that is characterized by uncontrolled, compulsive alcohol seeking and consumption, undeterred by adverse consequences. The 5th edition of the Diagnostics and Statistical Manual of Mental Disorders categorizes the disorder into mild, moderate, and severe sub-classifications. The more serious of the conditions, colloquially known as alcoholism, is a disease that includes symptoms of craving, loss of control in the amount consumed, dependence, and tolerance. Alcoholism is a world-wide public health problem, but in the United States alone, it is estimated that 18 million Americans can be classified as having AUD (NIAAA, 2012). Each year in the United States, 88,000 people die from alcohol-related causes, making it the third leading preventable cause of death in the country (CDC, 2014b). The economic impact of AUD is staggering, as it's estimated that in 2006 alcohol use problems cost the United States approximately 224 billion dollars (CDC, 2014a). Despite the overwhelming presence and burden AUD has on society, the exact molecular actions of ethanol in the brain are not entirely understood, as ethanol acts on diverse array of receptor signaling systems, across many different brain regions (Spanagel, 2009), and produces a spectrum of behavioral disorders. A better understanding of the neurobiology of ethanol-related disorders is needed in order to identify novel therapeutic treatments.

Alcoholism is a complex, multifactorial disease and the risk for developing addiction is determined by an interplay between an individual's genetic makeup, environmental factors, and neuroadaptations that occur following acute and repeated drug exposure (Spanagel, 2009). A major directive of the alcohol research field is to delineate the pathological progression to alcohol dependence. With initial exposure, changes in neurotransmission lead to intoxication, anxiolysis, and a sense of reward (Spanagel, 2009). After repeated exposure, alterations in cell signaling can generate changes in gene expression and synaptic function, thought to contribute to the development of tolerance, dependence and sensitization to ethanol (Gilpin & Koob, 2008). As drug administration continues, allostasis is established which may account for the essentially permanent changes in behavior associated with addiction (Koob, 2003).

A consequence of the interaction of ethanol with its molecular targets is altered synaptic functioning, otherwise known as synaptic plasticity. Previous research from our laboratory that examined ethanol regulation of gene expression across a variety of mouse strains has found significant enrichment of genes involved with synaptic plasticity, reproducibly amongst several brain regions (Kerns *et al.*, 2005; Wolen *et al.*, 2012). There is also evidence to support that adaptive responses underlying ethanol tolerance and dependence are synaptic in nature, in part involving changes in glutamate neurotransmission (Tsai & Coyle, 1998). Ethanol administration has been shown to induce structural synaptic plasticity as well. Alcohol-preferring rats exposed to 14 weeks of continuous access or subjected to repeated deprivations of ethanol exhibited decreased density and increased size of spines in a subpopulation of neurons in the nucleus accumbens (Zhou *et al.*, 2007). Cortical neurons exposed to chronic

intermittent ethanol administration had significant increases in NMDA receptor surface expression (Qiang *et al.*, 2007) and hippocampal cultures receiving prolonged ethanol exposures exhibited increased co-localization of PSD95 and f-actin (Carpenter-Hyland & Chandler, 2006) leading to enlargement of spine heads. Together these data suggest that dendritic spines may be an important target for the adaptive actions of ethanol.

The morphological specialization of neurons, where synapses appear to be regulated in an individual manner, advocates the need for local regulation. Local protein synthesis in dendrites is supported by the presence of synthesis machinery and mRNAs for a subset of genes (Steward & Levy, 1982; Steward & Reeves, 1988; Poon *et al.*, 2006; Matsumoto *et al.*, 2007). This complement of RNAs, known as the synaptic transcriptome, has been shown to be regulated by neuronal activation (Tongiorgi *et al.*, 1997; Steward & Worley, 2001; Grooms *et al.*, 2006). Yet, there are no known published studies that investigate the role the synaptic transcriptome plays in the expression of ethanol-induced behaviors. Therefore, since ethanol is known to induce widespread changes in gene expression (Miles *et al.*, 1992; Morrow *et al.*, 1992; Treadwell & Singh, 2004; Kerns *et al.*, 2005; Bell *et al.*, 2009), which can contribute to synaptic plasticity, and because local protein synthesis from synaptic mRNA populations is important for spatially restricted plasticity to occur (Steward & Levy, 1982), I set out to examine the function of the synaptic transcriptome in ethanol-induced behaviors. It is my hypothesis that behavioral responses to ethanol result, at least in part, from alterations in the synaptic transcriptome which contribute to synaptic remodeling and plasticity.

This investigation was approached in two ways. First, we observed the effect of repeated intermittent ethanol exposure on the profile of the synaptic transcriptome.

Behavioral sensitization is a process that occurs following repeated drug exposure, proposed as a result of neuroadaptations in the brain reward systems that contribute to such behaviors as drug craving and relapse in alcoholics (Piazza *et al.*, 1990; Robinson & Berridge, 1993). Not much is known about the exact molecular mechanisms that underlie ethanol sensitization, but evidence has indicated a potential involvement of the hypothalamic-pituitary-adrenal (HPA) axis and glucocorticoid receptors (Phillips *et al.*, 1997; Costin *et al.*, 2013a). Nonetheless, ethanol sensitization provides a model of neuroplasticity with a measureable behavioral endpoint. Selective analysis of the synaptic transcriptome through utilization of a synaptoneurosomal preparation allowed us to detect changes in synaptic mRNA profiles as a result of repeated ethanol exposure. In the second approach, we employed a transgenic mouse strain with altered dendritic trafficking of an ethanol-responsive gene, *Bdnf*, and determined that proper transcript localization is necessary for normal ethanol behavioral responses. Together, these results suggest an important function of the synaptic transcriptome in mediating the effects of ethanol. Future studies will continue to utilize the synaptoneurosomal model with the objective of potentially identifying molecular mechanisms that contribute to the actions of ethanol, which would otherwise go undetected when studying the entire transcriptome.

Chapter 2 – Background and Significance

Role of mRNA trafficking and local protein synthesis in synaptic plasticity

Neuroplasticity refers to the brain's ability to undergo structural and functional changes as a result of experience. This umbrella term describes the capability for neural pathway reorganization as well as the capacity for individual synaptic connections to be strengthened or weakened in response to activity. Repeated administration of drugs of abuse can lead to long-lasting adaptive changes that manifest as behaviors associated with addiction (Nestler, 2001a; Russo *et al.*, 2010). These modifications can be both structural (Robinson & Kolb, 1997) and molecular in nature (Nestler, 2001a). Development of long-lasting forms of behavioral and synaptic plasticity has been shown to require new protein synthesis (Davis & Squire, 1984; Kang & Schuman, 1996). These newly formed proteins are thought to be utilized specifically by activated synapses to stabilize modifications in synaptic strength (Kelleher *et al.*, 2004).

The prevailing theory had been that the soma represented the primary site of protein synthesis and synapses were dependent upon this synthesis for their function. This view was challenged by the work of Steward and others in the 1980's. The observation of dendritic polyribosomes localized near postsynaptic sites suggested the means for local protein synthesis (Steward & Levy, 1982; Steward, 1983). Quantitative

assessment of serial electron micrographs found approximately 70% of dendritic polyribosomes localized to structures positively identified as spine bases or membrane mounds that were highly probable to be spine bases (Steward & Levy, 1982). Subsequent work documented the presence of tRNA, translation factors, endoplasmic reticulum and golgi-like apparatus at postsynaptic sites (Steward & Reeves, 1988; Tiedge & Brosius, 1996; Gardiol *et al.*, 1999). Translocation of translational machinery into spines during hippocampal long term potentiation (LTP) has also been observed (Ostroff *et al.*, 2002). Soma-free synapse preparations retain the ability to translate proteins (Rao & Steward, 1991; Eberwine *et al.*, 2001), and this dendritic synthesis is crucial for some forms of synaptic plasticity (Huber *et al.*, 2000).

Local protein synthesis makes the prospect of regulating synapses on an individual basis a more efficient process (Steward & Levy, 1982). For instance, local translation is an effective way to obtain high protein concentrations at a particular synapse. Transport of relatively few mRNA molecules that can be translated multiple times as opposed to transporting each individual protein is more economical for the cell (Wilhelm & Vale, 1993). Local synthesis also allows for the spatial regulation of macromolecular assembly reactions and prevents expression of proteins in inappropriate locations which could have deleterious effects. For example, myelin basic protein (MBP) has high affinity for membranous structures. Binding of this protein to membranes causes compaction (St Johnston, 1995). On-site synthesis of MBP prevents harmful interactions that could occur during transport of the protein. Furthermore, efficiency in response to synaptic activation could be optimized by having a ready pool of transcripts available. Local translation to produce the proteins needed

for synaptic modification would conceivably be faster than excitation-transcription coupling. Another particularly attractive concept allows for locally transcribed proteins to have distinct functions as compared to somatic variants. It has been shown that dendritically localized *Bdnf* transcripts, but not somatic, are necessary for proper dendritic spine pruning in mice (An *et al.*, 2008). Hypotheses for how localization could dictate function include 1) temporal activation that would allow interaction with activity-initiated signaling cascades and 2) cis- or trans-acting regulatory elements associated with localized transcripts that could control conditions under which translation is initiated. Both provide thought-provoking avenues for investigation.

Supporting local protein synthesis, mRNA has been identified in the distal processes and is referred to as the synaptic transcriptome. *In situ* hybridization of hippocampal lamina (Lyford *et al.*, 1995; Tongiorgi *et al.*, 1997) as well as characterizations of synapse-enriched subcellular fractions (Chicurel *et al.*, 1993; Rao & Steward, 1993; Poon *et al.*, 2006; Matsumoto *et al.*, 2007) have confirmed the presence of specific transcripts in dendrites. The occurrence and functionality of mRNA in axons remains controversial. Local protein synthesis has clearly been detected in axons of invertebrate systems (Twiss & Fainzilber, 2009), however initial ultrastructural studies failed to detect ribosomes in mature mammalian CNS axons (Steward & Levy, 1982). Despite the apparent absence of ribosomes, some vertebrate axons were reported to contain mRNAs. For example, axons of hypothalamic neurons projecting to the posterior pituitary were shown to contain transcripts for vasopressin and oxytocin (Mohr *et al.*, 1991; Mohr & Richter, 1992). Additionally, message for the kappa-opioid receptor revealed axonal distribution in the dorsal root ganglia of rodents (Bi *et al.*, 2006). The

presence of peri-axoplasmic ribosome plaques (PARPs) have been identified intermittently along myelinated peripheral nerves (Koenig *et al.*, 2000), suggesting an inherent ability for axonal protein synthesis in the PNS. This may correlate with the capacity for spontaneous regeneration in peripheral nerves, not typically observed in the mature CNS (Twiss & Fainzilber, 2009). It has also been suggested that neuronal cell bodies are not the only source for translational machinery and message in distal axons, and that ribosomes and mRNA may be transferred from glia sources (Court *et al.*, 2008; Sotelo *et al.*, 2014). Regulated trafficking of mRNA in granules that also contain ribosomes and other translational factors has been detected in astrocytes and oligodendrocytes as well (Barbarese *et al.*, 1995; Gerstner *et al.*, 2012). Together these data suggest an important and varied role for local protein synthesis throughout the nervous system.

Transport of mRNA to distal processes has been shown to occur in an activity-dependent manner. For example, potassium depolarization of hippocampal neurons in culture resulted in anterograde movement of *Camk2a*, *Bdnf*, and *Ntrk2* mRNA along dendrites (Tongiorgi *et al.*, 1997; Rook *et al.*, 2000). Quantitative fluorescent *in situ* hybridization revealed bidirectional regulation of AMPA receptor mRNA localization as a result of NMDA and metabotropic glutamate receptor activation (Grooms *et al.*, 2006). *In vivo* synaptic stimulation of the dentate gyrus delivered *Arc* mRNA to the corresponding projection lamina and was found to be dependent upon NMDAR signaling (Steward *et al.*, 1998; Steward & Worley, 2001). A model for mRNA transport as a component of large ribonucleoprotein (RNP) granules has been described (Bramham & Wells, 2007). RNA binding proteins (RBPs) in the nucleus are thought to

stabilize the newly transcribed RNA and provide sequestration from translation during transport. Dendritic mRNA encoding fragile-X mental retardation protein (FMRP) and ARC remain associated with the translation initiation factor, eIF4AIII, indicating translation does not occur en route (Giorgi *et al.*, 2007). The speed of RNP movement along dendrites and the sensitivity of RNPs to microtubule (MT) depolymerizing drugs have implicated the MT cytoskeletal system in RNP granule transport (Kiebler & Bassell, 2006). Furthermore, characterization of affinity isolated RNP granules using the kinesin motor protein, KIF5, revealed a diverse composition (Kanai *et al.*, 2004). Constituents included multiple mRNA species and 42 different proteins involved in transport, stabilization, and translation. The observation of bidirectional transport of mRNAs within dendrites (Knowles *et al.*, 1996) suggests that activated synapses capture RNPs from a pool of patrolling granules (Doyle & Kiebler, 2011). The exact physical nature of the synaptic tag that marks an activated synapse has not been absolutely defined. Candidate molecular tags that have been proposed include post-translation modifications to existing synaptic proteins, alterations to protein conformational states, initiation of localized translation or proteolysis, and reorganization of the local cytoskeleton (Martin & Kosik, 2002; Kelleher *et al.*, 2004; Doyle & Kiebler, 2011). Following synaptic activation, granule localization into spines employs actin cytoskeleton myosin motor proteins, repressive RNA binding proteins are neutralized, and translation can occur (Bramham & Wells, 2007). Trafficking and local translation are regulated by particular cis-acting elements of both the transcript and proteins that bind them (Wells, 2006). mRNA localization elements that are typically, but not exclusively, located in 3'untranslated regions (UTR), help to distribute RNAs to their proper

subcellular location. These “zip codes” are heterogeneous in nature and range from short nucleotide sequences to complex secondary structure recognized by trans-acting RBPs (Doyle & Kiebler, 2011). The model of mRNA transport and local translation presented here exposes several regulatory mechanisms. Modulation by drugs of abuse at any point along the process would result in alterations to the synaptic transcriptome, potentially contributing to the development of behavioral plasticity.

Utilization of the synaptoneurosome preparation in neurogenomic research

Research into synaptic functioning, which includes local protein synthesis, has been advanced by the development of subcellular fractionation techniques that provide samples enriched for synaptic entities. A variety of preparations have been published in the literature (Whittaker *et al.*, 1964; Hollingsworth *et al.*, 1985; Rao & Steward, 1993). Each preparation differs slightly in protocol and consequently in the structure of enriched synaptic elements, retained molecular constituents, and functional capacity. Synaptosomes were first described by Gray and Whittaker (1960, 1964), who also showed that disruption of these particles by hypo-osmotic media and subsequent gradient filtration of the components would result in sub-fractions that corresponded to separate synaptic localizations (Whittaker *et al.*, 1964). Synaptosomes are typically defined as a subcellular particle that is derived from resealed axonal termini prepared from brain issue homogenized in iso-osmotic buffer followed by density-gradient fractionation. Initial centrifugation, usually at around 1000 x g, removes the nuclear pellet, the supernatant of which is then spun again at 17,000 x g to yield a mitochondrial pellet, which is then re-suspended and applied to a sucrose density gradient,

centrifuged at 50,000 x g to separate mitochondria from synaptosomes (Gray & Whittaker, 1960). This results in a fraction mainly composed of presynaptic elements which often retain part of the postsynaptic membrane. Synaptodendrosomes (Rao & Steward, 1993) and synaptoneurosomes (Hollingsworth *et al.*, 1985) are preparations that have been shown to retain a greater portion of the postsynaptic compartment, often in the form of a re-sealed portion of the dendritic spine. Synaptoneurosomes were first named as such in Hollingsworth *et al*. (1985), where a low centrifugation, size-filtration scheme was used to produce synaptosomal structures attached to resealed postsynaptic entities (neurosomes). The typical sizes of the identified particles were approximately 0.6 μm for the synaptosomes and 1.1 μm for the neurosomes (Hollingsworth *et al.*, 1985).

Together these subcellular fractionation procedures have been used in myriad studies that have aided the characterization of synapses as discrete biochemical units. It was demonstrated that depolarization of the synaptosomal membranes increased polysomal association of *Camk2a* mRNA and subsequent increase in protein (Bagni *et al.*, 2000). Synaptosomes prepared from striatum of rats injected with a single dose of 2.0 g/kg ethanol revealed a time-dependent initial increase followed by a decrease in the ability to synthesize dopamine (DA) (Pohorecky & Newman, 1977). Barbiturates were shown to increase Cl^- efflux from rat cerebral cortical synaptoneurosomes (Schwartz *et al.*, 1985). The observed differences in structure between synaptosomes and synaptoneurosomes may make them uniquely adept for particular types of experiments. While synaptosomes have been utilized more frequently, it can be surmised that synaptoneurosomes would be the more appropriate model to examine

postsynaptic functioning. For instance, the accumulation of cyclic AMP elicited by incubation of the preparations with adenosine, norepinephrine and histamine was significantly greater in the synaptoneurosomes as compared to the synaptosomes (Hollingsworth *et al.*, 1985). This is most likely explained by the neurosome being the functional entity that contains most of the receptors linked to the adenylyl cyclase (Hollingsworth *et al.*, 1985). Theoretically synaptoneurosomes should also provide the most complete complement of RNA present in the synapse. In fact, synaptoneurosomes have been used to identify the presence and activity-dependent modulation of Dicer and RNA-induced silencing complex (RISC) component, eIF2c, at the synapse (Lugli *et al.*, 2005). They have also been used to examine the synaptic transcriptome in the prefrontal cortex (PFC) of humans that were afflicted with Alzheimer's disease (Williams *et al.*, 2009). We therefore hypothesized that synaptoneurosomes could be used to survey the synaptic transcriptome for changes resulting from repeated administration of ethanol in an *in vivo* model.

Behavioral sensitization as a model of neuronal plasticity

Behavioral sensitization is the phenomenon defined by escalation of behavioral responses to repeated exposure of stimulus. Often measured as a long-lasting augmentation in psychomotor stimulating effects, behavioral sensitization is observed across different classes of drugs with abuse liability (Shuster *et al.*, 1975; Masur & Boerngen, 1980; Hirabayashi & Alam, 1981; Crabbe *et al.*, 1982). Sensitization is proposed to occur as the result of progressive neuroadaptations in brain regions that mediate reinforcement and reward resulting in incentive salience of the drug (Robinson

& Berridge, 1993). This is evidenced by studies with amphetamine and cocaine showing animals with an increased propensity for self-administration after sensitization (Horger *et al.*, 1990; Piazza *et al.*, 1990). Repeated pre-exposure to amphetamine, cocaine, and morphine can also enhance reward as measured by conditioned place preference (CPP) (Lett, 1989). The effect of sensitizing ethanol treatments on the rewarding properties of the drug is slightly convoluted. In a paper by Camarini and Hodge (2004), intermittent repeated ethanol exposure of 1.0 g/kg and 2.0 g/kg administered every other day resulted in increased two-bottle choice ethanol self-administration in B6 and D2 mice. However, the ethanol pretreatment in this study did not actually manifest as a significant sensitizing locomotor response in either genotype (Camarini & Hodge, 2004). In another study looking at the effect of ethanol sensitization on ethanol consumption in B6 and D2 mice, it was found that the ethanol preferring mice (B6) exhibited an increase in ethanol intake following induction of locomotor sensitization using 2.5 g/kg ethanol, that was elicited following a bout of pre-sensitized drinking (Lessov *et al.*, 2001). This increase was not observed in B6 mice that had been exposed to ethanol in the pre-sensitized drinking phase but only received repeated saline injections. Non-ethanol preferring mice (D2) did not increase their consumption subsequent to sensitization in this series of experiments. In another study that used Swiss Webster mice subjected to daily injections of 1.8 g/kg ethanol for 21 days, it was shown that mice that sensitized exhibited increased drinking of 20% ethanol, but not 10% ethanol, in a limited access, voluntary choice model compared to non-sensitized and saline control mice (Abrahao *et al.*, 2013). However, the genetic heterogeneity present in this outbred strain cannot be eliminated as the source for susceptibility to both sensitization and

increased ethanol consumption. Together these data suggest that the ability to modulate ethanol intake by sensitizing pretreatment is highly dependent upon mouse strain and schedule of administration.

Sensitization to specific effects of addictive drugs has also been observed in humans (Newlin & Thomson, 1991; Strakowski *et al.*, 1996; Schenk & Davidson, 1998; Sax & Strakowski, 2001). Clinical presentation of psychostimulant-induced psychosis that occurs with repeated dosing of stimulant drugs has been suggested to be the result of changes to the central nervous system, producing a form of 'kindling', that results in symptoms similar to schizophrenia (Ellinwood & Kilbey, 1980). Human experimental studies investigating sensitization are few due to ethical considerations, but one double-blind, placebo-controlled study (Strakowski *et al.*, 1996) showed significantly greater eye-blink rates, a process controlled by dopaminergic mechanisms (Karson, 1983), following a second dose of d-amphetamine. Newlin and Thompson (1991) found that sensitization to finger pulse amplitude was observed across ethanol sessions in sons of alcoholics, a group with increased propensity for development of alcoholism. In contrast, participants that reported no parental history of alcoholism, and whom were therefore deemed low-risk, tended to demonstrate tolerance. These results, where high-risk individuals seem to derive greater response to acute administration of alcohol than low-risk participants appears to contradict Schuckit's seminal work showing low level of response to an alcohol challenge in high-risk subjects (Schuckit, 1994). The former study is the only examination of response to equivalent doses of alcohol across multiple sessions (Newlin & Thomson, 1991).

The concurrence among different drug classes for development of sensitization, along with the observation of cross-sensitization, where pretreatment with one drug results in a sensitized response to another, suggests common neural substrates may mediate these effects (Wise & Bozarth, 1987; Robinson & Berridge, 1993). The mesocorticolimbic system is a major substrate for motivated behavior and responses to natural reinforcers and is suggested to mediate the rewarding properties of drugs. This pathway primarily consists of dopaminergic projections from the ventral tegmental area (VTA) to the nucleus accumbens (NAc), prefrontal cortex (PFC), amygdala, and hippocampus. The system is also innervated with reciprocal glutamatergic connections and GABAergic interneurons. Studies involving mesocorticolimbic lesions caused by 6-hydroxydopamine determined that the A10 dopamine neurons that project from the VTA to the NAc are important in mediating spontaneous and psychostimulant-induced locomotion (Fink & Smith, 1980; Koob *et al.*, 1981). Most drugs of abuse, including ethanol, cause a release of dopamine in the NAc, dorsal striatum (DS), and PFC (Di Chiara & Imperato, 1988; Maisonneuve *et al.*, 1990), and this is thought to be a major mediator of the positive reinforcing effects of addictive substances (Koob, 2000). Repeated intermittent treatment of psychostimulants results in augmented extracellular release of dopamine upon subsequent administrations. This molecular adaptation correlates with the observed enhanced motor stimulation (Kalivas & Duffy, 1990; Paulson & Robinson, 1995).

There are conflicting reports in the literature as to whether ethanol sensitization elicits an augmented DA response in the NAc (Rossetti *et al.*, 1993; Szumlinski *et al.*, 2005; Zapata *et al.*, 2006), but there are other lines of evidence that suggest that DA

does play a role in development of the behavior. D_1 and D_3 receptor knockout (KO) mice do not show a sensitized response to the locomotor-activating effects of ethanol (Harrison & Nobrega, 2009). while sensitization was potentiated in dopamine active transport (DAT) knockout mice on a D2 background (Morice *et al.*, 2010). In addition, neuroimaging studies of alcoholics during craving and relapse reveal altered dopamine transmission (George *et al.*, 2001). Overall the current data indicate that the mechanism of ethanol sensitization is complex, and requires investigation into the role of other neurotransmitters and signaling systems (Broadbent & Harless, 1999; Carrara-Nascimento *et al.*, 2011; Pastor *et al.*, 2012).

Various other neurochemical adaptations have been found in occur in response to sensitizing treatments of drugs of abuse including, but not limited, to dopamine autoreceptor subsensitivity (White & Wang, 1984; Ackerman & White, 1990), decreases in G protein subunits (Nestler *et al.*, 1990; Striplin & Kalivas, 1993), and increases in calmodulin message and protein (Gnegy *et al.*, 1991; Shimizu *et al.*, 1997). However many of these subcellular neurochemical adaptations are relatively transient, suggesting that they are not involved in the long-term expression of sensitization but are possibly necessary to trigger more lasting plastic changes required for maintenance of the behavior (White & Kalivas, 1998). Anatomical changes to dendritic spine morphology in response to sensitizing treatments of amphetamine and cocaine in rats have been shown to persist for longer periods of time (Robinson & Kolb, 1999), and other studies have focused on more enduring rearrangements of neural networks and circuitry to explain the long-lasting effects of repeated drug exposure (Ujike *et al.*, 2002). Together, these studies implicate behavioral sensitization as a valid, testable model to

study the neural plasticity that mediates drug related behavior and potentially contributes to development of addiction.

Application of microarrays and RNA-Seq to ethanol-related behaviors

Long-term cellular and molecular changes in the brain as a result of chronic drug exposure are believed to be crucial in the development of drug addiction (Nestler & Aghajanian, 1997). Alterations in gene expression caused by repeated administration of ethanol or other drugs of abuse are a proposed mechanism contributing to the neuroadaptations leading to addiction (Nestler & Aghajanian, 1997). Moreover, gene expression has been used as a surrogate measure of signaling mechanisms evoked by acute ethanol that contribute to a behavioral response (Kerns *et al.*, 2005; Farris & Miles, 2013). Genome-wide expression analysis allows for a non-biased, parallel examination of the entire transcriptome. The utility of expression profiling not only lies in its ability to identify individual genes that are associated with a particular phenotype, but also to provide insight into the inter-related nature of genes and their functions (Lockhart & Winzeler, 2000; Lockhart & Barlow, 2001). Gene networks can be defined and populated based on functional interactions or common regulatory mechanisms that manifest as highly correlated expression patterns. Investigating the response of the network, as opposed to single genes, may be more apt to explain a complex trait, like alcoholism (Farris & Miles, 2012).

In order to investigate the complex traits of alcohol abuse and dependence, genome-wide analysis has been applied to the study of various animal models, treatment paradigms, and tissues. Transcriptomic comparisons of inbred strains of mice

that differ in their response to ethanol have been important in elucidating genes and pathways that underlie divergent ethanol phenotypes (Xu *et al.*, 2001; Kerns *et al.*, 2005). These strains are frequently used as the progenitors for recombinant inbred (RI) lines which often exhibit a distribution in behavioral response to ethanol as a result of recombinational events between genomes. Genomic analysis combined with genetic mapping in these RI lines allow for the identification of genes that contribute to the variation in the behavioral response (Jansen & Nap, 2001). Gene profiling studies have also revealed brain regional differences in expression that are often greater than those induced by selective breeding (Kimpel *et al.*, 2007) or binge drinking (Mulligan *et al.*, 2011). Characterization of basal and ethanol-responsive differences in the VTA, NAc, and PFC between B6 and D2 mice uncovered region-specific expression profiles (Kerns *et al.*, 2005). This study found region-specific functional involvement for retinoic acid and development in the VTA, *Bdnf* signaling and neuropeptide expression in the NAc, and glucocorticoid signaling and myelination in the PFC (Kerns *et al.*, 2005). Expression profiling has also been instrumental in investigating various ethanol treatment paradigms (Rimondini *et al.*, 2002; Rodd *et al.*, 2008; McBride *et al.*, 2010), ethanol regulation of chromatin remodeling (Wolstenholme *et al.*, 2011; Zhou *et al.*, 2011; Ponomarev *et al.*, 2012) and the role of miRNAs in post-translation regulation (Lewohl *et al.*, 2011).

Most of ethanol transcriptomic studies to date have used microarray technology. Although there are differences among the various platforms, microarrays work according to the same molecular principle: complementary base pairing between fluorescently labeled target (either RNA or DNA based) and short probes attached to a

solid-phase support. After hybridization, the fluorescent signal detected correlates to mRNA abundance (Chee *et al.*, 1996). However, as next-generation sequencing technologies advance and decrease in cost, the use of high-throughput RNA sequencing (RNA-Seq) for expression profiling becomes an attractive option. Once again, the exact methodology depends on the platform being utilized, but the general approach involves creation of a sequencing library, typically in the form of cDNA. Following sequencing, the resulting short reads can either be aligned against a reference genome or assembled without the use of a reference genome to allow for identification of novel transcripts and splicing sites (Cloonan & Grimmond, 2008; Mortazavi *et al.*, 2008). Alignment provides structure to the transcriptome and the number of reads from each exon, splicing event, transcript, or gene can be determined and correlated to expression levels (Mortazavi *et al.*, 2008). RNA-Seq is currently believed to have distinct advantages to prior methods of quantifying the transcriptome, such as a larger dynamic range, determination of expression without the need for probe design, and detection of polymorphisms, novel splicing events, and transcriptional boundaries (Cloonan & Grimmond, 2008; Mortazavi *et al.*, 2008; Wang *et al.*, 2009; Zhou, 2014). Despite the promise of RNA-Seq, practical application is currently hindered by lack of consensus and support for analytical methodology, making microarrays still a viable and incredibility useful tool.

Activity-dependent regulation of BDNF and its role in alcoholism

Brain-derived neurotrophin factor (BDNF) is the most prevalent growth factor in the CNS and is a member of the neurotrophins (NTs) family of proteins. These

molecules are primarily associated with neuronal survival and differentiation in the developing nervous system. However, NTs have also been extensively investigated for their role in modulating synaptic transmission and facilitating plasticity in mature neurons (Poo, 2001). BDNF serves critical functions in the processes of learning and memory (Lu *et al.*, 2008), and the disruption of its proper functioning has been linked to numerous pathologies including Alzheimer's disease, Parkinson's disease, depression, obesity, schizophrenia, and addiction (Autry & Monteggia, 2012).

Every aspect of BDNF regulation is facilitated by neuronal activity, including transcription. The rodent *Bdnf* gene (Figure 2.1) contains nine promoters, each of which initiates transcription of a different exon (I – IX) (Aid *et al.*, 2007). A heterogeneous population of *Bdnf* transcripts is created by alternative splicing of each of the non-coding 5' exons onto the common 3' exon (IX) that contains the entire open reading frame for the protein. Expression profiles for the various splicing variants are developmental stage, tissue, and brain region-specific (Liu *et al.*, 2006b; Aid *et al.*, 2007). The transcription start sites are also differentially activated by neuronal activity. For example, transcription of exons I, IV, V, VII, VIII, and IX was enhanced in the hippocampus by kainic acid-induced seizures (Aid *et al.*, 2007). Furthermore, acute, but not chronic, administration of cocaine enhanced transcription of exon IV in the striatum and frontal cortex, but not hippocampus (Liu *et al.*, 2006b). The mRNAs for *Bdnf* are also polyadenylated at one of two alternative sites (Timmusk *et al.*, 1993). This creates two distinctive populations of mRNAs: those with short 3' untranslated regions (UTR) and those with long 3' UTR. Both long and short *Bdnf* mRNAs were expressed in all brain regions examined, however the ratio between long and short varied greatly between

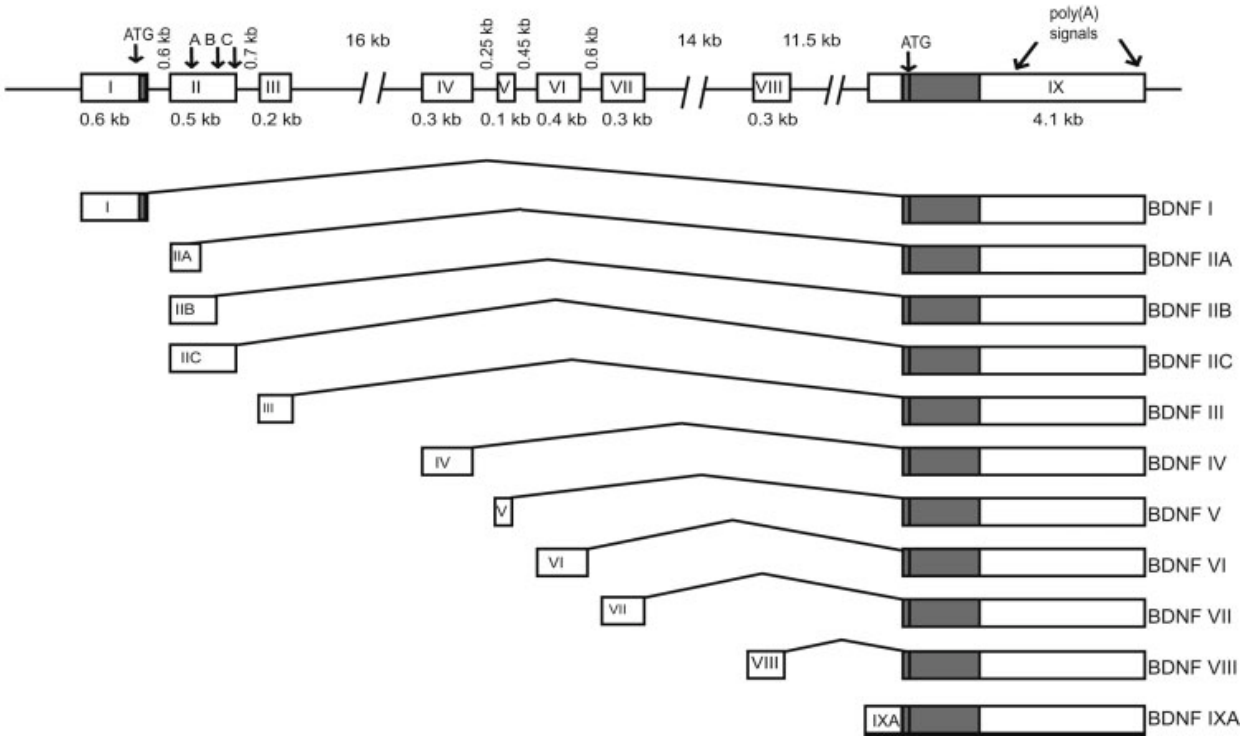

Figure 2.1 – Exon/intron structure and alternative transcripts of rodent *Bdnf*. Schematic representation of *Bdnf* transcripts in relation to the gene. Protein coding region is shown as filled box and untranslated regions are shown as open boxes. Each of the eight 5' untranslated exons splice to the common 3' protein coding exon IX. Transcription can also be initiated in the intron before the protein coding exon. The two alternative polyadenylation signals in the 3' untranslated region are marked by arrows. Exon II can generate three different transcript variants, IIA, IIB, and IIC, from the use of alternative splice-donor sites. Image reproduced with permission © 2006 Wiley-Liss, Inc. (Aid *et al.*, 2007).

brain regions (An *et al.*, 2008). The ratio of long to short isoforms also was significantly different depending on the promoter usage, within the single brain region (An *et al.*, 2008).

The redundancy that arises from two populations of *Bdnf* mRNAs that encode the exact same protein was hypothesized to allow for regulation of BDNF function in different subcellular locations. *Bdnf* mRNA has been shown to be targeted to dendrites under physiological conditions (An *et al.*, 2008). *Bdnf* mRNA also accumulates in the dendrites of cultured hippocampal neurons in a glutamate, Ca^{2+}, and TrkB receptor-dependent manner (Tongiorgi *et al.*, 1997; Tongiorgi *et al.*, 2004). An *et al*. (2008) concluded that it was long 3' UTR containing *Bdnf* transcripts that were preferentially targeted to synapses. Quantitative PCR was performed on RNA isolated from separated cell bodies and synaptic compartments of cultured rat cortical neurons, revealing a relative 7-fold enrichment of long 3' UTR in synaptic samples (An *et al.*, 2008). This was corroborated by fluorescent *in situ* hybridization (FISH) analysis of cultured cortical neurons as well as hippocampal neurons that had been transfected with constructs containing the *Bdnf* coding region attached to the short 3' UTR, the long 3' UTR, or just the portion between the two polyadenylation sites (An *et al.*, 2008). Alternatively, it has been suggested that the dendritic targeting element of *Bdnf* resides within the coding sequence (CDS), and can be overridden by inclusion of specific 5' UTR exons (Chiaruttini *et al.*, 2009). This was determined by FISH analysis of cultured hippocampal neurons transfected with constructs that contained *Bdnf* CDS preceded by 5' UTR sequences, yet missing the 3' UTR in its entirety (Chiaruttini *et al.*, 2009). They also determined that the RNA-binding protein, translin, bound the *Bdnf* CDS and that this

binding was blocked by the G196A mutation, which they showed impaired dendritic targeting of *Bdnf* mRNA. A model was proposed that suggested the CDS dendritic targeting element is specifically involved in constitutive trafficking of transcript to synapses while the 3' UTR acts as a inducible targeting signal (Chiaruttini *et al.*, 2009). The results of these two papers appear to contradict each other, but both conclude that cis-acting elements in the *Bdnf* mRNA are responsible for the synaptic targeting of transcript.

BDNF, like all neurotrophins, is synthesized as a prepro-BDNF precursor (Figure 2.2). Cleavage of the signal peptide after sequestration to the ER produces pro-BDNF, which can then form homo- and heterodimers with other pro-NTs (Lessmann *et al.*, 2003). The protein is then transferred to the golgi-network where it is packaged into both constitutive and regulated secretory vesicles. Cleavage of pro-BDNF to mature BDNF is catalyzed by furin-like enzymes and pro-hormone convertases that are associated with the golgi network and secretory vesicles (Lu, 2003). It has also been shown that pro-BDNF can be secreted and cleaved extracellularly by plasmin and metalloproteinases (Lee *et al.*, 2001). Recently it has been suggested that specific modes of neuronal activation can result in the concurrent secretion of pro-BDNF and tissue plasminogen activator, shifting the extracellular balance to mature-BDNF (Waterhouse & Xu, 2009). BDNF is released from presynaptic and postsynaptic sites. However it is believed that activity-dependent secretion occurs primarily from dendritic spines (Lu, 2003), and transfection experiments using BDNF-GFP constructs have indicated that postsynaptic release of BDNF upon presynaptic high frequency

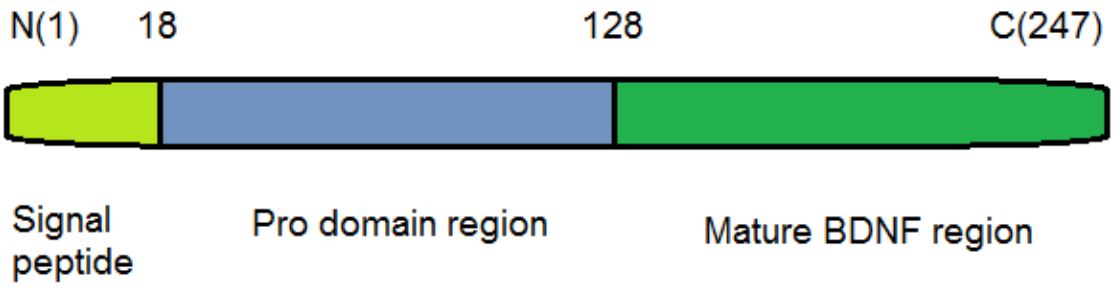

Figure 2.2 – Structural organization of prepro-BDNF. Schematic representation of the BDNF precursor protein. *Bdnf* mRNA encodes a 247 amino acid residue precursor protein. Following cleavage of the 18 amino acid signal peptide, pro-BDNF is transported to the Golgi for sorting into either the constitutive or regulated secretory granules. Pro-BDNF can be converted to the 119 amino acid mature BDNF by Golgi-associated furin, secretory granule prohormone convertases, or by extracellular matrix plasmin and metalloproteinases (Greenberg *et al.*, 2009).

stimulation depends on activation of postsynaptic glutamate receptors (Hartmann *et al.*, 2001).

Following secretion, the biological functions of BDNF are mediated by binding of two cell surface receptors. Tropomyosin related kinase B (TrkB) is a high affinity tyrosine kinase receptor that appears to mediate the cell survival and synaptic effects of BDNF. Truncated forms of TrkB have been identified on cultured astrocytes and appear to sequester BDNF, acting as a molecular sponge to remove the ligand from the extracellular environment, and inhibiting axonal regeneration following axonal injury (Fryer *et al.*, 1997). When BDNF binds TrkB, it induces dimerization and autophosphorylation of the receptor, leading to activation of three main signaling transduction pathways: phospholipase C (PLC)/protein kinase C (PKC), phosphatidylinositol 3-kinase (PI3K)/AKT, and mitogen-activated protein kinase (MAPK) pathways. Binding of BDNF to TrkB also results in receptor internalization followed by retrograde or anterograde transport, depending on the subcellular site of activation, to the axon where it activates cell survival signaling pathways (Lessmann *et al.*, 2003). The second receptor responsible for mediating the effects of BDNF is the low-affinity nerve growth factor receptor (LNGFR), also known as p75. The exact downstream signaling mechanism activated by the p75 receptor is unknown. However, it is thought to act in two ways. As a Trk co-receptor, p75 can enhance or suppress neurotrophin-Trk activity (Roux & Barker, 2002). Alternatively, data suggests that pro-BDNF can bind autonomous p75 resulting in the induction of apoptosis (Roux & Barker, 2002; Lessmann *et al.*, 2003).

BDNF signaling is able to modulate synaptic transmission through either presynaptic or postsynaptic mechanisms. Presynaptically, BDNF has been shown to cause phosphorylation of synapsin I and RIM1α via MAPK signaling, subsequently increasing synaptic vesicle exocytosis and glutamate efflux, respectively (Jovanovic *et al.*, 1996; Simsek-Duran & Lonart, 2008). In the postsynaptic cell, BDNF-induced phosphorylation of NR1 and NR2B subunits was shown to potentiate NMDA currents (Wang & Salter, 1994). It has also been suggested that BDNF may modulate synaptic plasticity by regulating local protein synthesis in dendrites (Waterhouse & Xu, 2009). Application of BDNF to cultured hippocampal neurons in the presence of transcriptional inhibitor, actinomycin, was able to increase levels of dendritic *Bdnf* and *Ntrk2* mRNA (Righi *et al.*, 2000). Facilitation of translation of existing dendritic *Arc* mRNA by BDNF was shown to be dependent upon a synergism between TrkB and NMDA receptors, as this function was blocked by both the NMDAR antagonist, MK-801, and the tyrosine kinase inhibitor, K252a, as well by inhibition of mammalian target of rapamycin (mTOR) (Takei *et al.*, 2004; Waterhouse & Xu, 2009).

The ability of BDNF to mediate synaptic plasticity and regulate neurotransmission, particularly of dopamine and serotonin release (Goggi *et al.*, 2002), would suggest that BDNF may be involved in the neuroadaptations that underlie the development of addiction. Human studies have indicated an association between BDNF and susceptibility to addiction (Uhl *et al.*, 2001; Matsushita *et al.*, 2004) along with lower plasma levels of BDNF in alcoholics, particularly in those with a family history of the disease (Joe *et al.*, 2007). Preclinically, alterations in *Bdnf* have been shown to modulate several behaviors associated with drugs of abuse (Horger *et al.*, 1999; Hall *et*

al., 2003; Hensler *et al.*, 2003). While studies of *Bdnf* homozygous knockout mice would be highly informative about the potential influences the neurotrophic factor has on the response to various drugs of abuse, these mice display substantial nervous system abnormalities and often die by their third postnatal week (Ernfors *et al.*, 1994; Conover & Yancopoulos, 1997). In contrast, *Bdnf* heterozygotes are viable and possess mRNA and protein levels that are half that of wildtype mice (Kolbeck *et al.*, 1999; Lyons *et al.*, 1999). As such, *Bdnf* heterozygous mice have been the primary reagent for studying the genetic impact on behavioral responses to a variety of drugs of abuse. On a mixed J129ftm/1Jae/C57BL/6 background, heterozygous mice exhibited increased ethanol consumption as well as augmented ethanol-induced sensitization and conditioned place preference as compared to their wildtype littermates (McGough *et al.*, 2004). It has also been reported that *Bdnf* mRNA is significantly augmented by single acute ethanol injection or voluntary self-administration (McGough *et al.*, 2004; Logrip *et al.*, 2009). Interestingly, Loprig *et al*. (2009) was able to show that escalating consumption of ethanol over 6 weeks resulted in the loss of ethanol's ability to increase *Bdnf* transcript levels, and that this was not recovered with a 2 week withdrawal period. The work of Dr. Dorit Ron and colleagues has suggested that BDNF signaling works as a parallel protective mechanism that prevents the neuroadaptations that lead to phenotypes associated with alcohol addiction and that a dysregulation of this protective mechanism can permit these adaptive responses to occur (McGough *et al.*, 2004). Therefore, due to BDNF's implicated function in ethanol-induced synaptic plasticity as well as the fact that *Bdnf* mRNA is targeted to the synapse where it can be translated and secreted in an

activity-dependent manner, BDNF is an excellent candidate for studying the effects of modulated dendritic trafficking on ethanol-induced behaviors.

Bdnf$^{klox/klox}$ *mouse as a model for altered synaptic transcript trafficking*

To examine the role of dendritically targeted *Bdnf* mRNA in response to ethanol administration, experiments here utilized an existing transgenic mouse model. This strain, referred to as *Bdnf*$^{klox/klox}$, was initially created as a mating partner for a cre-recombinase expressing mouse to produce brain region-restricted *Bdnf* mutants (Gorski *et al.*, 2003). The endogenous *Bdnf* allele was replaced with the gene diagramed in Figure 2.3. LoxP sites were inserted into the 5' UTR of the coding exon and 3' to the first polyadenylation site in the 3' UTR. In addition, three tandem SV40 polyadenylation signal sequences were inserted immediately upstream of the second loxP site, followed by a *lacZ* gene (An *et al.*, 2008). The insertion of the exogenous tandem polyadenylation sites resulted in truncation of the long *Bdnf* 3' UTR, creating a new species of mRNA. The short 3' UTR isoform was found to be unaffected in *Bdnf*$^{klox/klox}$ mice, however the long isoform was found to be absent (An *et al.*, 2008). The total amount of *Bdnf* mRNA was determined to be equivalent between *Bdnf*$^{klox/klox}$ and wildtype animals, however *in situ* hybridization revealed marked reduction of dendritic localization of *Bdnf* in both the dendrites of cortical and CA1 neurons (An *et al.*, 2008). This corresponded with elevated transcript levels in the soma of both cortical and hippocampal regions. Immunoblotting detected no alterations in global levels of either pro-BDNF or total-BDNF in the cortex, hippocampus, or striatum of *Bdnf*$^{klox/klox}$ mice, however dendritic targeting of BDNF protein was significantly reduced (An *et al.*, 2008).

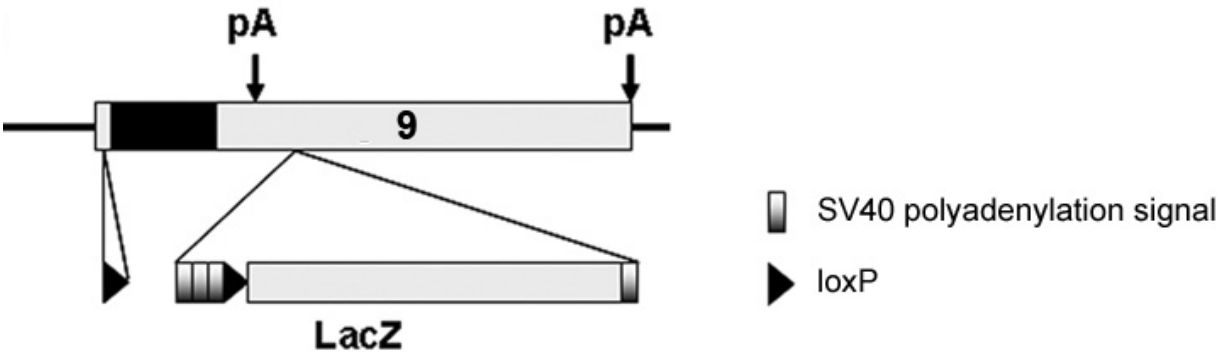

Figure 2.3 – Diagram of the *Bdnf*$^{\text{klox}}$ allele. The *Bdnf*$^{\text{klox}}$ allele contains one lox P site inserted into the 5' UTR within exon 9 and a sequence containing three tandem SV40 polyadenylation signals, a lox P site, and a *LacZ* gene inserted at a site 3' to the first *Bdnf* polyadenylation site. Image reproduced with permission © Nature Medicine (Liao *et al.*, 2012).

Immunostaining of cultured hippocampal neurons found that while BDNF protein could be detected in distal dendrites of wildtype mice, it was only detectable in proximal dendrites of *Bdnf*$^{klox/klox}$ mice. In addition, BDNF immunofluorescence in cell bodies was 44% higher in *Bdnf*$^{klox/klox}$ neurons as compared to wildtype neurons. Secretion of BDNF by cultured hippocampal neurons in response to KCl depolarization was impaired in *Bdnf*$^{klox/klox}$ mice (An *et al.*, 2008). Lastly, these mice were backcrossed and maintained on a C57BL/6J (B6) genome for 10 generations; a strain often utilized in ethanol research due to its proclivity for ethanol consumption. Therefore, these mice provided a unique genetic resource where the dendritic localization of an ethanol-responsive gene was significantly altered without affecting total transcript or protein levels. Administering ethanol and testing the resultant behavioral phenotypes in *Bdnf*$^{klox/klox}$ mice would provide insight to the role of proper transcript targeting in ethanol's neuronal effects.

The *Bdnf*$^{klox/klox}$ mice have been used to investigate certain physiological outcomes of reduced dendritic trafficking of *Bdnf* mRNA. The exhibited phenotypes either directly affected the design of experiments presented here, or were considered when interpreting the data. Cytoarchitecture and dendritic arborization in the cortex and hippocampus of 2 month old *Bdnf*$^{klox/klox}$ mice was no different from wildtype animals (An *et al.*, 2008). However, the dendritic spines of 2 month old *Bdnf*$^{klox/klox}$ mice were thinner and more numerous in CA1 pyramidal neurons. A 20% reduction in spine head diameter and a 54% increase in density was observed compared to wildtype neurons (An *et al.*, 2008). This altered morphology was confirmed to be the result of reduced dendritic BDNF synthesis and not due to increased levels of BDNF in cell bodies by using another transgenic mouse, BTg (Huang *et al.*, 1999). BTg mice expressed 2-3

fold higher levels of *Bdnf* mRNA in the dorsal forebrain, which remained restricted to the soma (An *et al.*, 2008). BTg mice exhibited average spine head diameter comparable to wildtype mice and spine density that was slightly increased, but significantly lower than *Bdnf*$^{klox/klox}$ mice. Further examination of *Bdnf*$^{klox/klox}$ mice at postnatal day 21 showed no difference in spine density as compared to wildtype mice, suggesting that the difference observed at 2 months resulted from a deficit in spine pruning, which occurs after the third postnatal week in mice (An *et al.*, 2008). Not unexpectedly, *Bdnf*$^{klox/klox}$ mice demonstrated impaired LTP at hippocampal CA1 synapses upon tetanic stimulation of the Schaeffer collaterals (An *et al.*, 2008). However *Bdnf*$^{klox/klox}$ mice exhibited normal paired pulse facilitation and synaptic responses to high frequency stimulation, phenotypes abnormal in conventional *Bdnf* knockout mice. There was also no difference in LTP recorded in cell bodies of neurons from *Bdnf*$^{klox/klox}$ mice.

Truncation of the long *Bdnf* 3' UTR was also found to cause severe obesity. Not only were *Bdnf*$^{klox/klox}$ male mice 171% heavier than sex-matched wildtype mice, they also showed longer linear growth, hyperleptinemia, enlarged adipose tissues, and impaired glucose homeostasis as a result of marked hyperphagia (Liao *et al.*, 2012). It was also shown that young (5-6 weeks), non-obese *Bdnf*$^{klox/klox}$ mice, which maintained similar serum leptin concentration as compared to wildtype, did not respond to a repeated dosing regimen of leptin (Liao *et al.*, 2012). Three doses of 3 μg/g of leptin over a 24 hour period significantly reduced food intake by wildtype, but had no effect on *Bdnf*$^{klox/klox}$ mice. This was not the result of impaired leptin receptor (LepR) activation, but in the ability for leptin-sensing neurons to communicate properly with non-LepR expressing cells (Liao *et al.*, 2012). Together, the studies utilizing *Bdnf*$^{klox/klox}$ mice

demonstrated a selective and distinctive function for the long 3' UTR *Bdnf* transcript preferentially trafficked to the synapse.

Behavioral models for assessing phenotypic responses to ethanol

Ethanol-induced locomotor activation

As mentioned previously, the mesolimbic dopamine pathway has been implicated in mediating drug-induced locomotor stimulation (Koob, 1992; Hooks & Kalivas, 1995). This system has also been implicated in reward perception, appetitive motivated behaviors, novelty/sensation seeking, and impulsivity (Alcaro *et al.*, 2007). Therefore, measurement of locomotor activity can be used as a surrogate for phenotypes more difficult to assess (Curzon *et al.*, 2009). In human studies, an individual's initial sensitivity to the drug has been shown to be predictive of susceptibility to develop alcoholism (Schuckit, 1994), and that this phenotype has a strong genetic influence (Heath *et al.*, 1999). Acute administration of ethanol reveals a dose-dependent biphasic effect. Low doses of ethanol during the rising phase of the blood ethanol curve cause a locomotor activation and higher doses can result in a sedative and even hypnotic response. Thus, testing transgenic animals in an acute locomotor dose response experiment will evaluate initial sensitivity to a range of ethanol doses. The results of which could increase understanding of acute ethanol-mediated signaling events that may lead to the genesis of behaviors associated with addition.

.

Loss of Righting Reflex (LORR)

Another model of acute sensitivity to ethanol is loss of righting reflex (LORR). Rodents administered a hypnotic dose of ethanol, when placed supine, are unable to return themselves to a prone position. The amount of time until an animal loses its LORR is referred to as latency and the length of "sleep time" is termed duration. Duration of LORR is a complex phenotype that is thought to depend on a combination of metabolic rate, initial brain sensitivity, and rapid development of functional tolerance (Tabakoff & Ritzmann, 1979). Functional tolerance is defined as the brain's ability to adapt in order to compensate for the disruption caused by alcohol (Tabakoff *et al.*, 1986). When this tolerance develops within a single session, it is referred to as acute functional tolerance (Tabakoff *et al.*, 1986). The molecular mechanism of ethanol acute functional tolerance is not completely elucidated. However, evidence suggests that compensatory adaptation of NMDA receptor function is important for mediating the behavior. Acute ethanol is a potent inhibitor of NMDA receptor function (Lovinger *et al.*, 1989). Nevertheless, administration of ethanol has been shown to increase phosphorylation of the NMDA receptor subunit, NR2B, which enhances channel function (Miyakawa *et al.*, 1997; Yaka *et al.*, 2002; Yaka *et al.*, 2003a). This modification is mediated by the Src family protein tyrosine kinase, FYN. Mice that are homozygous null for the *Fyn* gene ($Fyn^{-/-}$) have an increased duration of LORR (Miyakawa *et al.*, 1997). Excitatory postsynaptic potentials (EPSPs) measured in hippocampal slices from $Fyn^{-/-}$ mice did not recover from ethanol suppression over time as observed in control mice (Miyakawa *et al.*, 1997). It was also shown that administration of the NMDA antagonist, ifenprodil, abolished the difference in duration of LORR between the $Fyn^{-/-}$

and control mice (Yaka *et al.*, 2003b) and overexpression of FYN kinase resulted in shorter duration of LORR (Boehm *et al.*, 2004). Furthermore, previous work in our lab defined a *Fyn*-LORR gene network from genome-wide basal expression profiling of *Fyn*$^{-/-}$ mice PFC that was correlated to Fyn gene expression across the recombinant inbred strains, BXD and LXS, along with LORR data across BXDs (Farris & Miles, 2013). Functional over-representation analysis of this network identified enrichment of genes involved in ion channel activity and localization to the postsynaptic density (Farris & Miles, 2013). While the network was populated with genes that had potential roles in modulating NMDA receptor activity, there were also genes associated with other glutamate-related ion channels and white matter. This suggested additional mechanisms that contribute to the high-dose ethanol response that still need to be investigated (Farris & Miles, 2013).

Voluntary two-bottle choice paradigm

Free-choice ethanol consumption is a frequently employed test for general avidity of the drug in which animals are presented with one bottle of ethanol and one bottle of water for a prescribed amount of time. In the classic paradigm, animals have *ad libitum* access to the two bottles for 24 hours per day. However, manipulations designed to obtain high ethanol intake and consequently pharmacologically meaningful blood ethanol concentrations have been implemented throughout the literature (Melendez *et al.*, 2006; Melendez, 2011; Thiele *et al.*, 2014). These experiments are often used to study the genetic and neurobiological mechanisms underlying high ethanol drinking behavior through the use of animals models such as selectively bred, inbred,

recombinant inbred, and transgenic rodent lines (Crabbe *et al.*, 1992; Li *et al.*, 1993). While the paradigm does not inherently test for the rewarding properties of ethanol, it has been suggested that there is a positive correlation between ethanol drinking and the more formal assessment of reinforcement, operant self-administration (Green & Grahame, 2008). Strengthening the argument for validity, the μ-opioid receptor antagonist, naltrexone, which is used clinically to treat alcoholism and has been shown to decrease cue-induced cravings in alcoholics (Monti *et al.*, 1999), was able to reduce ethanol consumption in the two-bottle choice model (Franck *et al.*, 1998; Middaugh & Bandy, 2000; Ciccocioppo *et al.*, 2014). However, the effect is often transient, as tolerance to naltrexone develops. Acamprosate, another drug used clinically for treating alcohol dependence, was also able to diminish voluntary ethanol drinking (Zalewska-Kaszubska *et al.*, 2008; Oka *et al.*, 2013). Therefore, two-bottle choice drinking provides a useful screening test for genetic influences on ethanol consumption.

Conditioned Placed Preference (CPP)

Perception of the rewarding properties of drugs of abuse can be modeled though a Pavlovian conditioned stimulus test known as conditioned place preference (CPP). The premise behind CPP is that a learned association is formed between the rewarding drug (unconditioned stimulus) and the contextual environment in which it was administered (conditioned stimulus). The result of the association is that the conditioned stimulus is able to evoke a conditioned motivational response in the absence of the unconditioned stimulus, and consequently animals exhibit an increased preference for the drug-paired environment. The advantages of this model are that animals are tested

in a drug-free state, simultaneous measurement of reward and locomotor activity, sensitivity to reward and aversion, simplicity in execution (no need for surgical procedures), and utility for probing neural pathways involved in reward (Bardo & Bevins, 2000; Cunningham *et al.*, 2006). Limitations in the procedure include the confounding variables of novelty-seeking, apparatus bias, and general memory impairment (Bardo & Bevins, 2000). Additionally, validity of the CPP model for the motivational effects of abused drugs is not as robust as with self-administration protocols (Bardo & Bevins, 2000; Cunningham *et al.*, 2006). However, CPP can yield information regarding the rewarding effect of contextual cues associated with a drug stimulus (Bardo & Bevins, 2000).

Light-Dark Box (LDB) model of anxiety

The light-dark box (LDB) assay is based upon the spontaneous exploratory behavior of rodents which is offset by their natural averseness to novel environments and bright light (Crawley & Goodwin, 1980). When placed in an apparatus that provides choice between a light or dark compartment, rodents will spend more time and have greater locomotor activity in the dark side (Costall *et al.*, 1989; Onaivi & Martin, 1989). Clinically-prescribed anxiolytic drugs, such as benzodiazepines, will increase locomotion and time spent in the light and decrease latency to transition into the light, whereas anxiogenics have the opposite effects (Costall *et al.*, 1989; Imaizumi *et al.*, 1994a; Imaizumi *et al.*, 1994b). Therefore, preference for the light side is interpreted as an anxiolytic-like phenotype. Ethanol, a drug known to have anxiolytic effects in humans, when administered to mice predictably and significantly increases percent time

spent (PTS) and percent distance traveled (PDT) in the light. Thus, ethanol-induced anxiolytic-like activity provides an additional behavioral measurement of initial response to acute ethanol.

Chapter 3 – Characterization of the Synaptoneurosome Preparation

Introduction

Ever since the pioneering work of Cajal, the morphological polarity of neurons has been a major tenet of neuroscience. This specialized structure allows for compartmentalized functioning to occur in restricted subcellular domains, such as dendritic spines, which are able to respond individually to afferent signals (Holt & Schuman, 2013). This spatially limited response advocates the need for local regulation. Local synaptic protein synthesis is supported by the finding of synthesis machinery, including ribosomes, tRNA, translation factors, endoplasmic reticulum, and Golgi apparatus, at postsynaptic sites (Steward & Levy, 1982; Steward & Reeves, 1988). Furthermore, through hippocampal *in situ* hybridization (Lyford *et al.*, 1995; Poon *et al.*, 2006) and studies characterizing synapse-enriched subcellular fractions (Chicurel *et al.*, 1993; Rao & Steward, 1993; Poon *et al.*, 2006; Matsumoto *et al.*, 2007) and micro-dissected neuropil (Cajigas *et al.*, 2012), a number of mRNA species have been identified at synapses. Studies using protein synthesis inhibitors have shown that protein synthesis is required for behavioral and synaptic plasticity, assumedly for establishing enduring modifications (Kang & Schuman, 1996; Steward & Schuman, 2001). Thus, targeting of specific RNAs to dendrites may be an efficient way of localizing proteins involved in synaptic function by establishing local sites for their

synthesis and alterations in mRNA transport, stability, or translation could mediate synaptic plasticity (Steward & Banker, 1992; Chicurel *et al.*, 1993).

Synaptoneurosomes which retain resealed postsynaptic elements attached to isolated presynaptic terminals theoretically should provide a useful system to investigate regulation of the synaptic transcriptome in an *in vivo* model. Synaptoneurosomes, and preparations that enrich for similar synaptic entities, have been used previously to identify and evaluate dendritic RNA (Rao & Steward, 1993; Williams *et al.*, 2009). For the present study, we adapted a synaptoneurosome preparation from Williams, *et al.* (2009), which had been previously used in a genomic analysis of the synaptic transcriptome in PFC of Alzheimer's patients (Williams *et al.*, 2009). Characterization studies to ensure enrichment of synaptic elements that contain synaptically localized mRNA were necessary before proceeding with subsequent genomic profiling to examine the effect of repeated ethanol exposure on the synaptic transcriptome. Through molecular and transcriptomic analyses, we determined that an evaluation of transcripts within the synaptoneurosomal P2 fraction and its complementary supernatant, S2 would permit a comparison of synaptic and somatic transcriptomes in response to exogenous stimuli.

Materials and Methods

Animals. Characterization of the synaptoneurosome protocol utilized DBA/2J (D2) mice purchased from Jackson Laboratories (Bar Harbor, ME) at 8-9 weeks of age. All mice were housed 4-5 per cage and had *ad libitum* access to Teklad standard rodent chow (7912, Harlan, Madison, WI) and tap water in a 12-hour light/dark cycle (6 am on,

6 pm off). Mice were housed with Teklad corn cob bedding (7092, Harlan, Madison, WI)). All animal procedures were approved by the Institutional Animal Care and Use Committee of Virginia Commonwealth University (AM10332) and followed the NIH Guide for the Care and Use of Laboratory Animals.

Synaptoneurosome Preparation. The protocol for preparation of synaptoneurosomes was adapted from Williams *et al.* (2009) (Figure 3.1). Fresh tissue from 4 animals was pooled (approximately 0.45 g), manually homogenized utilizing a Potter-Elvehjem Safe-Grind® tissue grinder (Wheaton, Millville, NJ), and diluted 1:10 in synaptoneurosome homogenization buffer. The buffer consisted of 0.35 M nuclease free sucrose (Acros Organics, NJ), 10 mM HEPES (Life Technologies, Carlsbad, CA), and 1 mM EDTA (Ambion, Carlsbad, CA), which was brought to a pH of 7.4 and filter sterilized. Immediately before use, 0.25 mM DTT (Fisher Scientific, Waltham, MA), 30 U/ml RNase Out (Invitrogen, Carlsbad, CA), and 1x protease inhibitor cocktail containing AEBSF, Aprotinin, Bestatin, E64, Leupeptin, and Pepstatin A (Halt, Thermo Scientific, Rockford, IL), was added to the buffer. Centrifugation of whole homogenate (WH) at 500 x g for 10 minutes at 4˚C removed nuclei and cellular debris, yielding pellet, P1 and supernatant, S1. The S1 fraction was passed through a series of nylon filters with successively decreasing pore sizes of 70, 35, and 10 μm (SEFAR, Buffalo, NY). The filtrate was then re-suspended with 3 volumes of homogenization buffer, and centrifuged at 2000 x g for 15 minutes at 4˚C to yield the synaptoneurosome enriched pellet, P2 and supernatant, S2. Fractions were frozen on dry ice and then stored at -80˚C until further processing.

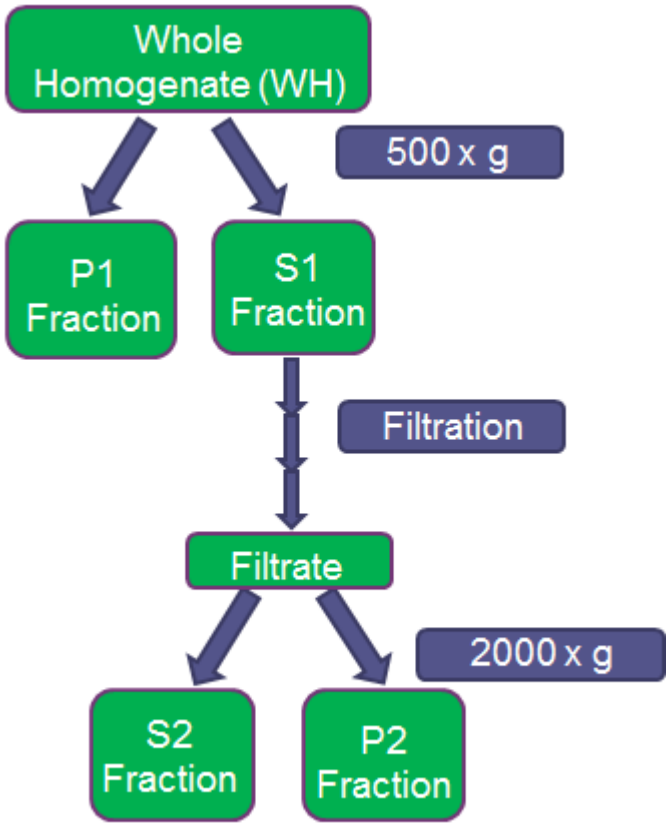

Figure 3.1 – Schematic depicting synaptoneurosome preparation. Whole homogenate (WH) processed from pooled frontal pole tissue of 4 mice was used in the centrifugation/filtration scheme depicted here. The initial pellet (P1) contained cellular debris and nuclei. The supernatant from the initial centrifugation (S1) was filtered and subjected to a second centrifugation. The pellet, P2, was enriched for synaptic elements and dendritically targeted RNA as compared to the supernatant, S2, which contained the remainder of the somatodendritic RNA.

Transmission Electron Microscopy (TEM). Morphological integrity of synaptoneurosomes was confirmed by transmission electron microscopy (TEM) performed by Dr. John Bigbee. A 1 ml aliquot of S1 supernatant was centrifuged at 2000 x g for 15 minutes to produce a pellet. P1, P2, and the pelleted S1 fractions were washed in PBS and centrifuged at 2000 x g for 8 minutes. The supernatant was decanted and pellet was fixed with 2% glutaraldhehyde in 0.1 M sodium cacodylate buffer at room temperature. After initial fixation, the sample was rinsed in 0.1 M cacodylate buffer for 5-10 minutes and then post-fixed in 1% osmium tetroxide in 0.1 M cacodylate buffer for 1 hour, followed by another 5-10 minutes rise in 0.1 M cacodylate buffer. Preparation continued with a serial dehydration with ethanol: 50%, 70%, 80%, 95% - for 5-10 minutes each, followed by 100% ethanol for 10-15 minutes (3x), and incubation in propylene oxide for 10-15 minutes (3x). The sample was then infiltrated with a 50/50 mix of propylene oxide and PolyBed 812 resin (Polysciences, Inc., Warrington, PA) overnight, which was then replaced with pure resin once again overnight. The sample was embedded in a mold, placed in a 60˚C oven overnight, and then sectioned with a Leica EM UC6i Ultramicrome (Leica Microsystems, Wetzlar, Germany), stained with 5% Uranyl acetate and Reynold's Lead Citrate, and examined on JEOL JEM-1230 transmission electron microscope (JEOL USA, Inc., Peabody, MA). Images of various magnifications (2,000x – 10,000x) were captured with the Gatan Ultrascan 4000 digital camera (Gatan, Inc., Pleasanton, CA).

DAPI Staining. Aliquots from each fraction of the synaptoneurosomal preparation were examined for the presence of contaminating nuclei using 4', 6-diamidino-2-phenylindole (DAPI) staining. 5 µl of WH, S1, and reconstituted P1 and P2 were

smeared onto microscope slides, allowed to air dry for 10 minutes, and were fixed in ice-cold acetone for 5 minutes. Specimens were mounted using DAPI containing media (Vectasheild, Burlingame, CA) and a cover slip. Ultraviolet light was used for DAPI excitation and emission was detected by Olympus IX-70 fluorescent microscope (Olympus America Inc., Tokyo, Japan) at 461 nm. Representative fields at 20x magnification were assessed for nuclear content.

Immunoblotting. Pellets (P1 and P2) and liquid aliquots (WH, S1, and S2) from synaptoneurosomal preparations were used to perform semi-quantitative immunoblotting. Pellets were triturated with NuPAGE lithium dodecyl sulfate (LDS) sample buffer (Life Technologies, Carlsbad, CA) diluted to 1x and containing 1x proteinase inhibitor cocktail (Halt, Thermo Scientific, Rockford, IL), while liquid aliquots were lysed directly with 4x LDS with added proteinase inhibitor. Samples were sonicated on ice water until samples were no longer viscous. Protein concentrations were determined using the bicinchoninic acid (BCA) assay (Thermo Scientific, Rockford, IL). Sample concentrations were balanced using 1x LDS, 10x NuPAGE reducing agent (Life Technologies, Carlsbad, CA) and boiled for 10 minutes. For each synaptoneurosome fraction, 10 µg of protein was loaded per lane on a 10% and on a 4% - 12% gradient NuPAGE bis-tris gel (Life Technologies, Carlsbad, CA). Electrophoresis was performed at 150V followed by transfer to 0.45 µm nitrocellulose membrane for 1.5 hours at 30V on ice. Membranes were incubated with Ponceau S for 10 minutes, and densitometric analysis of staining was performed using ImageJ processing and analysis software (National Institutes of Health). Prior to primary antibody incubation, the membranes were blocked with 5% non-fat dried milk in 1x Tris-

Buffered Saline with Tween 20 (TBST) for 45 minutes. Primary and secondary antibody catalog numbers, dilutions, and incubation times are provided in Table 3.1. Immunoblots were visualized on GeneMate Blue Autoradiography film (BioExpress, Kaysville, UT) using the Amersham ECLWestern Blotting Detection Reagent (GE Healthcare Life Sciences, Pittsburgh, PA) and quantified using ImageJ. All detected proteins were normalized to the total protein loaded per well as measured by Ponceau S staining. Statistical analysis of immunoblot data was performed by one-way ANOVA across synaptoneurosome fractions followed by Tukey's *post-hoc* analysis. Fold change between P2 and WH was also examined.

Quantitative Reverse Transcriptase Polymerase Chain Reaction (qRT-PCR). Synaptoneurosomal fractions were assayed for transcripts with known subcellular localizations using qRT-PCR. Three preparations were preformed to provide biological replicates of the fractions. Total RNA was isolated from aliquots of WH (0.5 ml) and S1 (0.75 ml) and from P1, P2, and S2 fractions in their entirety using the guanidine/phenol/chloroform method (Stat-60, Tel-Test Inc., Friendswood, TX) and a Tekmar homogenizer as per the STAT-60 protocol. RNA concentration and quality was determined using the SmartSpec 3000 (Bio-Rad, Hercules, CA) and the Experion Automated Electrophoresis Station (Bio-Rad, Hercules, CA). All RNA samples had RNA quality indices (RQI) ≥ 7.9, and 260/280 ratios were between 1.86 and 2.04. cDNA was generated from 995 ng of total DNase-treated RNA and 5 ng of luciferase mRNA (Promega, Madison, WI) using Deoxyribonuclease I (Invitrogen, Carlsbad, CA) and the iScript cDNA kit (Bio-Rad, Hercules, CA) according to manufacturer's instructions. qRT-PCR was performed using the iCycler iQ system (Bio-Rad, Hercules, CA) according to

Table 3.1: Immunoblotting antibodies

Antibody	Manufacturer	Catalog #	1˚ Dilution (Overnight Incubation at 4˚C)	2˚ Dilution (1h Incubation at Room Temp)
H4	Millipore	07-108	1 to 2000	1 to 5000
LDH	Santa Cruz	sc-33781	1 to 2000	1 to 5000
PSD95	BD Biosciences	610495	1 to 2500	1 to 5000
SYT	Abcam	ab51164	1 to 2000	1 to 5000
Donkey anti-Rabbit-HRP	GE Healthcare Life Sciences	NA934V	NA	see above
Sheep anti-Mouse-HRP	GE Healthcare Life Sciences	NA931V	NA	see above

manufacturer's instructions for iQ SYBER Green Supermix (Bio-Rad, Hercules, CA). Primer sequences, annealing temperatures, amplicon sizes, and cDNA dilutions used for each gene are listed in Table 3.2. Relative expression was calculated by comparing Ct values to a standard curve produced from WH cDNA (diluted 1:5, 1:25, 1:125, 1:625). Statistical analysis of qRT-PCR data was performed using a one-way ANOVA across all fractions and by Student's t-test between P2 and S2 fractions.

Small RNA qRT-PCR. The profile of selective small RNAs was assessed in P2 and S2 fractions of synaptoneurosomal preparations acquired from behaviorally sensitized mice (refer to Chapter 4 Materials and Methods). Pre-formulated TaqMan® primer/probe sets for small RNA detection (Life Technologies, Carlsbad, CA) were used to evaluate the levels of miR-149, miR-134, and miR-9 according to manufacturer's instructions. Briefly, individual reverse transcription reactions were set up using unique hairpinned primers that recognize a specific small RNA, MultiScribe™ reverse transcriptase, and 5 ng total RNA in a 15 µL reaction. cDNA was stored at -20˚C until the amplification reaction was prepared in triplicate using TaqMan® Universal PCR Master Mix II. The 5'end of the TaqMan® probes, which anneals specifically to a complementary sequence between the forward and reverse primer, are linked to FAM™ reporter dye. When DNA polymerase cleaves the probe during transcription of target, the reporter dye is separated from the non-fluorescent quencher dye, and detection can occur. Samples were analyzed using the iCycler iQ system (Bio-Rad, Hercules, CA). The PCR protocol was 95˚C for 10 minutes, followed by 50 cycles of 95˚C for 15 seconds, 60˚C for 60 seconds. Statistical analysis was performed using a Student's t-test between fractions for each small RNA.

Table 3.2: Primer sequences used for quantitative, real-time PCR

Target Gene	Forward Primer (5' to 3')	Reverse Primer (5' to 3')	Annealing Temp (˚C)	Amplicon Size (bp)	cDNA dilution
Camk2a	AGAGCACCAACACCACCATT	GGTTCAAAGGCTGTCATTCC	64	151	1:25 or 1:125
Arc	TGAAGCAGCAGACCTGACAT	GTGTGGTGATGCCCTTTCC	61	238	1:25
Gapdh	TTCCAGTATGACTCCACTCACGG	TGAAGACACCAGTAGACTCCACGAC	60	169	1:25
Snrpn	CACCTGTAGGCAGAGCAACC	GGTGGAGGGGGTCTCATTC	60	145	1:25 or 1:125
Gfap	AGAAAGGTTGAATCGCTGGA	GCTGTGAGGTCTGGCTTGG	60	137	1:25
Rn18s	GACTCAACACGGGAAACCTC	AGACAAATCGCTCCACCAAC	58	120	1:125
Luciferase	TACAACACCCCAACATCTTCGA	GGAAGTTCACCGGCGTCAT	63	Ref Johnson *et al.(2005)*	1:25 or 1:125

Microarray Sample Preparation, Hybridization and Scanning. Genomic expression analysis of P2 and S2 fractions of synaptoneurosomal preparations acquired from behaviorally sensitized mice (refer to Chapter 4 Materials and Methods) was performed using microarrays. Total RNA was isolated using the guanidine/phenol/chloroform method (Stat-60, Tel-Test Inc., Friendswood, TX) and a Tekmar homogenizer as per the STAT-60 protocol. RNA concentration was determined by measuring absorbance at 260 nm and RNA quality was assessed by electrophoresis on an Experion Analyzer (Bio-Rad, Hercules, CA) and 260/280 absorbance ratios. All RNA samples had RQI ≥ 7.6, and 260/280 ratios were between 1.97 and 2.06. Total RNA (100 ng) from each sample, spiked with poly-A RNA controls (Affymetrix, Santa Clara, CA), was used to generate amplified sense-strand cDNA utilizing the Ambion® WT Expression Kit (Life Technologies, Carlsbad, CA) according to the manufacturer's instructions. Using GeneChip® WT Terminal Labeling Kit (Affymetrix, Santa Clara, CA), purified cDNA was fragmented and biotin-labeled, followed by hybridization along with biotin-labeled hybridization controls to GeneChip® Mouse Gene 1.0 ST Arrays (Affymetrix, Santa Clara, CA) and scanning with Affymetrix GeneChip Scanner 3000 according to standard Affymetrix protocols. To avoid non-biological experimental variation that arises from sample batch structure, supervised randomization of samples into batches prior to each processing stage (RNA extraction, cRNA synthesis, and hybridization) was performed.

Microarray Data Analysis. Expression data from the S2 and P2 fractions were background corrected, quantile normalized, log2 transformed, and fit to a linear model using the robust multi-array average (RMA) expression measure (Irizarry *et al.*, 2003).

Microarray quality was assessed by inspecting the frequency distributions of log-transformed probe intensity values and by reviewing quality assessment metrics and graphs available from Expression Console™ software (Affymetrix, Santa Clara, CA). All arrays had pos_vs_neg_auc values (a metric that evaluates how well signal is separated from noise) greater than 0.92. Differential expression of genes across synaptoneurosomal fractions was assessed using linear models for microarray data (Limma) analysis (Smyth, 2004) using the Bioconductor package in the statistical platform, R (Team, 2011). For the comparison between fractions, false discovery rate (FDR) was set equal to 0.05.

RNA-Seq Library Preparation and Sequencing. Total RNA isolated for microarray analysis was subsequently used for RNA-Seq performed by the VCU Genomics Core Laboratory. The preparation of cDNA libraries was conducted following standard protocols using TruSeq RNA Sample Preparation Kit (Illumina, San Diego, CA). Briefly, mRNA was isolated from total RNA using poly-T oligo-attached magnetic beads. The mRNA was then fragmented in the presence of divalent cations at 94˚C. The fragmented RNA was converted into double stranded cDNA and the ends polished using T4 and Klenow DNA polymerases, with an adenine base added to the 3' ends followed by ligation of Illumina specific adaptors. The adaptor-ligated DNA was amplified with 15 cycles of PCR and purified using QIAquick PCR Purification Kit (Qiagen, Venlo, Netherlands). Library insert size was determined using an Agilent Bioanalyzer. Library quantification was performed by qRT-PCR assay using the KAPA Library Quant Kit (KAPA, Wilmington. MA). RNA-Seq libraries were analyzed using Illumina TruSeq Cluster V3 flow cells and TruSeq SBS Kit V3 (Illumina, San Diego, CA),

with six libraries of different indices pooled together in equal amounts loaded on to a single lane at a concentration of 13 pM and sequenced (2 x 100 paired end reads) on a Illumina HiSeq 2000. A summary of metrics that describe the RNA-Seq data can be found in Table 3.3. Once again, supervised randomization of samples prior to each processing stage (RNA extraction, library amplification, and lane assignment) was performed.

RNA-Seq Alignment, Transcript Assembly, Quantification and Differential Expression Analysis. Fastq formatted sequences generated on the Illumina HiSeq 2000, were mapped to the mouse reference genome (mm10) that had been edited for single nucleotide polymorphism (SNPs) between the C57BL/6 (B6) and DBA2/J (D2) strains (Williams, University of Tennessee) using Spliced Transcripts Alignment to a Reference, or STAR (v2.3.0) (Dobin *et al.*, 2013). The STAR algorithm consists of two phases: a seed searching phase and a clustering and scoring phase. The seed searching process is itself a two-part process. First, a sequential search of the reference genome is conducted to find the highest quality match to the read. Once this match is determined, a second sequential search of the reference is conducted using any unmapped portion of the reads if necessary. During the clustering process, STAR constructs full-length alignments of the reads by merging the hits detected by the first phase. BLAST-like local alignment scoring controls the process, which allows STAR to tolerate sequence mismatches as well as insertions and deletions relative to the reference.

To assemble transcripts and estimate abundance, BAM files from STAR and the annotated reference genome were analyzed using Cufflinks (v2.1.1, http://cufflinks.cbcb.umd.edu/) (Trapnell *et al.*, 2010). Once transcripts were assembled,

Table 3.3: RNA-Seq Data Quality Assessment							
Sample	Index	Lane	Library Yield (ng/μL)	# of Reads	% Alignment (STAR)	% Duplication	Mean Quality Score (PF)
SS3S2	CGATGT	L001	16.36724197	26742555	92.17%	6.8228	30.08
SS4S2	TGACCA	L002	17.22101902	24529561	91.20%	4.2094	31.2
SS5S2	ACAGTG	L004	14.14932264	15009481	91.24%	3.0409	31.41
SS6S2	GCCAAT	L004	12.95593431	14715360	90.96%	2.6361	30.62
SE3S2	CAGATC	L001	11.5074398	31923672	91.76%	5.8445	29.41
SE4S2	ATCACG	L003	12.55806866	16872692	91.23%	3.2339	29.56
SE5S2	TTAGGC	L003	15.610192	21390155	91.90%	3.8613	30.92
SE6S2	ACTTGA	L002	12.30075486	35049532	91.75%	4.5153	31.41
EE3S2	GTCCGC	L003	19.91357307	16014899	92.04%	4.125	30.93
EE4S2	GTTTCG	L001	21.75850598	28817464	92.24%	14.05	29.65
EE5S2	ATCACG	L001	16.25050427	23309321	92.48%	5.6212	30.59
EE6S2	GTGAAA	L003	11.87926146	59226719	91.67%	13.5016	30.72
SS3P2	GTGGCC	L004	8.9572335	51970374	88.18%	19.5221	30.96
SS4P2	CGTACG	L004	7.682275601	47088497	87.28%	19.4616	31.16
SS5P2	GAGTGG	L002	11.97488842	25868361	86.73%	16.0271	31.26
SS6P2	ACTGAT	L001	12.12427139	24061816	87.60%	17.5959	30.03
SE3P2	GATCAG	L002	20.78093368	30987158	87.27%	15.0665	31.15
SE4P2	TAGCTT	L001	18.5224577	40936024	86.98%	20.5494	29.81
SE5P2	GGCTAC	L004	11.0035649	23689045	87.15%	15.5153	31.15
SE6P2	GTTTCG	L003	10.50787671	25453380	87.03%	15.4818	30.52
EE3P2	AGTCAA	L004	12.64190201	17515744	86.50%	14.6318	30.81
EE4P2	AGTTCC	L002	9.852143188	24851512	86.13%	16.3764	30.81
EE5P2	ATGTCA	L002	11.80979669	23862288	86.91%	16.9291	30.88
EE6P2	CCGTCC	L003	7.616590362	38310485	85.44%	75.4096	32.12

their abundances were estimated by counting the number of aligned reads contained within a transcript, and normalizing to both the size of the transcript and to the total number of aligned reads in the sample (**F**ragments **P**er **K**ilobase of exon per **M**illion fragments mapped, **FPKM**). It should be noted that for paired end reads a read pair was counted as a single fragment. Cuffmerge was then used to merge all transcriptome assemblies, generating common IDs for each transcript, which were then tested for differential expression using Cuffdiff, which calculates pairwise comparisons of gene expression. For the comparison between fractions, false discovery rate (FDR) was set equal to 0.05.

Bioinformatics analysis. Integrative functional genomics analysis was performed using Gene Weaver (geneweaver.org) (Baker *et al.*, 2012), a curated repository of genomic experimental results. This web-based software allows users to evaluate gene set interactions and facilitates the assessment of gene set similarity through computation of the Jaccard Coefficient (size of the interaction divided by size of the union of the sample set). Independence between gene lists was additionally measured using Fisher's exact test in the statistical platform, R (Team, 2011) and by calculating the representation factor (RF) for overlap (http://nemates.org/MA/progs/overlap_stats.html). RF is the number of overlapping genes divided by the expected number of overlapping genes drawn from two independent groups. The expected number of overlapping genes is equal to the product of genes in both groups divided by the total number of genes in the genome. A RF > 1 indicates more overlap than expected of two independent groups.

Functional enrichment analysis was performed using ToppFun, a functional enrichment application available as part of the ToppGene suite of web based applications (toppgene.cchmc.org) (Chen *et al.*, 2009). Mouse gene symbols were submitted and analyzed for over-representation of genes that belong to Gene Ontology (GO) categories (molecular function, biological processes, and cellular component). To enhance informativeness of results, top ranked terms were filtered to remove broad and redundant definitions. Only categories that were comprised of greater than 3 and fewer than 400 genes were included, removing those that contained exactly the same query list as another term already listed in the displayed results.

MicroRNA Arrays. Total RNA isolated for the purpose of genomic expression profiling by microarray and RNA-Seq analyses was further assayed to characterize the complement of microRNAs present at the synapse (P2 samples) and compare to the microRNAs present in the somatic-RNA containing fraction (S2 samples). Samples were prepared using the FlashTag™ Biotin HSR RNA Labeling Kit (Affymetrix, Santa Clara, CA) in accordance to manufacturer's instructions. Total RNA (250 ng) from each sample, spiked with control oligos, was subjected to poly (A) tailing and biotin labeling. Qualitative assessment of proper target labeling was performed using an enzyme-linked oligosorbent assay (ELOSA). Samples were hybridized to GeneChip® miRNA 3.0 Arrays (Affymetrix, Santa Clara, CA) and scanned with the Affymetrix GeneChip Scanner 3000 according to standard Affymetrix protocols. Supervised randomization of samples into batches for RNA labeling and hybridization was performed. Data were summarized using the RMA algorithm and probe sets consistently called 'absent' across all samples using Detection Above Background' (DABG) p-values were removed

(McClintick & Edenberg, 2006). Differential expression between fractions was evaluated using the rank-based permutation method statistical analysis of microarrays (SAM) (Tusher *et al.*, 2001) setting the false discovery rate (FDR) at 0.01.

Results

Molecular characterization of the synaptoneurosome preparation.

Before the synaptoneurosomal preparation was used to investigate response of the synaptic transcriptome to repeated ethanol exposure, a molecular characterization was undertaken to establish enrichment of synaptic elements in the P2 fraction. The presence and morphological integrity of synaptoneurosomal structures within the P2 fraction was confirmed by transmission electron microscopy (TEM). The characteristic synaptoneurosomal profile consists of an intact presynaptic terminal with distinguishable synaptic vesicles and postsynaptic element with well-preserved postsynaptic density (Figure 3.2, **a**). An average (mean ± SD) of 20 ± 5 (n = 4) synaptoneurosomal structures was identified per 130 square micron field of the P2 fraction. Detected within the synaptoneurosomes were structures consistent with the size and density of polyribosomes (Figure 3.2, **b**). As suggested previously (Williams *et al.*, 2009), the intact pre- and postsynaptic terminals, identified by TEM, provides for selective extraction of synaptic mRNAs. Aliquots of the P1 fractions were also analyzed (Figure 3.2, **c**). Prominent features included nuclei, myelin structure, and blood vessels. Synaptoneurosomal structures were also identified within the P1. While electron microscopy provides visual detection of synaptoneurosomes, it is not a suitable method to evaluate the purity of the preparation since unequivocal identification requires the

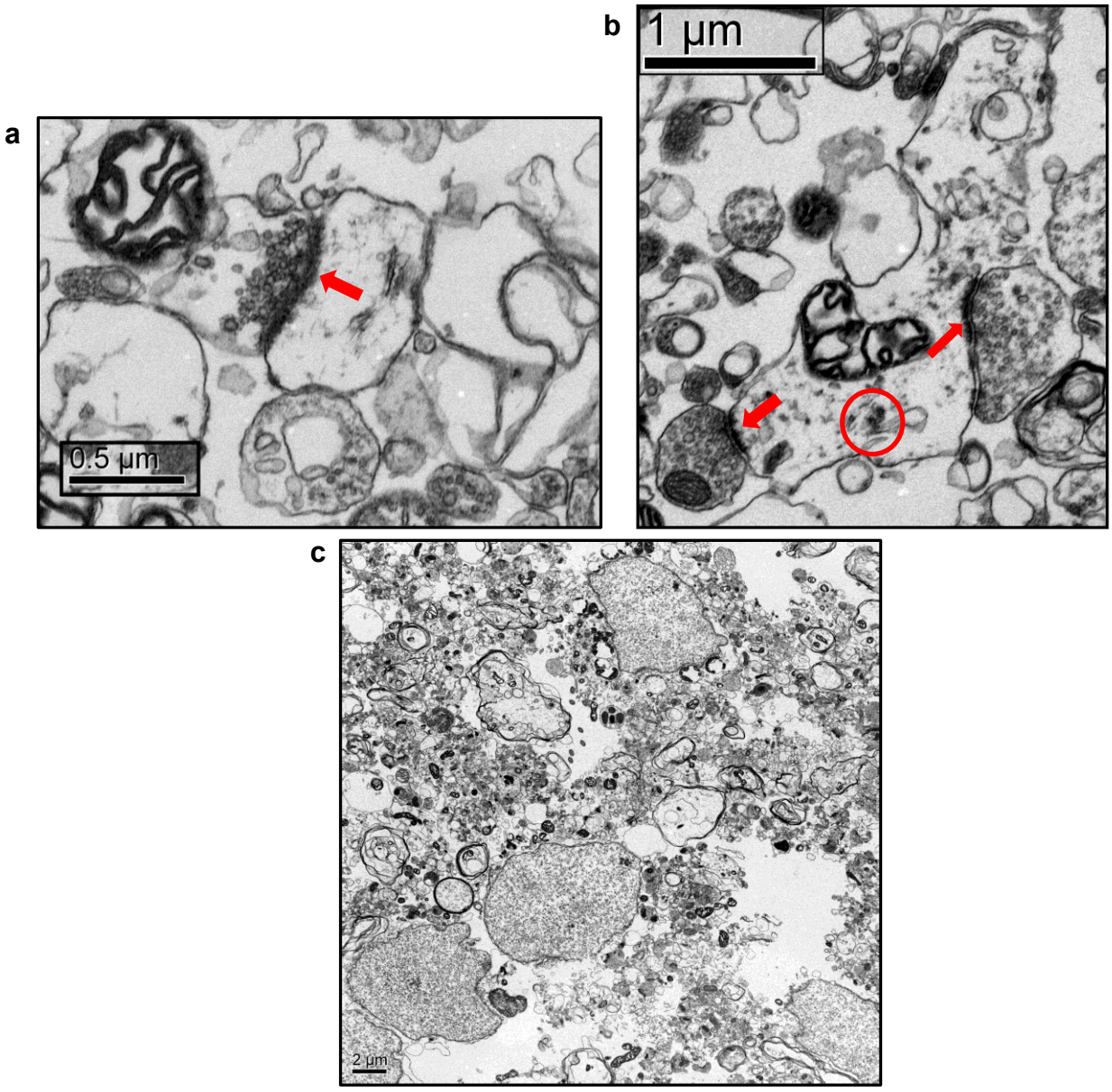

Figure 3.2 – Representative electron micrographs from P2 and P1 fractions. Characteristic synaptoneurosomal profiles in the P2 fraction were observed at (**a**) 10,000x magnification and (**b**) 8,000x magnification. Postsynaptic densities are labeled by red arrows and presynaptic elements with synaptic vesicles can be observed immediately adjacent. Polyribosome structures are highlighted by red circles. The P1 fraction (**c**) at 1,500x magnification contains prominent nuclei and myelin structure.

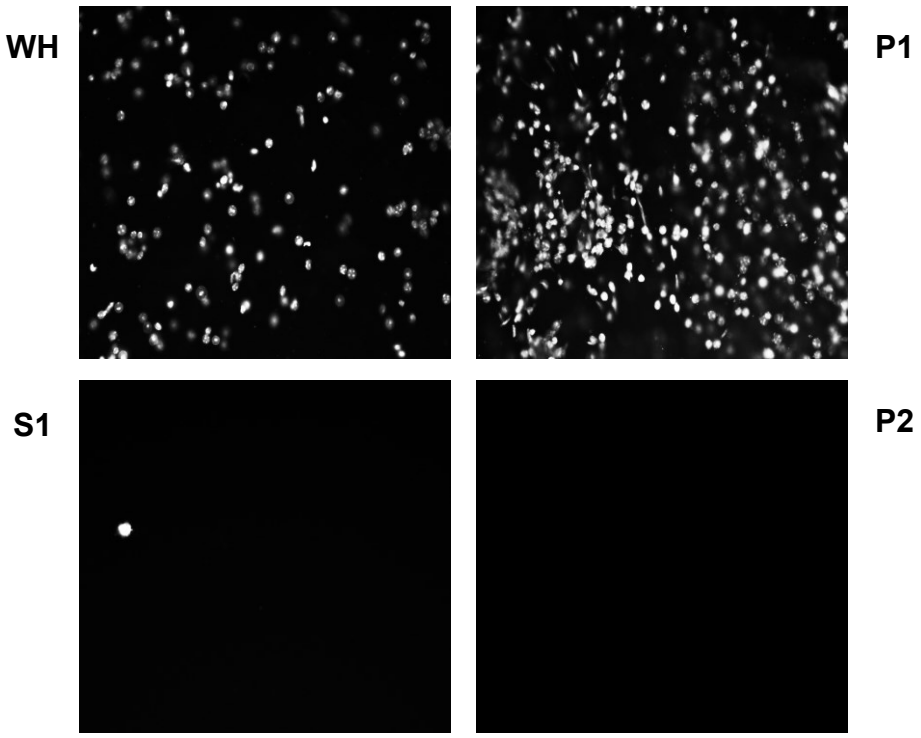

Figure 3.3 – DAPI staining of synaptoneurosome fractions. 4', 6-diamidino-2-phenylindole (DAPI) staining of DNA across the fractions indicated that most, if not all the nuclei were removed in the initial centrifugation step to produce the P1 pellet. All images were captured at 20x magnification.

plane of the section to cut through both the pre- and postsynaptic elements. Enrichment was better ascertained through other quantitative methods.

Presence of residual nuclei throughout synaptoneurosomal fractions was assessed by DAPI staining (Figure 3.3). No fluorescent signal was detected in any of the representative fields captured from P2 samples, and little to no DAPI staining was observed in the S1 supernatant from which P2 fractions were obtained. Most, if not all, nuclei were observed densely packed in the P1 fraction, produced during the initial centrifugation step. Concern over loss of synaptic elements during the first centrifugation prompted a change in protocol, from 1000 x g to 500 x g. To ensure that this modification in procedure did not result in greater nuclear contamination, synaptoneurosomal preparations were performed using both speeds and resulting P1 and P2 fractions were compared (Figure 3.4). DAPI staining was not detected in P2 fractions from either preparation. Therefore, to prevent the potential loss of synaptic structures, the slower centrifugation speed was chosen for subsequent preparations.

One method used to ascertain purity of the preparation and to verify enrichment was immunoblotting for subcellular protein markers (Figure 3.5). Due to the fractionating nature of the protocol, *a priori* determination of a proper loading control was impossible. Therefore, immunoreactivity for each protein was quantitated by densitometry and normalization to total protein loaded in each lane as measured by Ponceau S staining. Histone 4 (H4), a marker for the nuclear component, was detected only in the WH and P1 fraction. Lactate dehydrogenase (LDH), an abundant and ubiquitous protein used as the maker for the cytosolic component, was detected uniformly across all fractions. There was a significant increase in postsynaptic density protein 95 (PSD95) in the P2

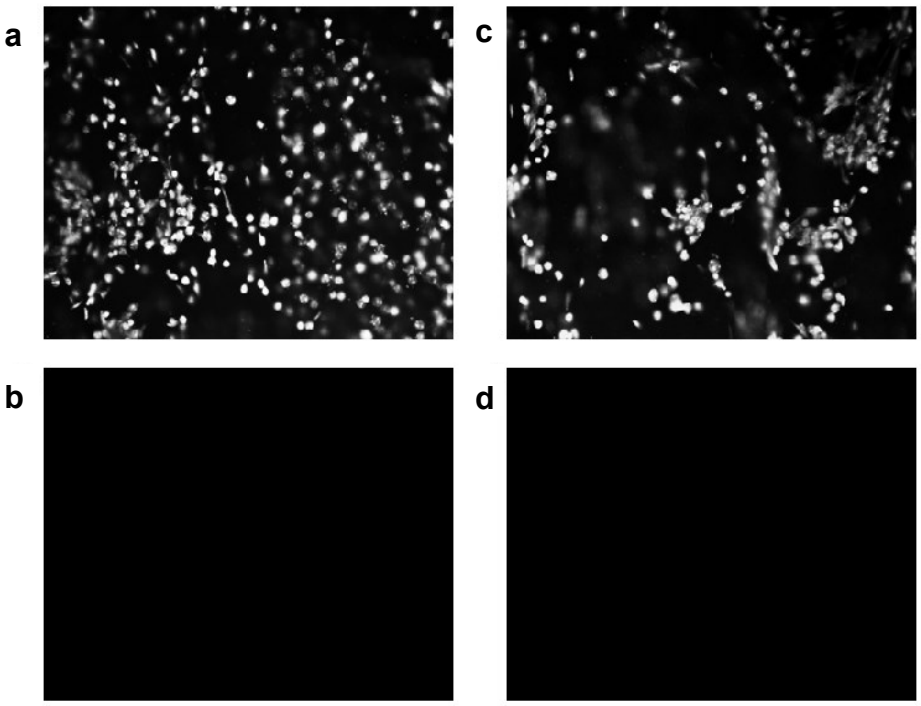

Figure 3.4 – Comparison of synaptoneurosomal preparation centrifugation speeds by DAPI staining. (**a**) P1, 1000 x g (**b**) P2, 1000 x g (**c**) P1, 500 x g (**d**) P2, 500 x g. All images were captured at 20x magnification.

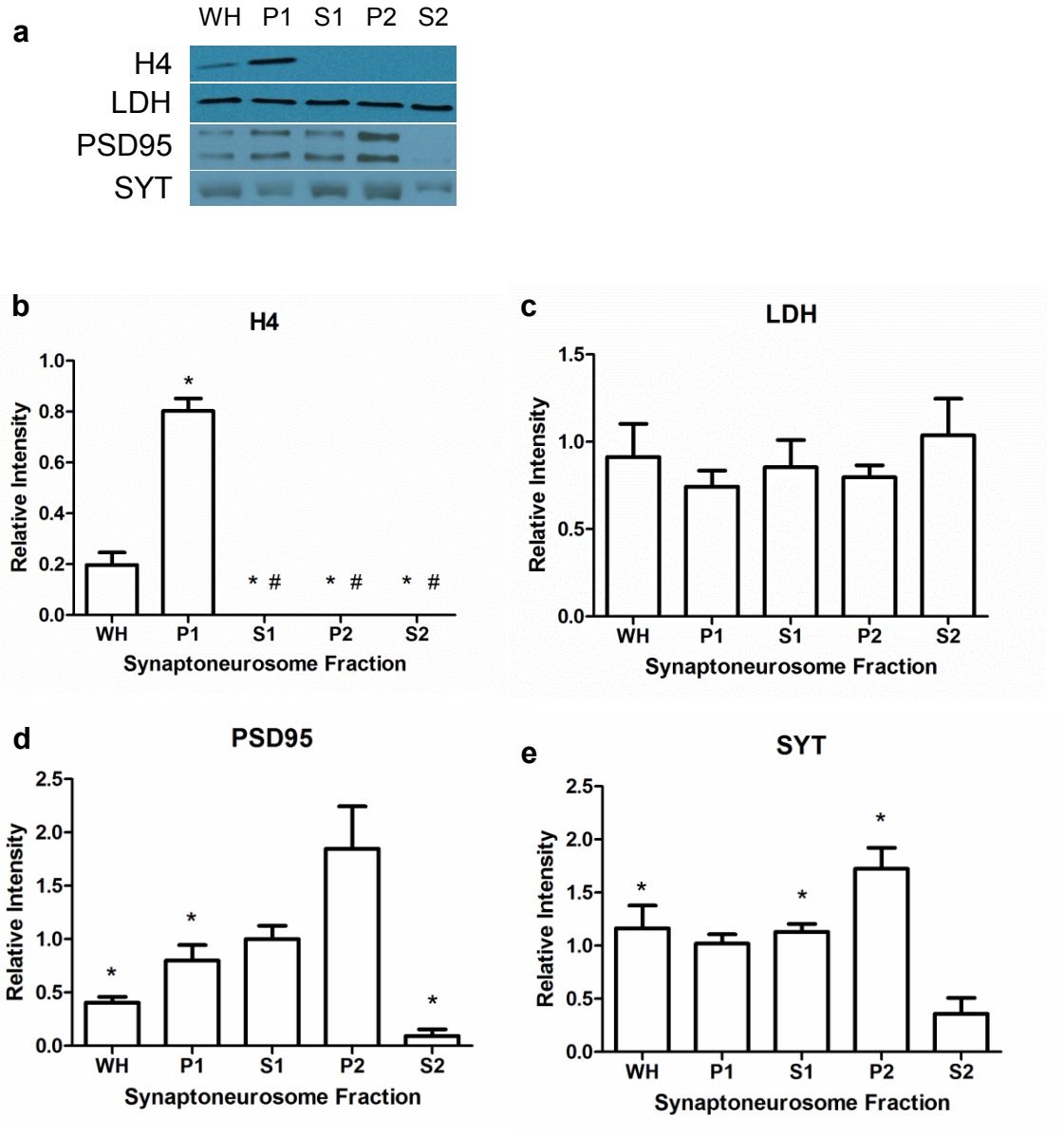

Figure 3.5 – Immunoblotting of subcellular protein markers across synaptoneurosome fractions. (**a**) Representative immunoblot images (**b**) quantification of H4 (F[4,10] = 125.3, *p < 0.01 compared to WH, #p < 0.01 compared to P1) (**c**) quantification of LDH (F[4,10] = 0.5492) (**d**) quantification of PSD95 (F[4,10] = 11.09, *p < 0.05 compared to P2) (**e**) quantification of SYT (F[4,10] = 9.828, *p < 0.05 compared to S2). Statistical analysis for each protein was performed by one-way ANOVA, followed by Tukey's HSD *post-hoc*, n = 3.

fraction, with a 4.6 fold enrichment compared to the WH. This enrichment of PSD95 in the synaptoneurosomal fraction is greater than what has been observed in previous publications, including the study this present protocol was adapted from, which only obtained 2.3 fold enrichment. (Villasana *et al.*, 2006; Williams *et al.*, 2009). The level of presynaptic marker, synaptotagmin (SYT), was significantly greater in the P2 fraction as compared to the S2, but there was no significant enrichment compared to the WH. This might suggest some loss of presynaptic elements in the P1. Together with the DAPI staining results, these data indicate P2 fractions contain synaptic elements enriched for synaptic protein markers as compared to the complementary supernatant fraction, S2, and are devoid of appreciable nuclear contamination.

To further ensure purity of the synaptoneurosomal preparation and to determine enrichment of known synaptically targeted transcripts, qRT-PCR was performed. Normalization to a cohort of endogenous control genes is currently the most accurate method to correct for potential biases that result from input or reaction efficiency. Ideal control genes are abundantly and consistently expressed across all sample types in the experimental design. Once again, since the objective of the synaptoneurosome preparation is distribution of mRNA species between the fractions based on subcellular location, it was assumed that typical housekeeping genes would not fulfill their intended purpose. Alternatively, an exogenous internal reference mRNA, luciferase, was added to the cDNA synthesis reaction. Detection of this reference transcript with primers designed by Johnson *et al.* (2005) was used to control for the losses and inefficiencies of downstream processing (Johnson *et al.*, 2005). Transcripts known to be synaptically targeted, *Camk2a* and *Arc* (Burgin *et al.*, 1990; Link *et al.*, 1995; Lyford *et al.*, 1995)

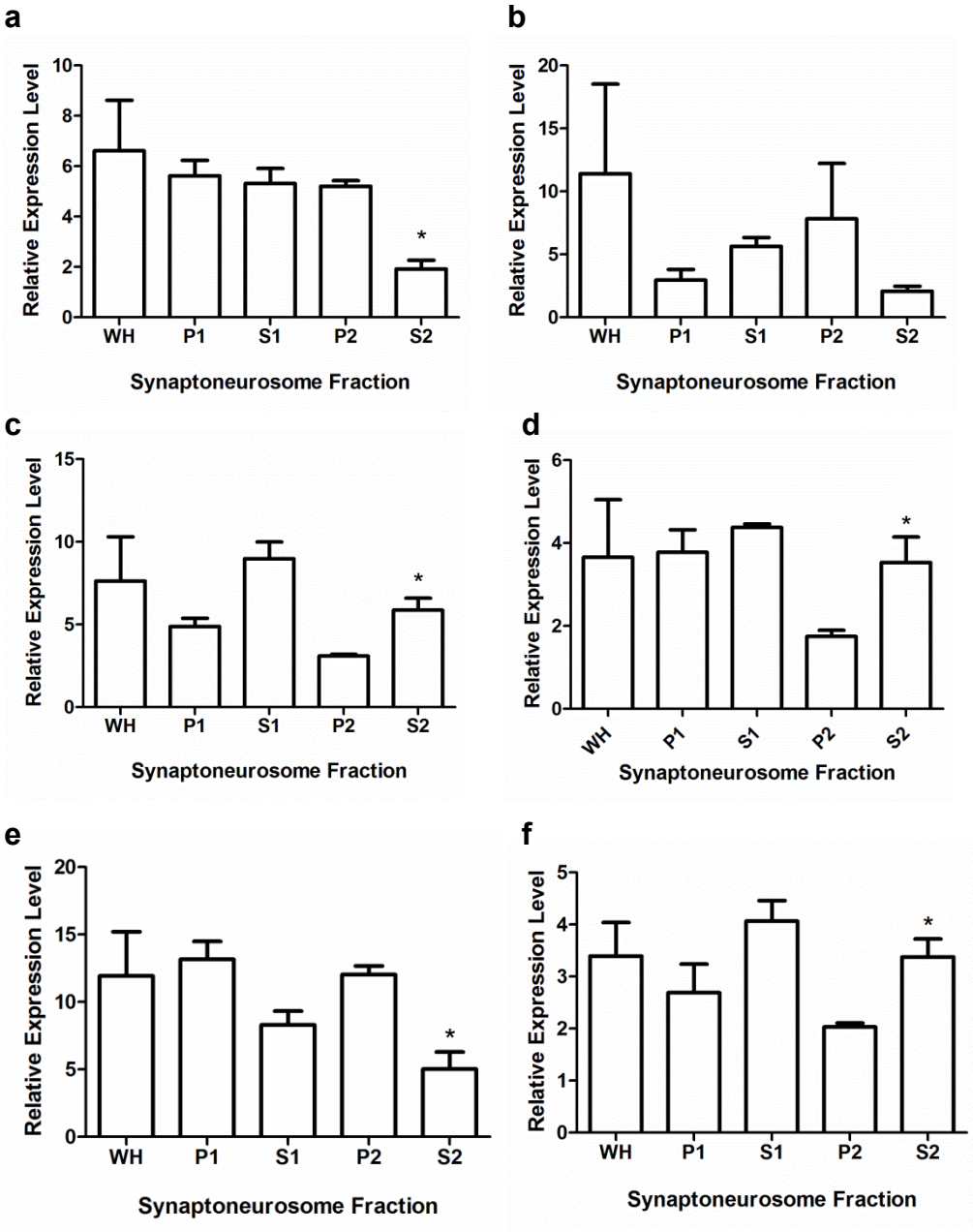

Figure 3.6 – qRT-PCR profile across synaptoneurosome fractions. (**a**) *Camk2a* (F[4,10] = 3.170, p = 0.0632, t[4] = 7.996, *p = 0.0013 compared to P2). (**b**) *Arc* (F[4,10] = 1.008, p = 0.4479, t[4] = 1.301, *p = 0.2631 compared to P2). (**c**) *Gapdh* (F[4,10] = 2.968, p = 0.0742, t[4] = 1.301, *p = 0.0190 compared to P2). (**d**) *Snrpn* (F[4,10] = 1.845, p = 0.1969, t[4] = 2.823, *p = 0.0477 compared to P2). (**e**) *Gfap* (F[4,10] = 3.642, p = 0.0443, t[4] = 4.933, *p = 0.0079 compared to P2). (**f**) *Rn18s* (F[4,10] = 3.022, p = 0.0711, t[4] = 3.835, *p = 0.0185 compared to P2). Statistical analysis for each gene was performed by one-way ANOVA across all fractions and a Student's t-test between P2 and S2 fractions, n = 3.

(Figure 3.6, **a, b**), as well as somatically restricted transcripts, *Gapdh* and *Snrpn (Litman et al., 1994; Poon et al., 2006)* (Figure 3.6, **c, d**) were assayed across all synaptoneurosomal fractions. *Gfap*, a prototypical astrocyte marker, and *Rn18s*, a ribosomal RNA, were also analyzed for further characterization of the preparation (Figure 3.6, **e, f**). These analyses were underpowered for detection of significant differences in transcript abundance when comparing all fractions. Nevertheless, the results produced a profile that depicted a pattern of differential expression between the P2 and S2 fractions. A Student's t-test to compare these fractions alone revealed significant differences in the expression of all genes, except *Arc*, which had a high level of variability. These results confirmed that subsequent genomic analyses should focus on differences between the P2 and S2 fractions.

To observe the percentage of total RNA present in each fraction and determine the approximate yield obtained from the synaptoneurosomal protocol, the three preparations from the qRT-PCR analysis were analyzed. An approximate value for total RNA present in the initial whole homogenate was extrapolated by multiplying the mass of RNA obtained from an aliquot of WH by the volume of buffer added in the initial step. The percent yield was estimated from the sum of the total RNA measured from each fraction. From the three preparations performed, an average (mean ± SD) yield of 75.8% ± 8.4 was attained. Using the sum of RNA from each fraction as an actual starting quantity, the percentage of total RNA present in the WH and S1 aliquots and P1, P2, and S2 fractions were calculated as (mean ± SD) 15.1 ± 2.2, 15.6 ± 2.7, 39.1 ± 8.4, 6.0 ± 1.7, and 24.2 ± 3.5 %, respectively. On average (mean ± SD), the yield of RNA isolated from the P2 fraction was 17.5 ± 3.4 µg per 0.45 g of starting tissue wet

weight. This quantity was greater than the amount obtained from Williams *et al.* (2009), which achieved a yield of 10 µg synaptoneurosomal RNA from 1 g of tissue.

Transcriptomic characterization of synaptoneurosome preparation.

Synaptoneurosomal fractions were prepared from the tissue of mice subjected to the ethanol behavioral sensitization paradigm (refer to Chapter 4 Materials and Methods) for the purpose of investigating the effect repeated ethanol exposure has on the synaptic transcriptome. These samples also provided the opportunity to further characterize the populations of RNA acquired from P2 and S2 fractions at the level of the entire transcriptome. Following RNA isolation and prior to preparation for microarray analysis, automated electrophoresis was performed to ascertain the quality of RNA from each sample. Figure 3.7, **a**, is a representative virtual gel which provides visualization of the molecular weight distribution of total RNA. Invariably, the P2 fractions appeared to be enriched for small molecular weight RNAs. Since it is known that microRNAs and their regulatory machinery are present in dendritic spines (Lugli *et al.*, 2005; Lugli *et al.*, 2008) and the low molecular weight bands consistently observed in the P2 fractions corresponded to the typical distance traveled by microRNAs on the automated electrophoretic gels, it was hypothesized that this enrichment consisted of microRNAs trafficked to the synapse for the purpose of local translation regulation. To examine microRNA distribution between the P2 and S2 fractions, qRT-PCR was performed using TaqMan® primers and probes selective for mir-149, mir-134, and mir-9 (Figure 3.7, **b**). Primers for miR-134 were used because this regulatory RNA is known to be present and function at the synapse (Schratt *et al.*, 2006). miR-9 was assayed since it has been

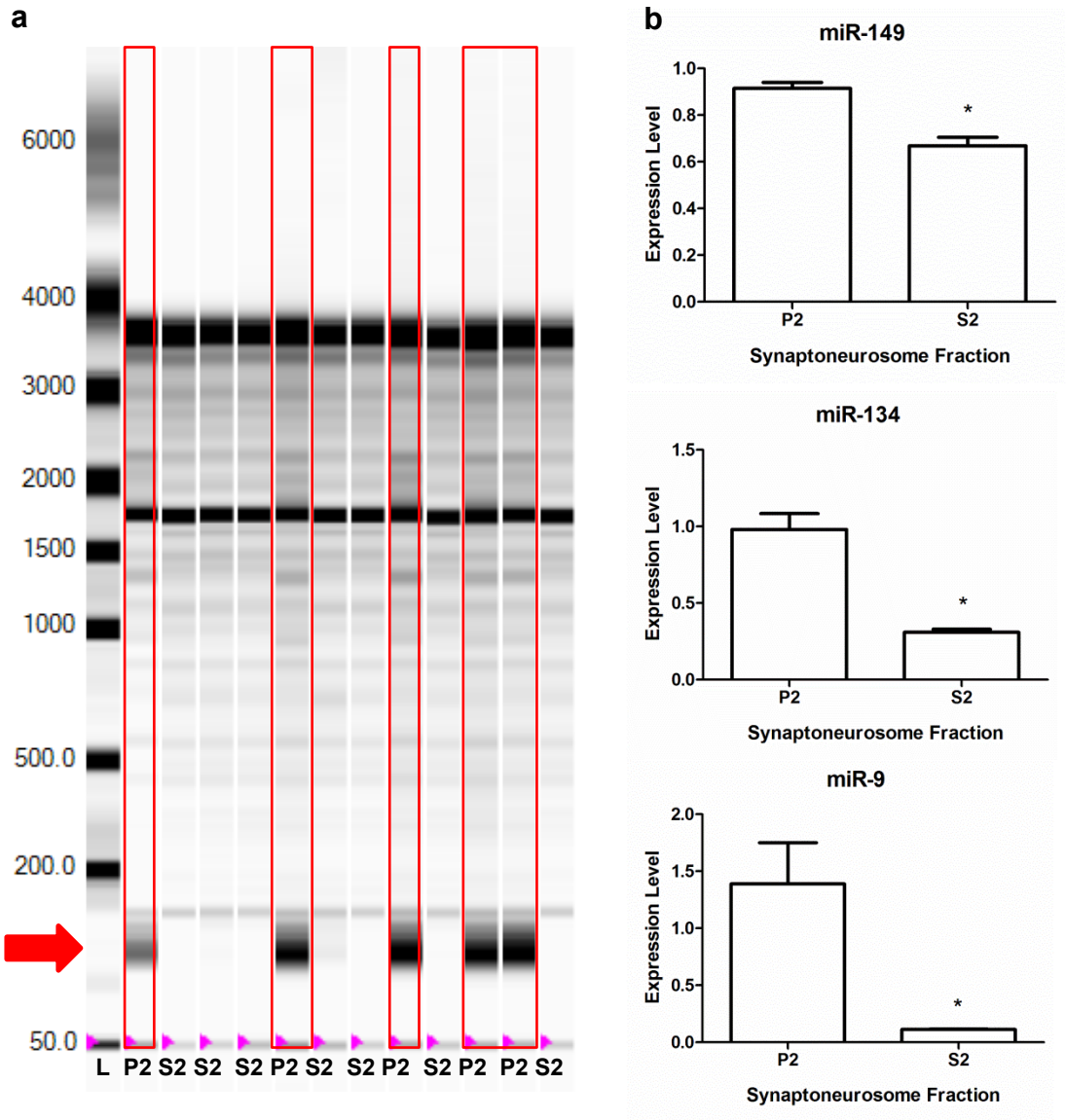

Figure 3.7 – Enrichment of small molecular weight RNAs in the P2 fraction (**a**) Representative virtual electrophoretic gel that shows distribution of total RNA isolated from synaptoneurosome fractions, P2 and S2. Lanes loaded with P2 samples are highlighted by the red boxes, and the enrichment of small molecular weight RNAs is indicated by the red arrow. (**b**) microRNA qRT-PCR results: miR-149 (t[6] = 5.511, p = 0.0015); miR-134 (t[6] = 6.324, p = 0.0007); miR-9 (t[6] = 3.521, p = 0.0125). Statistical analysis for each microRNA was performed by a Student's t-test between P2 and S2 fractions, n = 4.

shown to be regulated by ethanol (Pietrzykowski *et al.*, 2008). The assay for mir-149 had previously been used and validated in the laboratory. There was a significant increase in the level of these microRNA species in P2 versus S2 samples. These results prompted a global survey of the microRNA population using Affymetrix GeneChip® miRNA 3.0 arrays. SAM analysis, with an FDR correction set at 1%, identified 693 microRNAs that were differentially expressed between the fractions. Of these, 383 and 310 microRNAs were found enriched for in the P2 and S2 fractions, respectively (Supplemental Tables S3.1, S3.2). Chi squared analysis found a deviation from the null hypothesis frequency of 50%, indicating a significantly greater number of genes enriched for in the P2 ($\chi^2 = 7.690$, df = 1, p = 0.0056).

Once it was determined that the total RNA from P2 and S2 fractions had passed quality assurance measures, preparation of labeled targets for microarray analysis followed the protocol outlined in Figure 3.8, **a**. Starting with 100 ng of total RNA, each sample was spiked with poly-A RNA controls which permits monitoring of the entire target synthesis and labeling procedure. The quantity of anti-sense cRNA produced at an intermediary step was assessed revealing a significant reduction in the yield from S2 samples, despite using the exact same amount of starting material for both fractions (Figure3.8, **b**). Equal quantities of cRNA (10 µg) from each sample were used for subsequent reactions. The final product, labeled and fragmented cDNA, was spiked with hybridization controls and incubated on the microarray platform, allowing for hybridization between targets and probes. Despite equivalent amounts of labeled cDNA being added to each chip, a constant dissimilarity in overall fluorescent intensity between P2 and S2 fractions could be observed when looking at the digital images of

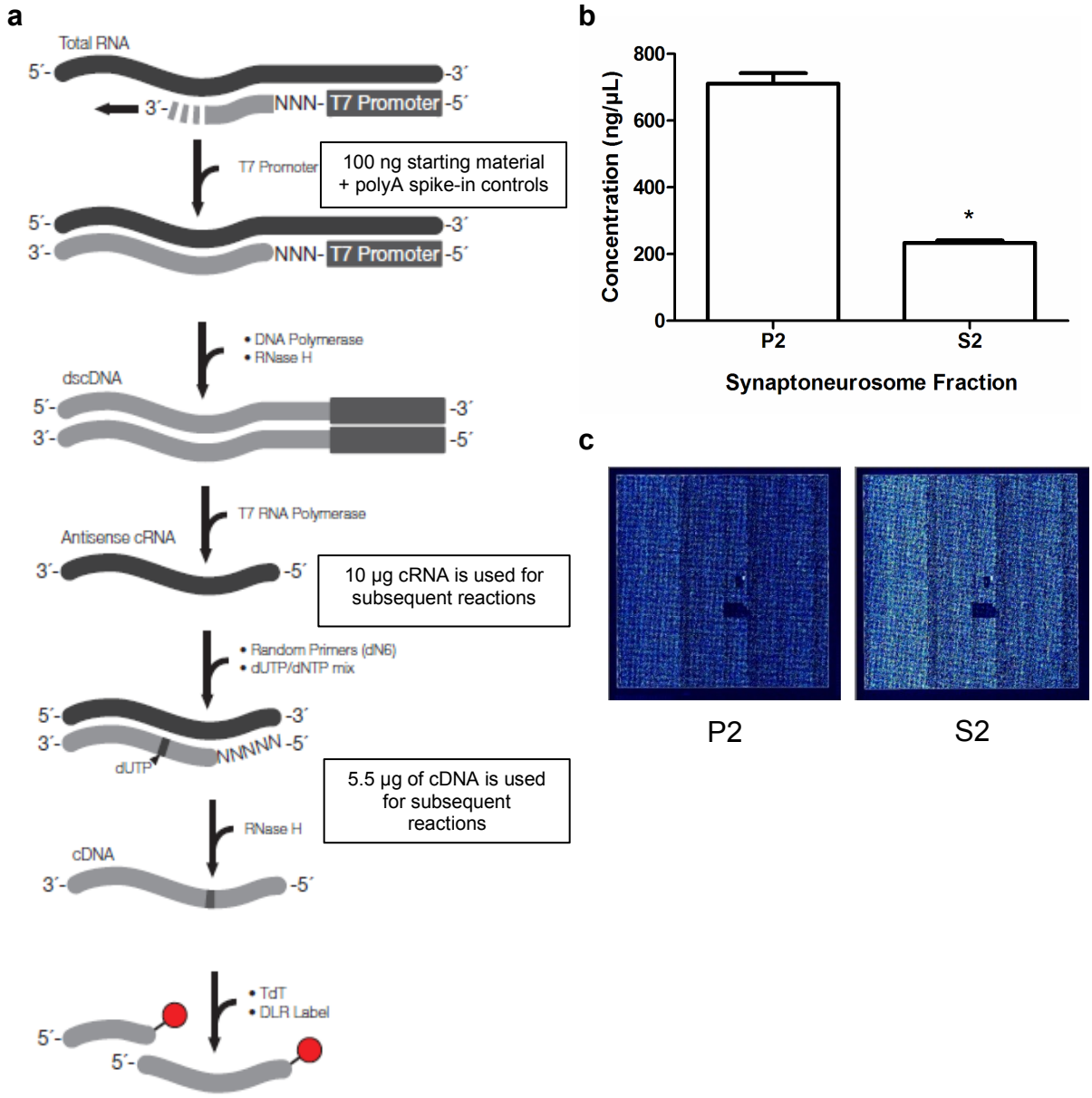

Figure 3.8 – Distinct RNA populations between P2 and S2 fractions affect microarray sample preparation. (**a**) Schematic of the protocol for microarray sample preparation. Image adapted from the Ambion® WT Expression Kit manual. (**b**) *In vitro* transcription cRNA yields (Student's t-test, $t[30] = 14.94$, $p < 0.0001$, $n = 16$) (**c**) Representative P2 and S2 sample DAT files, which store intensity calculations as pixel values.

the microarray (Figure 3.8, **c**). Concern that such disparity in signal intensity was the result of non-hybridizable material in the P2 that would prevent proper data normalization prompted a reanalysis by RNA-Seq. This methodology relies on next-generation sequencing which provides direct read counts of target RNA, ideally bypassing the potential bias that results from hybridization in the microarrays. The objectives of this analysis were: a) use RNA-Seq results to calculate a normalization factor that could be applied to the microarray intensity values b) compare and validate differential expression results obtained from the differing technologies.

To calculate a normalization factor, RNA-Seq results were filtered to provide a set of genes whose expression was not dependent on fraction. Genes were removed that had greater than 10% fold change and p-values less than 0.50 between P2 and S2 fractions. Additionally, low abundance genes (maximum FPKM less than 1 across all samples) were discarded. This provided a set of 193 genes that were stably expressed between the two fractions that were also present on the GeneChip® Mouse Gene 1.0 ST Arrays. By plotting the log2 transformed RMA microarray values for P2 versus S2 for this gene set, linear regression would indicate the degree to which the standard normalization scheme was amiss and the slope of the line of best fit could be used as a proper normalization factor (Figure 3.9). The resulting slope equaled 1.02, indicating that these genes were found to be equally distributed between P2 and S2 by both RNA-Seq and microarray analyses. This suggested that the RMA algorithm used for normalization of microarray data was able to properly correct for the large RNA population differences between P2 and S2 samples.

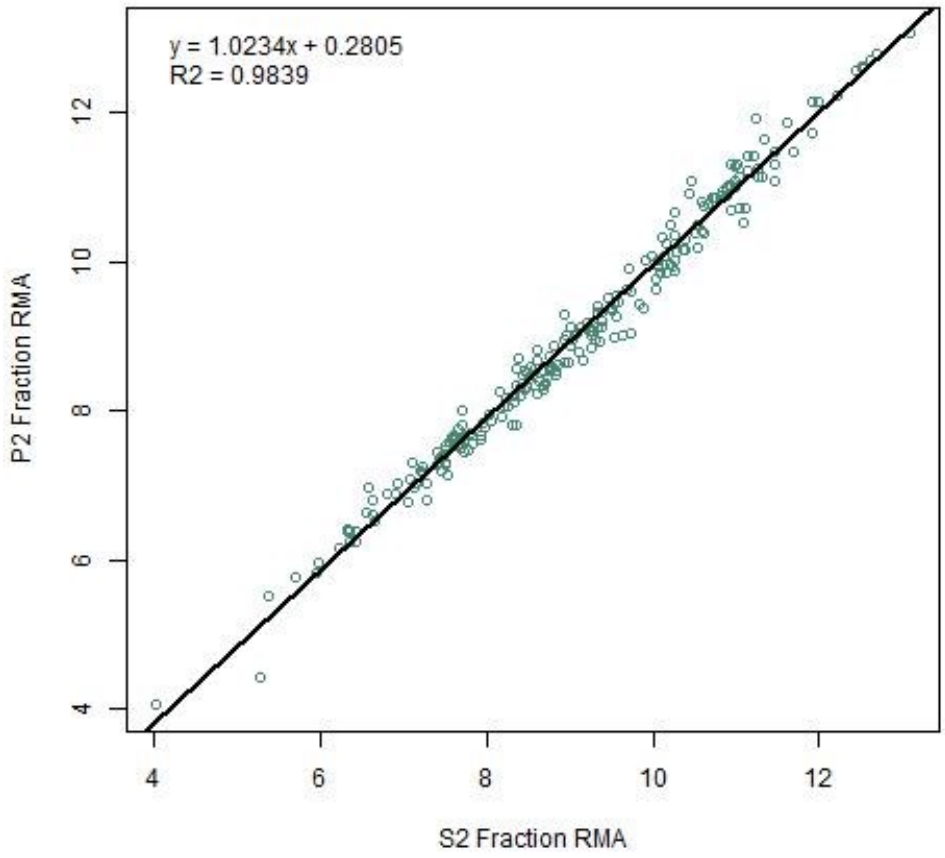

Figure 3.9 – Microarray normalization factor determination. S2 fraction RMA values plotted against P2 fraction RMA values for genes whose expression was found not be dependent on fraction by RNA-Seq. A significant correlation was found between S2 and P2 expression ($F\{1, 237] = 14520$, $p < 0.0001$). The slope of the line of best fit suggests no further normalization is required for RMA values calculated from P2 and S2 samples together.

RNA-Seq and microarrays both provide a genomic view of expression, yet their detection methods depend on distinct molecular principles. Calculated expression values for microarrays (RMA) and RNA-Seq (FPKM) for all genes can be found in Supplemental Tables 3.3, S3.4. Figure 3.10, **a** compares the number of fraction level significant genes as determined by the separate assays (Supplemental Table S3.5). The ability of RNA-Seq and microarrays to detect genes putatively enriched in the synaptic transcriptome was examined by looking at the number genes with greater expression in the P2 fraction compared to the S2 (Figure 3.10, **b**). Strikingly, there was an overlap of 1,945 genes enriched in the P2 fraction in both the microarray and RNA-Seq analyses (Supplemental Table S3.6). This overlapping set of genes was used for subsequent bioinformatics analyses to determine the underlying biological function of P2 enriched transcripts. Significant overlap with genes found through deep sequencing of RNA obtained from micro-dissected rat hippocampal neuropil structure (Cajigas *et al.*, 2012) and gene products present in the mouse postsynaptic proteome (Collins *et al.*, 2006) suggests a portion of the genes contained within the P2 fraction have been validated to be present or functioning in the synapse (Figure 3.11). Further evidence of this comes from functional enrichment analysis where the top ontological categories overrepresented in the P2 enriched gene list relate to neurotransmission and the synaptic compartment (Table 3.4) which contrasts from the somatic functions of the genes expressed in the S2 (Table 3.5, Supplemental Table S3.7). The complete list of functional enrichment categories for both the P2 fraction and S2 enriched genes can be found in Supplemental Tables S3.8, S3.9. The top 50 enriched genes from the P2 and

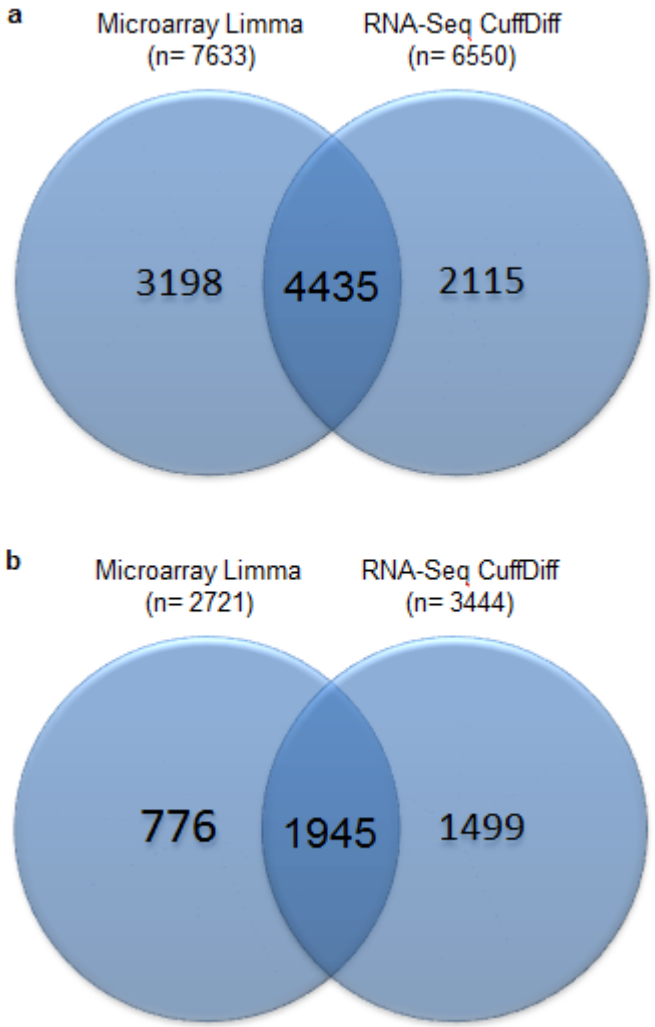

Figure 3.10 – Venn diagrams for P2 versus S2 fraction significant genes. (**a**) Total number of genes determined to be significantly different ($q < 0.05$) between P2 and S2 fractions by microarray Limma and RNA-Seq Cuffdiff analyses. Significance of overlap was measured by Fisher's exact test ($p < 2.2 \times 10^{-16}$, odds ratio = 0.65), Jaccard Coefficient ($J = 0.4835$, $p < 0.01$), and Representation Factor ($RF = 2.3$, $p < 1.2 \times 10^{-238}$). (**b**) Number of genes enriched in the P2 fraction as determined by microarray Limma and RNA-Seq Cuffdiff analyses. Fisher's exact test ($p < 2.2 \times 10^{-16}$, odds ratio = 3.71), Jaccard Coefficient ($J = 0.4833$, $p < 0.01$), and Representation Factor ($RF = 5.4$, $p < 1.2 \times 10^{-238}$).

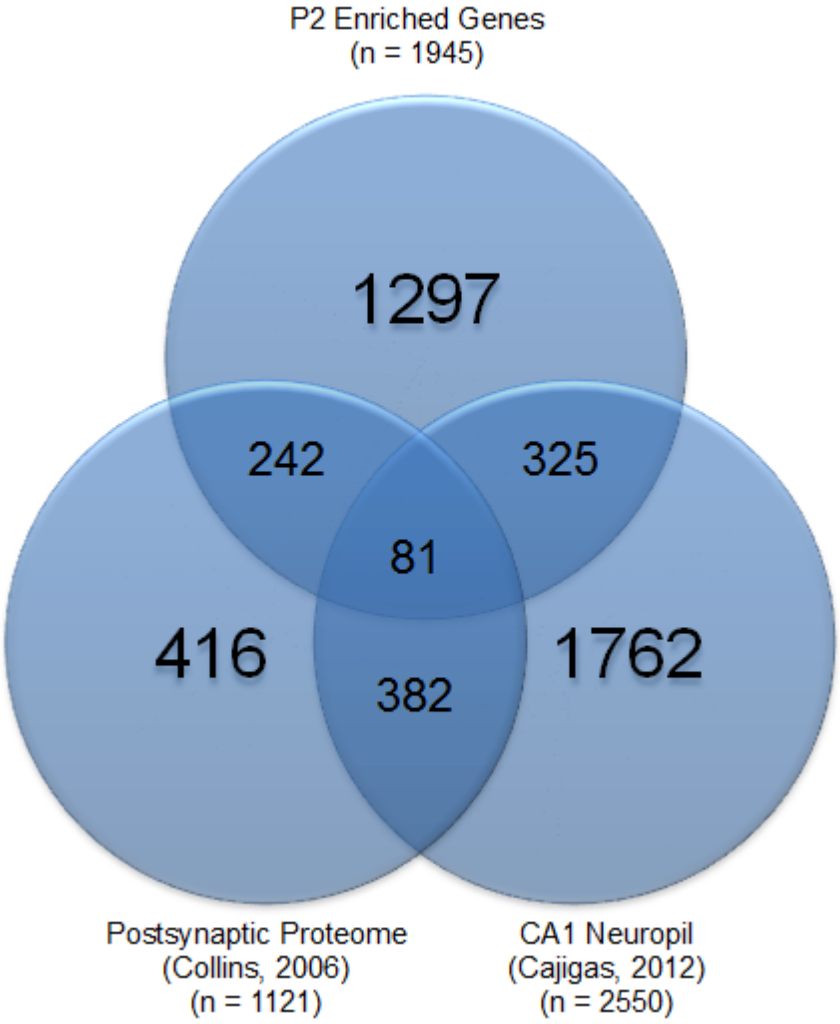

Figure 3.11 – Venn diagram depicting overlap between synapse related data sets. Significant overlap was found between the P2 enriched gene list and the postsynaptic proteome gene set (Collins *et al.*, 2006) (Fisher's exact test ($p < 2.2 \times 10^{-16}$, odds ratio = 2.52), Jaccard Coefficient ($J = 0.0888$, $p < 0.01$), and Representation Factor ($RF = 2.9$, $p < 1.05 \times 10^{-53}$)) and the CA1 neuropil gene set (Cajigas *et al.*, 2012) (Fisher's exact test ($p < 5.2 \times 10^{-7}$, odds ratio = 1.38), Jaccard Coefficient ($J = 0.0842$, $p < 0.01$), and Representation Factor ($RF = 1.7$, $p < 2.23 \times 10^{-23}$).

Table 3.4: Functional Enrichment Analysis, P2 Enriched Gene List

GO Category	Name	P-value	Terms in Query	Terms in Genome
Molecular Function	substrate-specific channel activity	2.84E-19	103	399
Molecular Function	divalent inorganic cation transmembrane transporter activity	4.43E-17	54	152
Molecular Function	transmembrane receptor protein kinase activity	7.96E-16	37	83
Molecular Function	active transmembrane transporter activity	5.51E-15	81	319
Molecular Function	PDZ domain binding	4.44E-13	41	117
Biological Process	neuron projection guidance	1.86E-22	106	376
Biological Process	regulation of transmembrane transport	9.15E-20	90	314
Biological Process	regulation of cell projection organization	1.36E-17	95	366
Biological Process	regulation of synaptic transmission	3.20E-17	74	251
Biological Process	glutamate receptor signaling pathway	1.97E-16	33	64
Cellular Component	axon	2.94E-27	115	389
Cellular Component	synaptic membrane	3.32E-22	81	251
Cellular Component	receptor complex	4.49E-21	83	271
Cellular Component	transmembrane transporter complex	4.98E-18	80	283
Cellular Component	cell leading edge	8.90E-18	86	320

Table 3.5: Functional Enrichment Analysis, S2 Enriched Gene List				
GO Category	**Name**	**P-value**	**Terms in Query**	**Terms in Genome**
Molecular Function	guanyl nucleotide binding	6.96E-13	104	390
Molecular Function	GTPase activity	2.82E-10	68	238
Molecular Function	translation factor activity, nucleic acid binding	4.51E-10	36	92
Molecular Function	protein transporter activity	2.64E-08	31	83
Molecular Function	small conjugating protein ligase activity	3.59E-08	73	292
Biological Process	ribonucleoprotein complex biogenesis	3.09E-27	110	282
Biological Process	ncRNA metabolic process	6.42E-27	120	326
Biological Process	RNA splicing	7.76E-26	123	347
Biological Process	negative regulation of ubiquitin-protein ligase activity	1.03E-19	43	73
Biological Process	positive regulation of protein ubiquitination	2.95E-18	62	145
Cellular Component	proteasome complex	2.58E-20	41	67
Cellular Component	transferase complex	5.59E-19	110	358
Cellular Component	spliceosomal complex	1.15E-18	65	159
Cellular Component	mitochondrial matrix	3.35E-18	102	327
Cellular Component	mitochondrial membrane part	2.09E-13	56	156

S2 fractions along with their average microarray RMA expression values and fold change are listed in Tables 3.6 and 3.7. Interestingly, the top P2 fraction enriched genes contained 4 transmembrane receptor protein tyrosine kinases (GO:0004714, p = 2.44E-5) and enrichment of genes related to neuro- and gliogenesis (GO:0022008, p = 1.45E-5; GO:0042063 p = 2.30E-5).

Discussion

In the present studies, we characterized the synaptoneurosomal preparation prior to subsequent analyses intended to investigate the effect of repeated ethanol on the synaptic transcriptome. We expected that an enrichment of synaptically localized RNA would allow for detection of gene expression changes potentially confined to the synapse that would otherwise go undetected when studying the entire transcriptome. Immunoblotting, qRT-PCR, microarray, and RNA-Seq analyses revealed marked differences in the proteins and transcripts present in the P2 and S2 fractions. A distinct pattern emerged indicating that a comparison of these two fractions would allow for an evaluation of the synaptically enriched and somatically restricted transcriptomes in response to an exogenously administered drug in an *in vivo* model.

The actual degree of enrichment of synaptic entities in the P2 fraction as compared to the whole homogenate (WH) is challenging to ascertain, as immunoblotting and qRT-PCR provided seemingly inconsistent results. For previously published studies that have used *Camk2a* as a marker for known synaptically trafficked transcripts, there is variability in whether this gene is enriched for in the synaptoneurosomal fraction as compared to the whole homogenate. Similar to our experiment, studies performed by Rao & Steward (1993) and Lugli *et al*. (2008) also

Table 3.6: Top 50 Enriched Genes for the P2 Fraction (RMA Expression Values)			
Top P2 Enriched Genes	**Avg P2 RMA**	**Avg S2 RMA**	**Fold Change**
Bcas1	9.908708563	7.7165745	4.569809617
Dio2	10.5112725	8.361132313	4.438709179
Kcnj16	9.716286438	7.680916938	4.099277056
Prex2	10.33622063	8.32982725	4.017765535
Hmgn5	7.142313563	5.139210063	4.008613991
Cyp2j9	10.44009188	8.577100813	3.637610472
Scd1	12.16146625	10.41146125	3.363597318
Kcnj10	11.58428875	9.85044025	3.326139091
Zbtb20	10.57668313	8.874199875	3.254606784
Unc13c	7.356212875	5.660362938	3.239676901
Myo6	10.15760481	8.4844335	3.189148578
Ly86	10.89960688	9.236156875	3.167731376
Hipk2	11.44230875	9.783465313	3.157632859
Ppp1r3c	10.07393275	8.424389313	3.137343375
Ctss	9.864882438	8.230374375	3.104816623
Shank1	11.01535625	9.382792125	3.100635903
Emp2	9.83387475	8.205306188	3.092060532
Slc15a2	10.09343056	8.517825625	2.980604464
Itgam	8.481647313	6.916405875	2.959270216
Epas1	10.50273375	8.943732875	2.946497159
Ptprz1	11.00774438	9.4564605	2.930778373
Scrg1	11.182115	9.641889375	2.908399848
Chpt1	9.948905938	8.418657938	2.888354858
Cdh19	8.049834625	6.54363375	2.840610205
Axl	9.9752645	8.469702313	2.839352932
Suclg2	9.083774563	7.594536875	2.807405941
Itih3	9.353696688	7.901444375	2.736349125
Aqp4	10.23541625	8.784841813	2.733168562
Pon2	8.864683563	7.420225125	2.721606398
Plxnb1	10.09605563	8.651819188	2.721187633
S100b	10.42180813	8.982548125	2.711817329
Gpc5	9.298272313	7.877714625	2.676889687
Kif5b	11.18507688	9.774207125	2.658974147
Ctso	10.32099125	8.926841188	2.628336628
Zcchc24	9.849041875	8.460466063	2.618200918
Agxt2l1	7.825990813	6.440697313	2.612250953
Fgfr3	10.40677125	9.022526813	2.610352133
Luzp2	11.67426813	10.29200313	2.606773077
Paqr8	11.0982675	9.716133375	2.606536613
Mertk	9.9821955	8.60537525	2.596953623
Lrp4	9.313314938	7.946084188	2.579749083
Sparc	12.1898275	10.82394063	2.577347157
Abhd3	10.91844688	9.557144563	2.569169924
Homer2	9.449535313	8.098367125	2.55118618
Fyb	6.809160938	5.464860063	2.539071242
Csf1r	10.2545725	8.91110925	2.537597491
Slc6a11	11.73678375	10.39680313	2.531479191
Sdc4	9.722872688	8.385073313	2.52765467
Kif1c	8.281282125	6.947754375	2.520181695
Aldh1a1	10.11923519	8.789005688	2.514426705

Table 3.7: Top 50 Enriched Genes for the S2 Fraction (RMA Expression Values)			
Top S2 Enriched Genes	**Avg P2 RMA**	**Avg S2 RMA**	**Fold Change**
Coro1a	8.464261	9.948133688	2.796985331
Psmg1	7.76762825	9.030230375	2.399280986
AI837181	9.031812875	10.2879025	2.38847475
Rem2	7.732485563	8.936279188	2.303445757
Pvalb	8.938885625	10.14045125	2.299891218
Ddx47	7.969834375	9.165814063	2.291003539
Tbc1d7	8.323964688	9.511408813	2.277489062
9430023L20Rik	7.545575313	8.728558625	2.270457942
Med27	9.136469375	10.31270438	2.259862507
Nprl2	8.692472188	9.834082938	2.206272131
Calb2	8.2623935	9.395536438	2.193360477
Naa38	8.385241563	9.514363375	2.187255586
Mrps27	7.738378188	8.86037225	2.176475926
Ruvbl1	7.731977938	8.8493775	2.169555605
Eif2b2	8.139883313	9.240228938	2.144060514
Rab33a	10.05362694	11.14929188	2.137115585
Nipsnap1	9.772151938	10.86016813	2.125815201
Snapc2	8.303404125	9.382869875	2.113253369
Hax1	8.526462125	9.604567375	2.111261454
2010107G23Rik	8.44934375	9.521665625	2.102814918
Dlx5	8.27979675	9.340618063	2.086118791
Neurod6	8.214160375	9.27474075	2.085770428
Rab3b	9.624252438	10.68428438	2.084977677
Cdkn1a	8.79371075	9.851396	2.08158901
Tbc1d25	7.838825688	8.892829813	2.076284478
Gstp1	11.130595	12.18360875	2.074859648
Glrx	9.0672105	10.11976881	2.074204749
Dusp1	9.39751975	10.4490275	2.072694874
Map1lc3a	10.09959206	11.15039125	2.071677145
BC037034	8.72322325	9.7722245	2.069096956
Rnf25	8.828368125	9.877004063	2.068573095
Tsen15	6.961364938	8.00779225	2.065408735
Pcgf1	8.295221938	9.338987313	2.061601333
Psmd13	9.011346188	10.05015775	2.054534508
Prmt7	8.424473188	9.456473813	2.044857947
Fn3k	8.36427025	9.394037688	2.041695104
Kbtbd4	8.493259	9.5192875	2.036410628
Zcchc12	8.379733313	9.40189475	2.030959453
Pdlim1	8.089376188	9.11063125	2.029683901
Gmpr	9.24582375	10.26523188	2.027087163
Naa20	9.10151325	10.12080731	2.026926904
Tmem199	8.05594125	9.0704205	2.020173567
Drg1	10.04116575	11.054215	2.018172162
Camk1g	9.159440875	10.16337831	2.005465903
Hist3h2a	9.498158563	10.5014975	2.004634111
Pip5k1a	9.095617125	10.09789563	2.003161167
Farsa	7.861806313	8.853419875	1.988407655
Ppif	9.680672938	10.65339563	1.962540855
Prmt1	8.2578405	9.22960675	1.961240216
Rwdd2a	8.202146188	9.172403	1.959189317

isolated synaptoneurosomal fractions from forebrain tissue, but only the later detected enrichment (> 2.0 fold) for *Camk2a* as compared to total homogenate (Rao & Steward, 1993; Lugli *et al.*, 2008). An issue with comparing results across publications is the number of procedural variations in synaptoneurosomal preparation. The protocol published by Lugli *et al.* (2008) performed the filtration prior to both centrifugation steps while Rao & Steward (1993) utilized a discontinuous Ficoll gradient to further promote fractionation. Both protocols used initial and final centrifugation speeds much higher than those used in the present study (2000 x g – 45,000 x g). Nevertheless, we did observe 4.3 fold enrichment of the postsynaptic protein marker, PSD95, as compared to the WH (Figure 3.5), and immunoblotting and qRT-PCR analyses both indicated enrichment of synaptic entities in the P2 fraction as compared to the S2 (Figures 3.5, 3.6). As a result, our subsequent analyses were the first to focus on expression differences between these two fractions instead of between the WH and P2.

The objective of the synaptoneurosome preparation is enrichment, since obtaining a pure neuron-specific synaptic fraction from tissue as complex as brain through a centrifugation and filtration scheme is improbable. As such, the P2 fractions were not completely devoid of somatically-restricted transcripts (Figure 3.6). Additionally, the qRT-PCR results revealed a significant increase in the level of *Gfap* present in the P2 as compared to the S2. High levels of *Gfap*, an intermediate filament used as a protein marker for reactive astrocytes, has previously been found to contaminate synaptoneurosome preparations (Rao & Steward, 1993). GFAP message has been identified in the processes of some astrocytes (Sarthy *et al.*, 1989; Trimmer *et al.*, 1991). Furthermore, evidence for regulated trafficking of astrocytic mRNA to

perisynaptic processes came from studies conducted with synaptoneurosomes (Gerstner *et al.*, 2012). As components of the tripartite synaptic structure, the role astrocytes play in regulation of neurotransmission makes them a major participant in brain plasticity (Halassa & Haydon, 2010). Therefore, the potential presence of glial processes makes the synaptoneurosomal preparation more representative of a comprehensive synaptic transcriptome. However, without distinguishing the populations of mRNA by cell type, we must evaluate our results with the knowledge that observed changes in expression may be non-neuronal in nature.

The conclusion that the P2 and S2 fractions yielded exceedingly disparate populations of RNA came from several lines of evidence during the characterization. The fact that automated electrophoresis revealed distinctive total RNA distributions (Figure 3.7, **a**) was the first indication of differences in RNA composition. The observation that synaptoneurosomal fractions are enriched with small molecular weight RNAs was previously made by Oswald Steward's group (Rao & Steward, 1993). Steward also found through subfractionation by oligo-dT chromatography that these small molecular weight RNAs were primarily found in the poly(A)-minus fraction. Our microarray results did confirm significant differences in the microRNA populations present in the P2 and S2 fractions, and even an enrichment within the P2. However, it is possible that the low molecular weight banding distribution represents a variety of small non-coding RNAs, such as tRNAs, snoRNAs, and piRNAs that could have undiscovered synaptic functions. A more complete assessment of this RNA will be necessary to make a definitive claim as to its composition.

If the complement of low molecular weight transcripts found in the P2 fraction did consist of large quantities of non-coding RNAs, this could partially explain the differences perceived in overall fluorescent intensity detected from the arrays hybridized with P2 and S2 samples. During microarray sample preparation, the *in vitro* transcription reaction utilizes primers that target both poly(A) and non-poly(A) containing RNAs. However, without complementary probes to hybridize to on the array, these non-poly(A) transcripts would lower the pool of targets available for detection. The proprietary primers used in the synthesis of cRNA are also designed to exclude rRNA. Our qRT-PCR results did show decreased levels of one particular rRNA, Rn18S, in the P2 fraction as compared to the S2 (Figure 3.6, **f**). If this pattern held for other rRNAs, P2 samples would theoretically have a larger proportion of RNAs available for reverse transcription and consequently for *in vitro* transcription, resulting in the larger yields of cRNA that were obtained.

Through our characterization of the synaptoneurosome preparation we determined that the P2 and S2 fractions exhibited the complementary expression profiles that we sought to investigate in response to repeated ethanol exposure. Functional enrichment analysis determined that genes enriched for in the P2, and therefore presumably trafficked to the synapse, are involved in the functioning of this subcellular compartment. However, the results of these studies indicate that further optimization may be required. For instance, modifications in particular centrifugation and filtration steps may increase the enrichment of known synaptically targeted transcripts in the P2 as compared to the WH. Furthermore, Johnson *et al*., 1997 published a protocol to isolate synaptoneurosomes from single rat hippocampal slices (Johnson *et al.*, 1997).

In that study, no effort at isolating RNA from the small scale fractions was attempted, but ideally this protocol could be adapted to produce enough RNA from smaller starting quantities of tissue. This could permit the examination of the synaptic transcriptome of individual brain regions. Nevertheless, we were satisfied with the prospect of using this preparation to study changes to the synaptic transcriptome in response to repeated ethanol exposure.

Chapter 4 – Regulation of the Synaptic Transcriptome by Repeated Ethanol Administration

Introduction

Alcoholism is a chronic disease characterized by compulsive drug-seeking undeterred by negative consequences, as well as cravings and potential for relapse that persist despite years of abstinence. The endurance of these long-lived pernicious behaviors support the theory that addiction arises from progressive and lasting cellular and molecular adaptations in response to repeated drug exposure (Nestler *et al.*, 1993; Nestler, 2001b). A more complete comprehension of neuronal plasticity that underlies the transition to compulsive drug use could lead to novel therapeutic strategies for alcohol use disorders.

Previous research from our laboratory looking at ethanol regulation of gene expression across a variety of mouse strains has found significant enrichment of genes involved with synaptic functioning and plasticity, reproducibly amongst several brain regions (Kerns *et al.*, 2005; Wolen *et al.*, 2012). Preliminary data obtained during my rotation project also suggested that chronic ethanol consumption could alter synaptic RNA populations. Yet, the functionally significant changes ethanol exposure has on RNA localized at the synapse remains largely unexplored. By mechanically separating the processes in primary rat neuronal cultures, it has been shown that axons, dendrites, and their synaptic terminals contain only about 3.9% of the total cellular RNA (Poon *et*

al., 2006). Therefore, it would be advantageous to discriminately examine the synaptic transcriptome to ascertain the cellular location of ethanol's effect on gene expression and potentially identify regulation that could go undetected when studying the entire transcriptome.

It has been proposed that behavioral sensitization is a process that occurs following repeated drug exposure as the result of neuroadaptations in brain reward systems that contribute to such phenomenon as drug craving and relapse in alcoholics (Piazza *et al.*, 1990; Robinson & Berridge, 1993). Intermittent administration of many drugs of abuse, including ethanol, propagates the development of long-lasting sensitized responses to their stimulant effects, often measured as augmented locomotor activation in rodent models (Shuster *et al.*, 1975; Hirabayashi & Alam, 1981; Masur *et al.*, 1986). Behavioral sensitization has been associated with neurochemical and molecular adaptations that effect neurotransmission (Kalivas & Stewart, 1991; White & Kalivas, 1998; Vanderschuren & Kalivas, 2000). There is also evidence that neuroadaptations to brain regions that mediate reinforcement and reward occurring in response to sensitizing treatments result in incentive salience of the drug. This is demonstrated by studies with amphetamine and cocaine where animals have increased propensity for self-administration after sensitization (Horger *et al.*, 1990; Piazza *et al.*, 1990). Increased voluntary consumption of ethanol has also been observed following intermittent repeated exposure (Lessov *et al.*, 2001; Camarini & Hodge, 2004).

We therefore sought to determine whether ethanol-induced sensitization may result, at least in part, from alterations in the synaptic transcriptome, contributing to synaptic remodeling and plasticity. To characterize the effect of ethanol on the synaptic

transcriptome as opposed to global changes in cells' expression, we utilized synaptoneurosomes, prepared from frontal pole tissue of sensitized DBA2/J mice, to enrich for synaptic mRNAs for the purpose of transcriptomic analysis. Our expression profile reveals that repeated ethanol exposure elicits distinctive changes to the complement of mRNA present at the synapse, substantiating the synaptoneurosome preparation as a practical technique in which to study ethanol-induced changes to gene expression on a subcellular basis.

Materials and Methods

Animals. Male DBA/2J (D2) mice were purchased from Jackson Laboratories (Bar Harbor, ME) at 8-9 weeks of age. Animals were housed 4 per cage and had *ad libitum* access to standard rodent chow (7912, Harlan, Madison, WI) and tap water in a 12-hour light/dark cycle (6 am on, 6 pm off). Mice were housed with Teklad corn cob bedding (7092, Harlan, Madison, WI) and cages were changed weekly. Subjects were allowed to habituate to the animal facility for one week prior to commencement of behavioral experiments. All behaviors were assayed during the light cycle between the hours of 8 am and 2 pm. All animal procedures were approved by the Institutional Animal Care and Use Committee of Virginia (AM10332) and carried out in accordance with the National Institute of Health guide for the Care and Use of Laboratory Animals.

Ethanol-Induced Behavioral Sensitization. Ethanol (EtOH) behavioral sensitization was induced according to a previously established laboratory protocol (Costin *et al.*, 2013a; Costin *et al.*, 2013b). Mice were divided into one of four treatment groups (n = 16): saline-saline (SS), saline-EtOH (SE), EtOH-saline (ES), and EtOH-

EtOH (EE) (Table 4.1). Mice were acclimated to the behavioral room for 1 hour prior to the start of the experiment on testing days. All locomotor activity was measured immediately following i.p. injection with either saline or ethanol during 10 minute sessions in sound-attenuating locomotor chambers (Med Associates, model ENV-515, St. Albans, VT). The system is interfaced with Med Associates software that assesses activity using a set of 16 infrared beam sensors along the X-Y plane. Animals received two days of habituating saline injections and placement in the testing apparatus. On test day 3, acute locomotor responses to saline (SS, SE) or 2.0 g/kg ethanol (ES, EE) were measured. On conditioning days 4-13, animals received daily injections in their home cages of either saline (SS, SE) or 2.5 g/kg ethanol (ES, EE). On final testing day 14, the SS and ES groups received saline and the SE and EE groups received 2.0 g/kg ethanol and all animals were placed in the activity chambers for 10 minutes. Statistical analysis for distance traveled was performed using a two-way repeated measures ANOVA followed by Tukey's *post-hoc* analysis.

Tissue Collection. On day 14 of the behavioral sensitization paradigm, mice were sacrificed by cervical dislocation 4 hours following i.p. injection. It has previously been shown that the 4-hour time-point captures a spectrum of early, intermediate, and late gene expression responses to alcohol (Kerns *et al.*, 2005). Immediately, brains were extracted and chilled for one minute in ice-cold 1x phosphate buffered saline. The frontal pole was dissected by making a cut rostral of the optic chiasm and excluding the olfactory bulbs. Excised tissue was stored in a tube on ice for as short of a period as possible before being processed in the synaptoneurosome preparation (refer to Chapter 3 Materials and Methods).

Table 4.1: Ethanol-induced behavioral sensitization experimental design

	Experimental Day			
Treattment Group	1 - 2 *	3 *	4 - 13	14 *
Saline-Saline (SS)	Saline	Saline	Saline	Saline
Saline-Ethanol (SE)	Saline	Saline	Saline	Ethanol (2.0 g/kg)
Ethanol-Saline (ES)	Saline	Ethanol (2.0 g/kg)	Ethanol (2.5 g/kg)	Saline
Ethanol-Ethanol (EE)	Saline	Ethanol (2.0 g/kg)	Ethanol (2.5 g/kg)	Ethanol (2.0 g/kg)
	* placement in locomotor boxes			

Quantitative Reverse Transcriptase Polymerase Chain Reaction (qRT-PCR). Synaptoneurosomal fractions, S2 and P2, prepared from mice subjected to the sensitization protocol were assessed for enrichment of known dendritically-trafficked and somatically-restricted transcripts using qRT-PCR. Total RNA was isolated using the guanidine/phenol/chloroform method (Stat-60, Tel-Test Inc., Friendswood, TX) and a Tekmar homogenizer as per the STAT-60 protocol. RNA concentration was determined by measuring absorbance at 260 nm and RNA quality was assessed by electrophoresis on an Experion Analyzer (Bio-Rad, Hercules, CA) and 260/280 absorbance ratios. All RNA samples had RNA quality indices (RQI) ≥ 7.6, and 260/280 ratios were between 1.97 and 2.06. cDNA was generated from 995 ng of total DNase-treated RNA and 5 ng of luciferase mRNA (Promega, Madison, WI) using Deoxyribonuclease I (Invitrogen, Carlsbad, CA) and the iScript cDNA kit (Bio-Rad, Hercules, CA) according to manufacturer's instructions. qRT-PCR was performed using the iCycler iQ system (Bio-Rad, Hercules, CA) according to manufacturer's instructions for iQ SYBER Green Supermix (Bio-Rad, Hercules, CA). Primer sequences, annealing temperatures, amplicon sizes, and cDNA dilutions used for each gene are listed in Table 3.1. Relative expression was calculated by comparing Ct values to a standard curve produced from S2 fraction cDNA (diluted 1:5, 1:25, 1:125, 1:625). Statistical analysis of qRT-PCR data was performed using a Student's t-test between the two fractions.

Microarray Data Analysis. For microarray sample preparation, hybridization and scanning refer to Chapter 3, Materials and Methods. Expression data from the S2 and P2 fractions were background corrected, quantile normalized, log2 transformed and fit

to a linear model using the robust multi-array average (RMA) expression measure (Irizarry *et al.*, 2003). Microarray quality was assessed by inspecting the distributions of log-transformed probe intensity values and reviewing quality assessment metrics and graphs available from Expression Console™ software (Affymetrix, Santa Clara, CA). All arrays had pos_vs_neg_auc values (a metric that evaluates how well signal is separated from noise) greater than 0.92. Differential expression of genes due to ethanol treatment was assessed in two ways. Initial examination of microarray data was performed on RMA values calculated separately for P2 and S2 fractions. One-way ANOVA was performed for each data set using TIGR Multiexperiment Viewer (MeV). P-values were corrected for multiple testing using the Bioconductor q-value package in the statistical platform, R (Team, 2011). Due to the exploratory nature of the study, a less stringent threshold for significance was applied (FDR = 0.3). *Post-hoc* pattern recognition analysis was performed using Pavlidis Template matching (PTM) (Pavlidis & Noble, 2001), an algorithm based on Pearson Correlation between template and the data, available in MeV. For a more direct comparison of microarray data to RNA-Seq results, differential expression was additionally assessed using linear models for microarray data (Limma) analysis (Smyth, 2004) using the Bioconductor package in R. This analysis was performed using RMA values calculated from P2 and S2 samples together and provided results for each pairwise comparison. FDR = 0.20 was applied for multiple testing correction.

RNA-Seq Data Analysis. For RNA-Seq library preparation, sequencing protocol, read alignment, transcript assembly, and quantification refer to Chapter 3 Materials and Methods. Only SS, SE, and EE samples were sequenced after initial microarray

analysis revealed little differential expression between the ES and EE ethanol treatment groups. Estimated abundances were reported as **F**ragments **P**er **K**ilobase of exon per **M**illion fragments mapped (**FPKM**). Differential expression was performed using Cuffdiff (v2.1.1, http://cufflinks.cbcb.umd.edu/) (Trapnell *et al.*, 2010) and pairwise comparisons of gene expression were calculated for each of the six groups (SS_S2, SE_S2, EE_S2, SS_P2, SE_P2, and EE_P2). For treatment comparisons within fraction, an FDR = 0.20 was applied for multiple testing correction.

Bioinformatics Analysis. Functional enrichment analysis was performed using ToppFun, a functional enrichment application available as part of the ToppGene suite of web based applications (toppgene.cchmc.org) (Chen *et al.*, 2009). Mouse gene symbols were submitted and analyzed for over-representation of genes that belong to Gene Ontology (GO) categories (molecular function, biological processes, and cellular component). To enhance informativeness of results, top ranked terms were filtered to remove broad and redundant definitions. Only categories that were comprised of greater than 3 and fewer than 400 genes were included, removing those that contained exactly the same query list as another term already listed in the displayed results. Literature association analysis of statistically significant genes was investigated using Ingenuity Pathway Analysis (IPA) (http://www.ingenuity.com/). IPA derives connections between genes based on their curated repository of biological interactions and functional annotations. Finally, the biological function of genes that adhered to specific patterns of regulation were independently assessed using GeneMANIA (genemania.org) (Mostafavi *et al.*, 2008). GeneMANIA creates interaction networks based on functional association data such as protein and genetic interactions,

pathways, co-expression, co-localization, and protein domain similarity as well as identifying candidate genes not directly detected from our analysis.

Results

Synaptoneurosome preparation allows for analysis of synaptic transcriptome in sensitized mice.

DBA/2J (D2) mice were chosen for these studies due to their characteristic sensitivity to ethanol psychomotor stimulation and development of sensitization (Phillips *et al.*, 1994). The four treatment groups (SS, SE, ES, and EE) were necessary not only to provide pertinent controls, but also to allow for a comprehensive examination of ethanol's effect on the synaptic transcriptome during the induction of behavioral sensitization. The saline-saline (SS) group provided baseline activity responses and controlled for changes that resulted solely from the stress of injections. The saline-ethanol (SE) group revealed synaptic responses to acute administration of ethanol. The ethanol-saline (ES) group exposed allostatic changes in gene expression at the synapse produced by repeated ethanol injections. Finally, the ethanol-ethanol (EE) group tested for alterations due to the induction of sensitization, following an acute ethanol administration. Distance traveled on test days 3 and 14 was compared, and a significant increase in activity on day 14 was interpreted as an induction of ethanol sensitization (Figure 4.1). Daily i.p. injections of 2.5 g/kg ethanol elicited an augmented locomotor response to 2.0 g/kg ethanol on day 14 as compared to day 3 in the EE treatment group. Frontal pole brain tissue obtained from mice, 4 hours following the final

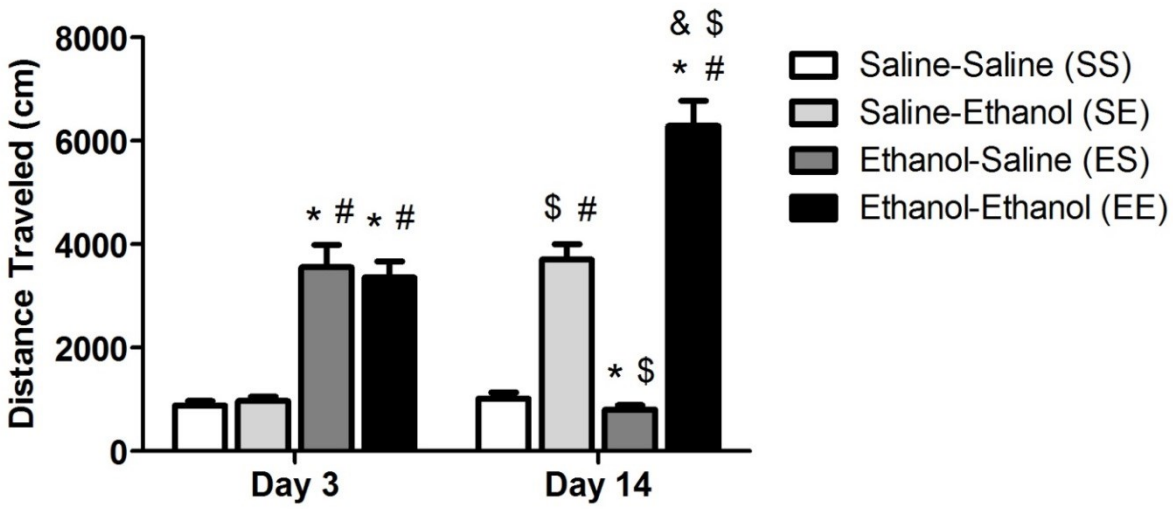

Figure 4.1 – Repeated ethanol exposure induced behavioral sensitization in D2 mice. On test day 3, acute ethanol elicited a significant locomotor activation compared to saline ($^{\#}p < 0.001$ compared to SS within same day; *p< 0.001 compared to SE within same day). One test day 14, daily injections of ethanol resulted in an augmented locomotor response compared to acute ethanol on day 3 ($^{\$}p < 0.001$ compared to same treatment on day 3) and acute ethanol on day 14 ($^{\&}p < 0.001$ compared to ES within same day). Repeated measures two-way ANOVA, main effect of treatment (F[3,60] = 63.143), main effect of day (F[1,60] = 14.567), significant interaction treatment x day (F[3,60] = 44.763), n = 16.

i.p. injection on day 14, was utilized in preparation of synaptoneurosome enriched samples (refer to Chapter 3 Materials and Methods).

To ensure enrichment in experimental tissues, qRT-PCR of total RNA isolated from mice subjected to the ethanol behavioral sensitization paradigm evaluated the profile of mRNA present in S2 and P2 fractions (Figure 4.2). P2 fractions had higher relative expression levels of known synaptically targeted transcripts, *CamK2a* and *Arc (Burgin et al., 1990; Link et al., 1995; Lyford et al., 1995)*, while transcripts known to be somatically restricted, *Gapdh* and *Snrpn (Litman et al., 1994; Poon et al., 2006)*, were more abundant in the S2 fraction. These results established that P2 fractions acquired from tissue harvested from sensitized D2 mice, which were used for subsequent analyses, did possess an enrichment of synaptically targeted RNA as compared to the S2 fractions.

Sensitizing ethanol treatment alters the synaptic transcriptome.

Microarray analysis. Initial examination of the synaptoneurosomal fractions obtained from sensitized D2 mice was performed by microarray analysis. This investigation was completed prior to demonstrating the validity of RMA data normalization (Chapter 3), which had required RNA-Seq be performed on these same samples. Therefore, to bypass any potential error that could have been introduced by applying an inappropriate normalization scheme across disparate fractions, expression measures were calculated separately for P2 and S2 samples. One-way ANOVA (FDR = 0.3) across ethanol treatments identified 214 probe sets, corresponding to 185 unique genes, which were significantly different within the P2 fraction (Supplemental Table

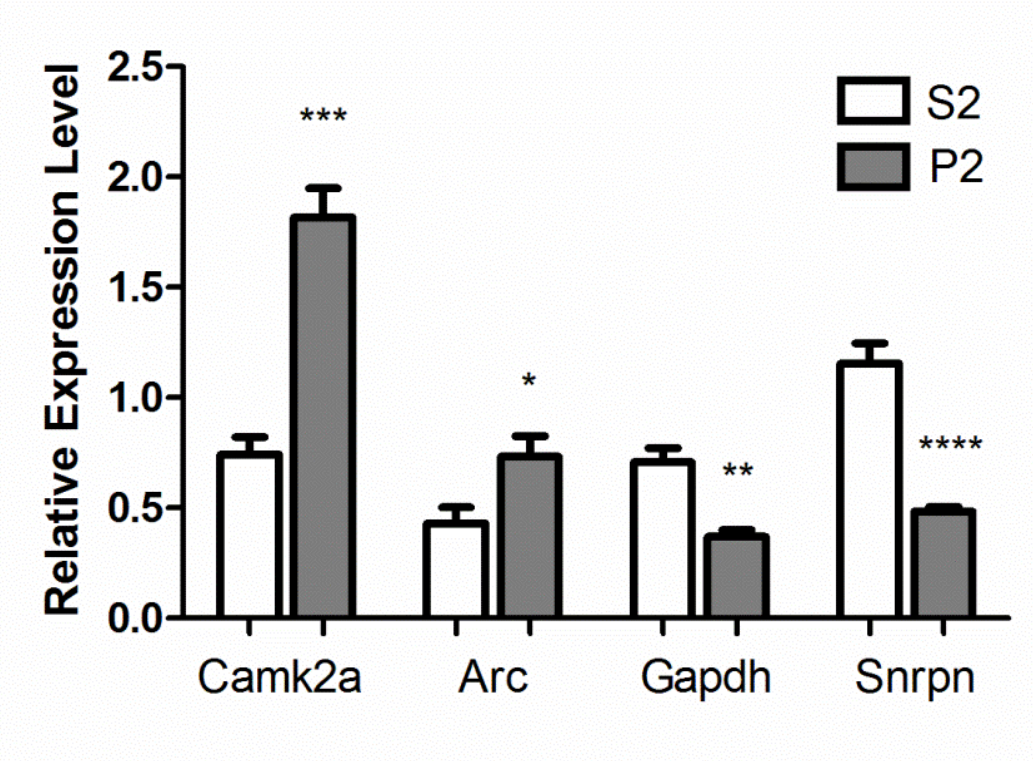

Figure 4.2 – qRT-PCR of S2 and P2 fractions from mice subjected to behavioral sensitization paradigm. RNA isolated from S2 and P2 fractions of behaviorally sensitized mice was assayed for transcripts of known subcellular localization to ensure enrichment of synaptic RNAs. Paired students t-test between fraction for each gene, *Camk2a* ($t[7] = 6.941$, ***p = 0.0002), *Arc* ($t[7] = 2.646$, *p = 0.0331), *Gapdh* ($t[7] = 4.181$, **p = 0.0041), *Snrpn* ($t[7] = 8.439$, ****p < 0.0001), n = 8.

S4.1). A similar analysis of the S2 fraction found 264 probe sets, corresponding to 243 unique genes that were regulated by ethanol (Supplemental Table S4.2). There were 44 genes that were found to be in common between the S2 and P2 significant gene lists, which left 141 genes that were being altered by ethanol in the P2 fraction only. This demonstrated that we were able to detect ethanol-responsive changes that were potentially unique to the synaptic transcriptome.

Functional enrichment analysis of genes found to be regulated by ethanol in the P2 fraction revealed significant over-representation of gene ontology categories involved with protein folding and association with the endoplasmic reticulum (ER) (Table 4.2, Supplemental Table S4.3). S2 functional enrichment analysis indicated that ethanol largely affected cell signaling processes in the fraction shown largely to contain somatically restricted transcripts (Table 4.3, Supplemental Table S4.4). However, there was also an over-representation of genes associated with the ER in the S2 significant gene list. Literature association analysis employing IPA identified 38 and 42 canonical pathways that were statistically enriched for in the P2 and S2 ethanol regulated gene sets, respectively (Tables 4.4, 4.5). Ethanol altered expression of both ER and glucocorticoid receptor signaling pathways in both fractions. However, the level of glucocorticoid receptor signaling enrichment was greater in the P2 fraction as compared to the S2. Additionally, there were only 10 canonical pathways in common between P2 and S2. This suggested that although there is overlap in the molecular processes being affected by ethanol in the synaptic and somatic RNA populations, there also appears to be differential regulation as well.

Table 4.2: Functional Enrichment Analysis,P2 Signficant Gene List (Initial Microarray Analysis, One-Factor ANOVA, q < 0.3)

GO Category	Name	P-value	Terms in Query	Terms in Genome
Molecular Function	isomerase activity	5.83E-04	7	156
Molecular Function	chaperone binding	1.29E-03	4	52
Molecular Function	NF-kappaB binding	2.07E-03	3	28
Molecular Function	unfolded protein binding	2.55E-03	5	103
Molecular Function	heat shock protein binding	4.06E-03	4	71
Biological Process	protein folding	5.80E-06	11	216
Biological Process	glycerol ether metabolic process	4.63E-05	4	22
Biological Process	positive regulation of nuclease activity	3.71E-04	5	66
Biological Process	negative regulation of lipid storage	4.05E-04	3	16
Biological Process	cerebellum development	1.06E-03	5	83
Cellular Component	endocytic vesicle lumen	3.83E-04	3	16
Cellular Component	endoplasmic reticulum lumen	1.43E-03	7	182
Cellular Component	PML body	8.28E-03	4	87
Cellular Component	nuclear body	2.66E-02	7	317
Cellular Component	endoplasmic reticulum Sec complex	2.71E-02	1	3

Table 4.3: Functional Enrichment Analysis,S2 Signficant Gene List (Initial Microarray Analysis, One-Factor ANOVA, q < 0.3)

GO Category	Name	P-value	Terms in Query	Terms in Genome
Molecular Function	protein kinase C binding	5.43E-06	7	57
Molecular Function	actin filament binding	8.27E-04	6	91
Molecular Function	transmembrane receptor protein tyrosine kinase activity	1.21E-03	5	66
Molecular Function	neutral amino acid transmembrane transporter activity	2.58E-03	3	23
Molecular Function	protein kinase regulator activity	3.26E-03	6	119
Biological Process	negative regulation of receptor biosynthetic process	3.60E-05	3	6
Biological Process	skeletal muscle organ development	4.93E-04	9	185
Biological Process	lipid storage	6.23E-04	5	56
Biological Process	cellular response to calcium ion	7.80E-04	4	34
Biological Process	positive regulation of multicellular organismal metabolic process	8.72E-04	4	35
Cellular Component	smooth endoplasmic reticulum	5.07E-04	4	31
Cellular Component	lipid particle	3.17E-02	3	57
Cellular Component	dense core granule membrane	3.59E-02	1	3
Cellular Component	integral component of endoplasmic reticulum membrane	4.10E-02	4	107
Cellular Component	CCAAT-binding factor complex	4.75E-02	1	4

Table 4.4: Ingenuity Pathway Analysis, P2 Signficant Gene List (Initial Microarray Analysis, One-Factor ANOVA, q < 0.3)

Ingenuity Canonical Pathways	-log(p-value)	Ratio (Query/Pathway Genes)	Molecules
Aldosterone Signaling in Epithelial Cells	4.3	0.0526	HSPA1A/HSPA1B,PIK3C2A,SGK1,HSP90B1,HSPA5,PDIA3,HSPH1,HSPE1
Glucocorticoid Receptor Signaling	4.06	0.0383	HSPA1A/HSPA1B,FKBP5,PIK3C2A,TSC22D3,POLR2A,SGK1,HSP90B1,HSPA5,CDKN1A,NFKBIA
Endoplasmic Reticulum Stress Pathway	3.14	0.143	CALR,HSP90B1,HSPA5
Production of Nitric Oxide and Reactive Oxygen Species in Macrophages	3.03	0.0389	PIK3C2A,PPP1R3C,PPARA,NFKBIA,RHOJ,PPP2R2A,RHOU
NAD Salvage Pathway II	2.86	0.115	NMNAT1,NT5E,NT5C2
Glioblastoma Multiforme Signaling	2.79	0.0411	PIK3C2A,WNT7A,CDKN1A,PDIA3,RHOJ,RHOU
Guanosine Nucleotides Degradation III	2.27	0.154	NT5E,NT5C2
Prostate Cancer Signaling	2.27	0.0488	PIK3C2A,HSP90B1,CDKN1A,NFKBIA
mTOR Signaling	2.25	0.0319	PIK3C2A,PLD1,PRR5,RHOJ,PPP2R2A,RHOU
Urate Biosynthesis/Inosine 5'-phosphate Degradation	2.21	0.143	NT5E,NT5C2
Glutamine Biosynthesis I	2.07	1	GLUL
Gİ±q Signaling	2.06	0.034	PIK3C2A,PLD1,NFKBIA,RHOJ,RHOU
Adenosine Nucleotides Degradation II	2.04	0.118	NT5E,NT5C2
p53 Signaling	2	0.0408	PIK3C2A,TP53BP2,CCNG1,CDKN1A
Telomerase Signaling	1.98	0.0404	PIK3C2A,HSP90B1,CDKN1A,PPP2R2A
Purine Nucleotides Degradation II (Aerobic)	1.9	0.1	NT5E,NT5C2
Glioma Invasiveness Signaling	1.89	0.0526	PIK3C2A,RHOJ,RHOU
Sphingosine-1-phosphate Signaling	1.84	0.0367	PIK3C2A,PDIA3,RHOJ,RHOU
Huntington's Disease Signaling	1.84	0.0261	HSPA1A/HSPA1B,PIK3C2A,POLR2A,SGK1,HSPA5,CAPN2
ERK5 Signaling	1.77	0.0476	SGK1,MAPK7,WNK1
UDP-D-xylose and UDP-D-glucuronate Biosynthesis	1.77	0.5	UGDH
Type II Diabetes Mellitus Signaling	1.74	0.0342	PIK3C2A,ADIPOR2,ABCC8,NFKBIA
PPARİ±/RXRİ± Activation	1.72	0.0279	HSP90B1,PPARA,ADIPOR2,PDIA3,NFKBIA
p70S6K Signaling	1.72	0.0336	PIK3C2A,PDIA3,PLD1,PPP2R2A
Lipid Antigen Presentation by CD1	1.68	0.0769	CALR,PDIA3
PI3K/AKT Signaling	1.67	0.0325	HSP90B1,CDKN1A,NFKBIA,PPP2R2A
Protein Ubiquitination Pathway	1.65	0.0235	HSPA1A/HSPA1B,HSP90B1,HSPA5,HSPH1,HSPE1,USP53
PEDF Signaling	1.64	0.0423	PIK3C2A,PNPLA2,NFKBIA
S-adenosyl-L-methionine Biosynthesis	1.59	0.333	MAT2A
eNOS Signaling	1.48	0.0284	HSPA1A/HSPA1B,PIK3C2A,HSP90B1,HSPA5
Heme Degradation	1.47	0.25	BLVRB
Branched-chain İ±-keto acid Dehydrogenase Complex	1.47	0.25	DBT
Stearate Biosynthesis I (Animals)	1.44	0.0571	DBT,GNPAT
Molecular Mechanisms of Cancer	1.42	0.0192	PIK3C2A,PTCH1,WNT7A,CDKN1A,NFKBIA,RHOJ,RHOU
Antigen Presentation Pathway	1.4	0.0541	CALR,PDIA3
Docosahexaenoic Acid (DHA) Signaling	1.36	0.0513	PIK3C2A,PNPLA2
PPAR Signaling	1.33	0.0319	HSP90B1,PPARA,NFKBIA
Protein Kinase A Signaling	1.32	0.0182	PPP1R3C,PDE11A,PTCH1,DUSP18,PTP4A1,PDIA3,NFKBIA

Table 4.5: Ingenuity Pathway Analysis, S2 Signficant Gene List (Initial Microarray Analysis, One-Factor ANOVA, q < 0.3)

Ingenuity Canonical Pathways	-log(p-value)	Ratio (Query/Pathway Genes)	Molecules
Endoplasmic Reticulum Stress Pathway	2.84	0.143	CALR,MBTPS2,HSPA5
cAMP-mediated signaling	2.56	0.0365	HTR1B,GRM2,HTR1A,MC4R,PKIG,ADRA2B,CAMK1G,PRKACA
Calcium Signaling	2.47	0.0393	CALR,TNNC1,RCAN1,CAMKK1,CAMK1G,PRKACA,HDAC9
ErbB2-ErbB3 Signaling	2.47	0.0702	JUN,NRG3,ERBB3,ELK1
Glucocorticoid Receptor Signaling	2.11	0.0307	JUN,FKBP5,TSC22D3,SGK1,HSPA5,CDKN1A,PRKACA,ELK1
Guanosine Nucleotides Degradation III	2.07	0.154	PNP,NT5E
Toll-like Receptor Signaling	2.07	0.0541	JUN,TLR3,PPARA,ELK1
Urate Biosynthesis/Inosine 5'-phosphate Degradation	2.01	0.143	PNP,NT5E
Gİ±i Signaling	2	0.0417	HTR1B,GRM2,HTR1A,ADRA2B,PRKACA
Xanthine and Xanthosine Salvage	1.96	1	PNP
Adenosine Nucleotides Degradation II	1.84	0.118	PNP,NT5E
ErbB Signaling	1.84	0.0465	JUN,NRG3,ERBB3,ELK1
ERK/MAPK Signaling	1.78	0.0321	KSR1,HSPB1,PRKACA,PLA2G3,EIF4EBP1,ELK1
Amyloid Processing	1.75	0.0588	CAPN3,BACE2,PRKACA
Purine Nucleotides Degradation II (Aerobic)	1.71	0.1	PNP,NT5E
Chondroitin Sulfate Biosynthesis	1.68	0.0556	HS3ST2,HS3ST1,XYLT1
Guanine and Guanosine Salvage I	1.67	0.5	PNP
Alanine Degradation III	1.67	0.5	GPT2
Alanine Biosynthesis II	1.67	0.5	GPT2
Adenine and Adenosine Salvage I	1.67	0.5	PNP
Dermatan Sulfate Biosynthesis	1.64	0.0536	HS3ST2,HS3ST1,XYLT1
Neuropathic Pain Signaling In Dorsal Horn Neurons	1.63	0.04	GRM2,CAMK1G,PRKACA,ELK1
Heparan Sulfate Biosynthesis	1.62	0.0526	HS3ST2,HS3ST1,XYLT1
Aldosterone Signaling in Epithelial Cells	1.6	0.0329	HSPB1,SGK1,HSPA5,HSPB8,DNAJC12
HGF Signaling	1.56	0.0381	JUN,CDKN1A,GAB1,ELK1
Gİ±s Signaling	1.51	0.0367	MC4R,PRKACA,ADD3,ELK1
ERK5 Signaling	1.51	0.0476	SGK1,WNK1,GAB1
Oxidized GTP and dGTP Detoxification	1.49	0.333	NUDT1
Corticotropin Releasing Hormone Signaling	1.47	0.0357	JUN,GLI3,PRKACA,ELK1
Cardiac Hypertrophy Signaling	1.45	0.0269	JUN,HSPB1,ADRA2B,PRKACA,RHOJ,ELK1
GDNF Family Ligand-Receptor Interactions	1.42	0.0441	JUN,GFRA2,GAB1
Agrin Interactions at Neuromuscular Junction	1.41	0.0435	JUN,NRG3,ERBB3
Sonic Hedgehog Signaling	1.38	0.0667	GLI3,PRKACA
PEDF Signaling	1.38	0.0423	PNPLA2,DOCK3,ELK1
Chemokine Signaling	1.38	0.0423	JUN,CXCR4,CAMK1G
Arsenate Detoxification I (Glutaredoxin)	1.37	0.25	PNP
LXR/RXR Activation	1.37	0.0331	LDLR,TLR3,IRF3,HMGCR
Basal Cell Carcinoma Signaling	1.36	0.0417	GLI3,WNT4,TCF7L1
Colorectal Cancer Metastasis Signaling	1.35	0.0254	JUN,TLR3,WNT4,PRKACA,TCF7L1,RHOJ
Sertoli Cell-Sertoli Cell Junction Signaling	1.34	0.0279	JUN,ACTN1,PRKACA,ELK1,PVRL3
Molecular Mechanisms of Cancer	1.34	0.0219	JUN,ARHGEF3,CDKN1A,WNT4,GAB1,PRKACA,RHOJ,ELK1
Axonal Guidance Signaling	1.33	0.0208	UNC5C,PLXND1,CXCR4,EPHB6,GLI3,WNT4,EFNA3,PRKACA,SEMA4A

Visualizing expression values by heat maps allows for biologically-relevant patterns of gene regulation to be identified. Two interesting expression patterns that were further investigated by PTM are displayed in Figure 4.3, **a, b**. Setting threshold parameters at absolute $R > 0.75$ and $p < 0.05$, 20 genes were found to be altered by repeated ethanol (ES, EE) compared to saline treatment (SS), which were not affected by treatment with acute ethanol (SE). Another 39 genes were found to be acutely regulated by ethanol (SE), but then exhibited a blunted or no response with repeated administration (ES, EE). This habituating gene expression profile has previously been observed in response to sensitizing ethanol treatments (Costin *et al.*, 2013a) and was examined further in the subsequent RNA-Seq analysis.

RNA-Seq analysis. As mentioned previously, RNA-Seq was performed to facilitate validation of data normalization and differential expression results. An independent bioinformatics examination of RNA-Seq data was also performed as a complement to microarray analysis. Cuffdiff analysis of RNA-Seq data provided differential expression results for each pairwise treatment comparison in the S2 and P2 fractions (Figure 4.4, **a, b**). Collapsing the significant genes across all comparisons, it was found that 2968 and 292 unique genes, corresponding to 2936 and 311 XLOC gene ids, changed with ethanol treatment in the S2 and P2 fractions, respectively (Figure 4.4, **c**, Supplemental Tables S4.5, S4.6). There were 176 genes that were found to be in common between the S2 and P2 significant gene lists, which left 116 genes that were being altered by ethanol in the P2 fraction only. Upon closer inspection of the 176 genes that overlapped between the S2 and P2 it was determined that 43 were regulated

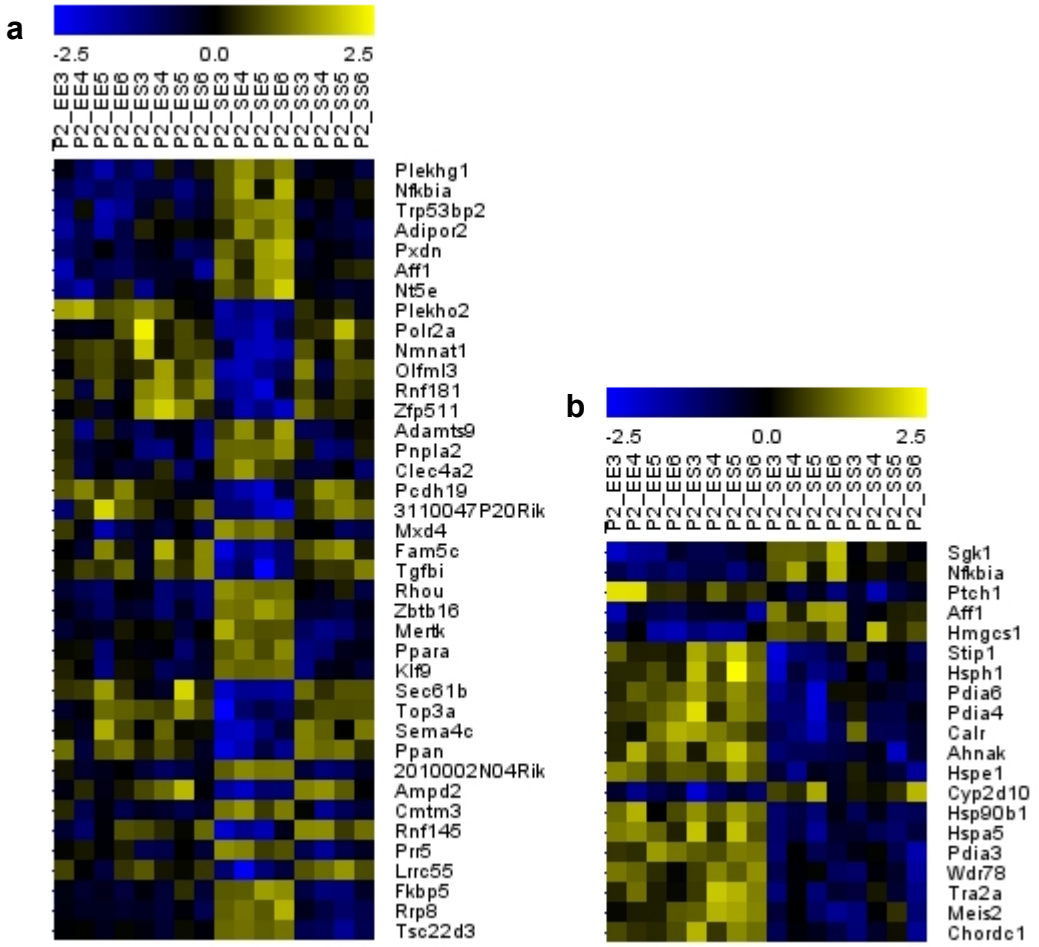

Figure 4.3 – Visual representation of gene expression patterns identified by PTM in the initial microarray analysis. These heatmaps depict the RMA values for genes found to be significantly regulated by ethanol in the P2 fraction by one-way ANOVA ($q < 0.3$). Templates were defined following a cursory examination of gene expression data using MeV. A threshold of absolute $R > 0.75$ and $p < 0.05$ identified (**a**) 39 genes that were acutely regulated by ethanol, but whose expression habituated with repeated ethanol and (**b**) 20 genes that were regulated by repeated ethanol administration.

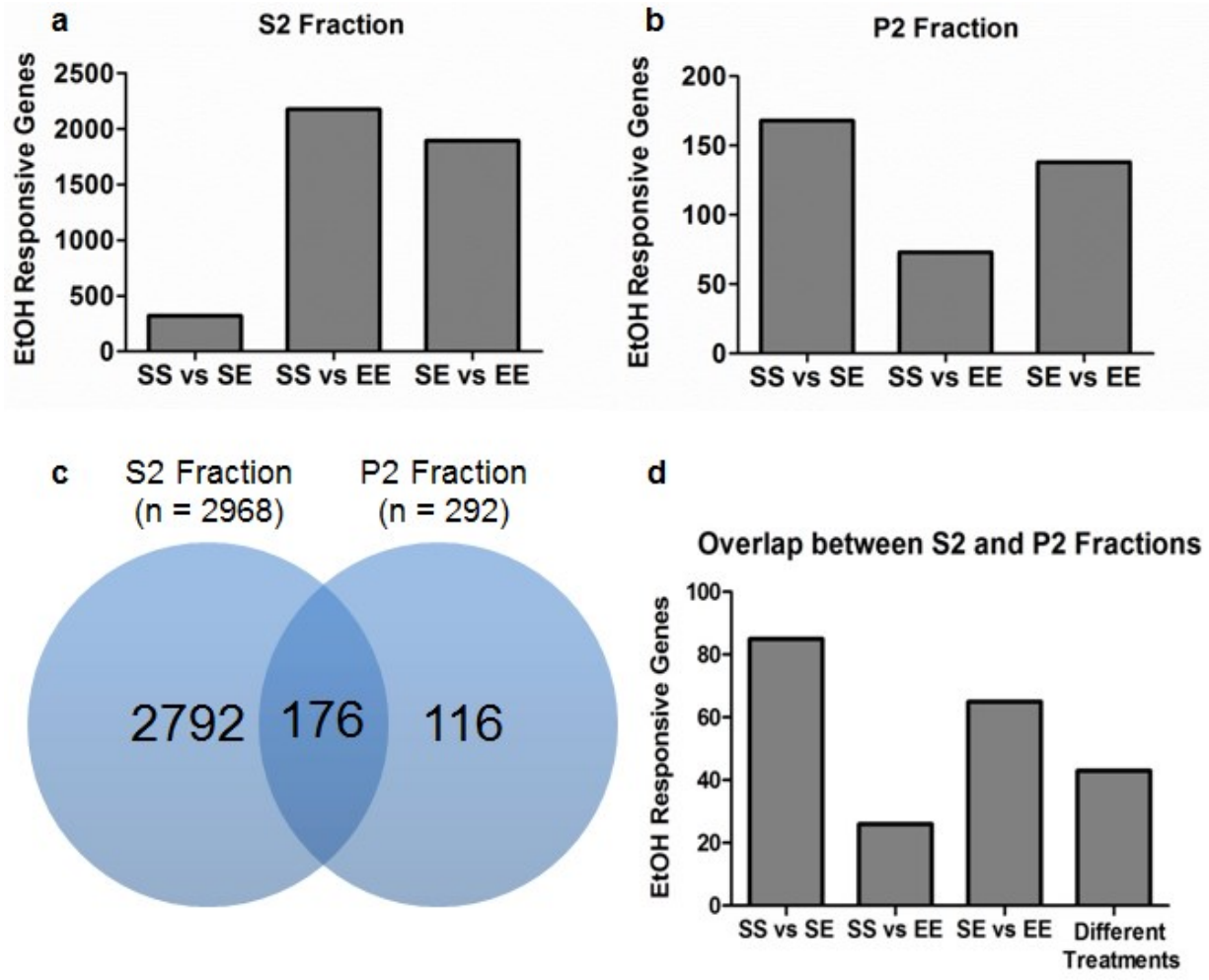

Figure 4.4 – RNA-Seq significant genes broken down by ethanol treatment and synaptoneurosome fraction. The number of genes found to be significantly altered across the behavioral sensitization treatments in the (**a**) S2 fraction and (**b**) P2 fraction. (**c**) A comparison of S2 and P2 ethanol regulated genes found 176 common genes. (**d**) A breakdown of the genes in common between the S2 and P2 fractions revealed that 43 were found to be regulated by different ethanol treatments. Of the remaining 133 genes, all but 4 exhibited the same direction of regulation by ethanol, either up- or down-regulated.

by different ethanol treatments between the fractions (Figure 4.4, **d**). These results corroborated the initial microarray analysis finding that detection of ethanol-responsive changes unique to the synaptic transcriptome was possible.

It was decided that it would be more informative to focus on changes that were localized to the synapse and compare those genes to the somatic RNA population. Therefore, a P2 fraction candidate gene list was compiled for subsequent bioinformatics analyses. For inclusion into the candidate gene list, genes were required to be differentially expressed only in the pairwise comparisons between the three P2 groups (SS_P2, SE_P2, and EE_P2) or a gene was regulated by ethanol in both the P2 and S2 fractions, but showed overall enrichment in the P2 fractions by collapsing and comparing all S2 and P2 samples.

Application of these criteria consolidated the list to 248 genes (Supplemental Table S4.7). The principal gene ontology categories derived from ToppFun functional enrichment analysis of the P2 candidate gene list revealed over-representation of ER activity and components of the extracellular matrix (Table 4.6). Alternatively, the top categories found to be over-represented in RNA-Seq S2 ethanol regulated genes reflected different biological functions, including cytoskeletal regulation and Ras protein signal transduction (Table 4.7). Genes regulated by ethanol in the S2 fraction were also related to the synapse, indicating global regulation of gene expression by ethanol has repercussions for synaptic functioning. However, the differences in functional enrichment between the P2 and S2 fractions support the conclusion that ethanol's regulation of gene expression is distinctive and contingent upon subcellular location. The complete list of functional enrichment categories for both the P2 fraction and S2

Table 4.6: Functional Enrichment Analysis, P2 Candidate Gene List (RNA-Seq Cuffdiff, q < 0.2)				
GO Category	**Name**	**P-value**	**Terms in Query**	**Terms in Genome**
Molecular Function	extracellular matrix structural constituent	2.40E-04	6	70
Molecular Function	protein-hormone receptor activity	6.33E-04	3	14
Molecular Function	growth factor binding	9.04E-04	7	123
Molecular Function	stem cell factor receptor binding	9.18E-04	2	4
Molecular Function	transmembrane receptor protein tyrosine kinase activity	1.40E-03	5	66
Biological Process	lung morphogenesis	5.49E-07	8	57
Biological Process	inner ear development	5.18E-06	12	189
Biological Process	branching morphogenesis of an epithelial tube	1.94E-05	11	181
Biological Process	positive regulation of melanocyte differentiation	1.94E-05	3	5
Biological Process	regulation of cellular response to growth factor stimulus	2.15E-05	11	183
Cellular Component	endoplasmic reticulum lumen	5.71E-07	13	187
Cellular Component	smooth endoplasmic reticulum	4.64E-06	6	36
Cellular Component	proteinaceous extracellular matrix	3.94E-04	13	348
Cellular Component	cytosolic ribosome	1.20E-03	6	96
Cellular Component	podosome	1.79E-03	3	20

Table 4.7: Functional Enrichment Analysis, S2 Significant Gene List (RNA-Seq Cuffdiff, q < 0.2)

GO Category	Name	P-value	Terms in Query	Terms in Genome
Molecular Function	actin binding	2.59E-09	104	388
Molecular Function	nucleoside-triphosphatase regulator activity	3.92E-08	86	318
Molecular Function	Ras GTPase binding	4.72E-06	49	170
Molecular Function	binding, bridging	1.17E-05	43	147
Molecular Function	guanyl-nucleotide exchange factor activity	1.96E-05	51	188
Biological Process	gliogenesis	8.86E-13	72	201
Biological Process	regulation of cell projection organization	2.12E-12	109	366
Biological Process	regulation of synaptic transmission	6.63E-12	82	251
Biological Process	regulation of Ras protein signal transduction	3.47E-10	105	376
Biological Process	axon guidance	3.44E-09	102	376
Cellular Component	axon	4.32E-14	116	389
Cellular Component	cell leading edge	1.63E-10	92	320
Cellular Component	synaptic membrane	2.98E-09	74	251
Cellular Component	neuron spine	1.54E-08	45	129
Cellular Component	postsynaptic density	8.21E-08	49	153

candidate genes can be found in the supporting information (Supplemental Tables S4.8, S4.9).

A posteriori, FPKM values for P2 candidate genes were evaluated across all treatment comparisons for the distinct patterns of regulation observed in the initial microarray analysis. Thirty-nine genes were classified as being altered by repeated ethanol as they were found to be significant in the SS vs EE comparison, but not in the SS vs SE. The habituating expression profile was defined as genes determined to be differentially regulated between SS and SE samples, but not SS and EE. This described 114 P2 candidate genes. Resulting gene lists were submitted to GeneMANIA to assess functional association across multiple independent datasets related to gene co-expression, co-localization, protein and genetic interactions, and predicted interactions (Figure 4.5, **a, b**). GeneMANIA also populates the composite network with predicted candidate genes related to the input genes, but not directly identified through our RNA-Seq analysis. The GeneMANIA algorithm predicted inclusion of *Sgk1* and *Mt1* into the habituating gene expression network. These two genes have previously been shown to be regulated by ethanol in the PFC of D2 mice, and are known to be glucocorticoid responsive (Kerns *et al.*, 2005). The repeated ethanol gene network was populated with 14 ribosomal proteins, 5 of which have been previously reported to be associated with the molecular and behavioral responses to ethanol (*Fau, Rpl26, Rpl27a, Rpl13,* and *Rpl10*) (Lewohl *et al.*, 2000; Saito *et al.*, 2004; Rodd *et al.*, 2008). The inclusion of these genes into the networks was primarily informed by co-expression relationships within the GeneMANIA databases.

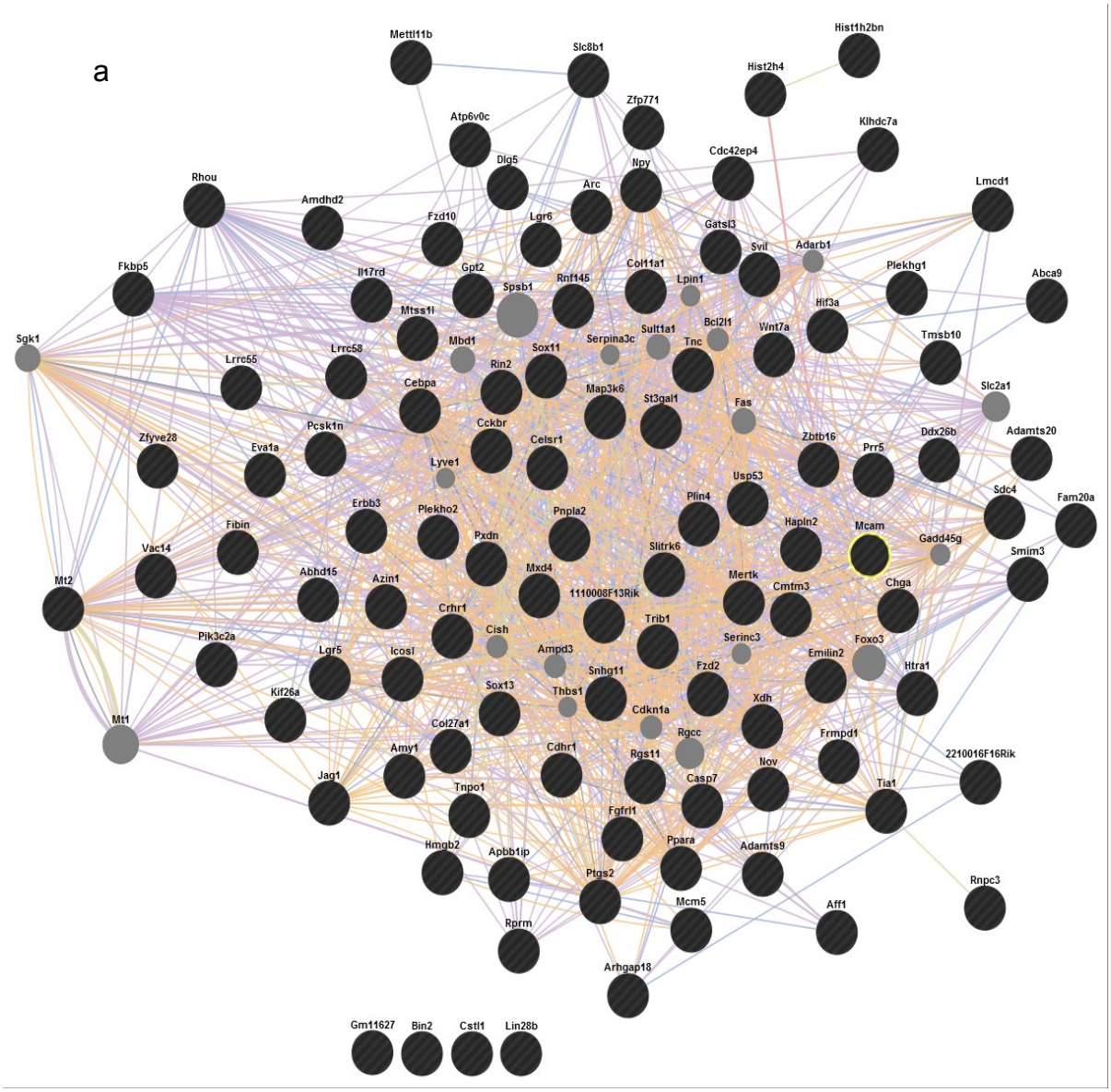
a
Mettl11b
Slc8b1
Hist1h2bn
Hist2h4
Zfp771
Atp6v0c
Klhdc7a
Dlg5
Npy
Cdc42ep4
Rhou
Arc
Lmcd1
Amdhd2
Fzd10
Lgr6
Gatsl3
Svil
Adarb1
Fkbp5
Il17rd
Gpt2
Spsb1
Rnf145
Col11a1
Lpin1
Plekhg1
Abca9
Mtss1l
Hif3a
Sgk1
Mbd1
Sult1a1
Bcl2l1
Wnt7a
Tmsb10
Lrrc58
Sox11
Serpina3c
Tnc
Lrrc55
Rin2
Cebpa
Map3k6
St3galt
Fas
Slc2a1
Pcsk1n
Cckbr
Celsr1
Zbtb16
Ddx26b
Adamts20
Zfyve28
Eva1a
Lyve1
Prr5
Usp53
Sdc4
Fam20a
Erbb3
Plekho2
Pnpla2
Pfin4
Hapln2
Mcam
Gadd45g
Fibin
Pxdn
Slitrk6
Smim3
Vac14
Mxd4
Mertk
Cmtm3
Chga
Mt2
Abhd15
Azin1
1110008F13Rik
Crhr1
Trib1
Cish
Serinc3
Foxo3
Pik3c2a
Lgr5
Icosl
Ampd3
Emilin2
Htra1
Fzd2
Snhg11
Kif26a
Sox13
Thbs1
Xdh
Cdkn1a
Mt1
Col27a1
Rgcc
Frmpd1
Amy1
Cdhr1
Rgs11
Nov
2210016F16Rik
Jag1
Casp7
Tia1
Tnpo1
Fgfrl1
Ppara
Hmgb2
Apbb1ip
Adamts9
Ptgs2
Rnpc3
Mcm5
Aff1
Rprm
Arhgap18
Gm11627
Bin2
Cstl1
Lin28b

b

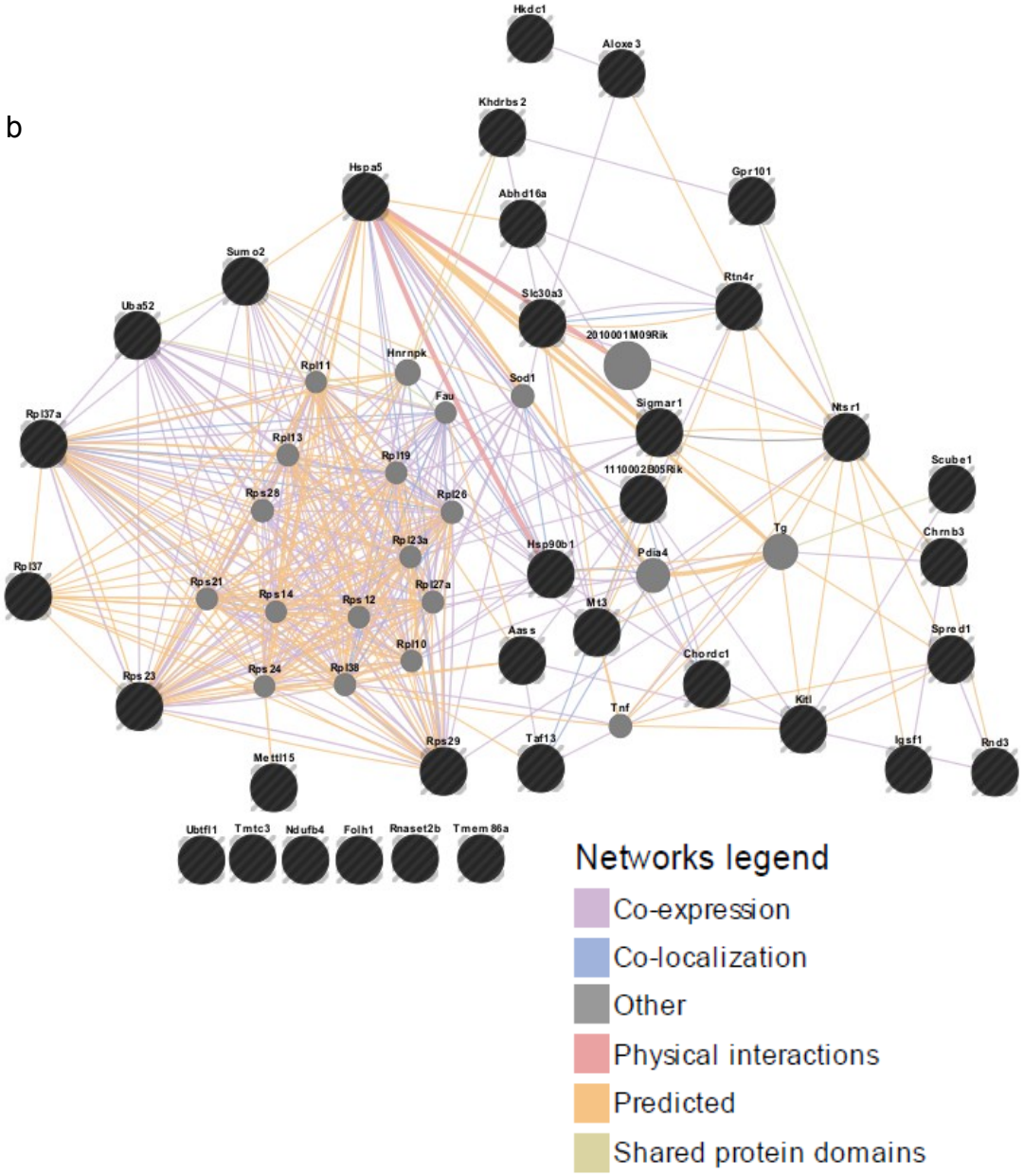

Figure 4.5 – RNA-Seq P2 candidate gene list functional association networks using GeneMANIA. (**a**) Interaction network for genes that were acutely regulated and then habituate following repeated ethanol is predicted to include *Mt1* and *Sgk1*. (**b**) Interaction network for genes that are regulated by repeated ethanol was populated with ribosomal proteins.

Trafficking of mRNA to the dendrites is facilitated by multiple RNA binding proteins (Bramham & Wells, 2007). Ethanol regulation of these proteins could contribute to alterations in the synaptic transcriptome and therefore impact synaptic plasticity. Functional enrichment analysis of the S2 fraction RNA-Seq significant gene list (Supplemental Table S4.9) found the ontological category, mRNA binding (GO:0003729), to be significantly over-represented ($p = 0.00103$). The S2 ethanol-responsive gene list was then compared to the RNA-Binding Protein DataBase's (RBPDB, http://rbpdb.ccbr.utoronto.ca/) (Cook *et al.*, 2011) collection of 413 curated mouse RNA-binding proteins. A significant number of genes (85) were found to overlap between the S2 gene set and RBPDB (Fisher's Exact Test, $p < 0.0004314$, odds ratio = 1.555425). *Cpeb1,* a RNA-binding protein shown to be involved in mRNA transport (Huang *et al.*, 2003), was regulated by ethanol in the S2 fraction. P2 candidate genes were compared to a set of genes that were identified as containing the cytoplasmic polyadenylation element (CPE), the consensus sequence for CPEB1 binding (Zhang *et al.*, 2010), and found that 32 genes were putative targets of CPEB1. One gene in particular, *Rhou*, has been determined to be regulated by ethanol under a number of different conditions. A survey of Gene Weaver (geneweaver.org) (Baker *et al.*, 2012), a curated repository of genomic experimental results, revealed *Rhou* to be regulated by both acute (Kerns *et al.*, 2005) and chronic administration as well as across various species, including mice and monkeys. *Rhou* was also identified in a study using gene expression patterns to distinguish between alcoholics and non-alcoholic controls in post-mortem samples (Liu *et al.*, 2006a).

Comparison of Array and RNA-Seq Result. For a more direct comparison to RNA-Seq data, microarrays were reanalyzed using Limma, a statistical algorithm that also examines differential expression for each pairwise treatment comparison in the S2 and P2 fractions. A candidate gene list was derived from Limma results in the same manner as the RNA-Seq analysis. 1078 genes were found to be significantly regulated by ethanol across all pairwise treatment comparisons in the P2, or in the S2 and P2, but enriched for in the P2 fraction in the microarray data (Figure 4.6, Supplemental Table S4.10). There was a significant overlap between the Limma and RNA-Seq data, where 82 genes were determined to be regulated by ethanol using both methodologies (Table 4.8). Functional enrichment analysis for the validated genes revealed over-representation of categories related to endoplasmic reticulum and protein folding (Figure 4.9, Supplemental Table 4.12). Therefore, microarray and RNA-Seq produced comparable results, verifying regulation of the synaptic transcriptome by sensitizing ethanol treatment.

This list of genes, which have been validated by two different methodologies dependent on distinct molecular principles, represents a starting foundation for selection of candidate genes from these studies. Other criteria to consider for choosing genes for following up experiments include synaptic localization of regulation, membership in significantly enriched ontological categories, high degree of connectivity to other ethanol responsive genes that would signify its potential as a hub gene for manipulation, and robustness of differential expression.

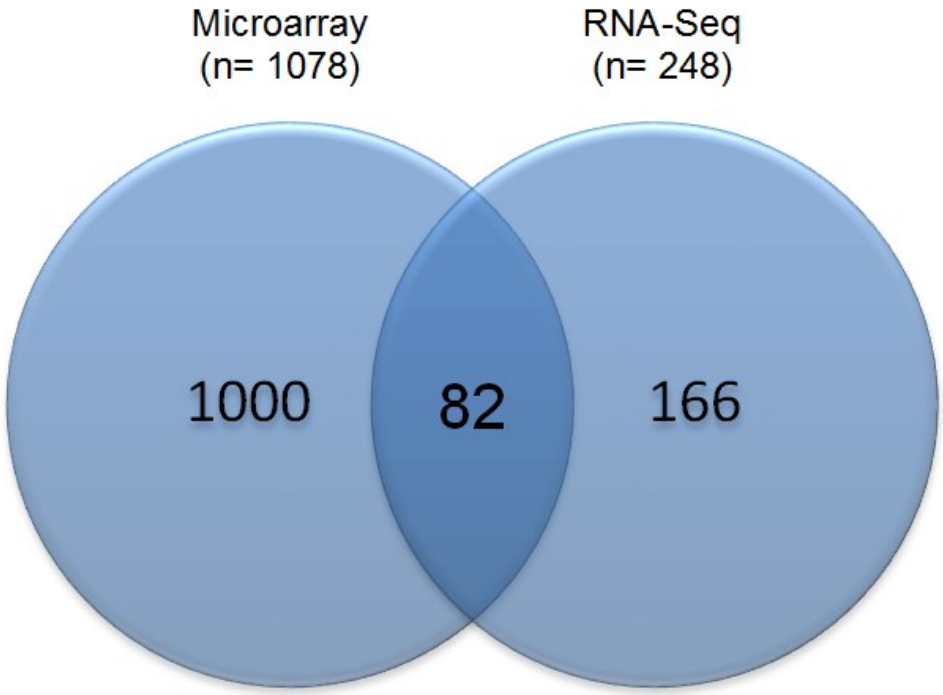

Figure 4.6 – Overlap of genes regulated by ethanol in the synaptic transcriptome between microarray and RNA-Seq analyses. Candidate genes were defined as being regulated by ethanol only in the P2, or in both the P2 and S2, but enriched for in the P2. Significance of overlap between microarray Limma and RNA-Seq Cuffdiff results was measured by Fisher's exact test ($p < 2.2 \times 10^{-16}$, odds ratio = 7.54), Jaccard Coefficient ($J = 0.066$, $p < 0.01$), and Representation Factor ($RF = 8.0$, $p < 3.795 \times 10^{-51}$).

Table 4.8: Validated P2 Fraction, Ethanol Treatment Candidate Genes from Overlap of Microarray Limma and RNA-Seq Cuffdiff

SSP2 v SEP2								SSP2 v EEP2				SEP2 v EEP2			
Jag1	Pamr1	Htra1	Tnc	Klhdc7a	Cmtm3	Mertk	Atp6v0c	Grm2	Agxt2l1	Aass	Scube1	Hsp90b1	Ppara	Pxdn	Unc5c
Frmpd1	Zdhhc22	Il17rd	Tnpo1	Lrrc55	Mxd4	Agxt2l1	Azin1	Ldlr	Angel1	Rtn4r	Xpo1	Hspa5	Prr5	Rhou	Fam5c
Fzd2	Abca9	Mcam	Adamts9	Pik3c2a	Plekhg1	Angel1	Tia1	Lpcat4	Fmo2	Sigmar1		Jag1	Cdc42ep4	Fgfr2	Gli3
Mt2	Amy1	Npy	Ppara	Rnf145	Plekho2	Fmo2		Pamr1	Ccng1	Slc30a3		Frmpd1	Erbb3	Man1a	Sox21
Slc24a6	Arhgap18	Ptgs2	Prr5	Usp53	Pxdn	Gpt2		Zdhhc22	Kirrel2	Spred1		Fzd2	Cmtm3	Sdf2l1	Dzip1l
Grm2	Cckbr	Sdc4	Gjb6	Cdc42ep4	Rhou	Ccng1		Gjb6	Mfsd2a	Tmem86a		Mt2	Mxd4	Sox9	
Ldlr	Celsr1	Sox11	Zdhhc8	Erbb3	Lonrf3	Kirrel2		Zdhhc8	Hsp90b1	Ubtfl1		Slc24a6	Plekhg1	Pdia4	
Lpcat4	Fgfrl1	Svil	Crhr1	Gatsl3	Hmgb2	Mfsd2a		Lonrf3	Hspa5	Ntsr1		Adamts9	Plekho2	Pdia6	

Table 4.9: Functional Enrichment Analysis, Validated P2 Fraction, Ethanol Treatment Candidate Genes from Overlap of Microarray Limma and RNA-Seq Cuffdiff

GO Category	Name	P-value	Terms in Query	Terms in Genome
Molecular Function	transmembrane receptor protein tyrosine kinase activity	2.07E-04	4	66
Molecular Function	misfolded protein binding	1.03E-03	2	11
Molecular Function	growth factor binding	2.16E-03	4	123
Molecular Function	peptide receptor activity	2.16E-03	4	123
Molecular Function	protein disulfide isomerase activity	4.21E-03	2	22
Biological Process	cardiac septum morphogenesis	3.69E-06	5	53
Biological Process	lung morphogenesis	5.31E-06	5	57
Biological Process	cardiac septum development	1.57E-05	5	71
Biological Process	inner ear development	2.08E-05	7	189
Biological Process	molting cycle process	5.52E-05	5	92
Cellular Component	endoplasmic reticulum lumen	1.34E-03	5	187
Cellular Component	podosome	3.37E-03	2	20
Cellular Component	endoplasmic reticulum - Golgi intermediate compartment	3.37E-03	3	69
Cellular Component	costamere	4.08E-03	2	22
Cellular Component	caveola	5.29E-03	3	81

Discussion

In this study, we examined the synaptic transcriptome in response to a behavioral sensitizing ethanol treatment in D2 mice. It was determined that by enriching tissue samples for synaptoneurosomal structures and then comparing somatic and synaptic fractions using transcriptomic analyses, we were able to distinguish ethanol's effects on localized populations of RNA. Differential expression was validated by the use of microarrays and RNA-Seq, which provided comparable results implicating the synaptic transcriptome in modulation of behavior by affecting local protein populations.

Neurons are highly specialized polarized cells, whose dendritic and axonal arborizations contain thousands of synapses that function and plasticize individually in response to stimulation (Steward & Levy, 1982; Steward *et al.*, 1998; Wallace *et al.*, 1998). It has been proposed that activity-dependent synaptic plasticity requires the transport and translation of specific mRNA species, creating a unique complement of proteins that are able to function in response to a specific stimulus (Bramham & Wells, 2007). Comparing the somatic and synaptic transcriptomes in response to sensitizing treatments of ethanol, we were able to detect discrete differences in ethanol regulation of gene expression. Through the characterization studies presented in Chapter 3, we were confident in the assessment that differences observed when analyzing P2 and S2 fractions represent ethanol's effect on gene expression in distinct subcellular locations. The exact means by which ethanol is exerting its regulation of the synaptic transcriptome has yet to be determined. Conceivably, ethanol could be affecting synaptic transcript abundances through overall modulation of transcription rates. This could have a global effect on mRNA levels within the cell, and, ultimately, through the mere altered availability of transcript, result in changes at the synapse. Our data

indicates that this is not an adequate explanation, as we were able to detect 141 genes by our initial microarray analysis and 116 genes by RNA-Seq, whose expression was changed in the P2 fraction alone and not in the somatic-RNA containing fraction, S2 (Figure 4.4).

Alternatively, the trafficking and localization of transcripts to the synapse offers another possible means of regulatory control. Synaptic tagging is a process whereby synaptic activation induces a transient synapse-specific change that allows the synapse to capture mRNA or proteins required for long-term plasticity, which has explicitly been studied for its role in long-term potentiation (Frey & Morris, 1997). The exact physical nature of the synaptic tag has not been absolutely defined, but candidate molecular tags that have been proposed include post-translation modifications to existing synaptic proteins, alterations to protein conformational states, initiation of localized translation or proteolysis, and reorganization of the local cytoskeleton (Martin & Kosik, 2002; Kelleher *et al.*, 2004; Doyle & Kiebler, 2011). All of these mechanisms have the potential of being initiated by signaling events that result from membrane receptor activation. For instance, one pharmacological effect of ethanol is the release of dopamine in the nucleus accumbens which, when acting at D1-like receptors, increases activity of adenylyl cyclase, thereby increasing cAMP levels and PKA activity. It has been shown that PKA activation is required for the formation of the synaptic tag (Casadio *et al.*, 1999; Barco *et al.*, 2002). The premise that signaling cascades downstream of ethanol could alter the ability of activated synapses to capture dendritically targeted mRNA requires examination.

In the proposed model of mRNA trafficking to the synapse, newly synthesized transcripts are bound by RNA-binding proteins in the nucleus and transported as part of large ribonucleoprotein particles (RNPs) along microtubules to the dendrites where, following synaptic activation, mRNA is localized to the spines by the actin cytoskeletal system (Bramham & Wells, 2007). Functional enrichment analysis of the RNA-Seq S2 ethanol-responsive gene list suggested that actin cytoskeletal reorganization and regulation of RNA-binding proteins may contribute to the mechanisms by which ethanol modulates the synaptic transcriptome. In the S2 fraction, we not only found regulation of *Cpeb1*, but also *Syncrip,* and *hnRNP-U*, whose two gene products have previously been shown to interact with kinesin family member 5 (KIF5), a myosin motor protein identified as a component of RNA transport granules (Kanai *et al.*, 2004). Ethanol's regulation of genes that participate in mRNA transport in the S2 fraction but not the P2 suggests that the synaptic plasticity elicited by repeated administration of ethanol can result from differential regulation of expression on a subcellular basis.

Bioinformatics analysis of the P2 candidate gene list (as well as the initial microarray analysis) indicated that transcripts altered in response to repeated ethanol exposure are significantly enriched for biological functions associated with endoplasmic reticulum function, in particular protein folding. Previously our laboratory has shown that ethanol regulates mRNA abundance of molecular chaperones *in vitro* and *in vivo* (Miles *et al.*, 1994; Kerns *et al.*, 2005). The present study extends these findings by providing evidence that this regulation may be localized or at least occurring at the synapse. In addition, biological network integration based upon functional annotation data using GeneMANIA predicted membership of 14 ribosomal proteins to the network constructed

from genes regulated by repeated ethanol (EE) but not acute ethanol (SE). Thus, our results that demonstrate ethanol regulation of genes that code for protein chaperones (*Hspa5, Hsp90b1),* co-chaperones (*Fkbp5, Chordc1*), and protein disulfide isomerases (*Pdia3, Pdia4, Pdia6*) suggest that repeated ethanol exposure modulate the local synaptic protein populations through synaptic genes involved in translation and protein folding. Alternatively, these changes in the P2 fraction of EE-treated animals may reflect increased demand for dendritic protein synthesis in response to repeated ethanol-evoked synaptic activity.

We also found enrichment of genes associated with the extracellular matrix, which is known for its role in altering synaptic architecture that contributes to the processes of learning and memory (Wright & Harding, 2009). It has been suggested that these processes are subverted during the development of addiction (Hyman *et al.*, 2006) and studies have linked extracellular matrix proteins to escalation of ethanol consumption (Smith *et al.*, 2011) and cocaine reward associative learning (Brown *et al.*, 2007). Our profiling of the synaptic transcriptome suggests that ethanol modifies expression of genes that participate in synaptic remodeling through regulation of synaptic and extracellular matrix proteins that may contribute to the induction of behavioral sensitization.

Our differential expression results were validated by performing both microarray and RNA-Seq analyses, techniques that rely on different sets of molecular principles. While RNA-Seq utilizes Next Generation Sequencing technology to provide direct read counts of transcripts, microarrays depend on the hybridization of target RNA to probe. Using both of these approaches allowed for a validation of data processing schemes

(Chapter 3) and differential expression results. A biologically relevant gene expression pattern detected in the P2 fraction, by both microarrays and RNA-Seq, was habituation following repeated administration of ethanol. It has previously been demonstrated in the Miles laboratory that this pattern of expression in response to ethanol behavioral sensitization occurs with glucocorticoid responsive genes, *Sgk1* and *Fkbp5*, and mimics the profile of the glucocorticoid, corticosterone, in response to ethanol (Costin *et al.*, 2013a). It also coincides with the literature that shows acute ethanol activates the hypothalamic-pituitary-adrenal (HPA) axis (Ellis, 1966), but that rodents and human alcoholics have blunted HPA responses while drinking and upon withdrawal (Wand & Dobs, 1991; Roberts *et al.*, 1995; Costa *et al.*, 1996; Rasmussen *et al.*, 2000; Richardson *et al.*, 2008). In the present study, we identified *Rhou*, which not only habituates in response to repeated ethanol, but also contains a glucocorticoid response element in its promoter region (http://opossum.cisreg.ca/oPOSSUM3/) and was found to be regulated in the P2 fraction only. This has implications for the synaptic transcriptome as a mediator of interactions between stress and alcoholism.

Despite a significant overlap of differential expression results from microarrays and RNA-Seq, there were still a number of genes that were only found to be regulated by ethanol in a single assay. This inconsistency may be the result of limitations of both technologies. While RNA-Seq is touted as having a greater dynamic range compared to arrays (Wang *et al.*, 2009; Zhao *et al.*, 2014), the ability to detect differences in low abundant transcripts is limited by sequencing depth, which is often begrudgingly sacrificed in efforts to balance cost and analytical power. It has been estimated that a minimum of 80 million reads per sample is required for accurate quantification of low

abundant genes (Consortium, 2011), while detection of up to 80% of differential expression events could possibly require as many as 300 million reads (Liu *et al.*, 2013). Our analysis averaged 28 million mapped reads per sample which could potentially prevent detection of differences in low abundant transcripts. This could especially be true in the complex mixed tissue sample of brain frontal pole which contains numerous cell types that exhibit diverse array of responses to exogenous stimulus. While at current sequencing depths, microarrays may still have greater sensitivity, they are at a disadvantage in discernable detection of differential expression of genes that are exceedingly abundant, resulting in over-saturation of the probe. Comprehensive coverage of the entire transcriptome by microarray analyses is also limited by representation of the genome on the chip. In the end, RNA-Seq and microarrays are both high-throughput approaches that can be used to complement each other, and analyses may benefit from investigating the union of their results as opposed to the intersection, with validation of individual candidate genes by other methodologies, such as quantitative reverse transcription PCR.

Using expression analysis, our study is the first to show regulation of the synaptic transcriptome by ethanol (or any exogenous drug) in an *in vivo* model. With repeated intermittent exposure to ethanol that resulted in a sensitized response, we observed changes to the complement of mRNA present at the synapse that we hypothesize contribute to the development of the behavioral phenotype in D2 mice. The individual genes and functional groups (e.g. molecular chaperones) identified in these studies provide important new information regarding the mechanisms of ethanol-induced synaptic plasticity. Functional analyses will be required to further validate these results

with the ultimate goal of selecting a candidate gene to disrupt synaptic targeting of its transcript in efforts to modulate ethanol behavior. Perhaps most importantly, this model has now been shown capable of identifying changes to the synaptic transcriptome and can be used to investigate other models of neuroplasticity in response to ethanol and other drugs of abuse.

Chapter 5 – Role of Synaptically Targeted *Bdnf* mRNA in Ethanol-Responsive Behaviors

Introduction

Brain-derived neurotrophic factor (BDNF) is a member of a class of molecules known as neurotrophins (NTs). These proteins are responsible for the differentiation and survival of developing neurons and the maintenance of mature neurons. NTs have also been investigated for their role in modulating synaptic transmission and facilitating plasticity (Poo, 2001). It is proposed that addiction arises from persistent and progressive cellular and molecular adaptations in response to repeated drug exposure (Wilke *et al.*, 1994; Nestler, 2001b), and research suggests that NTs, like BDNF, participate in the signaling and remodeling that contribute to the pathology (Russo *et al.*, 2009).

It has been proposed that activity-dependent local translation at the synapse is a mechanism of synaptic plasticity (Steward & Banker, 1992). It would stand to reason that regulation of local protein synthesis depends, at least in part, on the complement of RNA trafficked to the synapse. mRNA transport to distal processes has been shown to occur in an activity-dependent manner (Tongiorgi *et al.*, 1997; Steward & Worley, 2001; Grooms *et al.*, 2006). Our objective in this work was to investigate how the composition of the synaptic transcriptome contributes to ethanol-responsive behaviors. One

approach was through disrupting the dendritic trafficking of a known ethanol–responsive gene *in vivo*.

Bdnf has been identified as an ethanol-responsive gene through several of lines of evidence. Our lab has shown that *Bdnf* is up-regulated in the NAc of DBA/2J (D2) mice, 4 hours following a 2 g/kg i.p. injection of ethanol (Kerns *et al.*, 2005). Studies from the Ron lab have shown up-regulation of *Bdnf* in the hippocampus and dorsal striatum (DS) of C57BL/6J (B6) mice following an acute injection of 2 g/kg ethanol and in the DS after 4 weeks of self-administration of a 10% ethanol solution (McGough *et al.*, 2004). No change was observed in the expression of the closely related neurotrophin, nerve growth factor, following 4 weeks continuous access to ethanol. Interestingly, it was also demonstrated that escalating consumption of ethanol over 6 weeks resulted in the loss of ethanol's ability to increase *Bdnf* transcript levels, and that this was not recovered with a 2 week withdrawal period (Logrip *et al.*, 2009). The authors posit that the escalation in drinking resulted from dysregulation of BDNF signaling, which normally acts to prevent the neuroadaptations contributing to alcoholism (McGough *et al.*, 2004; Logrip *et al.*, 2009). Human studies have indicated an association between BDNF and susceptibility to addiction (Uhl *et al.*, 2001; Matsushita *et al.*, 2004) along with lower plasma levels of BDNF in alcoholics, particularly in those with a family history of the disease (Joe *et al.*, 2007). In animal studies, alterations in BDNF have been shown to modulate several behaviors associated with drugs of abuse (Horger *et al.*, 1999; Hall *et al.*, 2003; Hensler *et al.*, 2003). On a mixed J129ftm/1Jae/C57BL/6 background, heterozygous mice exhibited increased ethanol consumption as well as augmented ethanol-induced sensitization and

conditioned place preference as compared to their wildtype littermates (McGough *et al.*, 2004). Together these studies implicate *Bdnf* as an ethanol-responsive gene, whose altered expression can modify behavior.

The mRNA for *Bdnf* has been identified as a synaptically targeted transcript with evidence indicating that its dendritic transport is enhanced in an activity-dependent manner (Tongiorgi *et al.*, 1997). Using the existing $Bdnf^{klox/klox}$ mouse strain (Gorski *et al.*, 2003) in which the long 3' untranslated region (UTR) of this transcript was truncated, An *et al*. (2008) demonstrated that the long transcript variant was required for trafficking of *Bdnf* to dendrites (An *et al.*, 2008). $Bdnf^{klox/klox}$ mice possess reduced levels of BDNF transcript and protein in the dendrites, yet total levels remained unchanged. These mice also show a significant dysmorphogenesis of dendritic spines at 8 weeks of age indicating a role of dendritically translated BDNF in spine maturation and pruning (An *et al.*, 2008). Considering the involvement BDNF has shown in synaptic plasticity mediating addiction behaviors, these $Bdnf^{klox/klox}$ mice provide a valuable model for investigating whether targeting of certain transcripts to the synapse is necessary for ethanol response behaviors.

The aim of this study was to characterize the function of synaptically trafficked *Bdnf* in ethanol-responsive behaviors following acute low and high dose exposure. This was accomplished by testing $Bdnf^{klox/klox}$ mice for locomotor activity, sedation, and anxiolysis following ethanol administration. Furthermore, animals were tested for ethanol consumption in a two-bottle choice paradigm and ethanol's rewarding properties using conditioned placed preference (CPP). We hypothesized that *Bdnf* mRNA specifically targeted to the synapse would have a distinct function in response to

ethanol and that by disrupting its dendritic trafficking *in vivo* we would observe altered behavioral phenotypes as compared to wildtype littermates. Our results indicate an altered sensitivity to both low and high dose ethanol in *Bdnf*$^{klox/klox}$ mice, which was not exclusively pharmacokinetic in nature.

Materials and Methods

Animals. The Bdnf$^{klox/klox}$ strain of mice (Dr. Kevin Jones, University of Colorado-Boulder, CO, USA) were re-derived and bred in the VCU Transgenic Mouse Core, maintaining their C57BL/6J genetic background. Heterozygote matings were used to procure klox/klox homozygotes and wildtype littermates for experiments. Male mice were singly housed between 4 and 5 weeks of age and had *ad libitum* access to tap water in a 12-hour light/dark cycle (6 am on, 6 pm off). Mice were housed with Teklad corn cob bedding (7092, Harlan, Madison, WI). All behaviors were assayed during the light cycle between the hours of 8 am and 2 pm. All animal procedures were approved by the Institutional Animal Care and Use Committee of Virginia (AM10332) and carried out in accordance with the National Institute of Health guide for the Care and Use of Laboratory Animals.

Pair-Feeding. In a pair-feeding paradigm, daily food intake for Bdnf$^{klox/klox}$ mice was restricted to that of wildtype mice, which were given *ad libitum* access to Teklad standard rodent chow (7912, Harlan, Madison, WI). Each day, Bdnf$^{klox/klox}$ mice were provided with the average amount of food consumed by age-matched wildtype littermates on the previous day. Bdnf$^{klox/klox}$ mice were given two feedings per day: the first between 8 and 9 am and second between 4 and 5 pm. All mice were weighed on a

weekly basis to ensure Bdnf$^{klox/klox}$ mice were maintaining a body mass similar to wildtype mice. The pair-feeding protocol commenced at approximately 4 to 5 weeks of age, when Bdnf$^{klox/klox}$ mice were not obese, and continued throughout testing of the animals. Statistical analysis of body mass over time was performed using two-factor ANOVA and Bonferroni *post-hoc* analysis was used to compare differences between genotypes at each week.

Acute Locomotor Dose Response. The locomotor activity profile across various doses of ethanol was assessed using Med-Associates sound-attenuating locomotor activity chambers (Med Associates, model ENV-515, St. Albans, VT). Chambers are equipped with 100 mA lights, a fan to diminish ambient noise, and 16 infrared sensor beams along the x and y axis. The system is interfaced with Med Associates software that records the number of photobeam breaks which it converts to horizontal distance traveled. Mice approximately 8-10 weeks of age were acclimated to the behavioral testing room for 1 hour prior to i.p. injections. Two days of saline administration and 10 minutes placement in the testing apparatus allowed for habituation to injections and environment. On test day, mice received 1-, 1.5-, 2-, 2.5 g/kg ethanol or saline and distance traveled was recorded for 60 minutes. Statistical analysis for the locomotor dose response curves was performed using a two-way ANOVA on z-scored rank transformed data. Time course data across the full 60 minute testing period for each dose was analyzed using repeated measures two-way ANOVA. For analyses of body mass between genotypes and treatment groups, a two-way ANOVA was applied. Tukey's *post-hoc* analyses were performed where appropriate for all pairwise

comparisons. Correlation between body mass and distance traveled was analyzed using linear regression.

Loss of Righting Reflex (LORR). The sedative-hypnotic effects of ethanol were measured using the loss of righting reflex assay (LORR). Mice approximately 9.5-12 weeks of age were habituated to i.p. saline injections for 3 days. On test day mice received 4.0 g/kg ethanol at Time 0. Upon initial signs of intoxication, the mice were placed supine in a V-shaped trough. Latency for LORR, or Time 1, was recorded when a mouse was unable to right itself for 30 seconds. Mice taking longer than 5 minutes to acquire LORR were removed from the study due to possibility of improper injection. An animal was deemed to have regained its righting reflex, and Time 2 recorded, when it was able to right itself 2 times within 30 seconds. Duration of LORR was calculated by Time 2- Time 1. Statistical analyses of latency and duration of LORR as well as body mass were performed using a Student's t-test between genotypes. Correlation between body mass and LORR measurements was analyzed using linear regression.

Ethanol Two-Bottle Choice Drinking. General avidity for ethanol was measured using the voluntary two-bottle choice paradigm. Mice approximately 12-17 weeks of age were given 24 hour access to one bottle containing 7.5% (v/v) ethanol and one bottle containing tap water for 7 days followed by access to one bottle 15% (v/v) ethanol and one bottle tap water for an additional 7 days. Bottles were constructed from 15 ml glass centrifuge tubes (BioExpress, Kaysville, UT) plugged with a rubber stopper containing a 2.5 inch stainless steel sipper (Ancare, Bellmore, NY). Bottle position was varied in a double alternating fashion (left, left, right, right) as to account for arbitrary side preference. Daily fluid consumption was measured to the nearest 0.1 ml, average daily

intake was reported as g/kg, and preference was calculated from the ratio of ethanol intake divided by total amount of fluid consumed. Statistical analyses for total fluid and ethanol daily intake, as well as ethanol preference, were performed using repeated measures two-way ANOVA followed by Tukey's HSD *post-hoc* at $\alpha = 0.05$ to determine statistical significance between groups.

Saccharin and Quinine Taste Discrimination. Taste discrimination studies were performed to assess the selectivity of genotype effect on consumption. Taste preference for bitter or sweet solutions was measured using quinine hydrochloride (QHCl) or saccharin versus tap water in a two-bottle choice paradigm. Mice were cycled through a series of experiments: 30 μM QHCl, 2 mM saccharin, 75 μM QHCl, 0.5 mM saccharin. Consumption of each concentration was measured daily for 4 days with 4 days of access to water only between each experiment. It has been shown that tests lasting a minimum of 4 days are sensitive enough to discriminate strain differences in taste preference (Tordoff & Bachmanov, 2002). Bottles were constructed as described previously and were alternated every other day. Average daily intake was reported as g/kg and preference was calculated from the ratio of tastant solution intake divided by total amount of fluid consumed. Statistical analyses for intake, preference, and total fluid consumption was performed using a Student's t-test comparing genotype.

Conditioned Place Preference (CPP). Genotypic differences in the reward-like properties of ethanol were measured by conditioned place preference (CPP). Animals received cage enrichment and experimenter handling for one week prior to commencement of testing. The experimental apparatus (Med-Associates, ENV3013, St. Albans, VT) consisted of black and white chambers (20 x 20 x 20 cm each) which

differed in floor texture (white mesh and black rod) to help mice further differentiate between the two environments. Chambers were separated by a smaller intermediate compartment with grey walls, smooth PVC floor, and partitions that allowed access to the black and white chambers. On day 1 (pre-conditioning day), male mice were confined to the intermediate compartment for 5 minutes, partitions were lifted and mice were allowed to roam freely between chambers for 15 minutes. The time spent in the black and white chambers was used to establish baseline chamber preferences, if any. Mice were separated into vehicle and drug groups such that initial chamber biases were approximately balanced. On days 2–4 (conditioning days), twice per day, mice were injected (i.p.) with vehicle or drug and subsequently paired with either the black or white chamber, where they were allowed to roam for 15 minutes. Vehicle-treated animals were paired with saline in both chambers, and drug-treated animals received saline in one chamber and ethanol (2.0 g/kg) in the opposite chamber. Pairing of the ethanol with either the black or white chamber was randomized within the drug-treated group of mice. Daily injections were counterbalanced so that some mice received ethanol in the morning and others in the afternoon. On day 5 (test day), mice did not receive an injection. They were placed into the intermediate compartment for 5 minutes, the partitions were lifted and they were allowed to roam freely for 15 minutes. Locomotor activity counts and time spent in each chamber was recorded. For ethanol-treated mice, preference scores were calculated as time spent in the drug-paired side on test day minus time spent in drug-paired side during baseline. For saline-treated mice, preference scores were calculated as the average of time spent in the white side on test day minus the white side during baseline and the time spent in the black side on test

day minus the black side during baseline. Each animal was subjected to the CPP protocol twice, receiving the alternative conditioning treatment in the second experiment. There was a 6 week wash-out period between tests. Locomotor activity and body mass data was analyzed for the first experiment. Statistical analyses for preference score, locomotor activity, and body mass were performed using a two-way ANOVA followed by Tukey's HSD *post-hoc* to test pairwise comparisons where appropriate.

Light-Dark Box (LDB). Basal anxiety-like behavior and ethanol-induced anxiolysis were measured in the light-dark box (LDB) assay. The LDB apparatus (Med Associates, model ENV-515, St. Albans, VT) consists of a transparent square box 10.75" L x 10.75" W x 8" H, divided into two equally sized zones by a black insert, all enclosed within a sound-attenuating chamber. Chambers were illuminated with 170 mA stimulating lights. One hour prior to behavioral testing, mice approximately 8 to 9 weeks of age were relocated to the behavior room and the light-dark box chambers were turned on for habituation to testing environment. Mice were injected with either saline or 1.5 g/kg i.p. ethanol, returned to their home cage for 5 minutes, and then placed into the center of the LDB, facing the dark side, and allowed to roam for 10 minutes. Time (seconds) spent in each zone and distance traveled was recorded. Animals were removed from the study if they never entered the light side during the entire testing period. Statistical analyses were performed for percent time spent (PTS) in the light, percent distance traveled (PDT) in the light, latency to enter the light, and total locomotor activity by two-way ANOVA followed by Tukey's HSD *post-hoc* test for pairwise comparisons where applicable.

Ethanol Metabolism Time Course. Blood ethanol concentration (BEC) was measured at various time points following administration of high dose ethanol to determine the effect of genotype on ethanol metabolism. Male mice between 9 and 12 weeks of age were administered 4.0 g/kg ethanol and blood was collected via submandibular cheek punch at 10-, 30-, 60-, 120-, and 240 minutes following i.p. injection. On a single day, blood was collected from an individual mouse at either one or two given time points. Each mouse was subjected to the procedure for 3 days, with 3 to 5 days between ethanol administrations. Statistical analysis of the ethanol metabolism curve was performed using two-way ANOVA followed by Tukey's HSD *post-hoc* to determine significance between genotypes at each time point. Linear regression was used to compare the slope of the metabolism curves and to correlate body mass to BEC at each time point.

Tissue Collection and Preparation. As part of particular experiments, different tissue samples were taken for the purpose of correlating internal ethanol concentration to behavior. In two separate LORR experiments, blood was collected at Time 2 via submandibular cheek punch for the determination of BEC. In another LORR experiment, brain tissue was collected following cervical dislocation at Time 2 for the determination of brain ethanol concentration (BrEC). Blood samples procured during LORR and the for the ethanol metabolism time course were collected in BD microtainer tubes containing EDTA (Fisher Scientific, Waltham, MA) to prevent clotting. Samples were prepared for analysis by headspace gas chromatograph (GC) by aliquoting 20 µl of whole blood into 20 ml GC vials (Autosampler Guys, Alexandria, VA) containing 960 µl deionized (DI) water and 20 µl of 0.1 mg/ml 1-propanol standard. Vials were capped

with steel screw-top septa and stored at -20 ˚C until processed. For BrEC, whole brain was collected and rinsed in ice-cold DI water and blotted with filter paper. The tissue was then placed in an ice-cold, pre-weighed 14 ml polypropylene tube (BD Biosciences, Franklin Lakes, NJ) and weighed to determine brain mass. Samples were then flash frozen on dry ice and stored at -80 ˚C until processing could continue. On ice, tissue was partially thawed in a Pyrex glass homogenizer (#7727-07) and diluted 1:4 with ice-cold DI water. Homogenate was transferred to a GC vial and analyzed via headspace GC. Statistical analyses for BEC and BrEC were performed using Student's t-test or one-way ANOVA followed by a Tukey's *post-hoc* test where appropriate.

Results

Bdnf$^{klox/klox}$ mice maintained on a pair-feeding paradigm have comparable body mass to wildtype littermates.

It has been shown that Bdnf$^{klox/klox}$ mice's obesity phenotype is solely the result of hyperphagia and can be prevented by maintaining the animals on a pair-feeding schedule (Liao *et al.*, 2012). Preserving a comparable body mass between Bdnf$^{klox/klox}$ mice and their wildtype littermates was essential for the interpretation of many ethanol-induced behaviors. After ethanol is absorbed, it is distributed throughout the various body tissues in direct proportion to the water content of each tissue. Since adipose tissue contains relatively less water, an increase would reduce the volume of distribution (V_d) for ethanol, resulting in higher BECs despite administration of equal doses. Figure 5.1, **a-b**, demonstrates the pair-feeding paradigm's utility to prevent Bdnf$^{klox/klox}$ mice from developing an obese phenotype. When Bdnf$^{klox/klox}$ mice have *ad libitum* access to

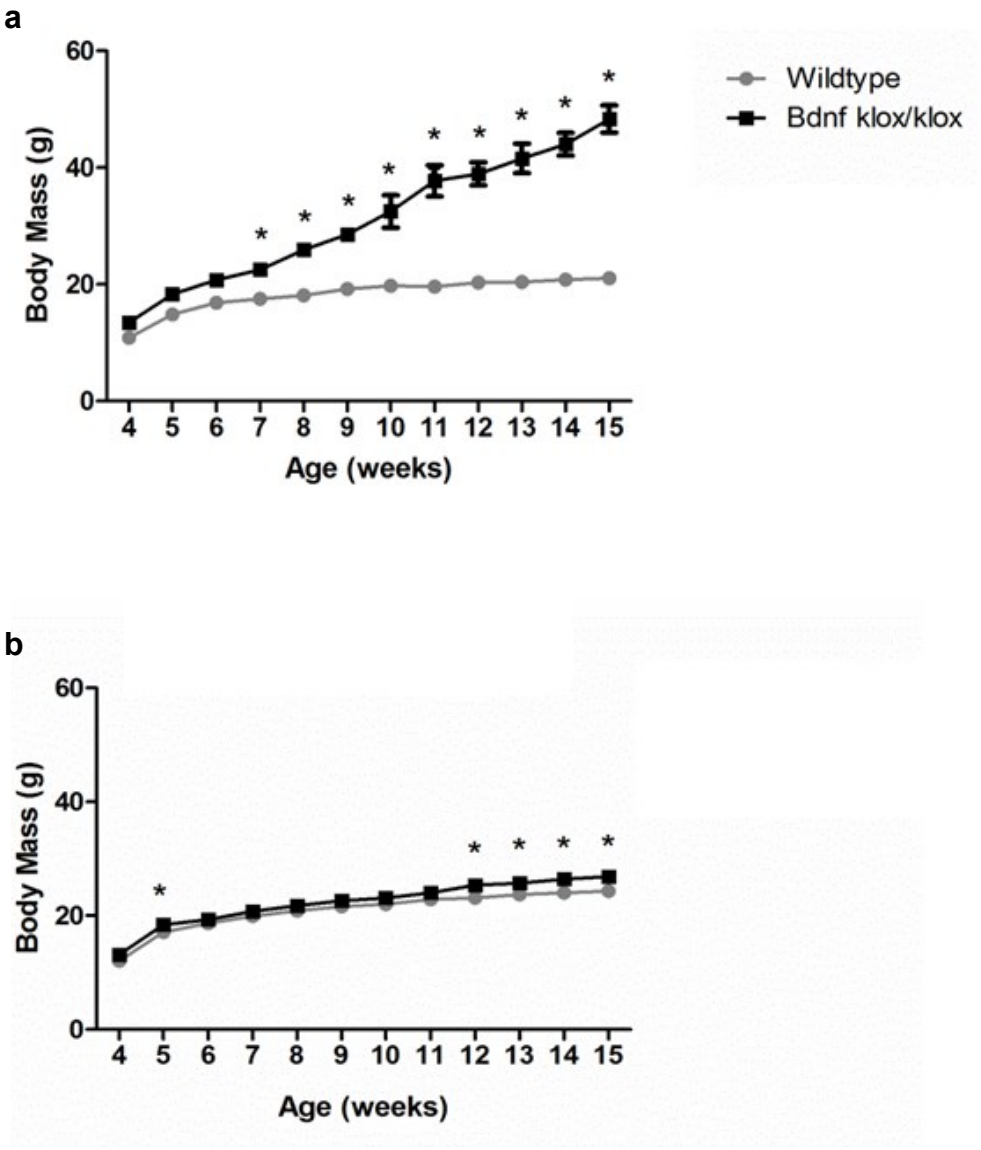

Figure 5.1 – Pair-feeding maintains comparable body mass between *Bdnf*$^{klox/klox}$ mice and wildtype littermates. (**a**) Female (and male) *Bdnf*$^{klox/klox}$ mice given *ad libitum* access to food have significantly different body masses compared to wildtype animals. Two-way ANOVA, Bonferroni *post-hoc* analysis, main effect of genotype $F[1,91] = 475.3$, main effect of week $F[12,91] = 62.57$, and significant interaction $F[12,91] = 21.84$, *$p < 0.05$, n = 1-6/group. (**b**) Pair-fed male *Bdnf*$^{klox/klox}$ mice maintained comparable body masses compared to wildtype animals. Two-way ANOVA, Bonferroni *post-hoc* analysis, main effect of genotype $F[1,699] = 96.44$, main effect of week $F[11,699] = 176.5$, but no significant interaction genotype x week, *$p < 0.05$, n = 16-46/group.

food, their body mass significantly differs from wildtype as early as 7 weeks of age. While Figure 5.1, **a**, depicts this phenomenon in female mice, this same trend has been observed in male mice (Liao *et al.*, 2012). Restricting male Bdnf$^{klox/klox}$ mice to the quantity of food consumed by their wildtype counterparts promoted maintenance of a "normal" body mass throughout the time frame of experimentation (Figure 5.1, **b**).

Bdnf$^{klox/klox}$ mice have an altered acute ethanol locomotor dose response profile.

The biphasic response to ethanol in rodent models, where relatively large doses are known to decrease locomotor activity while smaller doses are reported to increase locomotor activity, is well established (Wallgren & Barry, 1970; Pohorecky, 1997). However, the locomotor activating effect of low dose ethanol is strain dependent, and is considered virtually absent in C57BL/J6 (B6) mice (Phillips *et al.*, 1995). Since *Bdnf*$^{klox/klox}$ mice are maintained on a B6 genetic background, this could explain the shallow locomotor dose response observed in both the 10 and 60 minute time bins for both genotypes (Figure 5.2, **a, b**). Nevertheless, wildtype littermates exhibited significantly augmented locomotor activity following 2.0 and 2.5 g/kg ethanol as compared to saline in the 10 minute time bin immediately following injection (Figure 5.2, **a**). In contrast, *Bdnf*$^{klox/klox}$ mice demonstrated locomotor activation in response to 1.0 g/kg ethanol as compared to saline in both the 10 and 60 minute time bins and this level of activity was significantly different from wildtype mice when comparing the 60 minute time bin (Figure 5.2, **a, b**). Furthermore, *Bdnf*$^{klox/klox}$ mice revealed a biphasic locomotor response over the doses tested, displaying a reduced level of activity at 2.5 g/kg ethanol as compared to wildtype littermates in both 10 and 60 minute time bins (Figure 5.2, **a, b**). A time course of the data for each dose was plotted in 5 minute time bins throughout

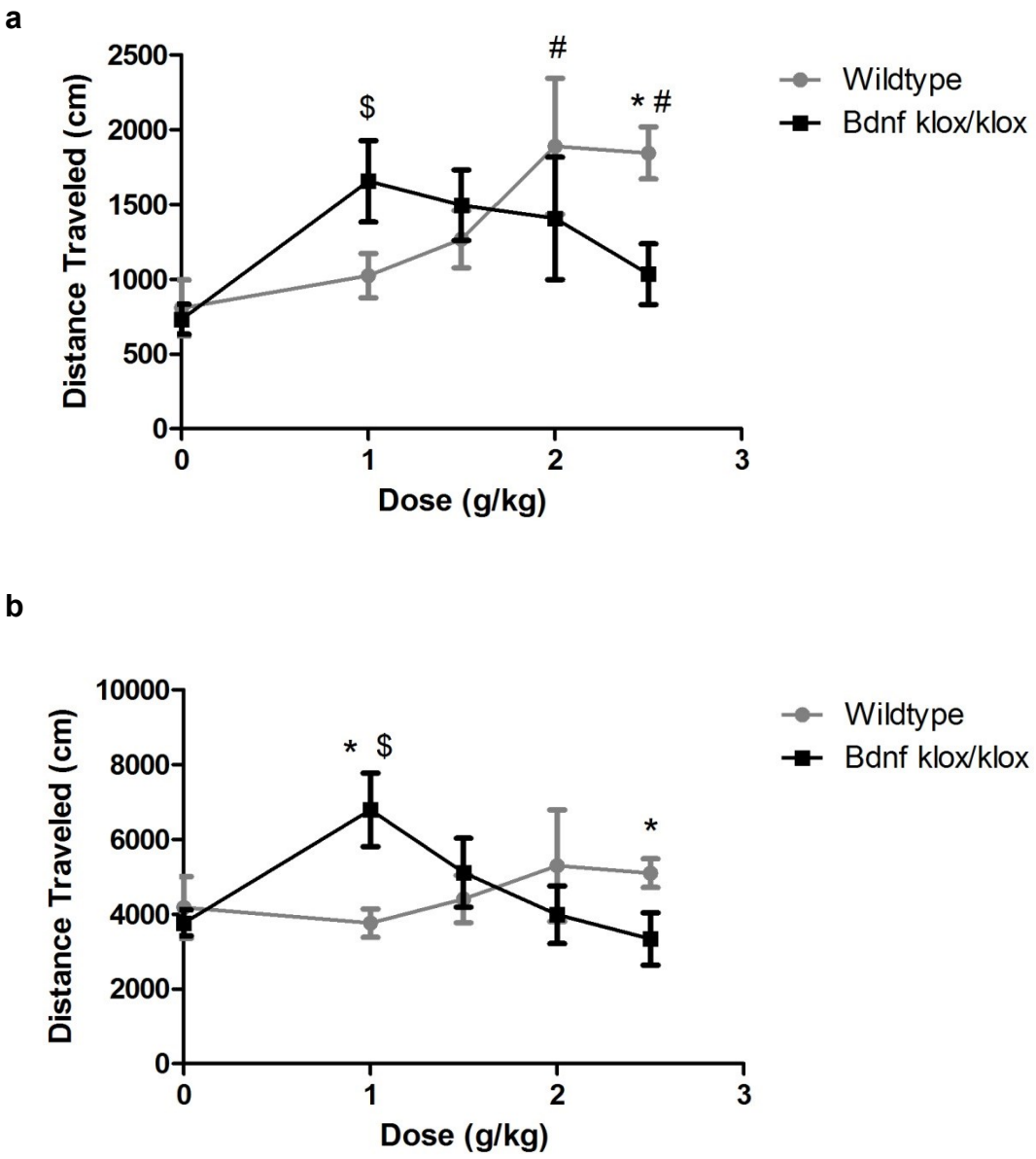

Figure 5.2 – Locomotor Activity Dose Response Curves. *Bdnf*$^{klox/klox}$ and wildtype mice that received various ethanol doses were placed in the locomotor activity chambers and locomotor activity was recorded. Distance traveled is reported for (**a**) the first 10 minute time bin (two-way ANOVA, Tukey's HSD *post-hoc*, main effect of dose $F[4,82] = 3.982$, significant interaction genotype x dose $F[4,82] = 2.864$, *$p < 0.05$ between genotypes, $^{\#}p < 0.05$ compared to wildtype saline, $^{\$}p < 0.05$ compared to klox/klox saline, n = 8-10/group) and (**b**) the full 60 minute testing session (two-way ANOVA, Tukey's HSD *post-hoc*, significant interaction genotype x dose $F[4,82] = 3.004$, *$p < 0.05$ between genotypes, $^{\$}p < 0.05$ compared to klox/klox saline, n = 8-10/group).

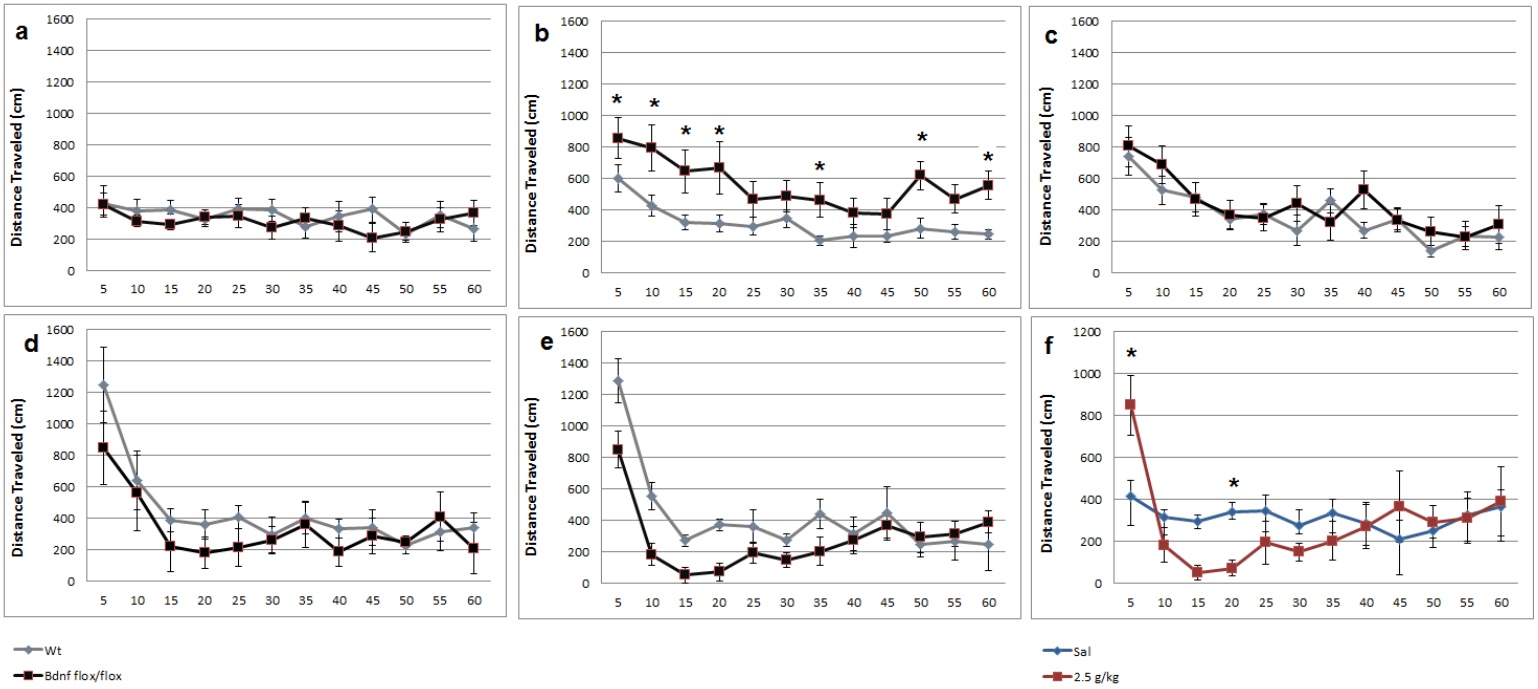

Figure 5.3 - Locomotor Activity Time Courses. The full 60 minute locomotor testing period was analyzed for each dose of ethanol. Repeated measures two-way ANOVA followed by Tukey's HSD *post-hoc* was used to analyze each dose, n = 8-10/group. (**a**) Saline: no main effect or significant interaction (**b**) 1.0 g/kg: main effect of genotype $F[1,176] = 9.705$, main effect of time bin $F[11,176] = 7.185$, no significant interaction genotype x time bin, *$p < 0.05$ between genotypes (**c**) 1.5 g/kg: main effect of time bin $F[11,198] = 10.696$ (**d**) 2.0 g/kg: main effect of time bin $F[11,176] = 11.434$ (**e**) 2.5 g/kg: main effect of genotype $F[1,175] = 5.978$, main effect of time bin $F[11,175] = 7.095$, significant interaction genotype x time bin $F[11,175] = 10.114$, *$p < 0.05$. (**f**) Comparison of saline and 2.5 g/kg ethanol within $Bdnf^{klox/klox}$, main effect of time bin $F[11,165] = 4.427$, significant interaction genotype x time bin $F[11,176] = 2.855$, *$p < 0.05$.

the 60 minute testing period (Figure 5.3, **a-e**). Interestingly, the locomotor activation of *Bdnf*$^{klox/klox}$ mice induced by 1.0 g/kg ethanol was sustained almost throughout the entire 60 minute testing period, remaining significantly different from wildtype mice at the 5, 10, 15, 20, 35, 50, and 60 minute time bins (Figure 5.3, **b**). Additionally, when examining the 2.5 g/kg ethanol treatment time course in *Bdnf*$^{klox/klox}$ mice, a significant decrease in activity below saline baseline levels was observed at the 20 minute time bin, with a trend at the 15 minute time bin (Figure 5.3, **f**). This suggests a sedative effect of 2.5 g/kg ethanol in the *Bdnf*$^{klox/klox}$ mice that was not observed in the wildtype littermates.

Although the *Bdnf*$^{klox/klox}$ mice used in this experiment were pair-fed, there was a concern that a difference in V_d as a result of dissimilar lean body mass between the genotypes would contribute to a shift in the locomotor dose response curve. While there was a main effect of genotype, no significant difference in body mass could be detected between the genotypes for any particular treatment group (Figure 5.4). Correlation between body mass and distance traveled was also examined for the ethanol doses that exhibited differences between the genotypes. No correlation was found between body mass and locomotor activity following 1.0 g/kg ethanol in the significant time bin of 60 minutes for the *Bdnf*$^{klox/klox}$ mice alone (Figure 5.5, **a**) or when considering *Bdnf*$^{klox/klox}$ and wildtype mice (Figure 5.5, **b**). Similarly, no correlation was found between body mass and locomotor activity following 2.5 g/kg in the significant time bin of 10 minutes (Figure 5.5, **c, d**). Therefore, it was unlikely that body mass was contributing to the genotypic effect on locomotor dose response profile.

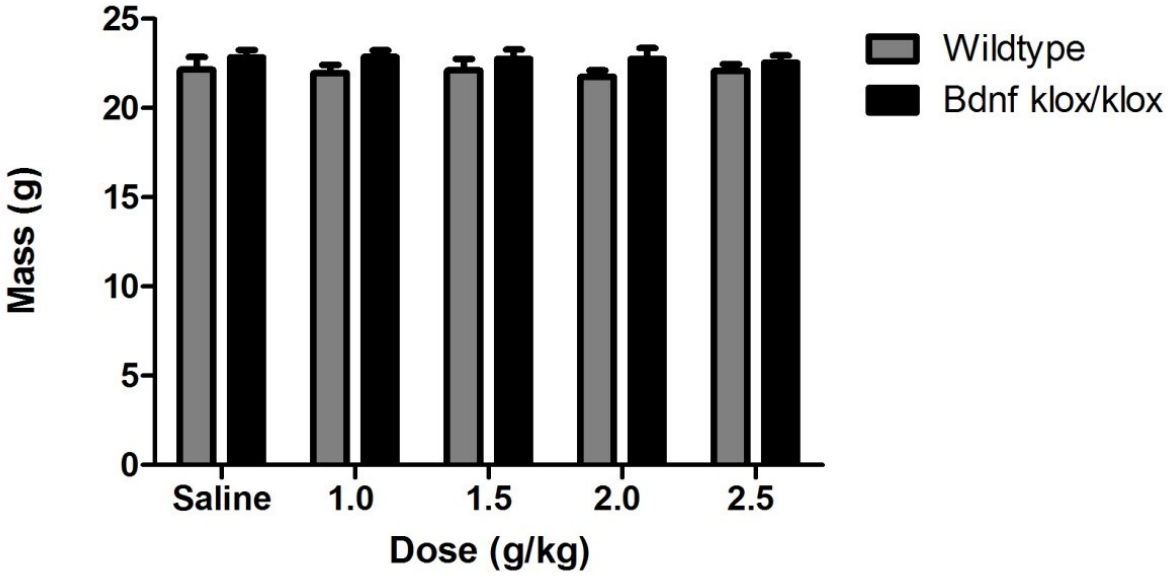

Figure 5.4 – Body mass of animals used for locomotor dose response. When comparing the body mass between the genotypes, broken down by treatment, there was a main effect of genotype (two-way ANOVA, $F[1, 82] = 5.348$), but no effect of dose and no significant interaction genotype x dose (n = 8-10/group).

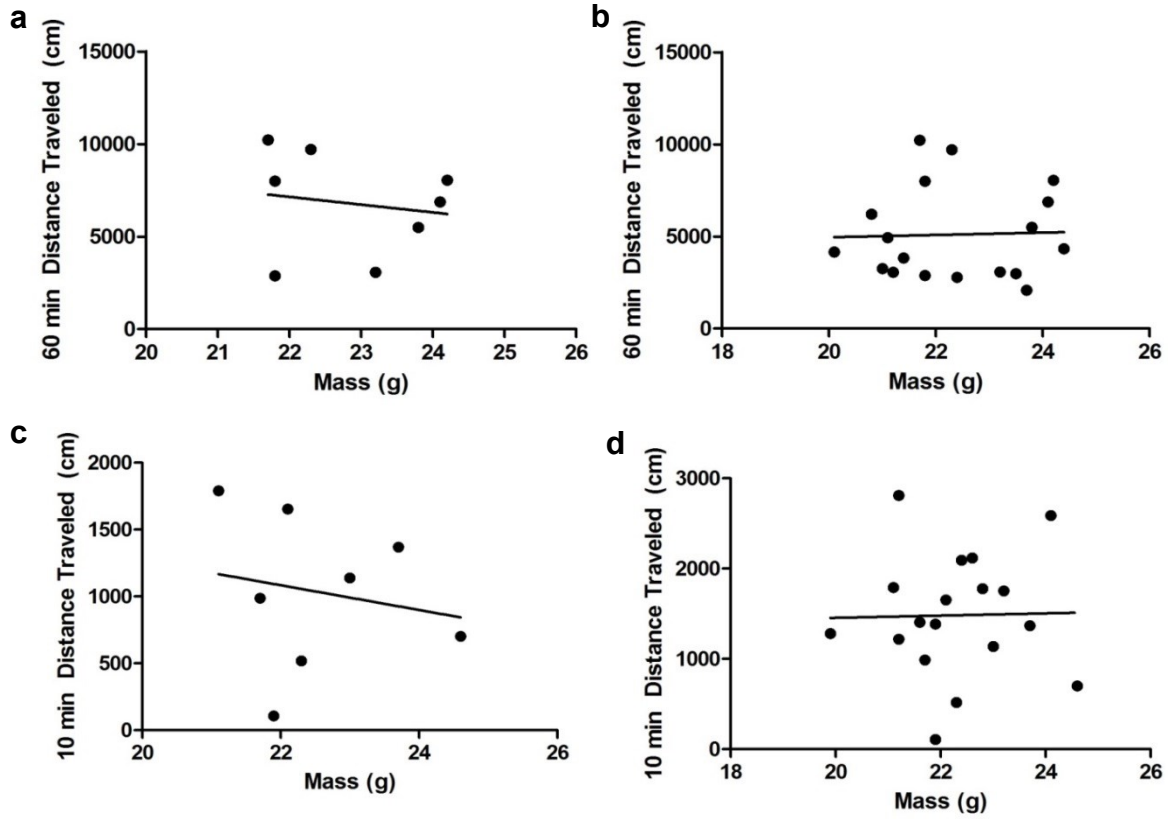

Figure 5.5 – Correlation between body mass and locomotor activity. There was no significant correlation between mass and locomotor activity under any of the conditions examined (**a**) 60 minute locomotor activity after 1.0 g/kg in *Bdnf*$^{klox/klox}$ mice (F[1,6] = 0.1640, r = 0.16, p = 0.6988) (**b**) 60 minute locomotor activity after 1.0 g/kg in all mice (F[1,6] = 0.01817, r = 0.03, p = 0.8945) (**c**) 10 minute locomotor activity after 2.5 g/kg in *Bdnf*$^{klox/klox}$ mice (F[1,6] = 0.2122, r = 0.18, p = 0.6612) (**d**) 10 minute locomotor activity after 2.5 g/kg in all mice (F[1,6] = 0.00697, r = 0.02, p = 0.9345).

Bdnf$^{klox/klox}$ *mice exhibit longer ethanol LORR sleep times.*

Initial investigations into the sedative-hypnotic properties of ethanol using LORR were performed with a cohort of non-pair-fed *Bdnf*$^{klox/klox}$ mice. This experiment also utilized two heterozygous klox mice which exhibited no detectable phenotypic differences from wildtype animals in the LORR assay. The data for these two genotypes was collapsed for the purpose of statistical analysis and the resulting group was referred to "Littermates". Animals lacking synaptically targeted *Bdnf* had significantly greater duration of LORR, sleeping 3.8x longer than "Littermate" controls (Figure 5.6, **c**). No difference in latency to LORR was observed (Figure 5.6, **b**). There was an obvious inequality in body mass between the non-pair-fed *Bdnf*$^{klox/klox}$ and "Littermate" animals (Figure 5.6, **d**). This prompted the concurrent measurement of BEC at multiple time points to examine relative contributions of pharmacokinetic and pharmacodynamic factors to the altered phenotype (Figure 5.6, **a**). No difference in BEC at the time *Bdnf*$^{klox/klox}$ and "Littermate" animals regain righting reflex (Time 2) would suggest the increased duration of LORR displayed by *Bdnf*$^{klox/klox}$ was solely the result of an altered pharmacokinetic profile, producing an elevated BEC for an extended period of time in *Bdnf*$^{klox/klox}$ mice. In contrast, *Bdnf*$^{klox/klox}$ mice had a significantly lower BEC at Time 2 as compared to "Littermates" (Figure 5.6, **e**), suggesting a possible deficit in acute functional tolerance (AFT). The BEC of "Littermate" animals was tested at a second time point, which corresponded approximately to the Time 2 for *Bdnf*$^{klox/klox}$ mice. This was referred to as "Littermate" Time 3. No difference between *Bdnf*$^{klox/klox}$ Time 2 BEC and "Littermate" Time 3 BEC implied a similar pharmacokinetic profile (Figure 5.6, **e**).

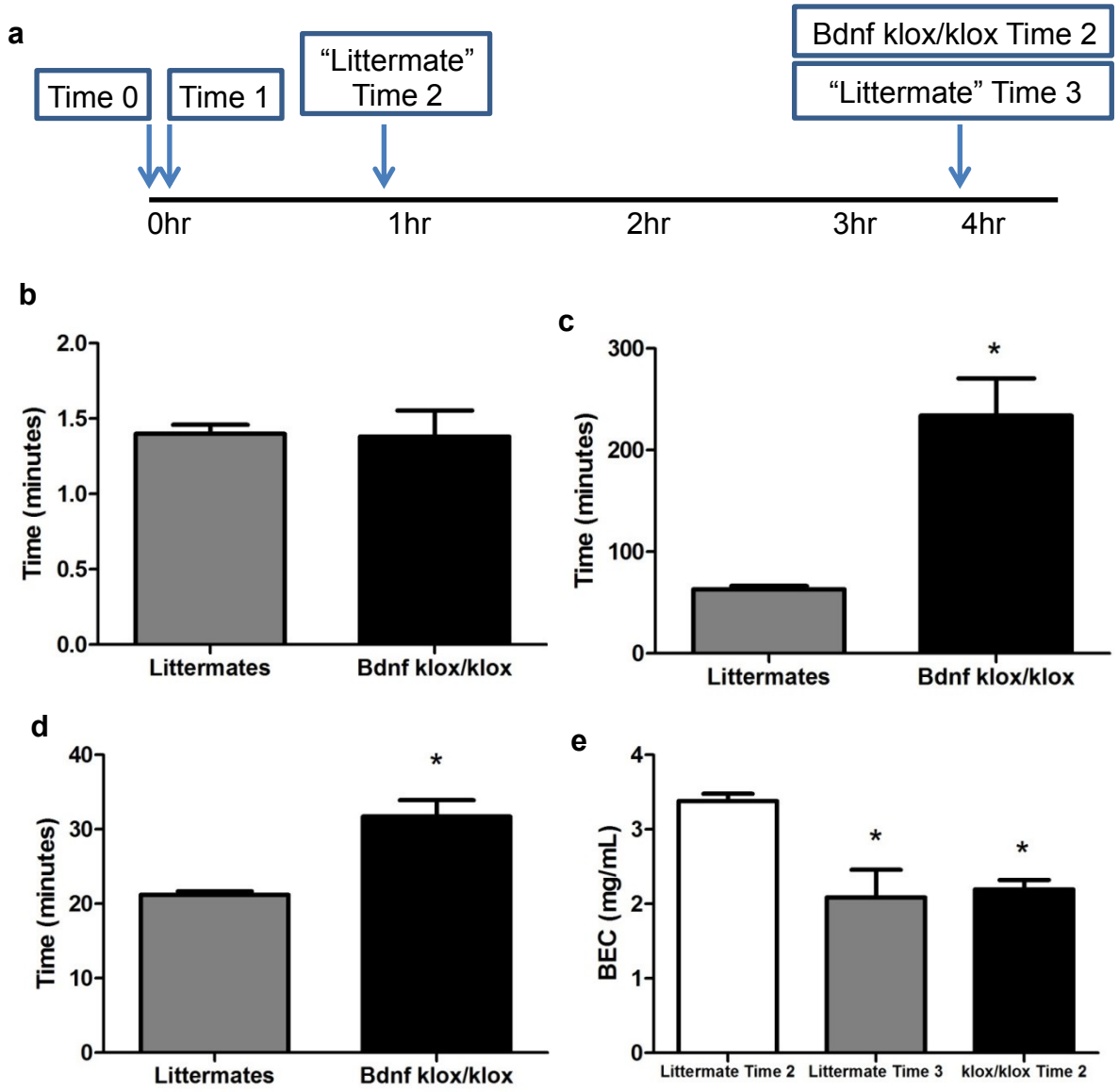

Figure 5.6 – LORR in non-pair-fed *Bdnf*$^{klox/klox}$ mice. (**a**) Diagram of the LORR experimental design. (**b**) No significant difference in latency to LORR was detected between "Littermates" and non-pair-fed *Bdnf*$^{klox/klox}$ mice (Student's t-test, *t*[12] = 0.1043) (**c**) A significant difference in duration of LORR between "Littermates" and non-pair-fed *Bdnf*$^{klox/klox}$ mice was detected (Student's t-test, t[12] =5.384, *p < 0.0001) (**d**) A significant difference in body mass between "Littermates" and non-pair-fed *Bdnf*$^{klox/klox}$ mice was detected (Student's t-test, t[12] =5.305, *p = 0.0025) (**e**) There was a significant difference in BEC between "Littermates" at Time 2 and "Littermates" at Time 3 and non-pair-fed *Bdnf*$^{klox/klox}$ at Time 2 (one-way ANOVA, t[2,15] = 19.28, *p < 0.001) (n = 6-8/group).

To further demonstrate that the enhanced sleep time in *Bdnf*$^{klox/klox}$ mice was not exclusively the result of increased body mass, LORR was performed in pair-fed *Bdnf*$^{klox/klox}$ and wildtype mice (Figure 5.7). A significant effect of genotype was found for duration of LORR (Figure 5.7, **b**) between groups of mice that had similar body masses (Figure 5.7, **c**). The observed effect was not as robust as with non-pair-fed animals, suggesting that the duration of LORR in non-pair-fed *Bdnf*$^{klox/klox}$ mice was probably attributable to a combination of altered pharmacokinetics and pharmacodynamics. BECs measured at Time 2 for this cohort of mice once again indicated that *Bdnf*$^{klox/klox}$ mice required lower blood ethanol concentrations to regain LORR (Figure 5.8, **a**). To establish there was not an altered blood: brain ethanol ratio in *Bdnf*$^{klox/klox}$ mice that contributed to the phenotype, another group of mice was subjected to LORR, and whole brain samples were collected for the determination of BrEC. A significant decrease in BrEC at Time 2 confirmed that the sedative effect of ethanol persisted at lower internal ethanol concentrations in *Bdnf*$^{klox/klox}$ mice compared to wildtype littermates (Figure 5.8, **b**).

Correlation analysis was used to further determine the potential impact of body mass on ethanol LORR. The latency and duration data for pair-fed *Bdnf*$^{klox/klox}$ and wildtype mice from all experiments were collapsed and plotted against body mass. A moderately strong positive linear relationship was found between body mass and duration when both genotypes were included, but no relationship was detected for latency to LORR (Figure 5.9, **a, b**). The data was broken down to examine the contribution of each genotype to the relationship between body mass and LORR. Interestingly, no significant correlation was detected for mass and duration within the

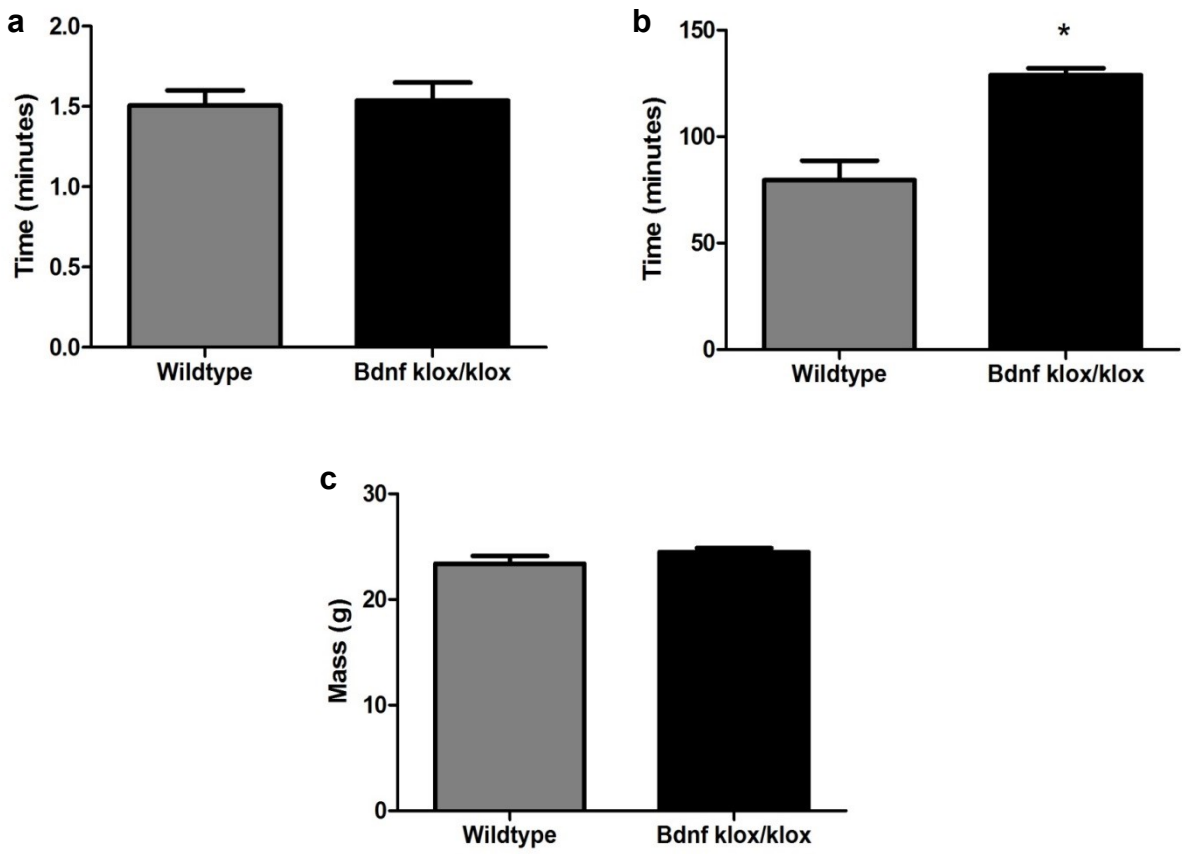

Figure 5.7 – LORR in pair-fed *Bdnf*$^{klox/klox}$ mice. (**a**) No significant difference in latency to LORR was detected between wildtype and pair-fed *Bdnf*$^{klox/klox}$ mice (Student's t-test, *t*[8] = 0.2198) (**b**) There was a significant difference in duration of LORR between wildtype and pair-fed *Bdnf*$^{klox/klox}$ mice (Student's t-test, t[8] =5.101, *p = 0.0009) (**d**) There was no difference in body mass between wildtype and pair-fed *Bdnf*$^{klox/klox}$ mice (Student's t-test, t[8] = 1.344), (n = 5/group).

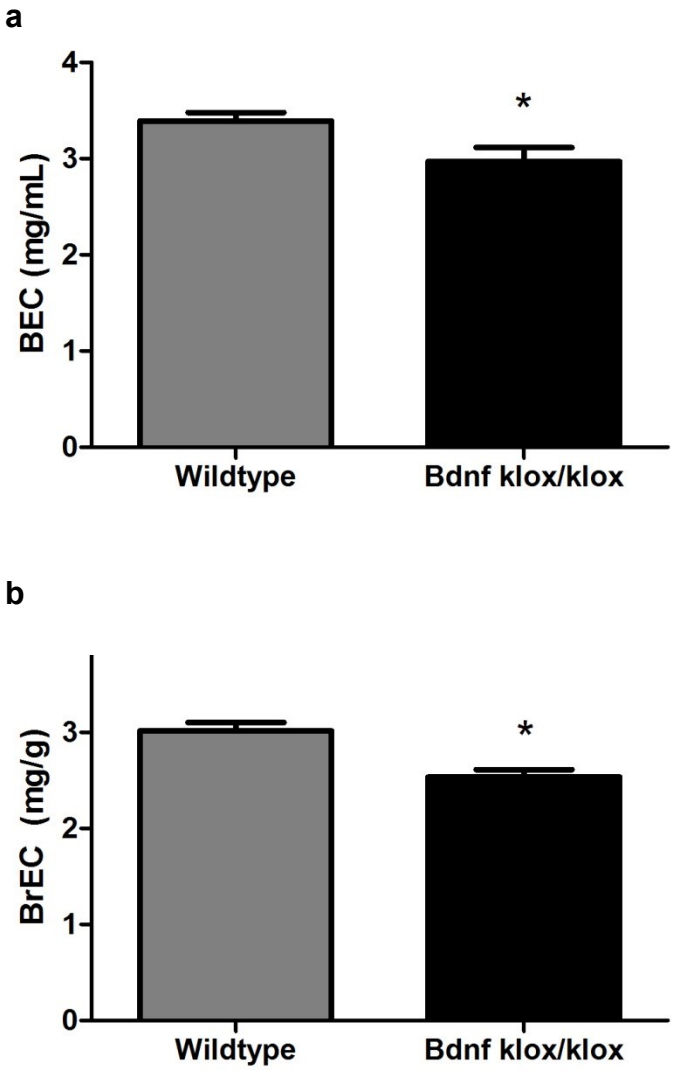

Figure 5.8 – Internal ethanol concentration of pair-fed *Bdnf*$^{klox/klox}$ mice at LORR Time 2. At the relative time of regaining loss of righting reflex, *Bdnf*$^{klox/klox}$ mice have lower (**a**) BEC (Student's t-test, *t*[8] = 2.49, *p = 0.0375) and (**b**) BrEC (Student's t-test, *t*[17] = 4.205, *p = 0.0006) as compared to wildtype animals (n = 5-10/group).

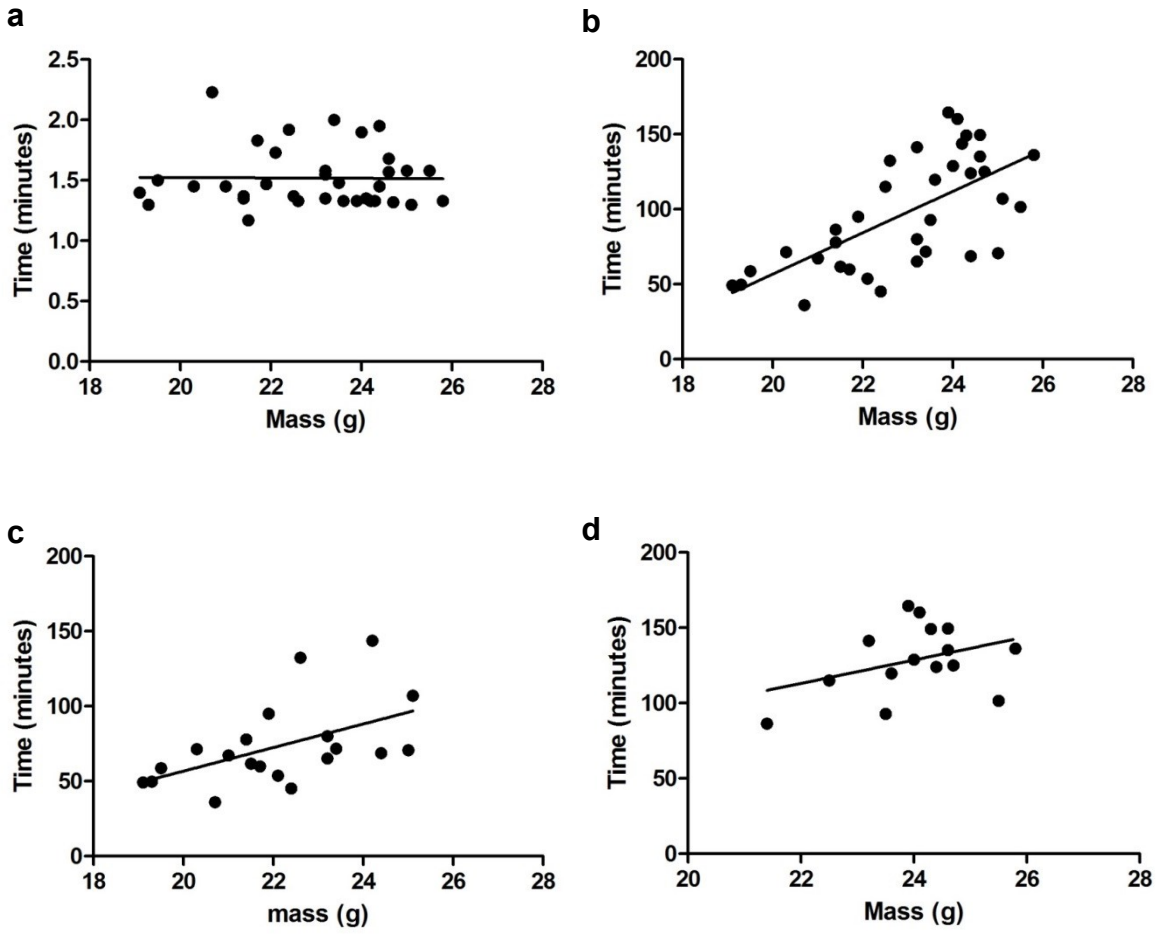

Figure 5.9 – Correlation between body mass and latency and duration of LORR. Subjects from all pair-fed animal LORR experiments were pooled for correlation analysis. (**a**) There was no significant correlation between body mass and latency to LORR (F[1,33] = 0.004, r = 0.011, p = 0.9459, n = 35/group) (**b**) A moderately strong positive linear relationship was found between body mass and duration (F[1,33] = 25.63, r = 0.66, p < 0.0001, n = 35/group) (**c**) A fairly strong positive relationship was found in the wildtype animals (F[1,18] = 6.549, r = 0.52, p = 0.0197, n = 20/group) (**d**) No significant correlation was detected for pair-fed *Bdnf*$^{klox/klox}$ mice (F[1,13] = 2.056, r = 0.37, p = 0.1752, n = 15/group).

pair-fed *Bdnf*$^{klox/klox}$ mice (Figure 5.9, **d**), while a fairly strong positive relationship was found in the wildtype animals (Figure 5.9, **c**). These results indicated that even amongst wildtype mice, pharmacokinetics may play a role in duration of LORR. This concept is compatible with data from the human literature that shows differences in lean body mass between males and females contributes to observed differences in impairment after administration of equivalent doses of alcohol adjusted for body weight (Mumenthaler *et al.*, 1999). This outcome suggests the need for increased awareness of balancing all variables, including weight, when dividing subjects into treatment groups for LORR.

Bdnf$^{klox/klox}$ *mice consume more ethanol, quinine, and saccharin in two-bottle choice.*

In the voluntary two-bottle choice paradigm, *Bdnf*$^{klox/klox}$ mice exhibited a concentration-dependent increase in ethanol intake, consuming significantly more 15% but not 7.5% ethanol as compared to wildtype littermates (Figure 5.10, **a**). Although not significant, there was an apparent trend toward increased consumption for the 7.5% concentration. *Bdnf*$^{klox/klox}$ mice also consumed a greater amount of 15% ethanol as compared to 7.5% ethanol whereas wildtype mice's level of consumption did not change between concentrations. For ethanol preference there was a main effect of concentration, as both genotypes had a greater preference ratio for 7.5% ethanol than 15% ethanol (Figure 5.10, **b**). Although there was a trend, no significant difference in preference between *Bdnf*$^{klox/klox}$ and wildtype mice was detected at either concentration. The concentration-dependent increase in ethanol intake by *Bdnf*$^{klox/klox}$ mice was not the result of differences in total fluid intake, as no effect of genotype or ethanol

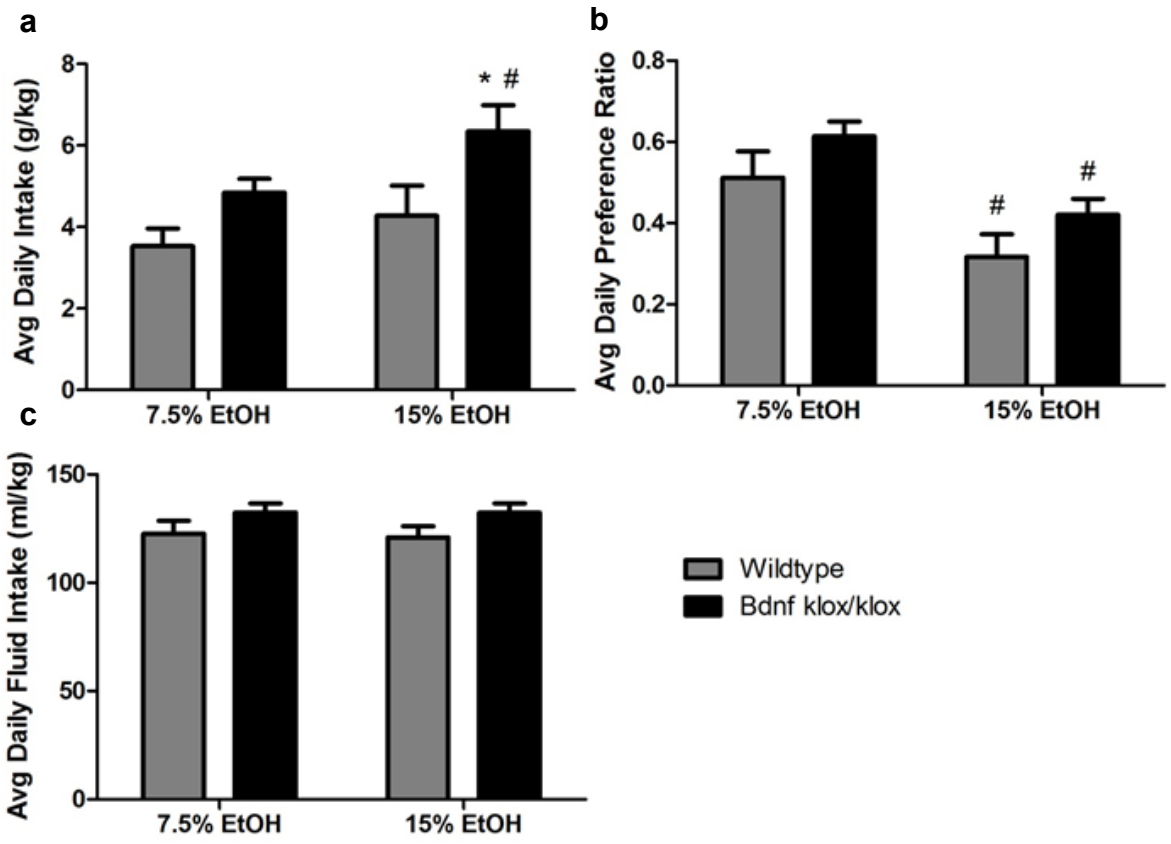

Figure 5.10 – Altered ethanol consumption in *Bdnf*$^{klox/klox}$ mice. In a classical two-bottle choice paradigm *Bdnf*$^{klox/klox}$ mice had (**a**) greater daily intake of 15% ethanol as compared to 7.5% (F[1,33] = 10.467, *p = 0.002) and greater daily intake of 15% ethanol as compared to wildtype (F[1,33] = 5.609, $^{\#}$p = 0.012). There was a trend for greater intake at 7.5% between genotypes (F[1,33] = 10.467, p = 0.106) (**b**) Both wildtype and *Bdnf*$^{klox/klox}$ mice exhibited decreased preference for 15% ethanol as compared to 7.5% (F[1,33] = 62.46, *p < 0.001), but no difference between genotype was detected (F[1,33] = 2.623, p = 0.115) (**c**) No difference in average daily fluid intake was detected between ethanol concentrations, but there was a trend for genotype (F[1,33] = 0.349, p = 0.559, F[1,33] = 3.395, p = 0.074). (Two-way, repeated measures ANOVA, Tukey's HSD *post-hoc*, n = 15-20/genotype).

concentration was detected (Figure 5.10, **c**). Of note, ethanol intake for both wildtype and *Bdnf*$^{klox/klox}$ mice was substantially lower than C57BL/6J intake levels previously reported by this lab (~10g/kg/18hr) (Khisti *et al.*, 2006), indicating a possible confounding effect of environmental factors specific to this study.

Ethanol is consumed orally and it has been shown that genetic manipulations that alter taste perception can lead to changes in ethanol preference and consumption (Blednov *et al.*, 2008). Therefore, taste preference studies are typically performed to test altered palatability of sweet and bitter tastes that could confound genotypic differences in ethanol consumption. Moderate aversion to bitter taste was tested using 30 μM QHCl, a concentration previously used in the literature (Bachmanov *et al.*, 1996; Tordoff, 2007). *Bdnf*$^{klox/klox}$ mice had a significantly greater intake of 30 μM QHCl as compared to wildtype mice (Figure 5.11, **a**), with no difference in total fluid consumed, but a trend towards increased preference in *Bdnf*$^{klox/klox}$ mice (Figure 5.11, **b, c**). This concentration of QHCl did not result in aversion for either genotype (one-sample t-test, $\mu = 0.50$, $t_{wildtype}[14] = 1.7023$, $p = 0.1108$, $t_{klox/klox}[19] = 0.2516$, $p = 0.8040$). Therefore animals were retested with 75 μM QHCl, in an attempt to alter preference. Once again, *Bdnf*$^{klox/klox}$ mice had greater intake of 75 μM QHCL (Figure 5.11, **d**), this time with a significant increase in preference for the bitter tastant as compared to wildtype (Figure 5.11, **e**). Proclivity for consumption of sweet tasting solutions was measured using 2 mM saccharin, a concentration previously used in the literature (Tordoff, 2007). *Bdnf*$^{klox/klox}$ mice consumed greater quantities of 2 mM saccharin as compared to wildtype (Figure 5.11, **g**), with no difference in preference between the genotypes as a result of the significantly greater volume of fluid consumed by *Bdnf*$^{klox/klox}$ animals

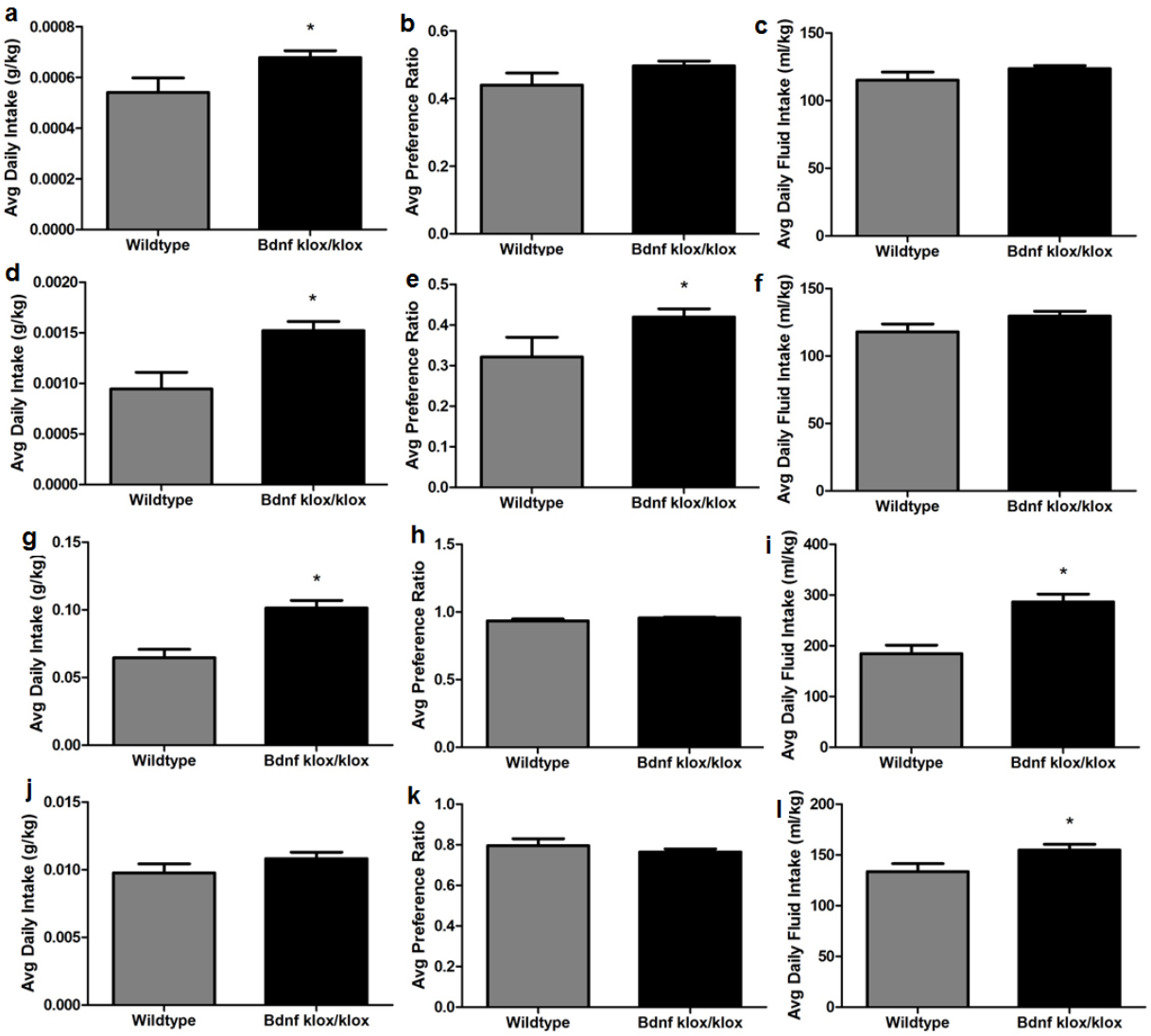

Figure 5.11 – Altered quinine and saccharin consumption in *Bdnf*$^{klox/klox}$ mice. Taste preference studies were performed to test taste palatability of sweet and bitter tastants. Average daily intake, preference, and total fluid consumption was measured for (**a-c**) 30 μM QHCl (t[33] = 2.349, *p = 0.03, t[33] = 1.636, p = 0.11, t[33] = 1.479, p = 0.11) (**d-f**) 75 μM QHCl (t[33] = 3.275, *p = 0.03, t[33] = 1.982, *p = 0.05, t[33] =1.791, p = 0.08) (**g-i**) 2 mM saccharin (t[33] = 4.352, *p = 0.0001, t[33] = 1.464, p = 0.15, t[33] =4.479, *p < 0.0001) (**j-k**) 0.5 mM saccharin (t[33] = 1.335, p = 0.19, t[33] = 0.8970, p = 0.38, t[33] =2.252, p = 0.03). Student's t-test, n = 15-20/genotype.

(Figure 5.11, **h, i**). In an attempt to determine if a difference in preference for saccharin actually existed between the genotypes, animals were retested with a 0.5 mM solution. At this concentration, no difference in intake or preference was found (Figure 5.11, **j, k**), despite a significant preference over water for both genotypes (one-sample t-test, $\mu = 0.50$, $t_{wildtype}[14] = 8.5988$, $p < 0.0001$, $t_{klox/klox}[19] = 18.1594$, $p < 0.0001$). The results of these taste preference experiments obfuscate the finding that *Bdnf*$^{klox/klox}$ mice had a concentration-dependent increase in ethanol intake. Differences in saccharin consumption do not necessarily negate the significance of increased ethanol intake, since hedonic responses to sweet tastes are considered a biomarker of predisposition to alcoholism in humans (Kampov-Polevoy *et al.*, 2004). However, in conjunction with the QHCl results, the voluntary consumption data is difficult to interpret.

Wildtype and Bdnf$^{klox/klox}$ *mice display similar preference in ethanol CPP.*

A previous study reported that *Bdnf*$^{+/-}$ mice exhibit enhanced preference scores in ethanol CPP (McGough *et al.*, 2004). Additionally, rats injected with a lentivirus over-expressing *Bdnf* in the dorsal lateral striatum had attenuated ethanol-induced conditioned preference (Bahi & Dreyer, 2013). A major component of the CPP paradigm is the learned association between conditioned stimulus and unconditioned stimulus (Bardo & Bevins, 2000) and synaptic plasticity is an important neurochemical foundation for the processes of learning and memory. It was therefore hypothesized that synaptically targeted *Bdnf* is involved in the conditioned response to ethanol, and that *Bdnf*$^{klox/klox}$ mice would have augmented preference scores as compared to wildtype animals. Following conditioning with saline-ethanol (2.0 g/kg) twice daily for 3 days,

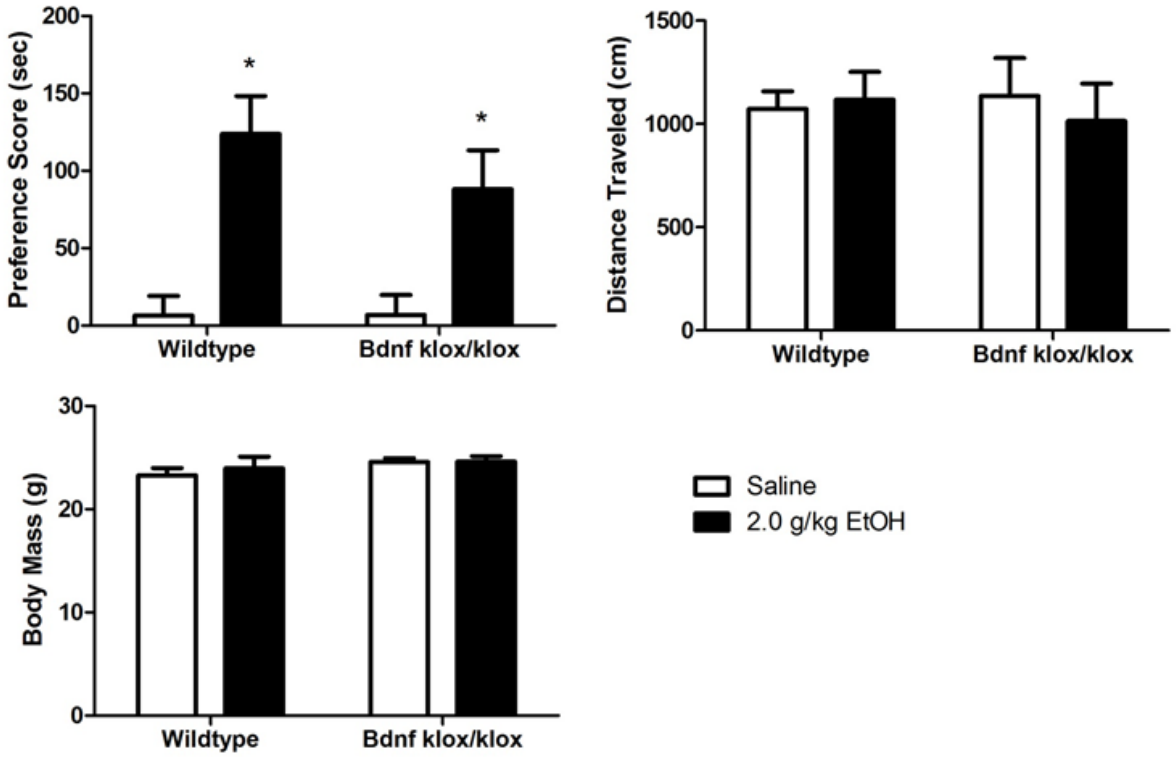

Figure 5.12 – Ethanol CPP in *Bdnf*$^{klox/klox}$ mice. The rewarding properties of 2.0 g/kg ethanol were tested in *Bdnf*$^{klox/klox}$ and wildtype mice. (**a**) Both genotypes exhibited a significant preference for the chamber paired with ethanol (F[1,51] = 23.312, *p < 0.01, n = 12-14/group). However, there was no difference in preference score between genotypes (F[1,51] = 0.740, p = 0.394, n = 12-14/group). (**b**) There was no difference in the locomotor activity amongst any of the groups on test day ($F_{genotype}$[1,23] = 0.0182, p = 0.894, $F_{treatment}$[1,23] = 0.0600, p = 0.809, n = 6-7/group). (**c**) While there was a trend, no significant difference in body mass was detected between genotypes (F[1,23] = 3.739, p = 0.066). Treatment groups were equally balanced for body mass (F[1,23] = 0.0763, p = 0.785, n = 6-7/group). (Two-way ANOVA, Tukey's HSD *post-hoc*).

Bdnf$^{klox/klox}$ and wildtype mice both exhibited a place preference greater than animals that were paired with saline in both chambers (Figure 5.12, **a**). No genotypic difference in ethanol preference score was detected. Additionally, there was no significant difference in body mass or locomotor activity on test day between any of the experimental groups (Figure 5.12, **b, c**). These results suggest that a lack of synaptically targeted *Bdnf* does not alter the reward-like properties of ethanol as measured by CPP.

Bdnf$^{klox/klox}$ *mice have reduced basal anxiety-like behavior.*

A pilot study to examine the function of synaptically targeted *Bdnf* in ethanol-induced anxiolysis was performed utilizing the light-dark box (LDB) model of anxiety. Basal anxiety-like behavior was assessed with administration of 0.9% saline. Ethanol-induced anxiolysis was evaluated using 1.5 g/kg ethanol, a dose that did not produce a differential locomotor response between the genotypes (Figure 5.2, 5.3, **c**). Previous dose-response studies in our laboratory had determined that a 1.8 g/kg dose of ethanol elicits a significant increase in PTS and PDT in the light. This dose was found to cause marked decreases in total distance traveled by *Bdnf*$^{klox/klox}$ mice in the LDB assay (data not shown). Figure 5.13 depicts the results of the present study, which found a main effect of genotype for both PTS and PDT in the light, with a significant increase for *Bdnf*$^{klox/klox}$ as compared to wildtype in saline treated animals (Figure 5.13, **a, b**). Although there was a trend, no difference was found between the genotypes when treated with ethanol and there was no main effect of treatment. The effect of genotype was not detected when looking at latency to enter the light (Figure 5.13, **c**). However,

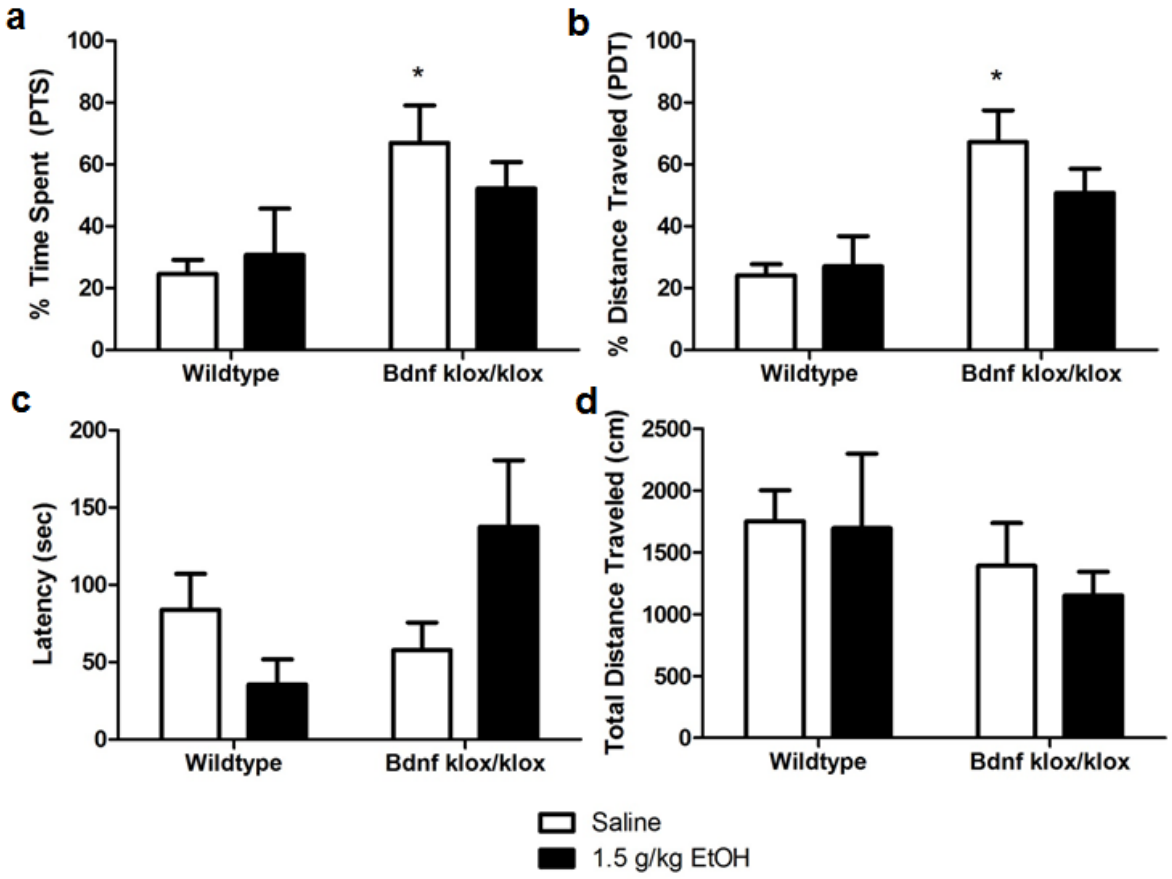

Figure 5.13 – Light-dark box (LDB) assay for anxiety-like behavior in *Bdnf*$^{klox/klox}$ mice. Basal anxiety-like behavior and ethanol-induced anxiolysis were measured in *Bdnf*$^{klox/klox}$ and wildtype mice. *Bdnf*$^{klox/klox}$ mice had a significant increase in basal (**a**) PTS (F[1,30] = 9.131, *p = 0.008) and (**b**) PDT in the light (F[1,30] = 9.131, *p = 0.002). There was a trend for a difference between genotypes in both PTS and PDT following 1.5 g/kg ethanol (F[1,30] = 9.131, p = 0.162, F[1,30] = 9.131, p = 0.072) (**c**) There was no effect of genotype or treatment on latency to enter the light compartment, although this measure exhibited high variability ((F[1,29] = 0.394, p = 0.535, F[1,29] = 0.219, p = 0.643). (**d**) Total distance traveled in the LDB assay was not affected by genotype or ethanol treatment ($F_{genotype}$[1,30] = 2.009, p = 0.167, $F_{treatment}$[1,30] = 0.215, p = 0.647). (Two-way ANOVA, Tukey's HSD *post-hoc*, n = 5-14/group).

there was a trend towards increased latency in the *Bdnf*$^{klox/klox}$ mice after ethanol as compared to wildtype, which was in contrast to the PTS and PDT data. Overall, there was no significant difference in total locomotor activity amongst any of the groups (Figure 5.13, **d**). These data indicate that *Bdnf*$^{klox/klox}$ mice have a lower basal anxiety-like behavior, and suggest no effect of 1.5 g/kg ethanol in either genotype. However, this was a preliminary assessment, and therefore experiments need to be repeated with larger sample sizes to make any definitive conclusions. Furthermore, since "anxiety" is a complex trait comprised of multiple phenotypic dimensions (Cryan & Holmes, 2005; Ramos, 2008), it may be prudent to test these mice in other anxiety-like behavior models, such as elevated plus maze or marble burying, to dissect the underlying factors contributing to the basal response in *Bdnf*$^{klox/klox}$ mice.

Bdnf$^{klox/klox}$ *mice have an altered ethanol metabolism time course.*

Ethanol metabolism was assessed to further investigate possible alterations in pharmacokinetic profiles between genotypes. As expected, BEC decreased significantly with time (Figure 5.14, **a**). There was also a main effect of genotype, but *post-hoc* analysis only found a significant difference between wildtype and *Bdnf*$^{klox/klox}$ mice at the 10 minute time point. Linear regression analysis concluded that the slopes of the metabolism curves were significantly different (Figure 5.14, **a**), suggesting a faster rate of metabolism in *Bdnf*$^{klox/klox}$ mice. For the mice used in this experiment, a main effect of genotype was detected when analyzing body mass (Figure 5.14, **b**). However, no difference was detected between animals used for any particular time point. Further

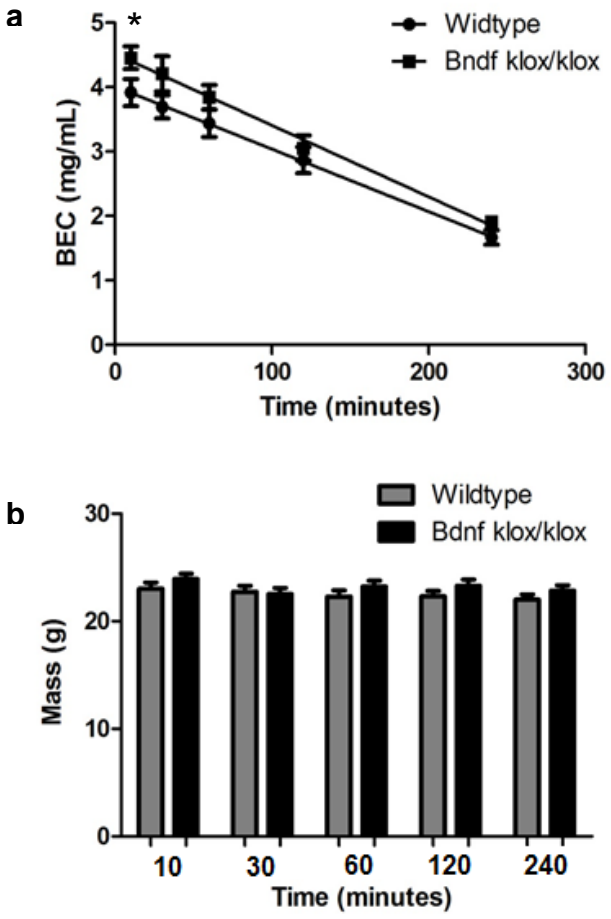

Figure 5.14 – Ethanol metabolism time course for *Bdnf*$^{klox/klox}$ and wildtype mice. (**a**) Analysis of the ethanol metabolism time course found a main effect of genotype and time, but no significant interaction of genotype x time ($F_{genotype}$[1,34] = 10.614, p = 0.003, F_{time}[4,34] = 59.232, p < 0.001, $F_{interaction}$[4,34] = 0.374, p = 0.825). *Bdnf*$^{klox/klox}$ mice had a significantly different BEC at the 10 minute time point as compared to wildtype (*p = 0.043). Linear regression determined that the metabolism curves for *Bdnf*$^{klox/klox}$ and wildtype mice had significantly different slopes, indicating a difference in rate of ethanol metabolism (wildtype slope = -0.009709 ± 0.0001182, *Bdnf*$^{klox/klox}$ slope = -0.01110 ± 0.0004791, F[1,6] = 7.89, p = 0.03). (**b**) Statistical analysis of body mass for the genotypes, broken down by time point, reveals a main effect of genotype, but no significant difference at any given time point (Two-way ANOVA, Tukey's HSD *post-hoc*, F[1,34] = 4.179, p = 0.049, n = 4-5/group).

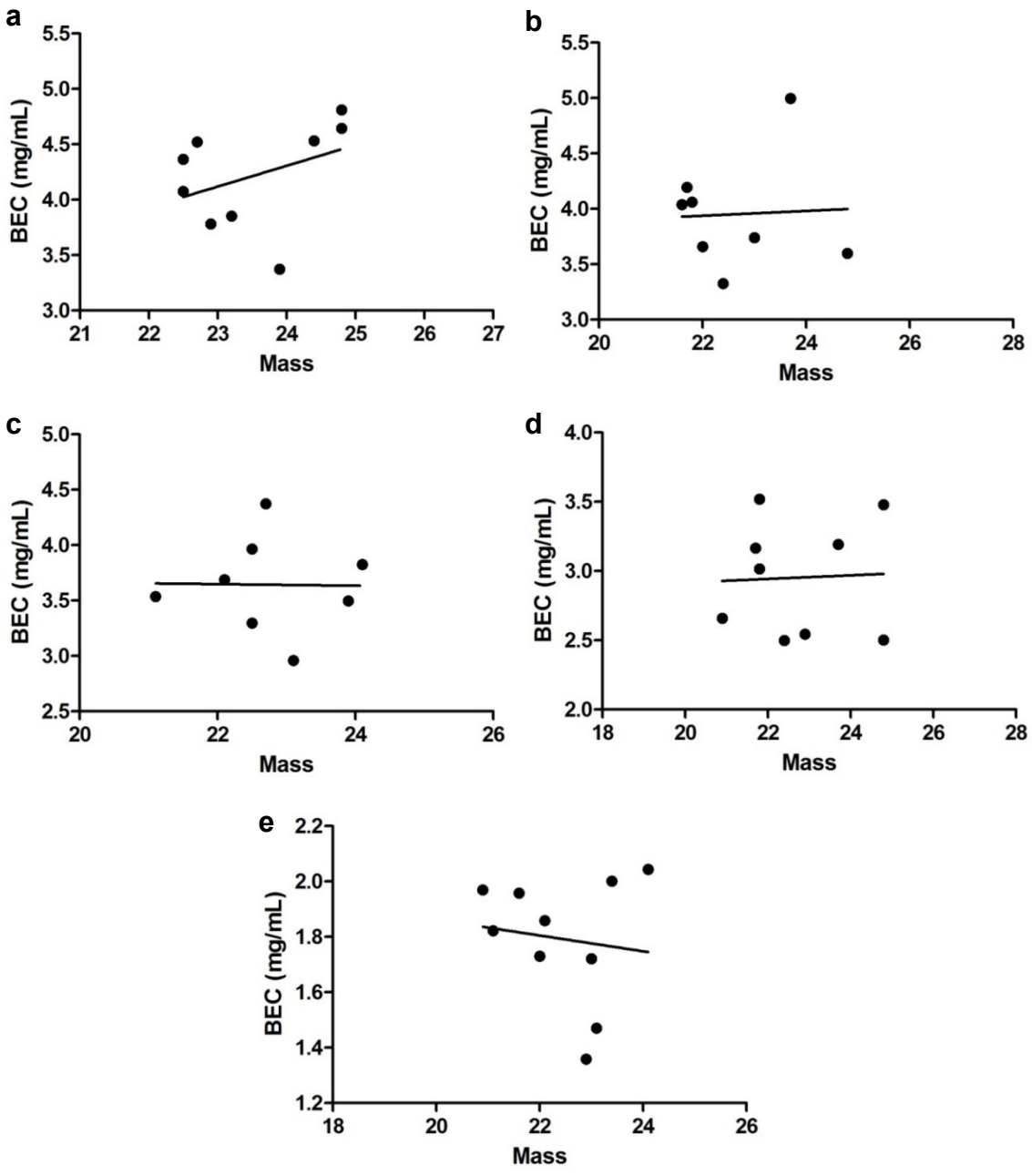

Figure 5.15 – Correlation between body mass and BEC. Linear regression was used to examine the correlation between body mass and BEC for *Bdnf*$^{klox/klox}$ and wildtype mice at each time point. (**a**) 10 minute $F[1,7] = 1.185$, r = 0.38, p = 0.31 (**b**) 30 minute $F[1,6] = 1.185$, r = 0.04, p = 0.91 (**c**) 10 minute $F[1,6] = 0.001$, r = 0.02, p = 0.9698 (**d**) 10 minute $F[1,7] = 0.013$, r = 0.04, p = 0.9109 (**e**) 10 minute $F[1,8] = 0.1379$, r = 0.13, p = 0.72).

examination into the relationship between body mass and BEC at each time point found no significant correlation (Figure 5.15, **a-e**).

Discussion

Bdnf$^{klox/klox}$ mice provided a unique model to study the implications of altered synaptic trafficking of an ethanol responsive gene. A behavioral characterization of these mice revealed the importance of proper mRNA localization in ethanol-responsive behaviors. In particular, ethanol-induced locomotor activation and LORR were found to be susceptible to changes in *Bdnf* transport. This series of experiments indicated that *Bdnf*$^{klox/klox}$ mice have an altered pharmacokinetic profile. However, evidence also suggests they have a greater sensitivity to both low and high dose ethanol that was the result of altered pharmacodynamic properties of the drug.

The biphasic behavioral response to ethanol is thought to reflect ethanol's action at multiple receptor and neurotransmitter systems (Grant, 1999; Quertemont *et al.*, 2003). Support for this comes from ethanol discriminative stimulus studies that show the substitution pattern of various receptor ligands, such as $GABA_A$, NMDA, and 5-HT, are dose and time dependent (Colombo & Grant, 1992; Grant & Colombo, 1993; Grant *et al.*, 1997; Green & Grant, 1998; Quertemont *et al.*, 2003). In particular, the actions of low and intermediate doses of ethanol appear to be mediated by $GABA_A$ positive modulation and 5-HT_1 agonism (Grant & Colombo, 1993; Grant *et al.*, 1997; Green & Grant, 1998). At higher doses, ethanol's antagonism of NMDA receptors appears more influential to the discriminative stimulus (Green & Grant, 1998). Our results showed that *Bdnf*$^{klox/klox}$ mice had increased sensitivity to both low dose ethanol (increased locomotor

activity at 1.0 g/kg ethanol, Figure 5.2) and high dose ethanol (decreased locomotor activity at 2.5 g/kg and enhanced duration of LORR, Figure 5.2 and Figure 5.7, **b**). This suggests that *Bdnf*$^{klox/klox}$ mice may have altered functioning of multiple receptor-signaling cascades as a result of reduced trafficking of *Bdnf* to the synapse. This is not unfounded conjecture, as BDNF signaling has been shown to modulate several neurotransmitter systems; including GABA and glutamate (Tanaka *et al.*, 1997; Levine *et al.*, 1998; Lin *et al.*, 1998; Brunig *et al.*, 2001; Jovanovic *et al.*, 2004). Additionally, *Bdnf* heterozygous knockouts (Korte *et al.*, 1995) and *Bdnf*$^{klox/klox}$ mice (An *et al.*, 2008) have been shown to have altered CA1 region long-term potentiation (LTP); an NMDA receptor-dependent form of LTP (Tsien *et al.*, 1996).

Alternatively, the observed difference in metabolism between *Bdnf*$^{klox/klox}$ mice and wildtype littermates (Figure 5.14, **a**) suggests that increased ethanol sensitivity to low and high doses may result from a shift in the dose response curve. An examination of our ethanol-induced locomotor activity data indicates this is not a sufficient explanation. *Bdnf*$^{klox/klox}$ mice exhibited an increased level of response to 1 g/kg ethanol that extended for the entire 60 minute testing period (Figure 5.3, **b)**. This protracted response was not observed in wildtype animals at any tested dose. Testing higher doses would elicit sedating effects of ethanol in wildtype mice, not an activating response. While a residual difference in lean body mass of the pair-fed animals cannot be overlooked as a potential factor, these data suggest a pharmacodynamic mechanism is involved.

Our LORR data also indicates that the increased sensitivity of *Bdnf*$^{klox/klox}$ mice is not exclusively the consequence of an altered pharmacokinetic profile. From blood

collected during LORR, we observed that wildtype mice regained their righting reflex at a BEC of 3.39 mg/mL (Figure 5.8, **a**), after a period of 79.6 minutes (Figure 5.7, **b**). Even if volume of distribution was a factor, *Bdnf*$^{klox/klox}$ mice should still have regained their righting reflex at a similar BEC to wildtype animals, but at a later time. From the ethanol metabolism curve, it was determined that *Bdnf*$^{klox/klox}$ animals were reaching a BEC of 3.39 mg/ml at an average time of 101.4 minutes. This was not significantly different from the time wildtype mice reached this BEC, but was significant from the average time at which *Bdnf*$^{klox/klox}$ mice were regaining their righting reflex, 128.9 minutes (one-sample, one-tailed t-test, $t[4] = -2.3469$, $p = 0.03939$). One explanation is that *Bdnf*$^{klox/klox}$ mice have an aberrant AFT, or a reduced capacity for the rapid neuroadaptations that occur during a single exposure to ethanol that result in less impairment during the falling phase of the BEC curve as compared to the same BEC in the rising phase. To confirm this hypothesis, BEC should be measured at Time 1 and a more accurate measurement of latency to LORR is required. The Crabbe/Ponomarev protocol for LORR improves detection of onset by utilizing a restraint apparatus that decreases the loss-of-function criterion from 30 second to 5 second intervals (Ponomarev & Crabbe, 2002). In conjunction with BEC determination at Time 1, this would increase sensitivity of AFT determination.

While our studies were in progress, a report was published using *Bdnf* heterozygous knockout mice which were shown to exhibit enhanced duration of LORR (Kim *et al.*, 2012). The authors of this paper also made use of adenylyl cyclase (AC) 5 KO and heterozygous *Camk2a* mice. AC5 null mice had an up-regulation of BDNF in the dorsal striatum (DS), but not the NAc, and exhibited a reduced duration of LORR. In

contrast, *Camk2a*$^{+/-}$ mice had decreased levels of BDNF in the DS and enhanced duration of LORR. In addition, the AC5 KO mice had increased basal levels of p-NR2B in the DS, but not the NAc. Phosphorylation of NR2B by the non-receptor tyrosine kinase, Fyn, has been shown to modulate the acute sedative-hypnotic properties of alcohol, and is thought to contribute to the development of AFT (Miyakawa *et al.*, 1997; Yaka *et al.*, 2003b). BDNF signaling, through its high affinity receptor, TrkB, has been shown to rapidly modulate NMDA receptor function through phosphorylation by Fyn kinase in the hippocampus and mPFC (Levine *et al.*, 1998; Lin *et al.*, 1998; Xu *et al.*, 2006; Otis *et al.*, 2014). This specific pathway has yet to be verified in the striatum. The Kim *et al*. (2012) study, in conjunction with our work, was the first to demonstrate a function of BDNF in duration of LORR following acute ethanol exposure. Together they suggest that BDNF, perhaps specifically through translation of its synaptically trafficked message, is involved in the modulation of NMDA receptors, contributing to AFT.

While the lack of synaptically targeted *Bdnf* seems to alter sensitivity to both low and high dose ethanol, its effect on the rewarding properties of the drug is more ambiguous. Due to the hyperphagic nature of *Bdnf*$^{klox/klox}$ mice, the use of a pair-feeding paradigm was necessary to maintain body masses comparable to wildtype animals. This required a restriction on the amount of food these mice would naturally consume. It has been suggested that the rewarding effects of drugs of abuse are mediated by neural substrates that control the incentive-motivating effects of natural reinforcers, such as food (Wise, 1982; Koob, 1992). The fact that food restriction enhances the central rewarding effects of abused drugs is well established (Carroll *et al.*, 1979; Cabeza de Vaca & Carr, 1998; Stuber *et al.*, 2002). For instance, food restriction has

been shown to enhance self-administration and CPP by the psychostimulants cocaine and amphetamine (Carroll *et al.*, 1979; Bell *et al.*, 1997; Cabeza de Vaca & Carr, 1998; Stuber *et al.*, 2002). There is ample evidence that the regulation occurs through molecular adaptations in the NAc involving the dopamine signaling pathway, particularly downstream of the D1 receptor (Haberny *et al.*, 2004; Pan *et al.*, 2006; Zhen *et al.*, 2006; Carr *et al.*, 2009). Despite the pair-feeding schedule, $Bdnf^{klox/klox}$ mice did not show a difference in ethanol-induced CPP compared to wildtype (Figure 5.12, **a**). This suggests that ethanol's rewarding properties are not altered in these mice. However, a more appropriate interpretation of results would require an experimental deign that uses both pair-fed and non-pair animals.

Food restriction has also been shown to affect ethanol consumption, in a strain-specific manner. Schroff, *et al*., (2004) showed that after a 12 day food restriction, which resulted in a 20% loss of body weight followed by a recovery period, B6 but not D2 mice had higher ethanol intake and preference in a two-bottle choice paradigm (Schroff *et al.*, 2004). Our two-bottle choice drinking studies do show that $Bdnf^{klox/klox}$ mice have an increased avidity for consumption of ethanol (Figure 5.10, **a**). However, food restriction cannot be eliminated as a cause. Not only is there a potential for altered brain chemistry, but a simple attempt to supplement caloric intake may be the underlying basis for the behavior. Various controls were considered for the drinking studies, including giving the mice access to saccharin-adulterated ethanol and isocaloric sucrose. These solutions would have been made equivalent in caloric value, and balanced for level of sweetness. Unfortunately, our taste preference studies indicated

differential consumption of saccharin between the genotypes (Figure 5.11, **j**) that would have confounded these studies as well.

Evidence in the literature suggests that the increased consumption of saccharin in the Bdnf$^{klox/klox}$ mice may be the result of altered leptin signaling. Bdnf$^{klox/klox}$ mice lack the long 3' UTR containing *Bdnf* transcript that is preferentially trafficked to the synapse. This has been shown to compromise the ability of leptin, an anorectic hormone, to activate hypothalamic neurons and perform its central function of inhibiting food intake, contributing to the hyperphagic obesity in these mice (Liao *et al.*, 2012). Administration of leptin has been shown to reduce sucrose self-administration in rats through a centrally mediated mechanism (Figlewicz *et al.*, 2006). It has also been shown to suppress responses of peripheral taste nerves to both saccharin and sucrose (Kawai *et al.*, 2000). However, leptin administration did not affect response of peripheral taste nerves to quinine (Kawai *et al.*, 2000). Further research will be required to determine the cause of altered quinine palatability in Bdnf$^{klox/klox}$ mice, but it could indicate disrupted orosensory functioning or a deficit in taste processing.

While Bdnf$^{klox/klox}$ mice did provide a distinctly unique model to investigate disruption in mRNA trafficking of a known ethanol-responsive gene, it was not without its limitations. First, these mice are a traditional knock-in strain. An inherent disadvantage being that the missing transcript variant was not expressed throughout development. This is especially of concern since BDNF is particularly influential in the developing nervous system. However, simply because these phenotypes could be the result of developmental abnormalities does not diminish our findings. One could hypothesize that since synaptically targeted *Bdnf* has been shown to modulate dendritic

spine morphology (An *et al.*, 2008), a developmental alteration in synaptic functioning could set up a neural circuitry that is differentially sensitive to ethanol. This system would still provide a resource for advancing the understanding of ethanol's neuropharmacological actions.

Another limitation is that these studies were not able to distinguish between the effects of reduced dendritic or increased somatic *Bdnf* on ethanol phenotypes. Evidence for a possible role of decreased dendritic *Bdnf* was established in the paper by An *et al.* (2008). Here they showed that overexpression of somatically restricted *Bdnf* in dorsal forebrain did not result in the same aberrant hippocampal dendritic spine morphology that was exhibited by $Bdnf^{klox/klox}$ mice. As a control for the present studies, a viral vector designed to overexpress the short 3' UTR isoform of *Bdnf* into various brain regions could distinguish the function of the two populations of *Bdnf* mRNA. This would further test the hypothesis that synaptic trafficking of *Bdnf* is necessary for the synaptic plasticity that contributes to ethanol behavioral responses.

Despite these limitations, this investigation was the first to show that disrupted mRNA localization of a known ethanol-responsive gene is sufficient to cause altered ethanol phenotypes. The manifestation of these behaviors was shown not to be completely dependent on pharmacokinetic mechanisms. The lack of synaptically targeted *Bdnf* resulted in greater ethanol sensitivity to both low and high dose ethanol which suggests an alteration to multiple neurotransmitter systems. In particular, loss of locally translated BDNF may hinder the compensatory regulation of NMDA receptors in response to ethanol, disrupting the development of AFT. In addition to the long 3' UTR, a polymorphism, Val66Met, has also been shown to disrupt dendritic trafficking of *Bdnf*

(Chiaruttini *et al.*, 2009). Data on the association between this variant and alcohol abuse disorders is inconsistent and appears dependent on ethnic population differences in allele frequency (Gratacos *et al.*, 2007; Shin *et al.*, 2010; Muschler *et al.*, 2011; Nedic *et al.*, 2013). However it suggests that further examination into genetic regulation of the synaptic mRNA populations and its potential effect on predisposition towards alcoholism is warranted.

Chapter 6 – Viral Vector Rescue of Bdnf $^{klox/klox}$ Altered Ethanol-Phenotypes

Introduction

Local translation of the synaptic transcriptome is one mechanism by which the neuron achieves localized activity-dependent regulation of function at the level of the individual synapse (Steward & Levy, 1982). We have demonstrated through the research presented in previous chapters, that not only is ethanol administration able to alter the complement of mRNA enriched at the synapse, but that at least some ethanol-responsive behaviors require proper synaptic targeting of specific transcripts. In particular, this latter finding was shown by altering the dendritic targeting of *Bdnf*.

The *Bdnf*$^{klox/klox}$ mouse provided a unique model in which to examine the effect of altered dendritic trafficking of a known ethanol-responsive gene. These mice, which possess a truncated variant of the long 3' UTR *Bdnf* isoform, were shown to have reduced synaptic *Bdnf* transcript and protein (An *et al.*, 2008). Our studies revealed that *Bdnf*$^{klox/klox}$ mice exhibited altered sensitivity to both low and high dose ethanol. However, determining whether these behaviors resulted from diminished synaptic or increased somatic *Bdnf* was not possible from the studies presented in Chapter 5 of this thesis.

Xu and colleagues, however, have previously used adeno-associated viral (AAV) vectors to express *Bdnf* constructs, compensating for loss of dendritically targeted *Bdnf* in *Bdnf*$^{klox/klox}$ *mice.* These vectors were designed to express *Bdnf*'s protein coding

sequence (CDS) linked to either the short 3' UTR (AAV-BDNF-A) or the long 3' UTR (AAV-BDNF-A*B) (Liao *et al.*, 2012). AAV-BDNF-A included the sequence up to and including the first endogenous polyadenylation signal, while AAV-BDNF-A*B encoded the entire 3' UTR, where the first polyadenylation signal was mutated. In a study of the effects of altered synaptic trafficking of *Bdnf* on obesity, AAV-BDNF-A injected bilaterally into the ventromedial hypothalamus of 2 week old *Bdnf*$^{klox/klox}$ pups only slightly reduced the body mass of the animals at 7 weeks of age (Liao *et al.*, 2012). However, AAV-BDNF-A*B was able to completely ameliorated the obesity phenotype (Liao *et al.*, 2012). This implicated a specific function for long 3' UTR *Bdnf* required for development of the phenotype that could not be completely overcome with simple over-expression of *Bdnf*.

As described in Chapter 5, *Bdnf*$^{klox/klox}$ mice had a significantly prolonged duration of ethanol loss of righting reflex (LORR). This was a consequence, at least in part, of altered pharmacodynamic actions of ethanol, and not simply the result of an altered pharmacokinetic profile. Through the use of *Bdnf* heterozygotes and siRNA knock-down of *Bdnf*, Kim *et al.* (2012) concluded that biochemical changes in the level of *Bdnf* in the dorsal striatum (DS) plays a critical role in ethanol-induced LORR (Kim, 2012). Additionally, Ron and colleagues have shown selective regulation of *Bdnf* expression in the DS, specifically the dorsolateral region, in response to ethanol (McGough *et al.*, 2004; Jeanblanc *et al.*, 2009; Logrip *et al.*, 2009). Thus, we selected the DS as a target area for delivery of AAV-BDNF vectors to more directly test the role of *Bdnf* dendritic targeting in the ethanol behavioral responses described in Chapter 5.

It was hypothesized that injection of AAV-BDNF-A*B, but not AAV-BDNF-A, into the DS of *Bdnf*$^{klox/klox}$ mice would rescue the altered ethanol phenotypes exhibited as a result of the mutation. Furthermore, if the observed behaviors derived from lack of dendritic and not increased somatic *Bdnf*, injection of AAV-BDNF-A into the DS of wildtype mice was expected to have no effect on ethanol-induced LORR or locomotor activation. This experiment still does not explicitly identify the action of synaptically targeted *Bdnf* as the cause of the observed genotypic differences. However, discovering a unique function for long 3' UTR containing *Bdnf*, which has been shown to be preferentially targeted to the dendrites, would be the first step in making this determination.

Materials and Methods

Plasmids. DNA for three plasmids (pAAV-BDNF-A, pAAV-BDNF-A*B, and pAAV-GFP) were received on Whatman filter paper from Dr. Baoji Xu at Georgetown University Medical Center, Washington, DC, USA. The BDNF-expressing AAV constructs (Figure 6.1, **a**) were previously generated by first subcloning the cytomegalovirus (CMV) promoter, the mouse *Bdnf* coding sequence that is extended at its 3' end with *Myc* epitope sequence, and the mouse genomic sequence encoding the short *Bdnf* 3' UTR (A) or the long *Bdnf* 3' UTR (A*B) into pBluescript II KS (-) (Liao *et al.*, 2012). The entire CMV-BDNF-Myc-A and CMV-BDNF-Myc-AB were removed from the plasmid by NotI restriction digest. The plasmid, pAAV-MCS (Stratagene, La Jolla, CA) (Figure 6.1, **b**) was digested with NotI to remove a 1.7 kb fragment and the two NotI

a

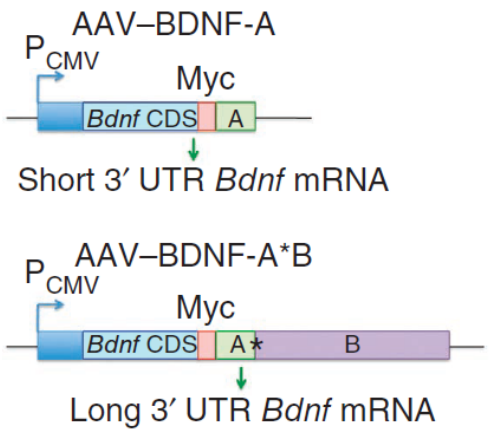

b

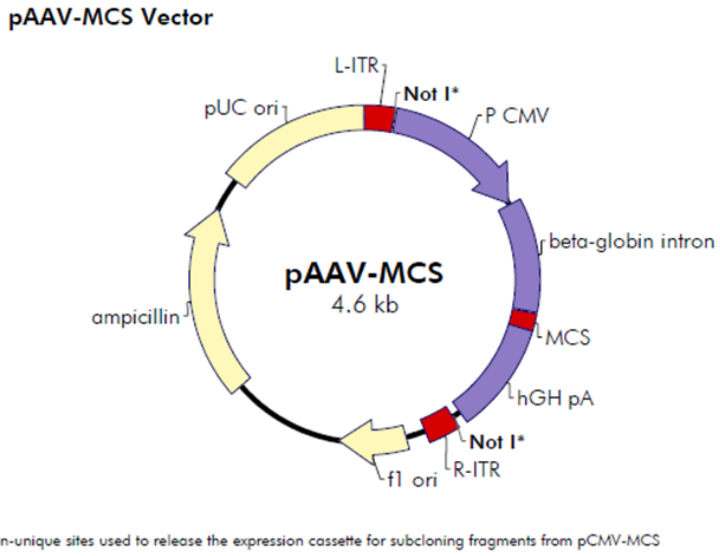

Figure 6.1 – Plasmid diagrams. Schematic of the (**a**) pAAV-BDNF-A and pAAV-BDNF-A*B plasmid constructs. Image reproduced with permission © Nature Medicine (Liao *et al.*, 2012). (**b**) Backbone structure for the pAAV-MCS vector from Stratagene.

fragments, CMV-BDNF-Myc-A (1.8 kb) and CMV-BDNF-Myc-AB (4.2 kb), were subcloned into the pAAV-MCS (Liao *et al.*, 2012). To extract the plasmids from the filter paper, a sterilized razor blade was used to cut around the outline that indicated the placement of DNA. The DNA-containing filter paper was then placed in a 1.5 ml microcentrifuge tube with 200 µL TE buffer and allowed to incubate for 2.5 hours at room temperature. A transformation reaction with XL-10 Gold *E. Coli* competent cells (Stratagene, La Jolla, CA) was set up for each of the three experimental plasmids, a positive control (pUC18), and a negative control (TE buffer) following the protocol from the Stratagene manual. Into a 14 ml cell culture tube, 100 µL of cells and 4 µL of 2-mercaptoethanol were added and allowed to incubate with intermittent swirling for 10 minutes. To each tube, either 5 µL of pAAV-BDNF-A, pAAV-BDNF-AB, pAAV-GFP or 1 µL 0.01 ng/µL pUC18 was added. Reactions were kept on ice for 30 minutes. Cells were heat shocked for 30 seconds at 42˚C, and then placed on ice for 2 minutes. Pre-warmed SOC media (900 µL) was added to each sample, which was then incubated at 37˚C with shaking (200 rpm) for 3 hours. Transformed cells (100 µL for experimental plasmids, 5 µL for pUC18) were plated onto pre-warmed sterile 1.5% agar plates infused with100 µg/ml ampicillin. All plates were incubated at 37˚C overnight. After 13.5 hours, single colonies were isolated and used to inoculate 5 ml of either Luria Broth (LB) containing NaCl and 100 µg/ml ampicillin or Terrific Broth (TB) containing 100 µg/ml ampicillin in 14 ml cell culture tubes. Cultures were allowed to grow for 8 hours at 37˚C while shaking. Bacterial glycerol stocks were made for each experimental plasmid from a 0.5 ml aliquot of culture and 0.5 ml 50% glycerol stock. Cryopreservation tubes were flash frozen on dry ice and then stored at -80˚C for long term storage. Remaining liquid

cultures were centrifuged at 6000 rpm at 4˚C for 10 minutes and bacterial pellets were stored at -80˚C until further processing. Lysis, cleanup and DNA precipitation were performed using the QIAquick Spin Miniprep Kit (Qiagen, Venlo, Netherlands) according to the manufacturer's instructions. This DNA was used to evaluate the purity and integrity of the plasmids by UV spectroscopy (NanoDrop 2000, Thermo Scientific, Rockford, IL), restriction enzyme digest/agarose gel electrophoresis, and sequencing. To prepare enough plasmid for AAV production, the same process was repeated using the bacterial glycerol stocks. However, after the 8 hour incubation, the liquid starter cultures (3 ml) were added to 500 ml of LB containing 100 µg/ml ampicillin in a 1 L Erlenmeyer flask. The flasks were incubated for no more than 16 hours at 37˚C at 200 rpm. Once again cells were pelleted and lysis and DNA precipitation was performed using the endotoxin-free Qiagen Megaprep Kit according to manufacturer's instructions. Plasmid DNA was diluted to 1 µg/uL in TE and 300 µL of each was sent to the University of North Carolina (UNC) – Chapel Hill Vector Core for AAV production.

In vitro Viral Transduction. As per recommendation from Stratagene, a human fibrosarcoma cell line, AAV-HT1080 (Agilent Technologies, Santa Clara, CA) maintained in high-glucose DMEM containing 10% FBS, 2 mM L-glutamine and 50 U/ml penicillin/streptomycin, was used for all transduction experiments. For subsequent qRT-PCR, immunoblotting, or immunocytochemistry assays, $0.25x10^6$, $0.20x10^6$, or $0.12x10^6$ cells respectively, were plated in 6-well dishes on the afternoon prior to transduction. The morning of transduction, media was removed from each well and replaced with 1 ml of fresh media containing viruses at a concentration sufficient for a multiplicity of infection (MOI) of 12,400 (this MOI had been previously determined to transduce an

adequate number of cells in an experiment using AAV-GFP). According to SignaGen® Laboratories (a supplier of AAV viruses) a range of 2,000 – 10,000 MOI for AAV is used for most cell lines; however some cells can require an MOI up to 500,000. Controls with no virus were also prepared. Plates were incubated with intermittent swirling for 6 hours in a humidified 37˚C/5% CO_2 environment. Virus containing media was then removed from each well and replaced with 3 ml of DMEM (for cells to be used in qRT-PCR 18% FBS DMEM was used rather than 10% FBS DMEM). Cells were either harvested or fixed, depending on the downstream analysis, 48 hours following transduction.

Quantitative Reverse Transcriptase Polymerase Chain Reaction (qRT-PCR). AAV-HT1080 cells transduced with AAV-BDNF-A, AAV-BDNF-A*B, AAV-GFP, or no virus, were pelleted, washed three times with 1x sterile PBS, and stored at -80˚C until further processing. Cells were lysed using Buffer RLT and RNA was extracted following the cell culture protocol from the RNeasy Mini Kit (Qiagen, Venlo, Netherlands). RNA concentration and purity was assessed using a NanoDrop 2000 (Thermo Scientific, Rockford, IL). All RNA samples had 260/280 ratio between 2.07 and 2.09. Total RNA from each sample (2 µg) was treated with Deoxyribonuclease I (Invitrogen, Carlsbad, CA). DNase-treated RNA (1 µg) was used to generate cDNA using the iScript cDNA kit (Bio-Rad, Hercules, CA) according to manufacturer's instructions. A balanced amount of DNase-treated RNA from each sample was used as a control for viral DNA contamination. qRT-PCR was performed using the CFX Connect™ system (Bio-Rad, Hercules, CA) according to manufacturer's instructions for iQ SYBER Green Supermix (Bio-Rad, Hercules, CA). Primer sequences, annealing temperatures, amplicon sizes, and cDNA dilutions used for each gene are listed in Table 6.1. Expression was

Table 6.1: Primer sequences used for *Bdnf* qRT-PCR

Target Gene	Forward Primer (5' to 3')	Reverse Primer (5' to 3')	Annealing Temp (˚C)	Amplicon Size (bp)	cDNA dilution
Proximal 3' UTR of *Bdnf*	TGGTTATTTCATACTTCGGTTGC	AGTGTCAGCCAGTGATGTCG	60	170	1:25
Distal 3' UTR of *Bdnf*	AGGCAAACAATCGCTTCATC	TGGTAAACGGCACAAAACAA	60	203	1:25

calculated by comparing Ct values to a standard curve created from cDNA (diluted 1:5, 1:25, 1:125, 1:625) produced from RNA obtained from AAV-BDNF-A*B transduced cells. Statistical analysis of *Bdnf* expression was performed by one-way ANOVA across all treatment groups, followed by Tukey's HSD *post-hoc* for all pairwise comparisons.

Immunoblotting. AAV-HT1080 cells transduced with virus were pelleted, washed three times with 1x sterile PBS, and stored at -80˚C until further processing. To each pellet, 100 µL of 1x RIPA buffer (1% NP40, 0.5% Na deoxycholate, 0.1% SDS, 150 mM NaCl, 50 mM Tris) with added protease inhibitor cocktail (Halt, Thermo Scientific, Rockford, IL) was added. Samples were triturated using a pipette and then stored on ice for 30 minutes. Lysates were passed through a 28g syringe five times and then stored at -80˚C. Protein concentrations were determined using the BCA assay (Thermo Scientific, Rockford, IL). Sample concentrations were balanced using 1x RIPA, 10x dithiothreitol (Fisher Scientific, Waltham, MA), and 2x stop solution (29.35 g Tris-HCl, 300 ml 10% w/v SDS, 150 ml glycerol, QS H_20), boiled for 10 minutes, and then placed on ice for 30 minutes. For each sample, 10 or 20 µg of protein was loaded per lane on a 4% - 12% NuPAGE bis-tris gel (Life Technologies, Carlsbad, CA). Mouse PFC and entorhinal cortex (EC) samples lysed with 1x LDS buffer were used as positive controls for BDNF detection. Electrophoresis was performed at 150V followed by transfer to 0.20 µm nitrocellulose or PVDF membrane for 1.5 hours at 30V on ice. Coomassie blue stain was used to ensure complete transfer of protein to membrane. Prior to primary antibody incubation, the membranes were blocked with 5% non-fat dried milk in 1x TBST for 45 minutes. Immunoblots were visualized on GeneMate Blue Autoradiography film

(BioExpress, Kaysville, UT) using the Amersham ECL Western Blotting Detection Reagent (GE Healthcare Life Sciences, Pittsburgh, PA).

Immunocytochemistry. Cells were washed three times for 15 minutes with 1X Dulbecco's PBS (DPBS) containing calcium and magnesium (Life Technologies, Carlsbad, CA). All incubations in this protocol took place at room temperature and the plate was protected from light using tin foil. For fixation, cells were incubated with 4% paraformaldehyde in 1X PBS for 20 minutes. Following another three – 15 minute washes with DPBS, cells were blocked and permeablized with 10% goat serum, 0.5% Triton X-100 in 1x PBS for 30 minutes. For detection of the Myc epitope that should be expressed by AAV-BDNF-A and AAV-BDNF-A*B, cells were incubated at room temperature for 60 minutes with anti-Myc tag antibody (ab9106, Abcam, Cambridge, England) diluted 1:2000 and 1:5000 in 3% goat serum/1X PBST. After being washed (3X – 15 minutes) with DPBS, goat-α-rabbit secondary antibody (Alexa Fluor 488, Life Technologies, Carlsbad, CA) diluted 1:2000 in 3% goat serum/1X PBST was applied to cells for 2 hour incubation. Cells were washed a final three times in DPBS, followed by imaging using a fluorescent microscope measuring green channel emission (Zeiss Microscope, Q Imaging Camera).

Enzyme-Linked Immunosorbent Assay (ELISA). Dorsal striatum (DS) tissue from *Bdnf*$^{klox/klox}$ and wildtype mice was lysed using a modified protein extraction protocol shown to significant increase yield of BDNF from brain (Szapacs *et al.*, 2004). Frozen tissue was weighed and 400 µL of lysis buffer was added to each sample. Lysis buffer consisted of 100 mM PIPES, pH 7.0 (Boston Bioproducts, Ashland, MA), 500 mM NaCl (Fisher Scientific, Waltham, MA), 0.2% Triton X-100 (Fisher Scientific, Waltham, MA),

0.1% NaN_3 (Fisher Scientific, Waltham, MA), 2% BSA (Fisher Scientific, Waltham, MA), 2 mM EDTA · Na_2 · $2H_2O$ (Fisher Scientific, Waltham, MA), and 1x protease inhibitor cocktail (Halt, Thermo Scientific, Rockford, IL), which was added immediately before use. Samples were homogenized with a Polytron® (Kinematica AG, Germany), and then placed on ice until being centrifuged for 30 minutes at 16,000 x g at 4˚C. Supernatant was removed and stored at -80˚C until the assay was performed. The Promega BDNF Emax® ImmunoAssay System (Promega, Madison, WI) was employed to measure BDNF levels for each sample. Each well of a 96-well Nunc® Immobilizer™, flat bottom, amino plate (Thermo Scientific, Rockford, IL), was incubated overnight at 4˚C with 100 µL anti-BDNF monoclonal antibody (mAb) diluted 1:1000 in carbonate coating buffer (25 mM sodium bicarbonate and 25 mM sodium carbonate, pH 9.7). Unadsorbed mAb was removed and plate was vigorously washed once with TBST wash buffer, which was made from 20 mM Tris (Bio-Rad, Hercules, CA), 150 mM NaCl (Fisher Scientific, Waltham, MA), and 0.05% (v/v) Tween 20 (Fisher Scientific, Waltham, MA). Just prior to blocking, lysed tissue extracts were allowed to come to room temperature (RT). The plate was blocked using 200 µL 1X Promega Block and Sample buffer followed by incubation for 1 hour at RT. The plate was then vigorously washed once with TBST. One hundred µL of each sample or standard (500, 250, 125, 62.5, 31.3, 15.6, 7.8, 0 pg/ml) were added in triplicate to the plate and incubated for 2 hours at RT with shaking. The plate was then washed five times with TBST. One hundred µL of anti-human BDNF polyclonal antibody (pAb) diluted 1:500 in 1X Block and Sample buffer was added to each well and the plate was once again incubated for 2 hours at RT with shaking. After the plate was washed five times with TBST, 100 µL of anti-Igγ

horseradish peroxidase conjugate diluted 1:200 in 1X Block and Sample buffer was added to each well and the plate was incubated for 1 hour at RT with shaking. The plate was washed again five times with TBST. Finally, the plate was developed using 100 µL of room temperature Promega TMB One Solution which was allowed to incubate for 10 minutes with shaking. The reaction was stopped using 100 µL of 1N HCl and absorbance was measured at 450 nm. BDNF levels were normalized to wet tissue weight and reported as ng/g. Statistical analysis of DS BDNF levels was performed by Student's t-test between the two genotypes.

Animals. Bdnf$^{klox/klox}$ and wildtype mice were bred in the VCU Transgenic Mouse Core. Male mice were singly housed between 4 and 5 weeks of age and kept on a 12-hour light/dark cycle (6 am on, 6 pm off) in the out-of-vivarium animal room located on the 6th floor of Kontos Medical Sciences Building. Mice were housed with Teklad corn cob bedding (7092, Harlan, Madison, WI). All animals had *ad libitum* access to tap water, and *Bdnf*$^{klox/klox}$ mice were subjected to the pair-feeding paradigm from the time they were singly housed until the experiment ended. In brief, *Bdnf*$^{klox/klox}$ mice were restricted to the amount of standard rodent chow (7912, Harlan, Madison, WI) that was consumed by age-matched wildtype littermates on the previous day. All behaviors were assayed during the light cycle between the hours of 8 am and 2 pm. All animal procedures were approved by the Institutional Animal Care and Use Committee of Virginia (AM10332) and carried out in accordance with the National Institute of Health guide for the Care and Use of Laboratory Animals.

Stereotaxic Microinjection. Surgeries were staggered over time as animals became available from the transgenic core. *Bdnf*$^{klox/klox}$ and wildtype mice, 9.5 to 11.5

weeks of age, received *ad libitum* access to 0.188 mg/ml cherry-flavored children's ibuprofen in their drinking water from 24 hours prior to surgery until 72 hours after surgery. Induction of anesthesia was performed with 5% isoflurane and 7 L O_2 per minute. Sedation was maintained with 2-3% isoflurane/7 L O_2 per minute. In preparation for surgery ophthalmic ointment (Henry Schein) was applied to the eyes, the scalp was shaved and wiped with isopropanol, and the animal was placed in the stereotaxic rig (myNeuroLab, St Louis, MO). After ear bars were inserted to immobilize the head and adjusted for levelness, the incision site was cleaned with ethanol, betadine, and ethanol and numbed with an injection of 0.1 ml of 0.25% bupivacaine. An anterioposterior (AP) incision was made to expose the skull and needles were centered at bregma. If necessary, adjustments to the animal's head were made to be within the same AP and mediolateral (ML) planes as bregma. AP and ML coordinates from bregma were recorded. DS coordinates (AP: + 0.10 mm, ML: + 0.22 mm, DV: -0.31 mm, with needles at a 10% angle) were added/subtracted from those recorded at bregma and AP and ML coordinates adjusted. Needles were lowered to the skull surface, where marks were made with a fine-point sharpie for drilling. Holes were drilled (Dremel, Mount Prospect, IL) into the skull with a 3/64" bit, needles rinsed with autoclaved water, 100% ethanol, and autoclaved water before being loaded with one of three viruses: AAV-BDNF-A, AAV-BDNF-A*B, or AAV-GFP. Needles were placed at the edge of the skull and dorsoventral (DV) readings were taken. DV coordinates were subtracted and the needles were lowered into the DS. One tenth of a µL of virus (0.1 µL) was injected bilaterally over a two minute period, for a total of 1 µL of virus. Needles were allowed to sit at the injection site for 10 minutes and then slowly removed and cleaned. Incisions

were sealed with VetBond (3M, St. Paul, MN) and mice were placed in a clean cage on a heating pad until coming out from anesthesia. Sterile technique was maintained throughout surgery and absence of toe pinch reflex and breathing was assessed and recorded at least every 15 minutes. The number of animals that received each AAV treatment was as follows: 2 wildtype, GFP; 2 wildtype, BDNF-A; 3 wildtype, BDNF-AB; 3 *Bdnf*$^{klox/klox}$, GFP; 5 *Bdnf*$^{klox/klox}$, BDNF-A; 5 *Bdnf*$^{klox/klox}$, BDNF-AB. Mice were allowed 3 weeks for recovery and viral expression before behavioral testing commenced.

Loss of Righting Reflex (LORR). The sedative-hypnotic effects of ethanol were measured using the loss of righting reflex assay (LORR). Three to four weeks following stereotaxic injection of AAV-BDNF-A, AAV-BDNF-A*B, or AAV-GFP, mice were habituated to i.p. saline injections for 3 days. On test day mice received 4.0 g/kg ethanol and were placed supine in a V-shaped trough after losing righting reflex. Latency for LORR, or Time 1, was recorded when a mouse was unable to right itself for 30 seconds. Mice taking longer than 5 minutes to acquire LORR were removed from the study due to possibility of improper injection. An animal was deemed to have regained its righting reflex, and Time 2 recorded, when it was able to right itself 2 times within 30 seconds. Duration of LORR was calculated by Time 2- Time 1. Statistical analyses of latency and duration of LORR was performed using a two-way ANOVA followed by Tukey's HSD *post-hoc* to test pairwise comparisons where appropriate.

Locomotor Activity Assay. Locomotor activity in response to acute low-dose ethanol was assessed using Med-Associates sound-attenuating locomotor activity chambers (Med Associates, model ENV-515, St. Albans, VT). Chambers are equipped with 100 mA lights, a fan to diminish ambient noise, and 16 infrared sensor beams

along the x and y axis. The system is interfaced with Med Associates software that records the number of photobeam breaks which it converts to horizontal distance traveled. Nine weeks following AAV injections, mice were acclimated to the behavioral testing room for 1 hour prior to i.p. injections. Two days of saline administration and 10 minutes placement in the testing apparatus allowed for habituation to injections and environment. On test day, mice received 1.0 g/kg ethanol and distance traveled was recorded for 60 minutes. Preliminary statistics were performed due to the limited number of animals. Analysis for locomotor activity measured in the 10 and 60 minute time bins was performed using a two-way ANOVA. Analysis of time course data for AAV-treated *Bdnf*$^{klox/klox}$ mice and time course data collapsed across genotypes for the full 60 minute testing period was analyzed using a repeated measures two-way ANOVA. Tukey's HSD *post-hoc* analyses were performed where appropriate for all pairwise comparisons.

Results

*In vitro transduction of AAV containing BDNF-A and BDNF-A*B into AAV-HT1080 cells resulted in expression of Bdnf mRNA.*

To verify that the viruses made by the UNC Vector Core were capable of overexpressing *Bdnf*, they were first tested *in vitro*. DNase treated RNA from cells transduced with AAV-BDNF-A, AAV-BDNF-A*B, AAV-GFP and a no virus control was used to produce cDNA for analysis by qRT-PCR. A no-reverse transcription control was also run to detect any viral DNA contamination. Primers designed to test for all isoforms of *Bdnf* transcript (primers directed proximal to the initial polyadenylation site) and for

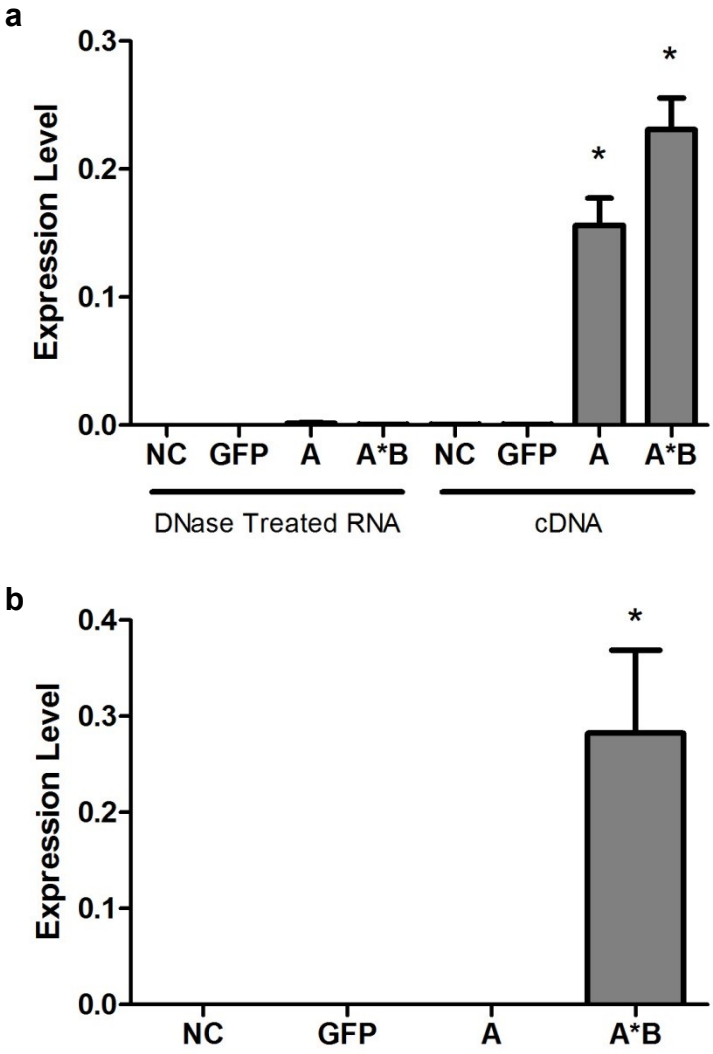

Figure 6.2 – qRT-PCR of AAV transduced HT1080 cells. HT1080 cells were transduced with AAV-BDNF-A (A), AAV-BDNF-A*B (AB), AAV-GFP (GFP), or no virus as a negative control (NC). qRT-PCR using primers designed to target the proximal 3' UTR and detect total *Bdnf* levels (**a**) determined that both virus A and A*B were able to produce *Bdnf* transcript (one-way ANOVA, $F[7,16] = 62.74$, *$p < 0.001$, n =3). Reactions using DNase treated RNA as starting material confirmed that amplified product did not result from viral DNA contamination. (**b**) Using primers directed towards the distal 3' UTR, it was determined that only virus A*B could produce the long 3' UTR transcript isoform (one-way ANOVA, $F[3,8] = 10.72$, *$p < 0.01$, n =3).

long 3' UTR isoforms only (primers that target distal to the initial polyadenylation site) were used to capture the profile of *Bdnf* mRNA transcribed by each virus. AAV-HT1080 cells do not express *Bdnf*, therefore no *Bdnf* was detected in cells transduced with AAV-GFP or no virus (Figure 6.2, **a, b**). Transduction with both AAV-BDNF-A and AAV-BDNF-A*B resulted in expression that could be detected when using primers designed to test for *Bdnf* total transcript levels (Figure 6.2, **a**). This was not due to DNA contamination, as no *Bdnf* was detected in the samples that used DNase treated RNA as template. Equally as important, we were able to demonstrate that long 3' UTR *Bdnf* was only expressed by AAV-BDNF-A*B and not AAV-BDNF-A. Thus, AAV-BDNF-A and AAV-BDNF-A*B expressed the appropriate *Bdnf* transcript isoforms *in vitro*.

Results of in vitro BDNF protein expression by transduction of AAV into AAV-HT1080 cells were inconclusive.

To confirm that expression of *Bdnf* mRNA by AAV-BDNF-A and AAV-BDNF-A*B resulted in production of BDNF protein *in vitro*, immunocytochemical (ICC) studies of transduced AAV-HT1080 cells were undertaken. An antibody directed at the Myc epitope tag whose sequence was in frame with the BDNF CDS was used to qualitatively detect protein levels. Initial examination of cells transduced with AAV-BDNF-A and AAV-BDNF-A*B indicated a low level of fluorescent signal that was not detected in the no primary control cells (Figure 6.3, **a-d**). However, a similar level of fluorescence was detected in cells that had been treated with no virus (Figure 6.3, **e, f**). This suggested that the observed signal was likely background fluorescence from the primary antibody binding non-specific target. Robust GFP signal was detected from cells transduced with

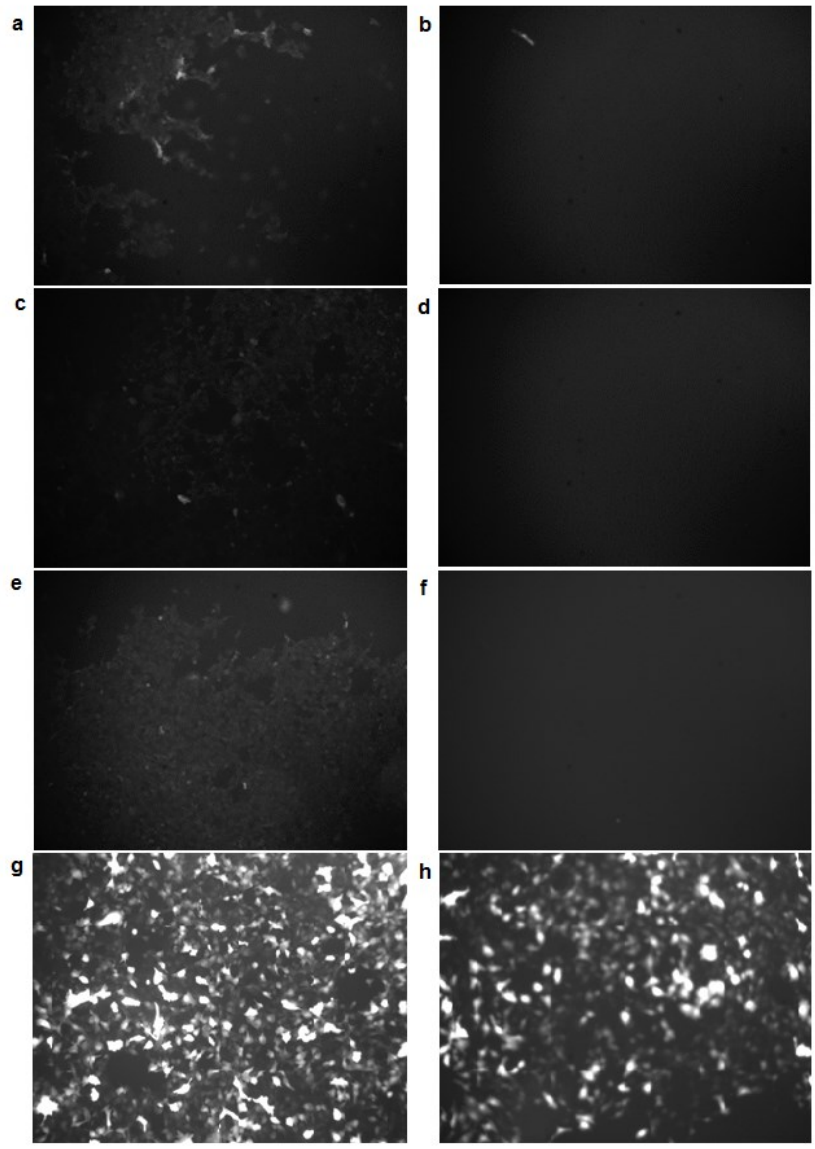

Figure 6.3 – *In vitro* expression of BDNF protein by AAV. HT1080 cells were transduced with AAV-GFP, AAV-BDNF-A, AAV-BDNF-A*B, and no virus as a negative control. Detection of *in vitro* BDNF protein expression was attempted by immunocytochemical studies using anti-myc tag antibody (**a**) AAV-Bndf-A, 1:2000 anti-myc tag, 2000 msec exposure (**b**) AAV-Bdnf-A , No 1˚, 2000 msec exposure (**c**) AAV-Bdnf-AB, 1:2000 anti-myc tag, 2000 msec exposure (**d**) AAV-Bdnf-AB, No 1˚, 2000 msec exposure (**e**) No virus, 1:2000 anti-myc tag, 2000 msec exposure (**f**) No virus, No 1˚, 2000 msec exposure (**g**) AAV-GFP, 1:2000 anti-myc tag, 2000 msec exposure (**h**) AAV-GFP, No 1˚, 2000 msec exposure.

AAV-GFP, which indicated that this virus was able to produce its gene product as expected (Figure 6.3, **g, h**).

Since the design of the ICC experiment provided no positive control to compare results to, immunoblotting was performed on protein isolated from cells that had been transduced with AAV-BDNF-A, AAV-BDNF-A*B, AAV-GFP and a no virus control. For a positive control, protein isolated from mouse PFC and EC were also analyzed. No protein was detected at the expected molecular weight for BDNF (~18 kDa for monomers) in either the transduced AAV-HT1080 cells or the animal tissue lysates when probing with anti-Myc-tag antibody (data not shown). Surprisingly, two anti-BDNF antibodies not only failed to detect BDNF in transduced AAV-HT1080 cells, but were also unsuccessful in detecting BDNF in the positive controls. The results of these studies are inconclusive until conditions can be worked out to definitely demonstrate the presence or absence of BDNF protein.

*In vivo pilot study using AAV to express BDNF-A and BDNF-A*B in to the dorsal striatum of Bdnf$^{klox/klox}$ mice did not rescue altered LORR or locomotor phenotypes.*

Due to time constraints and limited availability of *Bdnf*$^{klox/klox}$ mice, it was determined that the best course of action would be to proceed with an *in vivo* pilot study while preliminary cell culture work was still ongoing. To confirm that wildtype and *Bdnf*$^{klox/klox}$ mice possessed similar global expression of BDNF in the DS, an ELISA assay was performed. No significant difference in BDNF protein was detected between the two genotypes (Figure 6.4), indicating that the observed phenotypic differences described in Chapter 5 were not the result of altered BDNF levels in the DS.

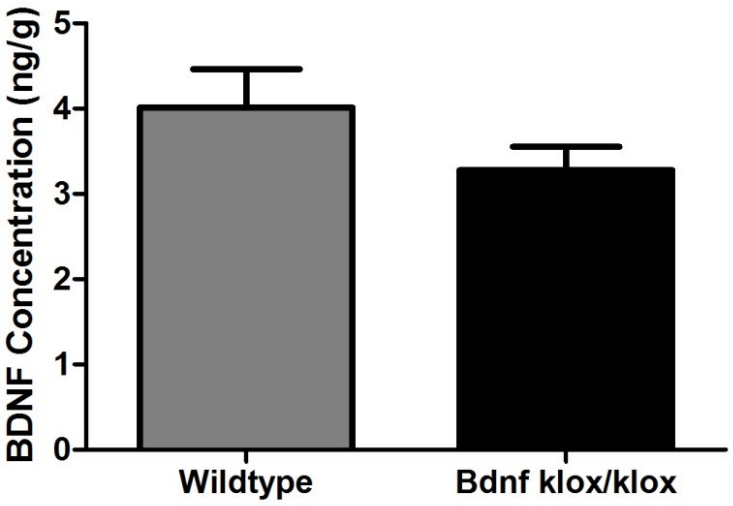

Figure 6.4 – BDNF protein levels in the dorsal striatum of *Bdnf*$^{klox/klox}$ mice. Subsequent studies into the role of synaptically targeted *Bdnf* required conformation that *Bdnf*$^{klox/klox}$ mice possessed similar global levels of BDNF protein in the dorsal striatum (DS) as compared to wildtype animals. No genotypic difference in DS BDNF expression was detected by ELISA (Student's t-test, $t[8] = 1.381$, $p = 0.2045$).

Beginning 3 weeks after viral injection, animals were tested for LORR and ethanol-induced locomotor activity; the two behaviors in which *Bdnf*$^{klox/klox}$ mice exhibited the most robust phenotypic differences. A significant main effect of genotype was found for duration of LORR, however no effect of viral treatment was observed (Figure 6.5, **b**). Since the sample size was low and the data variable for AAV treated wildtype mice, a one-way ANOVA of *Bdnf*$^{klox/klox}$ animals was performed to evaluate effect of viral treatment. Once again, no difference was detected in duration of LORR between *Bdnf*$^{klox/klox}$ mice that received AAV-GFP, AAV-BDNF-A, or AAV-BDNF-A*B. Interestingly, there was a main effect of genotype, but not viral treatment, for latency to LORR (Figure 6.5, **a**).

Within 48 hours of receiving 4.0 g/kg ethanol for the LORR assay, the two wildtype mice that had been previously injected with AAV-GFP died. This adversely affected the ability to interpret data regarding viral treatment in wildtype animals going forward. However, as a pilot study, testing the remaining animals still permitted information to be gathered about the efficacy of viral treatment in *Bdnf*$^{klox/klox}$ mice. Locomotor activity was assessed in response to 1.0 g/kg ethanol. This dose had been shown to elicit an activated response in *Bdnf*$^{klox/klox}$ mice not observed in wildtype animals. This activation was found to persist for almost the entire 60 minutes testing period (reference Figure 5.3, **b**). In the AAV-injected animals, this genotypic difference in activation was detected when comparing the sum of activity for the full 60 minutes (Figure 6.6, **b**), but not when analyzing the first 10 minute time bin (Figure 6.6, **a**). A time course of the data was plotted in 5 minute time bins throughout the 60 minute

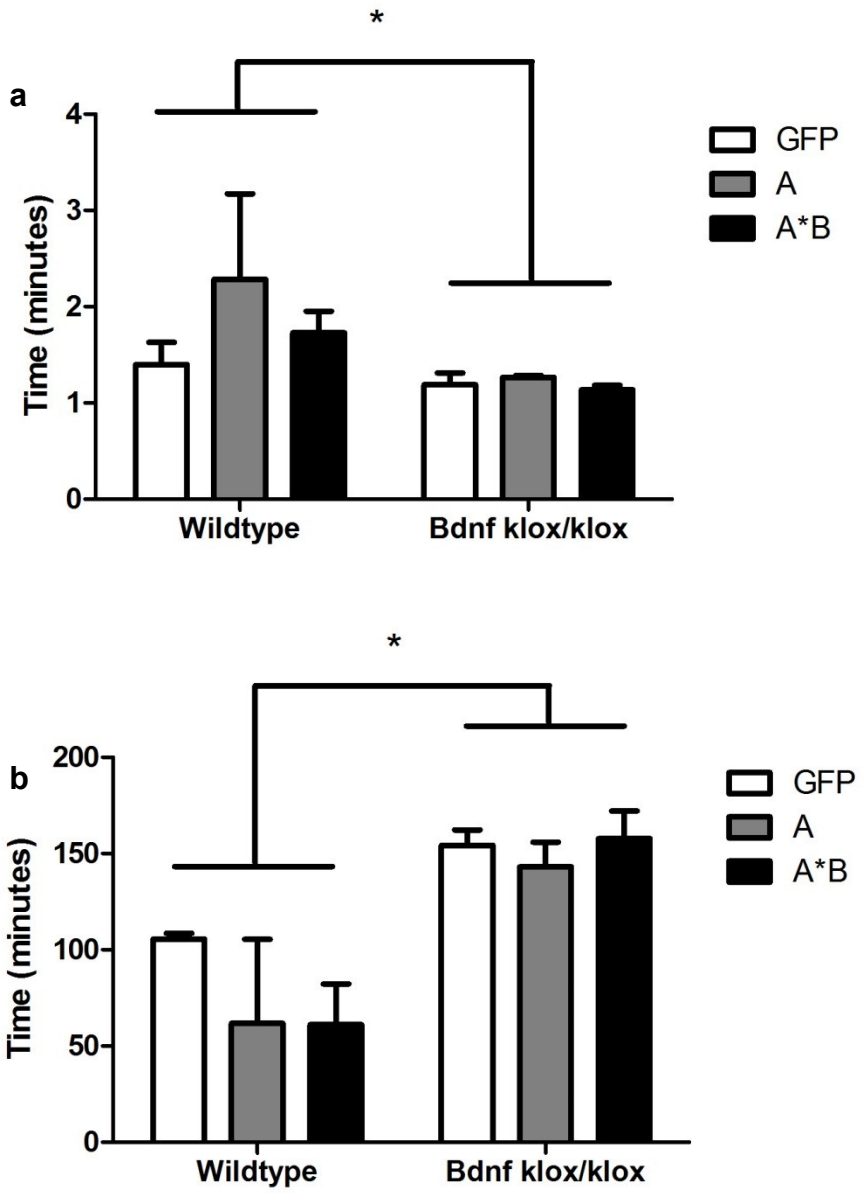

Figure 6.5 – LORR in AAV injected mice. Mice injected with AAV-GFP, AAV-BDNF-A, and AAV-BDNF-A*B into the DS were subjected to LORR. (**a**) For latency ($F_{genotype}$[1,14] = 14.108, *p = 0.002) and (**b**) duration of LORR ($F_{genotype}$[1,14] = 24.269, *p < 0.001) there was a main effect of genotype, but not viral treatment.

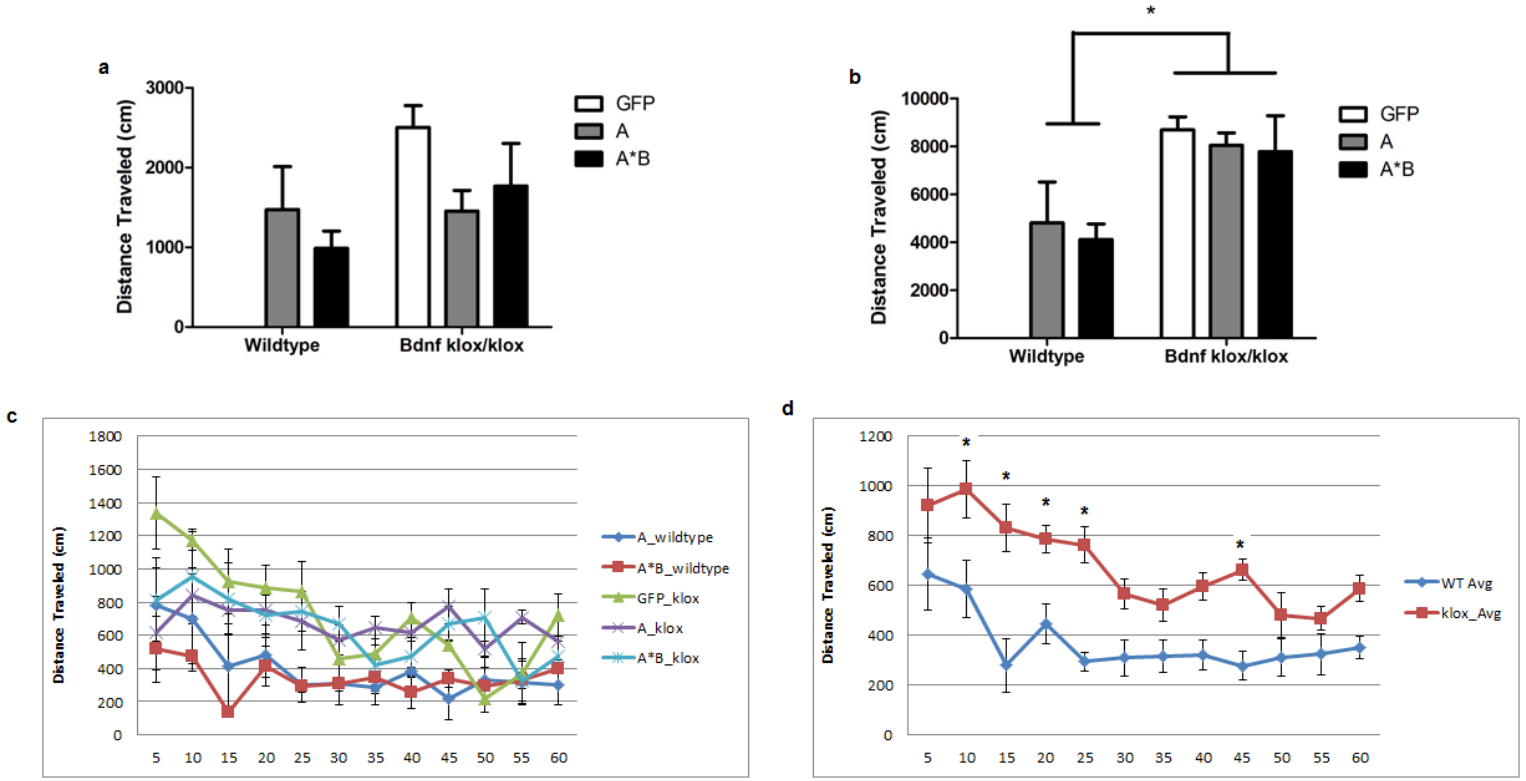

Figure 6.6 – Locomotor response to low dose ethanol in AAV injected mice. Mice injected with AAV-GFP, AAV-BDNF-A, and AAV-BDNF-A*B into the DS were tested for locomotor response following 1.0 g/kg ethanol. (**a**) There was no difference in distance traveled between the genotypes or the virus treatments within the first 10 minute time bin (two-way ANOVA, $F[1,14] = 0.973$, $p = 0.341$; $F[2,14] = 1.458$, $p = 0.266$) (**b**) A main effect of genotype was found when examining the entire 60 minute testing period (two-way ANOVA, $F[1,14] = 9.294$, * $p = 0.009$). However, there was no effect of viral treatment on distance traveled ($F[2,14] = 0.229$, $p = 0.798$) (**c**) The time course of locomotor activity for the full 60 minutes was plotted for all genotype/treatment groups. Statistical analysis focused on viral treatment across the *Bdnf*$^{klox/klox}$ mice. There was no main effect of treatment (two-way, repeated measures ANOVA, $F[2,110] = 0.149$, $p = 0.863$). However there were trends towards significant differences between the BDNF expressing viruses and AAV-GFP (Tukey's HSD *post-hoc*, $p = 0.006$; $p = 0.058$). (**d**) When time course locomotor activity was collapsed across genotypes, a significant protracted activation to ethanol was observed in *Bdnf*$^{klox/klox}$ mice compared to wildtype (two-way, repeated measures ANOVA, $F[1,11] = 12.698$, *$p < 0.050$).

testing period (Figure 6.6, **c**). A three-factor ANOVA to analyze AAV-treatment, time, and genotype could not be performed due to the lack of AAV-GFP treated wildtype mice. Therefore, statistical analysis focused on AAV-treatment within *Bdnf*$^{klox/klox}$ mice. A main effect of time and a significant interaction between time and AAV treatment were detected. *Post-hoc* analysis revealed a significant difference in distance traveled during the first 5 minute time bin between AAV-GFP and AAV-BDNF-A treated *Bdnf*$^{klox/klox}$ mice. There was also a trend towards significance when comparing AAV-GFP and AAV-BDNF-A*B treatments. When the locomotor activity data was collapsed across genotypes, the previously identified pattern of protracted activation was observed. *Bdnf*$^{klox/klox}$ mice remained significantly different from wildtype mice at the 10, 15, 20, 25, and 45 minute time bins (Figure 6.6, **d**). Together, these behavioral analyses suggest that injection of AAV-BDNF-A*B into the DS of *Bdnf*$^{klox/klox}$ mice did not rescue the altered phenotypes.

Discussion

The objective of this series of experiments was to confirm that altered ethanol phenotypes exhibited by *Bdnf*$^{klox/klox}$ mice were due to loss of a distinctive function by long 3' UTR *Bdnf*, theoretically performed at the synapse. In order to test this hypothesis, AAV-BDNF-A and AAV-BDNF-A*B were injected into the DS of *Bdnf*$^{klox/klox}$ and wildtype mice. The intended outcome was a behavioral profile that could be interpreted to determine the unique actions of short and long 3' UTR *Bdnf* in expression of ethanol-induced LORR and locomotor activation. However, a lack of significant behavioral findings in this pilot study could be the result of various limitations.

Of primary concern was the inability to detect BDNF protein expression in an *in vitro* system. The 48 hour post transduction time point appears to be appropriate, as *Bdnf* transcript (Figure 6.2, **a, b**) and GFP protein (Figure 6.3, **g, h**) expression were detectable. For absolute conformation that AAV-BDNF-A and AAV-BDNF-A*B are incapable of producing BDNF, a validated BDNF or Myc epitope antibody will be required. In an ongoing attempt to evaluate antibody efficacy, a BDNF protein standard has been purchased to test the two BDNF antibodies that failed to detect BDNF by immunoblotting. In the qRT-PCR analysis, primers were designed to detect short and long 3' UTR isoforms, but gave no indication as to the presence of *Bdnf* CDS. Therefore, as an additional control, DNA sequencing of the BDNF CDS is also underway to ensure that this sequence is intact.

If AAV-BDNF-A and AAV-BDNF-A*B are capable of producing BDNF protein *in vitro* and *in vivo*, there are other factors that could contribute to a lack of effect. This includes location and timing of injections. First, the DS was chosen for the site of viral injection based upon findings in the literature that suggest BDNF signaling in the DS is important for mediating ethanol-responsive behaviors, particularly LORR (Jeanblanc *et al.*, 2009; Logrip *et al.*, 2009; Kim *et al.*, 2012). However there is evidence that other neural substrates are associated with this ethanol action, including cortex (Harris *et al.*, 1995) and hippocampus (Proctor *et al.*, 2003). The hippocampus and isocortex happen to be the brain regions with the greatest BDNF expression levels (Wetmore *et al.*, 1994). Although there is no direct evidence that BDNF's effect on ethanol LORR is mediated by these regions, it does not exclude the possibility.

As mentioned previously, an inherent limitation of the *Bdnf*$^{klox/klox}$ model is the fact that *Bdnf* is not expressed throughout development. This makes it unclear as to whether BDNF regulates neuronal development or neuronal function to affect ethanol-induced phenotypes (Liao *et al.*, 2012). *Bdnf* expression is fairly low prenatally, and significantly rises postnatally, peaking at around 3 weeks of age in mice (Qiao *et al.*, 1996; Gorski *et al.*, 2003).Therefore, injection of *Bdnf*-containing AAV into mouse pups would allow for overexpression of BDNF to have an effect on synaptic development, synaptic function, or both, thereby bypassing the confounding variable (Liao *et al.*, 2012).

Even though injections of AAV-BDNF-A*B did not reverse ethanol phenotypes in *Bdnf*$^{klox/klox}$ mice as hypothesized, there were interesting findings in this pilot study that should be addressed. First, although not affected by AAV treatment, there was an apparent genotypic difference in latency to LORR (Figure 6.6, **a**). This prompted a *post-hoc* analysis of all previous LORR data from experiments that used pair-fed *Bdnf*$^{klox/klox}$ mice. When the data was collapsed there was a trend, although not significant, for decreased latency to LORR in *Bdnf*$^{klox/klox}$ mice as compared to wildtype (unpaired, two-tailed t-test, $t[27] = 1.7208$, $p = 0.0967$). Since the interpretation of LORR results depends on the accuracy of latency determination, a more in-depth analysis may be warranted in *Bdnf*$^{klox/klox}$ mice and wildtype littermates.

Another relevant outcome from this pilot study was confirmation that *Bdnf*$^{klox/klox}$ mice exhibit protracted activation to 1.0 g/kg ethanol (Figure 6.6, **d**). This result did come with the caveat of an AAV-treatment dependent reduction in activation during the first 5 minute time bin for *Bdnf*$^{klox/klox}$ mice treated with AAV-BDNF-A and a trend for AAV-BDNF-A*B (Figure 6.6, **c**). If these two viruses are able to express BDNF protein

in vivo, this result would necessitate further investigation as it could suggest that general overexpression of BDNF could alter initial activation. However, without AAV-GFP wildtype treated mice for comparison, this is simply conjecture.

For any insightful interpretation to come from this pilot study, unequivocal determination of the efficacy of AAV-BDNF-A and AAV-BDNF-AB to express BDNF protein is essential. However, moving forward with this line of investigation may require that new viral constructs be designed and characterized, and modifications to the experimental design may be necessary.

Chapter 7 – Concluding Discussion and Future Directions

Discussion

It is generally accepted that alcoholism is a disease that develops over time as a consequence of genetic make-up, environmental factors, and cumulative exposure to the drug. The latter of which results in neuroadaptations that lead to long-lasting alterations in neuronal activity, which are proposed to underlie the development of behaviors associated with addiction. Of particular focus in this dissertation was how specifically the synaptic transcriptome contributes to the molecular mechanisms underlying addiction. The long term objective is to have a more complete understanding of the mechanisms of alcohol-induced neuronal plasticity to facilitate the development of novel therapeutic treatments for addiction. Through a two-pronged approach, we have demonstrated the importance of the synaptic transcriptome in mediating ethanol-responsive behaviors and have identified potential synaptic candidate genes that warrant further investigation.

Ever since Steward's influential work showing that synapses possess the capacity for local translation (Steward & Levy, 1982), the importance of synapses as the effector, as opposed to merely the target, of long-term change has become abundantly clear. It therefore would make sense that regulation of the synaptic transcriptome would be an inherent mechanism by which to mediate changes in synaptic structure and

function. Synaptic plasticity has been studied extensively for its role in learning and memory (Kandel, 2001); neuronal processes that are suggested to be subverted during the development of addiction (Hyman *et al.*, 2006). A large body of literature exists describing the role of learning in ethanol-induced behavioral sensitization (Trujillo & Akil, 1995; Quadros *et al.*, 2003; Brebner *et al.*, 2005), the model of neuronal plasticity that was utilized for these investigations. Sensitized responses to psychostimulant effects of drugs also appear to be affected by stress. Cross-sensitization between stress and ethanol suggests a potential role for HPA axis associated changes in ethanol sensitization (Phillips *et al.*, 1997). Glucocorticoid hormones are the final step in activation of the HPA axis and have been shown to have acutely positive and chronically negative effects on learning and memory (Tasker *et al.*, 2006). Glucocorticoid effects on memory appear to result from regulation of gene expression (Tasker *et al.*, 2006). Upon binding and activation, the glucocorticoid receptor translocates to the nucleus and acts as a transcription factor, where it mediates the transcription of a number of genes including, *Sgk1* and *Fkbp5* (Webster *et al.*, 1993; Binder, 2009). The Miles laboratory has previously identified glucocorticoid-responsive gene expression changes that potentially contribute to the development of behavioral sensitization (Kerns *et al.*, 2005; Costin *et al.*, 2013a). In the present work, we found that a number of synaptically targeted genes conform to the gene expression pattern elicited by the dysregulation of the HPA access that occurs with repeated ethanol exposure (Figure 4.3). This suggests that local synaptic function may be a chief target for the interaction between ethanol and glucocorticoid signaling.

If the development of ethanol-responsive behaviors exploits the same molecular mechanisms as learning and memory, BDNF would be an ideal candidate for initiating an examination into the interaction between ethanol and the synaptic transcriptome. BDNF signaling has been shown to be intimately involved in the facilitation of NMDA receptor-dependent hippocampal LTP and LTD (Patterson *et al.*, 1996; Woo *et al.*, 2005) and the trafficking of its mRNA to the synapse suggests a localized role for BDNF function (An *et al.*, 2008). BDNF, and other NTs, have also been shown to modulate functional tolerance following ethanol withdrawal (Szabo & Hoffman, 1995). It has been proposed that functional tolerance is a CNS adaptation, like learning and memory, which depends on changes in synaptic efficacy (Hoffman *et al.*, 1978). Potential adaptive mechanisms contributing to functional tolerance following chronic alcohol include selective targeting of NR2B-contianing NMDA receptors to the synapse (Carpenter-Hyland *et al.*, 2004) and increases in F-actin and PSD95 co-localization promoting dendritic spine enlargement (Carpenter-Hyland & Chandler, 2006). BDNF could conceivably contribute to these phenomena, since it has been shown that BDNF application to hippocampal neuronal cultures increases NMDA receptor subunit levels and trafficking to the membrane (Caldeira *et al.*, 2007). Additionally, BDNF increases phosphorylation of the NR2B subunit of NMDA receptors via Fyn kinase, thereby increasing receptor activity (Lin *et al.*, 1998). This same molecular adaptation occurs in response to acute ethanol administration, and is thought to contribute to AFT (Miyakawa *et al.*, 1997; Yaka *et al.*, 2003b). Acute ethanol has also been shown to increase BDNF expression in the hippocampus and dorsal striatum (McGough *et al.*, 2004). It is suggested that the dorsal striatum (DS) is the neuronal center that regulates duration of

LORR (Kim *et al.*, 2012). Therefore, if the enhanced duration of LORR exhibited by *Bdnf*$^{klox/klox}$ mice (Figure 5.7) is in fact the result of a deficit in AFT, one could hypothesize that development of ethanol AFT requires signaling pathways initiated specifically by locally translated *Bdnf* in the DS. Overall, the studies presented in this dissertation suggest that ethanol alters the synaptic transcriptome, appropriating the processes that contribute to normal synaptic functioning, and leading to the neuronal and behavioral adaptations that occur during the development of addiction. Our studies on *Bdnf*$^{klox/klox}$ mice highlight how synaptic targeting of specific mRNA can modulate ethanol behavioral responses.

Future Directions

Investigations into the synaptic transcriptome were enabled through the use of a synaptic enrichment protocol known as the synaptoneurosome preparation. A portion of the studies presented here demonstrated the utility of this method to examine *in vivo* alterations to the synaptic transcriptome as a result of systemic drug administration. A significant outcome of this work was the establishment of the synaptoneurosome protocol in our laboratory, which can now be utilized to further probe the effect of ethanol on localized mRNA and protein populations. It was determined that sensitizing treatments of ethanol in D2 mice perturbed the synaptic transcriptome of the frontal pole (Chapter 4). This heterogeneous brain region was initially chosen for this series of experiments due to its inclusion of brain regions believed to mediate the rewarding and reinforcing properties of ethanol, such as NAc, DS, and PFC (Robinson & Berridge, 1993). However, numerous studies have indicated brain region specific differences that

contribute to ethanol behavioral phenotypes (Kerns *et al.*, 2005; Mulligan *et al.*, 2011; Wolstenholme *et al.*, 2011). Regional expression profiles may be dampened by examining the frontal pole synaptic transcriptome as a whole, obscuring the actual mechanism underlying behavioral sensitization. Furthermore, taking a systems network approach to examine brain-region specific synaptic transcriptomes could provide insight into how the brain's circuity adapts in concert to repeated drug administration (Mulligan *et al.*, 2011).

Selection of the frontal pole region also allowed sufficient quantities of RNA to be obtained for subsequent analyses. Therefore, an impediment to examining brain-regional differences in synaptic expression patterns associated with behavioral sensitization is the large amount of tissue necessary. While an obvious solution is to increase the number of test subjects, this needs to be balanced by the time and cost of preforming such an experiment. A conservative estimate for a brain region the size of the DS would require a minimum of 60 mice per sensitization treatment groups, in order to obtain biological replicates. Alternatively, optimization of the synaptoneurosome preparation could significantly lessen the starting tissue requirements. A protocol by Johnson *et al.* (1997) was able to obtain fractions enriched for intact synaptoneurosomes from 400 μm slices of individual rat hippocampi (Johnson *et al.*, 1997). No attempts at RNA isolation from these samples were made. Thus, in order to be useful in expression profiling studies this protocol would need to be characterized and optimized for RNA yield.

As mentioned previously, the propensity for development of alcohol dependence arises from a combination of genetics, environmental factors, and prior history of drug

use. The identification of a cohort of genes regulated by ethanol exclusively at the synapse (Figure 4.4, Table 4.8) raised the question as to whether there could also be genetic regulation that occurs on the subcellular level contributing to behavioral responses. B6 and D2 mice are two inbred strains that have highly polymorphic genomes (Walter *et al.*, 2007) and show divergent phenotypic responses to ethanol (McClearn & Rodgers, 1959; Goldstein, 1973; Phillips *et al.*, 1994; Metten *et al.*, 1998). Therefore, the B6 and D2 strains were used as progenitors for the BXD recombinant inbred panel often used for genetic mapping of quantitative traits related to ethanol. The breeding of these two inbred stains, followed by intercrossing of their obligate heterozygote F_1 offspring, results in random recombinational events across the genomes. Further inbreeding of the F_2 generation creates a mosaic of B6 and D2 haplotypes along every chromosome, uniquely apt for genetic mapping studies. Examining ethanol sensitization responses across a subset of the BXD panel, along with the B6 and D2 progenitors, indicates that this behavior is a heritable phenotype that varies substantially with genotype (Figure 7.1). The synaptoneurosome preparation could therefore be used to profile the synaptic transcriptome of specific BXD strains subjected to the sensitization paradigm in efforts to identify synaptic expression quantitative trait loci (eQTL). An eQTL is a genomic loci that contributes to the variability in expression of a particular transcript. The hypothesis being that a genetical genomics approach could identify novel loci that contribute to transcript levels in the synapse, contributing to the synaptic plasticity underlying behavioral sensitization.

A list of candidate genes was derived from analysis of RNA isolated from the synaptoneurosomal fraction, P2, indicating that repeated ethanol exposure is able to

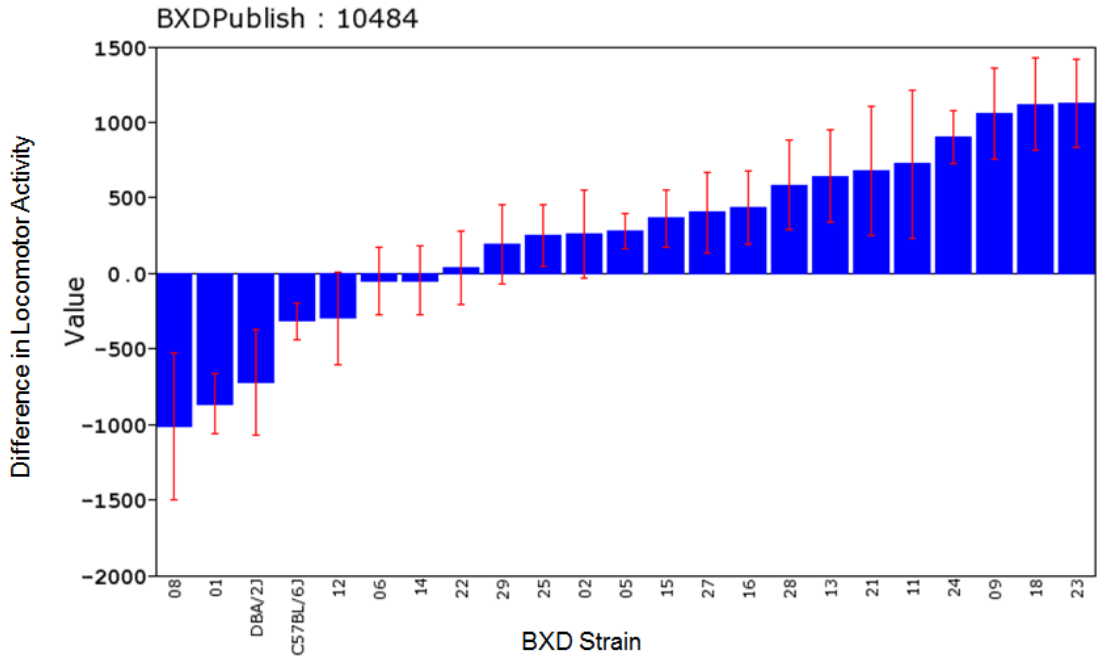

Figure 7.1 – Ethanol behavioral sensitization across the BXD line. The heritable nature of the ethanol sensitization response can be observed when testing the BXD recombinant inbred line of mice. In response to 2.0 g/kg ethanol, the difference in locomotor activity between the fifth and first ethanol treatment, 1-5 minutes after injection in female BXD mice is graphed (Phillips *et al.*, 1995). Plot was obtained from GeneNetwork (www.genenetwork.org), record ID 10484.

regulate the synaptic transcriptome (Supplemental Table S4.7). *Rhou*, which encodes for a small G protein of the Rho family of GTPases, fulfills the majority of criteria established to select candidates for additional investigation. Nothing is known regarding the function of *Rhou* in brain, but it has been previously identified as regulated by ethanol under various experimental conditions (Unpublished-Data; Kerns *et al.*, 2005). In the present study, results indicated that *Rhou* expression was significantly altered in the P2 fraction only (Supplemental Table S4.7). This suggests that *Rhou*'s function in response to ethanol may be localized to the synapse. Additionally, *Rhou* exhibited the habituating gene expression profile characteristic of glucocorticoid responsive genes following repeated ethanol exposure (Figure 4.3). The gene structure of *Rhou* contains a glucocorticoid responsive element (GRE), implicating that *Rhou* could be involved in glucocorticoid regulation of the interaction between stress and alcohol dependence (Costin *et al.*, 2013a). *Rhou* is also a putative target for the CPEB1 RNA-binding protein (Zhang *et al.*, 2010). This makes *Rhou* amenable for experiments to test the effect of altering dendritic trafficking of a known ethanol responsive gene. Mutating the putative CPEB1 binding site would theoretically alter synaptic levels of *Rhou* transcript which, if done *in vivo,* would offer a unique model for examining the role of the synaptic transcriptome in glucocorticoid regulation of ethanol behavioral sensitization.

This approach is not without precedence, as the second line of investigation presented herein demonstrated that disrupted trafficking of a known ethanol-responsive gene, *Bdnf*, results in altered behavioral phenotypes. *Bdnf*$^{klox/klox}$ mice, which have a truncated long 3' UTR variant of the *Bdnf* mRNA and reduced levels of BDNF protein and transcript at the synapse, exhibited a prolonged duration of LORR (Figure 5.7). As

mentioned previously, I hypothesize that AFT to the sedative effects of ethanol tested in LORR may be mediated by signaling cascades initiated by locally translated BDNF. This remains contingent on validation studies required to confirm that *Bdnf*$^{klox/klox}$ mice have a deficit in AFT. Alternatively, since *Bdnf*$^{klox/klox}$ mice exhibited increased sensitivity to both 1.0 and 2.5 g/kg ethanol, the fact that *Bdnf*$^{klox/klox}$ mice also regained righting reflex at a lower BEC may simply reflect an increased sensitivity to 4.0 g/kg ethanol. Our latency measurement may not be sensitive enough to detect the altered initial sensitivity at this high dose of ethanol. However, if *Bdnf*$^{klox/klox}$ mice do have a deficit in AFT, this could also be detected through a series of experiments to test the molecular events that underlie the behavior. For instance, I would predict that ethanol-induced phosphorylation of NR2B would be lower in *Bdnf*$^{klox/klox}$ mice as compared to wildtype mice. It has been shown that brain-region selective compartmentalization of NR2B and Fyn kinase by RACK1 confers region specificity to the effects of ethanol (Yaka *et al.*, 2003a). Upon ethanol administration, RACK1 dissociates from the NR2B/Fyn/RACK complex (Yaka *et al.*, 2003a). This allows for Fyn to phosphorylate NR2B and RACK1 to translocate the nucleus, where it alters the transcription of BDNF (Yaka *et al.*, 2003a). BDNF signaling through TrkB, negatively regulates ethanol-induced behavioral effects by altering levels of neuropeptide Y, dopamine receptor 3 and dynorphin (Jeanblanc *et al.*, 2006; Logrip *et al.*, 2008). This establishes a parallel signaling mechanism to protect against ethanol induced neuroadaptations (Jeanblanc *et al.*, 2009). Therefore the level of RACK1 nuclear translocation and subsequent effects on transcription in response to ethanol should be altered in *Bdnf*$^{klox/klox}$ mice. Mice selectively bred for their acquisition of AFT to ethanol (Erwin & Deitrich, 1996) could be used in a complementary study to

determine the role of synaptic *Bdnf*. qRT-PCR on total RNA isolated from synaptoneurosomes prepared from the tissue of High-AFT (HAFT) and Low-AFT (LAFT) mice may reveal differential targeting of *Bdnf* to the synapse, contributing to expression of the selected trait.

Bdnf$^{klox/klox}$ mice also exhibited an altered behavioral response to low dose ethanol, wherein we observed increased locomotor activity following a 1.0 g/kg dose of ethanol (Figure 5.2, 5.3). Acute, ethanol has been shown to dose-dependently activate DAergic neuronal firing (Gessa *et al.*, 1985), which results in an increase of DA released in the NAc shell (Pontieri *et al.*, 1995). Midbrain A10 DA neurons have been characterized as the neurochemical substrate of reinforcement (Wise & Rompre, 1989; Wise, 2004), and have been shown to underlie spontaneous and psychomotor-induced locomotor activity (Fink & Smith, 1980; Koob *et al.*, 1981). Therefore, one might predict that the increased ethanol-induced locomotor response of *Bdnf*$^{klox/klox}$ mice may result from altered dopamine release from mesolimbic DA neurons. Dopamine, as measured by microdialysis, should reveal an augmented release in the NAc shell of *Bdnf*$^{klox/klox}$ mice as compared to wildtype. This increased DA level would theoretically remain elevated for an extended period of time, contributing to the protracted activation that was observed to last at least 60 minutes (Figure 5.3).

The lengthy duration of LORR displayed by non-pair-fed *Bdnf*$^{klox/klox}$ mice suggested a combination of pharmacokinetic and pharmacodynamic effects underlying the phenotype (Figure 5.6). Despite being maintained at a body mass comparable to wildtype animals, pair-fed *Bdnf*$^{klox/klox}$ mice still had an altered ethanol metabolism profile (Figure 5.14). Therefore, follow up studies to investigate the potential pharmacokinetic

contributions should be undertaken. Lean body mass determination through chemical analysis or NMR spectrometry (Tinsley *et al.*, 2004) could determine if a discrepancy in V_d still exists between pair-fed *Bdnf*$^{klox/klox}$ mice and wildtype littermates. Although, decreased volume of distribution in *Bdnf*$^{klox/klox}$ mice would not explain the apparent increased ethanol metabolism rate (Figure 5.14). An examination into the level or activity of ethanol metabolic enzymes, such as alcohol and aldehyde dehydrogenase, CYP2E1, and catalase, may be warranted.

Expression profiling could be used as an initial examination for altered neuronal and metabolic systems in *Bdnf*$^{klox/klox}$ mice. Transcriptomic analyses measure steady state mRNA abundance, a composite of transcription and degradation rates. Differences between naïve *Bdnf*$^{klox/klox}$ and wildtype mice could therefore be informative as to the basally perturbed pathways that could contribute to altered ethanol responses. This has been demonstrated in Fyn$^{-/-}$ mice, which showed a coordinate basal decrease in myelin-associated gene expression that was an underlying factor in enhanced sensitivity to high dose ethanol (Farris & Miles, 2013). Microarray analysis of *Bdnf*$^{klox/klox}$ DS has been initiated, prompted by our LORR findings. Future microarray studies could be performed on the PFC or NAc to determine if reduced dendritic *Bdnf* alters basal myelin-associated genes, as observed in the Fyn$^{-/-}$ mice (Farris & Miles, 2013). Analysis of the liver would contribute to an overall comparison of pharmacokinetic profiles between *Bdnf*$^{klox/klox}$ and wildtype mice. Proper controls will be essential to these studies to ensure that observed differences in expression are the result of altered dendritic trafficking of *Bdnf* and not due to food restriction. As such, microarray studies will

require samples to be run from not only wildtype and pair-fed animals, but non-pair-fed animals as well.

Overall, the studies presented in this dissertation highlight the importance of the synaptic transcriptome in ethanol-responsive behaviors. As the capability to positively identify targeted transcripts and the regulatory mechanisms that control RNA trafficking advances, I expect that the true extent of the synaptic transcriptome's effect on localized activity-dependent plasticity will become apparent. In particular, the concept that dendritic transcripts act as a template for proteins that have a distinct function as compared to their somatically translated counterparts may reveal unconventional functions for otherwise well characterized proteins. In conclusion, the synaptic transcriptome provides a new frontier for investigating the molecular and cellular mechanisms that contribute to the development of alcoholism, with the ultimate goal of identifying novel and more effective therapeutic interventions.

Literature Cited

Abrahao, K.P., Ariwodola, O.J., Butler, T.R., Rau, A.R., Skelly, M.J., Carter, E., Alexander, N.P., McCool, B.A., Souza-Formigoni, M.L. & Weiner, J.L. (2013) Locomotor sensitization to ethanol impairs NMDA receptor-dependent synaptic plasticity in the nucleus accumbens and increases ethanol self-administration. *J Neurosci*, 33, 4834-4842.

Ackerman, J.M. & White, F.J. (1990) A10 somatodendritic dopamine autoreceptor sensitivity following withdrawal from repeated cocaine treatment. *Neurosci Lett*, 117, 181-187.

Aid, T., Kazantseva, A., Piirsoo, M., Palm, K. & Timmusk, T. (2007) Mouse and rat BDNF gene structure and expression revisited. *J Neurosci Res*, 85, 525-535.

Alcaro, A., Huber, R. & Panksepp, J. (2007) Behavioral functions of the mesolimbic dopaminergic system: an affective neuroethological perspective. *Brain Res Rev*, 56, 283-321.

Altar, C.A., Boylan, C.B., Fritsche, M., Jackson, C., Hyman, C. & Lindsay, R.M. (1994) The neurotrophins NT-4/5 and BDNF augment serotonin, dopamine, and GABAergic systems during behaviorally effective infusions to the substantia nigra. *Exp Neurol*, 130, 31-40.

Altar, C.A., Boylan, C.B., Jackson, C., Hershenson, S., Miller, J., Wiegand, S.J., Lindsay, R.M. & Hyman, C. (1992) Brain-derived neurotrophic factor augments rotational behavior and nigrostriatal dopamine turnover in vivo. *Proc Natl Acad Sci U S A*, 89, 11347-11351.

An, J.J., Gharami, K., Liao, G.Y., Woo, N.H., Lau, A.G., Vanevski, F., Torre, E.R., Jones, K.R., Feng, Y., Lu, B. & Xu, B. (2008) Distinct role of long 3' UTR BDNF mRNA in spine morphology and synaptic plasticity in hippocampal neurons. *Cell*, 134, 175-187.

Autry, A.E. & Monteggia, L.M. (2012) Brain-derived neurotrophic factor and neuropsychiatric disorders. *Pharmacol Rev*, 64, 238-258.

Bachmanov, A.A., Tordoff, M.G. & Beauchamp, G.K. (1996) Ethanol consumption and taste preferences in C57BL/6ByJ and 129/J mice. *Alcohol Clin Exp Res*, 20, 201-206.

Bagni, C., Mannucci, L., Dotti, C.G. & Amaldi, F. (2000) Chemical stimulation of synaptosomes modulates alpha -Ca2+/calmodulin-dependent protein kinase II mRNA association to polysomes. *J Neurosci*, 20, RC76.

Bahi, A. & Dreyer, J.L. (2013) Striatal modulation of BDNF expression using microRNA124a-expressing lentiviral vectors impairs ethanol-induced conditioned-place preference and voluntary alcohol consumption. *Eur J Neurosci*, 38, 2328-2337.

Baker, E.J., Jay, J.J., Bubier, J.A., Langston, M.A. & Chesler, E.J. (2012) GeneWeaver: a web-based system for integrative functional genomics. *Nucleic Acids Res*, 40, D1067-1076.

Barbarese, E., Koppel, D.E., Deutscher, M.P., Smith, C.L., Ainger, K., Morgan, F. & Carson, J.H. (1995) Protein translation components are colocalized in granules in oligodendrocytes. *J Cell Sci*, 108 (Pt 8), 2781-2790.

Barco, A., Alarcon, J.M. & Kandel, E.R. (2002) Expression of constitutively active CREB protein facilitates the late phase of long-term potentiation by enhancing synaptic capture. *Cell*, 108, 689-703.

Bardo, M.T. & Bevins, R.A. (2000) Conditioned place preference: what does it add to our preclinical understanding of drug reward? *Psychopharmacology (Berl)*, 153, 31-43.

Bell, R.L., Kimpel, M.W., McClintick, J.N., Strother, W.N., Carr, L.G., Liang, T., Rodd, Z.A., Mayfield, R.D., Edenberg, H.J. & McBride, W.J. (2009) Gene expression changes in the nucleus accumbens of alcohol-preferring rats following chronic ethanol consumption. *Pharmacol Biochem Behav*, 94, 131-147.

Bell, S.M., Stewart, R.B., Thompson, S.C. & Meisch, R.A. (1997) Food-deprivation increases cocaine-induced conditioned place preference and locomotor activity in rats. *Psychopharmacology (Berl)*, 131, 1-8.

Bi, J., Tsai, N.P., Lin, Y.P., Loh, H.H. & Wei, L.N. (2006) Axonal mRNA transport and localized translational regulation of kappa-opioid receptor in primary neurons of dorsal root ganglia. *Proc Natl Acad Sci U S A*, 103, 19919-19924.

Binder, E.B. (2009) The role of FKBP5, a co-chaperone of the glucocorticoid receptor in the pathogenesis and therapy of affective and anxiety disorders. *Psychoneuroendocrinology*, 34 Suppl 1, S186-195.

Blednov, Y.A., Walker, D., Martinez, M., Levine, M., Damak, S. & Margolskee, R.F. (2008) Perception of sweet taste is important for voluntary alcohol consumption in mice. *Genes Brain Behav*, 7, 1-13.

Boehm, S.L., 2nd, Peden, L., Jennings, A.W., Kojima, N., Harris, R.A. & Blednov, Y.A. (2004) Over-expression of the fyn-kinase gene reduces hypnotic sensitivity to ethanol in mice. *Neurosci Lett*, 372, 6-11.

Bramham, C.R. & Wells, D.G. (2007) Dendritic mRNA: transport, translation and function. *Nat Rev Neurosci*, 8, 776-789.

Brebner, K., Wong, T.P., Liu, L., Liu, Y., Campsall, P., Gray, S., Phelps, L., Phillips, A.G. & Wang, Y.T. (2005) Nucleus accumbens long-term depression and the expression of behavioral sensitization. *Science*, 310, 1340-1343.

Broadbent, J. & Harless, W.E. (1999) Differential effects of GABA(A) and GABA(B) agonists on sensitization to the locomotor stimulant effects of ethanol in DBA/2 J mice. *Psychopharmacology (Berl)*, 141, 197-205.

Brown, T.E., Forquer, M.R., Cocking, D.L., Jansen, H.T., Harding, J.W. & Sorg, B.A. (2007) Role of matrix metalloproteinases in the acquisition and reconsolidation of cocaine-induced conditioned place preference. *Learn Mem*, 14, 214-223.

Brunig, I., Penschuck, S., Berninger, B., Benson, J. & Fritschy, J.M. (2001) BDNF reduces miniature inhibitory postsynaptic currents by rapid downregulation of GABA(A) receptor surface expression. *Eur J Neurosci*, 13, 1320-1328.

Burgin, K.E., Waxham, M.N., Rickling, S., Westgate, S.A., Mobley, W.C. & Kelly, P.T. (1990) In situ hybridization histochemistry of Ca2+/calmodulin-dependent protein kinase in developing rat brain. *J Neurosci*, 10, 1788-1798.

Cabeza de Vaca, S. & Carr, K.D. (1998) Food restriction enhances the central rewarding effect of abused drugs. *J Neurosci*, 18, 7502-7510.

Cajigas, I.J., Tushev, G., Will, T.J., tom Dieck, S., Fuerst, N. & Schuman, E.M. (2012) The local transcriptome in the synaptic neuropil revealed by deep sequencing and high-resolution imaging. *Neuron*, 74, 453-466.

Caldeira, M.V., Melo, C.V., Pereira, D.B., Carvalho, R.F., Carvalho, A.L. & Duarte, C.B. (2007) BDNF regulates the expression and traffic of NMDA receptors in cultured hippocampal neurons. *Mol Cell Neurosci*, 35, 208-219.

Camarini, R. & Hodge, C.W. (2004) Ethanol preexposure increases ethanol self-administration in C57BL/6J and DBA/2J mice. *Pharmacol Biochem Behav*, 79, 623-632.

Carpenter-Hyland, E.P. & Chandler, L.J. (2006) Homeostatic plasticity during alcohol exposure promotes enlargement of dendritic spines. *Eur J Neurosci*, 24, 3496-3506.

Carpenter-Hyland, E.P., Woodward, J.J. & Chandler, L.J. (2004) Chronic ethanol induces synaptic but not extrasynaptic targeting of NMDA receptors. *J Neurosci*, 24, 7859-7868.

Carr, K.D., Cabeza de Vaca, S., Sun, Y. & Chau, L.S. (2009) Reward-potentiating effects of D-1 dopamine receptor agonist and AMPAR GluR1 antagonist in nucleus accumbens shell and their modulation by food restriction. *Psychopharmacology (Berl)*, 202, 731-743.

Carrara-Nascimento, P.F., Griffin, W.C., 3rd, Pastrello, D.M., Olive, M.F. & Camarini, R. (2011) Changes in extracellular levels of glutamate in the nucleus accumbens after ethanol-induced behavioral sensitization in adolescent and adult mice. *Alcohol*, 45, 451-460.

Carroll, M.E., France, C.P. & Meisch, R.A. (1979) Food deprivation increases oral and intravenous drug intake in rats. *Science*, 205, 319-321.

Casadio, A., Martin, K.C., Giustetto, M., Zhu, H., Chen, M., Bartsch, D., Bailey, C.H. & Kandel, E.R. (1999) A transient, neuron-wide form of CREB-mediated long-term facilitation can be stabilized at specific synapses by local protein synthesis. *Cell*, 99, 221-237.

CDC (2014a) Excessive Drinking Costs U.S. $223.5 Billion.

CDC (2014b) Fact Sheets - Alcohol Use and Health.

Chee, M., Yang, R., Hubbell, E., Berno, A., Huang, X.C., Stern, D., Winkler, J., Lockhart, D.J., Morris, M.S. & Fodor, S.P. (1996) Accessing genetic information with high-density DNA arrays. *Science*, 274, 610-614.

Chen, J., Bardes, E.E., Aronow, B.J. & Jegga, A.G. (2009) ToppGene Suite for gene list enrichment analysis and candidate gene prioritization. *Nucleic Acids Res*, 37, W305-311.

Chiaruttini, C., Vicario, A., Li, Z., Baj, G., Braiuca, P., Wu, Y., Lee, F.S., Gardossi, L., Baraban, J.M. & Tongiorgi, E. (2009) Dendritic trafficking of BDNF mRNA is mediated by translin and blocked by the G196A (Val66Met) mutation. *Proc Natl Acad Sci U S A*, 106, 16481-16486.

Chicurel, M.E., Terrian, D.M. & Potter, H. (1993) mRNA at the synapse: analysis of a synaptosomal preparation enriched in hippocampal dendritic spines. *J Neurosci*, 13, 4054-4063.

Ciccocioppo, R., Stopponi, S., Economidou, D., Kuriyama, M., Kinoshita, H., Heilig, M., Roberto, M., Weiss, F. & Teshima, K. (2014) Chronic Treatment with Novel Brain-Penetrating Selective NOP Receptor Agonist MT-7716 Reduces Alcohol Drinking and Seeking in the Rat. *Neuropsychopharmacology*.

Cloonan, N. & Grimmond, S.M. (2008) Transcriptome content and dynamics at single-nucleotide resolution. *Genome Biol*, 9, 234.

Collins, M.O., Husi, H., Yu, L., Brandon, J.M., Anderson, C.N., Blackstock, W.P., Choudhary, J.S. & Grant, S.G. (2006) Molecular characterization and comparison of the components and multiprotein complexes in the postsynaptic proteome. *J Neurochem*, 97 Suppl 1, 16-23.

Colombo, G. & Grant, K.A. (1992) NMDA receptor complex antagonists have ethanol-like discriminative stimulus effects. *Ann N Y Acad Sci*, 654, 421-423.

Conover, J.C. & Yancopoulos, G.D. (1997) Neurotrophin regulation of the developing nervous system: analyses of knockout mice. *Rev Neurosci*, 8, 13-27.

Consortium, E.P. (2011) A user's guide to the encyclopedia of DNA elements (ENCODE). *PLoS Biol*, 9, e1001046.

Cook, K.B., Kazan, H., Zuberi, K., Morris, Q. & Hughes, T.R. (2011) RBPDB: a database of RNA-binding specificities. *Nucleic Acids Res*, 39, D301-308.

Costa, A., Bono, G., Martignoni, E., Merlo, P., Sances, G. & Nappi, G. (1996) An assessment of hypothalamo-pituitary-adrenal axis functioning in non-depressed, early abstinent alcoholics. *Psychoneuroendocrinology*, 21, 263-275.

Costall, B., Jones, B.J., Kelly, M.E., Naylor, R.J. & Tomkins, D.M. (1989) Exploration of mice in a black and white test box: validation as a model of anxiety. *Pharmacol Biochem Behav*, 32, 777-785.

Costin, B.N., Dever, S.M. & Miles, M.F. (2013a) Ethanol regulation of serum glucocorticoid kinase 1 expression in DBA2/J mouse prefrontal cortex. *PLoS One*, 8, e72979.

Costin, B.N., Wolen, A.R., Fitting, S., Shelton, K.L. & Miles, M.F. (2013b) Role of adrenal glucocorticoid signaling in prefrontal cortex gene expression and acute behavioral responses to ethanol. *Alcohol Clin Exp Res*, 37, 57-66.

Court, F.A., Hendriks, W.T., MacGillavry, H.D., Alvarez, J. & van Minnen, J. (2008) Schwann cell to axon transfer of ribosomes: toward a novel understanding of the role of glia in the nervous system. *J Neurosci*, 28, 11024-11029.

Crabbe, J.C., Jr., Johnson, N.A., Gray, D.K., Kosobud, A. & Young, E.R. (1982) Biphasic effects of ethanol on open-field activity: sensitivity and tolerance in C57BL/6N and DBA/2N mice. *J Comp Physiol Psychol*, 96, 440-451.

Crabbe, J.C., Phillips, T.J., Cunningham, C.L. & Belknap, J.K. (1992) Genetic determinants of ethanol reinforcement. *Ann N Y Acad Sci*, 654, 302-310.

Crawley, J. & Goodwin, F.K. (1980) Preliminary report of a simple animal behavior model for the anxiolytic effects of benzodiazepines. *Pharmacol Biochem Behav*, 13, 167-170.

Cryan, J.F. & Holmes, A. (2005) The ascent of mouse: advances in modelling human depression and anxiety. *Nat Rev Drug Discov*, 4, 775-790.

Cunningham, C.L., Gremel, C.M. & Groblewski, P.A. (2006) Drug-induced conditioned place preference and aversion in mice. *Nat Protoc*, 1, 1662-1670.

Curzon, P., Zhang, M., Radek, R.J. & Fox, G.B. (2009) The Behavioral Assessment of Sensorimotor Processes in the Mouse: Acoustic Startle, Sensory Gating, Locomotor Activity, Rotarod, and Beam Walking. In JJ, B. (ed) *Methods of Behavior Analysis in Neuroscience*, Boca Raton, FL.

Davis, H.P. & Squire, L.R. (1984) Protein synthesis and memory: a review. *Psychol Bull*, 96, 518-559.

Di Chiara, G. & Imperato, A. (1988) Drugs abused by humans preferentially increase synaptic dopamine concentrations in the mesolimbic system of freely moving rats. *Proc Natl Acad Sci U S A*, 85, 5274-5278.

Dobin, A., Davis, C.A., Schlesinger, F., Drenkow, J., Zaleski, C., Jha, S., Batut, P., Chaisson, M. & Gingeras, T.R. (2013) STAR: ultrafast universal RNA-seq aligner. *Bioinformatics*, 29, 15-21.

Doyle, M. & Kiebler, M.A. (2011) Mechanisms of dendritic mRNA transport and its role in synaptic tagging. *EMBO J*, 30, 3540-3552.

Eberwine, J., Miyashiro, K., Kacharmina, J.E. & Job, C. (2001) Local translation of classes of mRNAs that are targeted to neuronal dendrites. *Proc Natl Acad Sci U S A*, 98, 7080-7085.

Ellinwood, E.H., Jr. & Kilbey, M.M. (1980) Fundamental mechanisms underlying altered behavior following chronic administration of psychomotor stimulants. *Biol Psychiatry*, 15, 749-757.

Ellis, F.W. (1966) Effect of ethanol on plasma corticosterone levels. *J Pharmacol Exp Ther*, 153, 121-127.

Ernfors, P., Lee, K.F. & Jaenisch, R. (1994) Mice lacking brain-derived neurotrophic factor develop with sensory deficits. *Nature*, 368, 147-150.

Erwin, V.G. & Deitrich, R.A. (1996) Genetic selection and characterization of mouse lines for acute functional tolerance to ethanol. *J Pharmacol Exp Ther*, 279, 1310-1317.

Farris, S.P. & Miles, M.F. (2012) Ethanol modulation of gene networks: implications for alcoholism. *Neurobiol Dis*, 45, 115-121.

Farris, S.P. & Miles, M.F. (2013) Fyn-dependent gene networks in acute ethanol sensitivity. *PLoS One*, 8, e82435.

Figlewicz, D.P., Bennett, J.L., Naleid, A.M., Davis, C. & Grimm, J.W. (2006) Intraventricular insulin and leptin decrease sucrose self-administration in rats. *Physiol Behav*, 89, 611-616.

Fink, J.S. & Smith, G.P. (1980) Mesolimbic and mesocortical dopaminergic neurons are necessary for normal exploratory behavior in rats. *Neurosci Lett*, 17, 61-65.

Franck, J., Lindholm, S. & Raaschou, P. (1998) Modulation of volitional ethanol intake in the rat by central delta-opioid receptors. *Alcohol Clin Exp Res*, 22, 1185-1189.

Frey, U. & Morris, R.G. (1997) Synaptic tagging and long-term potentiation. *Nature*, 385, 533-536.

Fryer, R.H., Kaplan, D.R. & Kromer, L.F. (1997) Truncated trkB receptors on nonneuronal cells inhibit BDNF-induced neurite outgrowth in vitro. *Exp Neurol*, 148, 616-627.

Gardiol, A., Racca, C. & Triller, A. (1999) Dendritic and postsynaptic protein synthetic machinery. *J Neurosci*, 19, 168-179.

George, M.S., Anton, R.F., Bloomer, C., Teneback, C., Drobes, D.J., Lorberbaum, J.P., Nahas, Z. & Vincent, D.J. (2001) Activation of prefrontal cortex and anterior thalamus in alcoholic subjects on exposure to alcohol-specific cues. *Arch Gen Psychiatry*, 58, 345-352.

Gerstner, J.R., Vanderheyden, W.M., LaVaute, T., Westmark, C.J., Rouhana, L., Pack, A.I., Wickens, M. & Landry, C.F. (2012) Time of day regulates subcellular trafficking, tripartite synaptic localization, and polyadenylation of the astrocytic Fabp7 mRNA. *J Neurosci*, 32, 1383-1394.

Gessa, G.L., Muntoni, F., Collu, M., Vargiu, L. & Mereu, G. (1985) Low doses of ethanol activate dopaminergic neurons in the ventral tegmental area. *Brain Res*, 348, 201-203.

Gilpin, N.W. & Koob, G.F. (2008) Neurobiology of Alcohol Dependence: Focus on Motivational Mechanisms. *Alcohol Res Health*, 31, 185-195.

Giorgi, C., Yeo, G.W., Stone, M.E., Katz, D.B., Burge, C., Turrigiano, G. & Moore, M.J. (2007) The EJC factor eIF4AIII modulates synaptic strength and neuronal protein expression. *Cell*, 130, 179-191.

Gnegy, M.E., Hewlett, G.H., Yee, S.L. & Welsh, M.J. (1991) Alterations in calmodulin content and localization in areas of rat brain after repeated intermittent amphetamine. *Brain Res*, 562, 6-12.

Goggi, J., Pullar, I.A., Carney, S.L. & Bradford, H.F. (2002) Modulation of neurotransmitter release induced by brain-derived neurotrophic factor in rat brain striatal slices in vitro. *Brain Res*, 941, 34-42.

Goldstein, D.B. (1973) Letter: Inherited differences in intensity of alcohol withdrawal reactions in mice. *Nature*, 245, 154-156.

Gorski, J.A., Zeiler, S.R., Tamowski, S. & Jones, K.R. (2003) Brain-derived neurotrophic factor is required for the maintenance of cortical dendrites. *J Neurosci*, 23, 6856-6865.

Grant, K.A. (1999) Strategies for understanding the pharmacological effects of ethanol with drug discrimination procedures. *Pharmacol Biochem Behav*, 64, 261-267.

Grant, K.A. & Colombo, G. (1993) Pharmacological analysis of the mixed discriminative stimulus effects of ethanol. *Alcohol Alcohol Suppl*, 2, 445-449.

Grant, K.A., Colombo, G. & Gatto, G.J. (1997) Characterization of the ethanol-like discriminative stimulus effects of 5-HT receptor agonists as a function of ethanol training dose. *Psychopharmacology (Berl)*, 133, 133-141.

Gratacos, M., Gonzalez, J.R., Mercader, J.M., de Cid, R., Urretavizcaya, M. & Estivill, X. (2007) Brain-derived neurotrophic factor Val66Met and psychiatric disorders: meta-analysis of case-control studies confirm association to substance-related disorders, eating disorders, and schizophrenia. *Biol Psychiatry*, 61, 911-922.

Gray, E.G. & Whittaker, V.P. (1960) The isolation of synaptic vesicles from the central nervous system. *J Physiol*, 153, 35P-37P.

Green, A.S. & Grahame, N.J. (2008) Ethanol drinking in rodents: is free-choice drinking related to the reinforcing effects of ethanol? *Alcohol*, 42, 1-11.

Green, K.L. & Grant, K.A. (1998) Evidence for overshadowing by components of the heterogeneous discriminative stimulus effects of ethanol. *Drug Alcohol Depend*, 52, 149-159.

Greenberg, M.E., Xu, B., Lu, B. & Hempstead, B.L. (2009) New insights in the biology of BDNF synthesis and release: implications in CNS function. *J Neurosci*, 29, 12764-12767.

Grooms, S.Y., Noh, K.M., Regis, R., Bassell, G.J., Bryan, M.K., Carroll, R.C. & Zukin, R.S. (2006) Activity bidirectionally regulates AMPA receptor mRNA

abundance in dendrites of hippocampal neurons. *J Neurosci*, 26, 8339-8351.

Haberny, S.L., Berman, Y., Meller, E. & Carr, K.D. (2004) Chronic food restriction increases D-1 dopamine receptor agonist-induced phosphorylation of extracellular signal-regulated kinase 1/2 and cyclic AMP response element-binding protein in caudate-putamen and nucleus accumbens. *Neuroscience*, 125, 289-298.

Halassa, M.M. & Haydon, P.G. (2010) Integrated brain circuits: astrocytic networks modulate neuronal activity and behavior. *Annu Rev Physiol*, 72, 335-355.

Hall, F.S., Drgonova, J., Goeb, M. & Uhl, G.R. (2003) Reduced behavioral effects of cocaine in heterozygous brain-derived neurotrophic factor (BDNF) knockout mice. *Neuropsychopharmacology*, 28, 1485-1490.

Harris, R.A., McQuilkin, S.J., Paylor, R., Abeliovich, A., Tonegawa, S. & Wehner, J.M. (1995) Mutant mice lacking the gamma isoform of protein kinase C show decreased behavioral actions of ethanol and altered function of gamma-aminobutyrate type A receptors. *Proc Natl Acad Sci U S A*, 92, 3658-3662.

Harrison, S.J. & Nobrega, J.N. (2009) Differential susceptibility to ethanol and amphetamine sensitization in dopamine D3 receptor-deficient mice. *Psychopharmacology (Berl)*, 204, 49-59.

Hartmann, M., Heumann, R. & Lessmann, V. (2001) Synaptic secretion of BDNF after high-frequency stimulation of glutamatergic synapses. *EMBO J*, 20, 5887-5897.

Heath, A.C., Madden, P.A., Bucholz, K.K., Dinwiddie, S.H., Slutske, W.S., Bierut, L.J., Rohrbaugh, J.W., Statham, D.J., Dunne, M.P., Whitfield, J.B. & Martin, N.G. (1999) Genetic differences in alcohol sensitivity and the inheritance of alcoholism risk. *Psychol Med*, 29, 1069-1081.

Hensler, J.G., Ladenheim, E.E. & Lyons, W.E. (2003) Ethanol consumption and serotonin-1A (5-HT1A) receptor function in heterozygous BDNF (+/-) mice. *J Neurochem*, 85, 1139-1147.

Hirabayashi, M. & Alam, M.R. (1981) Enhancing effect of methamphetamine on ambulatory activity produced by repeated administration in mice. *Pharmacol Biochem Behav*, 15, 925-932.

Hoffman, P.L., Ritzmann, R.F., Walter, R. & Tabakoff, B. (1978) Arginine vasopressin maintains ethanol tolerance. *Nature*, 276, 614-616.

Hollingsworth, E.B., McNeal, E.T., Burton, J.L., Williams, R.J., Daly, J.W. & Creveling, C.R. (1985) Biochemical characterization of a filtered synaptoneurosome preparation from guinea pig cerebral cortex: cyclic adenosine 3':5'-monophosphate-generating systems, receptors, and enzymes. *J Neurosci*, 5, 2240-2253.

Holt, C.E. & Schuman, E.M. (2013) The central dogma decentralized: new perspectives on RNA function and local translation in neurons. *Neuron*, 80, 648-657.

Hooks, M.S. & Kalivas, P.W. (1995) The role of mesoaccumbens--pallidal circuitry in novelty-induced behavioral activation. *Neuroscience*, 64, 587-597.

Horger, B.A., Iyasere, C.A., Berhow, M.T., Messer, C.J., Nestler, E.J. & Taylor, J.R. (1999) Enhancement of locomotor activity and conditioned reward to cocaine by brain-derived neurotrophic factor. *J Neurosci*, 19, 4110-4122.

Horger, B.A., Shelton, K. & Schenk, S. (1990) Preexposure sensitizes rats to the rewarding effects of cocaine. *Pharmacol Biochem Behav*, 37, 707-711.

Huang, Y.S., Carson, J.H., Barbarese, E. & Richter, J.D. (2003) Facilitation of dendritic mRNA transport by CPEB. *Genes Dev*, 17, 638-653.

Huang, Z.J., Kirkwood, A., Pizzorusso, T., Porciatti, V., Morales, B., Bear, M.F., Maffei, L. & Tonegawa, S. (1999) BDNF regulates the maturation of inhibition and the critical period of plasticity in mouse visual cortex. *Cell*, 98, 739-755.

Huber, K.M., Kayser, M.S. & Bear, M.F. (2000) Role for rapid dendritic protein synthesis in hippocampal mGluR-dependent long-term depression. *Science*, 288, 1254-1257.

Hyman, S.E., Malenka, R.C. & Nestler, E.J. (2006) Neural mechanisms of addiction: the role of reward-related learning and memory. *Annu Rev Neurosci*, 29, 565-598.

Imaizumi, M., Miyazaki, S. & Onodera, K. (1994a) Effects of xanthine derivatives in a light/dark test in mice and the contribution of adenosine receptors. *Methods Find Exp Clin Pharmacol*, 16, 639-644.

Imaizumi, M., Suzuki, T., Machida, H. & Onodera, K. (1994b) A fully automated apparatus for a light/dark test measuring anxiolytic or anxiogenic effects of drugs in mice. *Nihon Shinkei Seishin Yakurigaku Zasshi*, 14, 83-91.

Irizarry, R.A., Hobbs, B., Collin, F., Beazer-Barclay, Y.D., Antonellis, K.J., Scherf, U. & Speed, T.P. (2003) Exploration, normalization, and summaries of high density oligonucleotide array probe level data. *Biostatistics*, 4, 249-264.

Jansen, R.C. & Nap, J.P. (2001) Genetical genomics: the added value from segregation. *Trends Genet*, 17, 388-391.

Jeanblanc, J., He, D.Y., Carnicella, S., Kharazia, V., Janak, P.H. & Ron, D. (2009) Endogenous BDNF in the dorsolateral striatum gates alcohol drinking. *J Neurosci*, 29, 13494-13502.

Jeanblanc, J., He, D.Y., McGough, N.N., Logrip, M.L., Phamluong, K., Janak, P.H. & Ron, D. (2006) The dopamine D3 receptor is part of a homeostatic pathway regulating ethanol consumption. *J Neurosci*, 26, 1457-1464.

Joe, K.H., Kim, Y.K., Kim, T.S., Roh, S.W., Choi, S.W., Kim, Y.B., Lee, H.J. & Kim, D.J. (2007) Decreased plasma brain-derived neurotrophic factor levels in patients with alcohol dependence. *Alcohol Clin Exp Res*, 31, 1833-1838.

Johnson, D.R., Lee, P.K., Holmes, V.F. & Alvarez-Cohen, L. (2005) An internal reference technique for accurately quantifying specific mRNAs by real-time PCR with application to the tceA reductive dehalogenase gene. *Appl Environ Microbiol*, 71, 3866-3871.

Johnson, M.W., Chotiner, J.K. & Watson, J.B. (1997) Isolation and characterization of synaptoneurosomes from single rat hippocampal slices. *J Neurosci Methods*, 77, 151-156.

Jovanovic, J.N., Benfenati, F., Siow, Y.L., Sihra, T.S., Sanghera, J.S., Pelech, S.L., Greengard, P. & Czernik, A.J. (1996) Neurotrophins stimulate phosphorylation of synapsin I by MAP kinase and regulate synapsin I-actin interactions. *Proc Natl Acad Sci U S A*, 93, 3679-3683.

Jovanovic, J.N., Thomas, P., Kittler, J.T., Smart, T.G. & Moss, S.J. (2004) Brain-derived neurotrophic factor modulates fast synaptic inhibition by regulating GABA(A) receptor phosphorylation, activity, and cell-surface stability. *J Neurosci*, 24, 522-530.

Kalivas, P.W. & Duffy, P. (1990) Effect of acute and daily cocaine treatment on extracellular dopamine in the nucleus accumbens. *Synapse*, 5, 48-58.

Kalivas, P.W. & Stewart, J. (1991) Dopamine transmission in the initiation and expression of drug- and stress-induced sensitization of motor activity. *Brain Res Brain Res Rev*, 16, 223-244.

Kampov-Polevoy, A.B., Eick, C., Boland, G., Khalitov, E. & Crews, F.T. (2004) Sweet liking, novelty seeking, and gender predict alcoholic status. *Alcohol Clin Exp Res*, 28, 1291-1298.

Kanai, Y., Dohmae, N. & Hirokawa, N. (2004) Kinesin transports RNA: isolation and characterization of an RNA-transporting granule. *Neuron*, 43, 513-525.

Kandel, E.R. (2001) The molecular biology of memory storage: a dialogue between genes and synapses. *Science*, 294, 1030-1038.

Kang, H. & Schuman, E.M. (1996) A requirement for local protein synthesis in neurotrophin-induced hippocampal synaptic plasticity. *Science*, 273, 1402-1406.

Karson, C.N. (1983) Spontaneous eye-blink rates and dopaminergic systems. *Brain*, 106 (Pt 3), 643-653.

Kawai, K., Sugimoto, K., Nakashima, K., Miura, H. & Ninomiya, Y. (2000) Leptin as a modulator of sweet taste sensitivities in mice. *Proc Natl Acad Sci U S A*, 97, 11044-11049.

Kelleher, R.J., 3rd, Govindarajan, A. & Tonegawa, S. (2004) Translational regulatory mechanisms in persistent forms of synaptic plasticity. *Neuron*, 44, 59-73.

Kerns, R.T., Ravindranathan, A., Hassan, S., Cage, M.P., York, T., Sikela, J.M., Williams, R.W. & Miles, M.F. (2005) Ethanol-responsive brain region expression networks: implications for behavioral responses to acute ethanol in DBA/2J versus C57BL/6J mice. *J Neurosci*, 25, 2255-2266.

Khisti, R.T., Wolstenholme, J., Shelton, K.L. & Miles, M.F. (2006) Characterization of the ethanol-deprivation effect in substrains of C57BL/6 mice. *Alcohol*, 40, 119-126.

Kiebler, M.A. & Bassell, G.J. (2006) Neuronal RNA granules: movers and makers. *Neuron*, 51, 685-690.

Kim, K.S., Kim, H., Park, S.K. & Han, P.L. (2012) The dorsal striatum expressing adenylyl cyclase-5 controls behavioral sensitivity of the righting reflex to high-dose ethanol. *Brain Res*, 1489, 27-36.

Kimpel, M.W., Strother, W.N., McClintick, J.N., Carr, L.G., Liang, T., Edenberg, H.J. & McBride, W.J. (2007) Functional gene expression differences between inbred alcohol-preferring and -non-preferring rats in five brain regions. *Alcohol*, 41, 95-132.

Knowles, R.B., Sabry, J.H., Martone, M.E., Deerinck, T.J., Ellisman, M.H., Bassell, G.J. & Kosik, K.S. (1996) Translocation of RNA granules in living neurons. *J Neurosci*, 16, 7812-7820.

Koenig, E., Martin, R., Titmus, M. & Sotelo-Silveira, J.R. (2000) Cryptic peripheral ribosomal domains distributed intermittently along mammalian myelinated axons. *J Neurosci*, 20, 8390-8400.

Kolbeck, R., Bartke, I., Eberle, W. & Barde, Y.A. (1999) Brain-derived neurotrophic factor levels in the nervous system of wild-type and neurotrophin gene mutant mice. *J Neurochem*, 72, 1930-1938.

Koob, G.F. (1992) Drugs of abuse: anatomy, pharmacology and function of reward pathways. *Trends Pharmacol Sci*, 13, 177-184.

Koob, G.F. (2000) Neurobiology of addiction. Toward the development of new therapies. *Ann N Y Acad Sci*, 909, 170-185.

Koob, G.F. (2003) Alcoholism: allostasis and beyond. *Alcohol Clin Exp Res*, 27, 232-243.

Koob, G.F., Stinus, L. & Le Moal, M. (1981) Hyperactivity and hypoactivity produced by lesions to the mesolimbic dopamine system. *Behav Brain Res*, 3, 341-359.

Korte, M., Carroll, P., Wolf, E., Brem, G., Thoenen, H. & Bonhoeffer, T. (1995) Hippocampal long-term potentiation is impaired in mice lacking brain-derived neurotrophic factor. *Proc Natl Acad Sci U S A*, 92, 8856-8860.

Lee, R., Kermani, P., Teng, K.K. & Hempstead, B.L. (2001) Regulation of cell survival by secreted proneurotrophins. *Science*, 294, 1945-1948.

Lessmann, V., Gottmann, K. & Malcangio, M. (2003) Neurotrophin secretion: current facts and future prospects. *Prog Neurobiol*, 69, 341-374.

Lessov, C.N., Palmer, A.A., Quick, E.A. & Phillips, T.J. (2001) Voluntary ethanol drinking in C57BL/6J and DBA/2J mice before and after sensitization to the locomotor stimulant effects of ethanol. *Psychopharmacology (Berl)*, 155, 91-99.

Lett, B.T. (1989) Repeated exposures intensify rather than diminish the rewarding effects of amphetamine, morphine, and cocaine. *Psychopharmacology (Berl)*, 98, 357-362.

Levine, E.S., Crozier, R.A., Black, I.B. & Plummer, M.R. (1998) Brain-derived neurotrophic factor modulates hippocampal synaptic transmission by increasing N-methyl-D-aspartic acid receptor activity. *Proc Natl Acad Sci U S A*, 95, 10235-10239.

Lewohl, J.M., Nunez, Y.O., Dodd, P.R., Tiwari, G.R., Harris, R.A. & Mayfield, R.D. (2011) Up-regulation of microRNAs in brain of human alcoholics. *Alcohol Clin Exp Res*, 35, 1928-1937.

Lewohl, J.M., Wang, L., Miles, M.F., Zhang, L., Dodd, P.R. & Harris, R.A. (2000) Gene expression in human alcoholism: microarray analysis of frontal cortex. *Alcohol Clin Exp Res*, 24, 1873-1882.

Li, T.K., Lumeng, L. & Doolittle, D.P. (1993) Selective breeding for alcohol preference and associated responses. *Behav Genet*, 23, 163-170.

Liao, G.Y., An, J.J., Gharami, K., Waterhouse, E.G., Vanevski, F., Jones, K.R. & Xu, B. (2012) Dendritically targeted Bdnf mRNA is essential for energy balance and response to leptin. *Nat Med*, 18, 564-571.

Lin, S.Y., Wu, K., Levine, E.S., Mount, H.T., Suen, P.C. & Black, I.B. (1998) BDNF acutely increases tyrosine phosphorylation of the NMDA receptor subunit 2B in cortical and hippocampal postsynaptic densities. *Brain Res Mol Brain Res*, 55, 20-27.

Link, W., Konietzko, U., Kauselmann, G., Krug, M., Schwanke, B., Frey, U. & Kuhl, D. (1995) Somatodendritic expression of an immediate early gene is regulated by synaptic activity. *Proc Natl Acad Sci U S A*, 92, 5734-5738.

Litman, P., Barg, J. & Ginzburg, I. (1994) Microtubules are involved in the localization of tau mRNA in primary neuronal cell cultures. *Neuron*, 13, 1463-1474.

Liu, J., Lewohl, J.M., Harris, R.A., Iyer, V.R., Dodd, P.R., Randall, P.K. & Mayfield, R.D. (2006a) Patterns of gene expression in the frontal cortex discriminate alcoholic from nonalcoholic individuals. *Neuropsychopharmacology*, 31, 1574-1582.

Liu, Q.R., Lu, L., Zhu, X.G., Gong, J.P., Shaham, Y. & Uhl, G.R. (2006b) Rodent BDNF genes, novel promoters, novel splice variants, and regulation by cocaine. *Brain Res*, 1067, 1-12.

Liu, Y., Ferguson, J.F., Xue, C., Silverman, I.M., Gregory, B., Reilly, M.P. & Li, M. (2013) Evaluating the impact of sequencing depth on transcriptome profiling in human adipose. *PLoS One*, 8, e66883.

Lockhart, D.J. & Barlow, C. (2001) Expressing what's on your mind: DNA arrays and the brain. *Nat Rev Neurosci*, 2, 63-68.

Lockhart, D.J. & Winzeler, E.A. (2000) Genomics, gene expression and DNA arrays. *Nature*, 405, 827-836.

Logrip, M.L., Janak, P.H. & Ron, D. (2008) Dynorphin is a downstream effector of striatal BDNF regulation of ethanol intake. *FASEB J*, 22, 2393-2404.

Logrip, M.L., Janak, P.H. & Ron, D. (2009) Escalating ethanol intake is associated with altered corticostriatal BDNF expression. *J Neurochem*, 109, 1459-1468.

Lovinger, D.M., White, G. & Weight, F.F. (1989) Ethanol inhibits NMDA-activated ion current in hippocampal neurons. *Science*, 243, 1721-1724.

Lu, B. (2003) BDNF and activity-dependent synaptic modulation. *Learn Mem*, 10, 86-98.

Lu, Y., Christian, K. & Lu, B. (2008) BDNF: a key regulator for protein synthesis-dependent LTP and long-term memory? *Neurobiol Learn Mem*, 89, 312-323.

Lugli, G., Larson, J., Martone, M.E., Jones, Y. & Smalheiser, N.R. (2005) Dicer and eIF2c are enriched at postsynaptic densities in adult mouse brain and are modified by neuronal activity in a calpain-dependent manner. *J Neurochem*, 94, 896-905.

Lugli, G., Torvik, V.I., Larson, J. & Smalheiser, N.R. (2008) Expression of microRNAs and their precursors in synaptic fractions of adult mouse forebrain. *J Neurochem*, 106, 650-661.

Lyford, G.L., Yamagata, K., Kaufmann, W.E., Barnes, C.A., Sanders, L.K., Copeland, N.G., Gilbert, D.J., Jenkins, N.A., Lanahan, A.A. & Worley, P.F. (1995) Arc, a growth factor and activity-regulated gene, encodes a novel cytoskeleton-associated protein that is enriched in neuronal dendrites. *Neuron*, 14, 433-445.

Lyons, W.E., Mamounas, L.A., Ricaurte, G.A., Coppola, V., Reid, S.W., Bora, S.H., Wihler, C., Koliatsos, V.E. & Tessarollo, L. (1999) Brain-derived neurotrophic factor-deficient mice develop aggressiveness and hyperphagia in conjunction with brain serotonergic abnormalities. *Proc Natl Acad Sci U S A*, 96, 15239-15244.

Maisonneuve, I.M., Keller, R.W. & Glick, S.D. (1990) Similar effects of D-amphetamine and cocaine on extracellular dopamine levels in medial prefrontal cortex of rats. *Brain Res*, 535, 221-226.

Martin, K.C. & Kosik, K.S. (2002) Synaptic tagging -- who's it? *Nat Rev Neurosci*, 3, 813-820.

Masur, J. & Boerngen, R. (1980) The excitatory component of ethanol in mice: a chronic study. *Pharmacol Biochem Behav*, 13, 777-780.

Masur, J., Oliveira de Souza, M.L. & Zwicker, A.P. (1986) The excitatory effect of ethanol: absence in rats, no tolerance and increased sensitivity in mice. *Pharmacol Biochem Behav*, 24, 1225-1228.

Matsumoto, M., Setou, M. & Inokuchi, K. (2007) Transcriptome analysis reveals the population of dendritic RNAs and their redistribution by neural activity. *Neurosci Res*, 57, 411-423.

Matsushita, S., Kimura, M., Miyakawa, T., Yoshino, A., Murayama, M., Masaki, T. & Higuchi, S. (2004) Association study of brain-derived neurotrophic factor gene polymorphism and alcoholism. *Alcohol Clin Exp Res*, 28, 1609-1612.

McBride, W.J., Kimpel, M.W., Schultz, J.A., McClintick, J.N., Edenberg, H.J. & Bell, R.L. (2010) Changes in gene expression in regions of the extended amygdala of alcohol-preferring rats after binge-like alcohol drinking. *Alcohol*, 44, 171-183.

McClearn, G.E. & Rodgers, D.A. (1959) Differences in alcohol preference among inbred strains of mice. *QJ Stud Alcohol*, 20, 691-695.

McClintick, J.N. & Edenberg, H.J. (2006) Effects of filtering by Present call on analysis of microarray experiments. *BMC Bioinformatics*, 7, 49.

McGough, N.N., He, D.Y., Logrip, M.L., Jeanblanc, J., Phamluong, K., Luong, K., Kharazia, V., Janak, P.H. & Ron, D. (2004) RACK1 and brain-derived neurotrophic factor: a homeostatic pathway that regulates alcohol addiction. *J Neurosci*, 24, 10542-10552.

Melendez, R.I. (2011) Intermittent (every-other-day) drinking induces rapid escalation of ethanol intake and preference in adolescent and adult C57BL/6J mice. *Alcohol Clin Exp Res*, 35, 652-658.

Melendez, R.I., Middaugh, L.D. & Kalivas, P.W. (2006) Development of an alcohol deprivation and escalation effect in C57BL/6J mice. *Alcohol Clin Exp Res*, 30, 2017-2025.

Metten, P., Phillips, T.J., Crabbe, J.C., Tarantino, L.M., McClearn, G.E., Plomin, R., Erwin, V.G. & Belknap, J.K. (1998) High genetic susceptibility to ethanol withdrawal predicts low ethanol consumption. *Mamm Genome*, 9, 983-990.

Middaugh, L.D. & Bandy, A.L. (2000) Naltrexone effects on ethanol consumption and response to ethanol conditioned cues in C57BL/6 mice. *Psychopharmacology (Berl)*, 151, 321-327.

Miles, M.F., Diaz, J.E. & DeGuzman, V. (1992) Ethanol-responsive gene expression in neural cell cultures. *Biochim Biophys Acta*, 1138, 268-274.

Miles, M.F., Wilke, N., Elliot, M., Tanner, W. & Shah, S. (1994) Ethanol-responsive genes in neural cells include the 78-kilodalton glucose-regulated protein (GRP78) and 94-kilodalton glucose-regulated protein (GRP94) molecular chaperones. *Mol Pharmacol*, 46, 873-879.

Miyakawa, T., Yagi, T., Kitazawa, H., Yasuda, M., Kawai, N., Tsuboi, K. & Niki, H. (1997) Fyn-kinase as a determinant of ethanol sensitivity: relation to NMDA-receptor function. *Science*, 278, 698-701.

Mohr, E., Fehr, S. & Richter, D. (1991) Axonal transport of neuropeptide encoding mRNAs within the hypothalamo-hypophyseal tract of rats. *EMBO J*, 10, 2419-2424.

Mohr, E. & Richter, D. (1992) Diversity of mRNAs in the Axonal Compartment of Peptidergic Neurons in the Rat. *Eur J Neurosci*, 4, 870-876.

Monti, P.M., Rohsenow, D.J., Hutchison, K.E., Swift, R.M., Mueller, T.I., Colby, S.M., Brown, R.A., Gulliver, S.B., Gordon, A. & Abrams, D.B. (1999) Naltrexone's effect on cue-elicited craving among alcoholics in treatment. *Alcohol Clin Exp Res*, 23, 1386-1394.

Morice, E., Denis, C., Giros, B. & Nosten-Bertrand, M. (2010) Evidence of long-term expression of behavioral sensitization to both cocaine and ethanol in dopamine transporter knockout mice. *Psychopharmacology (Berl)*, 208, 57-66.

Morrow, A.L., Herbert, J.S. & Montpied, P. (1992) Differential effects of chronic ethanol administration on GABA(A) receptor alpha1 and alpha6 subunit mRNA levels in rat cerebellum. *Mol Cell Neurosci*, 3, 251-258.

Mortazavi, A., Williams, B.A., McCue, K., Schaeffer, L. & Wold, B. (2008) Mapping and quantifying mammalian transcriptomes by RNA-Seq. *Nat Methods*, 5, 621-628.

Mostafavi, S., Ray, D., Warde-Farley, D., Grouios, C. & Morris, Q. (2008) GeneMANIA: a real-time multiple association network integration algorithm for predicting gene function. *Genome Biol*, 9 Suppl 1, S4.

Mulligan, M.K., Rhodes, J.S., Crabbe, J.C., Mayfield, R.D., Harris, R.A. & Ponomarev, I. (2011) Molecular profiles of drinking alcohol to intoxication in C57BL/6J mice. *Alcohol Clin Exp Res*, 35, 659-670.

Mumenthaler, M.S., Taylor, J.L., O'Hara, R. & Yesavage, J.A. (1999) Gender differences in moderate drinking effects. *Alcohol Res Health*, 23, 55-64.

Muschler, M.A., Heberlein, A., Frieling, H., Vogel, N., Becker, C.M., Kornhuber, J., Bleich, S. & Hillemacher, T. (2011) Brain-derived neurotrophic factor, Val66Met single nucleotide polymorphism is not associated with alcohol dependence. *Psychiatr Genet*, 21, 53-54.

Nedic, G., Perkovic, M.N., Sviglin, K.N., Muck-Seler, D., Borovecki, F. & Pivac, N. (2013) Brain-derived neurotrophic factor Val66Met polymorphism and alcohol-related phenotypes. *Prog Neuropsychopharmacol Biol Psychiatry*, 40, 193-198.

Nestler, E.J. (2001a) Molecular basis of long-term plasticity underlying addiction. *Nat Rev Neurosci*, 2, 119-128.

Nestler, E.J. (2001b) Molecular neurobiology of addiction. *Am J Addict*, 10, 201-217.

Nestler, E.J. & Aghajanian, G.K. (1997) Molecular and cellular basis of addiction. *Science*, 278, 58-63.

Nestler, E.J., Hope, B.T. & Widnell, K.L. (1993) Drug addiction: a model for the molecular basis of neural plasticity. *Neuron*, 11, 995-1006.

Nestler, E.J., Terwilliger, R.Z., Walker, J.R., Sevarino, K.A. & Duman, R.S. (1990) Chronic cocaine treatment decreases levels of the G protein subunits Gi alpha and Go alpha in discrete regions of rat brain. *J Neurochem*, 55, 1079-1082.

Newlin, D.B. & Thomson, J.B. (1991) Chronic tolerance and sensitization to alcohol in sons of alcoholics. *Alcohol Clin Exp Res*, 15, 399-405.

NIAAA (2012) Alcohol Use Disorders.

Oka, M., Hirouchi, M., Tamura, M., Sugahara, S. & Oyama, T. (2013) Acamprosate {monocalcium bis(3-acetamidopropane-1-sulfonate)} reduces ethanol-drinking behavior in rats and glutamate-induced toxicity in ethanol-exposed primary rat cortical neuronal cultures. *Eur J Pharmacol*, 718, 323-331.

Onaivi, E.S. & Martin, B.R. (1989) Neuropharmacological and physiological validation of a computer-controlled two-compartment black and white box for the assessment of anxiety. *Prog Neuropsychopharmacol Biol Psychiatry*, 13, 963-976.

Ostroff, L.E., Fiala, J.C., Allwardt, B. & Harris, K.M. (2002) Polyribosomes redistribute from dendritic shafts into spines with enlarged synapses during LTP in developing rat hippocampal slices. *Neuron*, 35, 535-545.

Otis, J.M., Fitzgerald, M.K. & Mueller, D. (2014) Infralimbic BDNF/TrkB enhancement of GluN2B currents facilitates extinction of a cocaine-conditioned place preference. *J Neurosci*, 34, 6057-6064.

Pan, Y., Berman, Y., Haberny, S., Meller, E. & Carr, K.D. (2006) Synthesis, protein levels, activity, and phosphorylation state of tyrosine hydroxylase in mesoaccumbens and nigrostriatal dopamine pathways of chronically food-restricted rats. *Brain Res*, 1122, 135-142.

Pastor, R., Reed, C., Meyer, P.J., McKinnon, C., Ryabinin, A.E. & Phillips, T.J. (2012) Role of corticotropin-releasing factor and corticosterone in behavioral sensitization to ethanol. *J Pharmacol Exp Ther*, 341, 455-463.

Patterson, S.L., Abel, T., Deuel, T.A., Martin, K.C., Rose, J.C. & Kandel, E.R. (1996) Recombinant BDNF rescues deficits in basal synaptic transmission and hippocampal LTP in BDNF knockout mice. *Neuron*, 16, 1137-1145.

Paulson, P.E. & Robinson, T.E. (1995) Amphetamine-induced time-dependent sensitization of dopamine neurotransmission in the dorsal and ventral striatum: a microdialysis study in behaving rats. *Synapse*, 19, 56-65.

Pavlidis, P. & Noble, W.S. (2001) Analysis of strain and regional variation in gene expression in mouse brain. *Genome Biol*, 2, RESEARCH0042.

Phillips, T.J., Dickinson, S. & Burkhart-Kasch, S. (1994) Behavioral sensitization to drug stimulant effects in C57BL/6J and DBA/2J inbred mice. *Behav Neurosci*, 108, 789-803.

Phillips, T.J., Huson, M., Gwiazdon, C., Burkhart-Kasch, S. & Shen, E.H. (1995) Effects of acute and repeated ethanol exposures on the locomotor activity of BXD recombinant inbred mice. *Alcohol Clin Exp Res*, 19, 269-278.

Phillips, T.J., Roberts, A.J. & Lessov, C.N. (1997) Behavioral sensitization to ethanol: genetics and the effects of stress. *Pharmacol Biochem Behav*, 57, 487-493.

Piazza, P.V., Deminiere, J.M., le Moal, M. & Simon, H. (1990) Stress- and pharmacologically-induced behavioral sensitization increases vulnerability to acquisition of amphetamine self-administration. *Brain Res*, 514, 22-26.

Pietrzykowski, A.Z., Friesen, R.M., Martin, G.E., Puig, S.I., Nowak, C.L., Wynne, P.M., Siegelmann, H.T. & Treistman, S.N. (2008) Posttranscriptional regulation of BK channel splice variant stability by miR-9 underlies neuroadaptation to alcohol. *Neuron*, 59, 274-287.

Pohorecky, L.A. (1997) Biphasic action of ethanol. *Biobehav Rev*, 1, 231-240.

Pohorecky, L.A. & Newman, B. (1977) Effect of ethanol on dopamine synthesis in rat striatal synaptosomes. *Drug Alcohol Depend*, 2, 329-334.

Ponomarev, I. & Crabbe, J.C. (2002) A novel method to assess initial sensitivity and acute functional tolerance to hypnotic effects of ethanol. *J Pharmacol Exp Ther*, 302, 257-263.

Ponomarev, I., Wang, S., Zhang, L., Harris, R.A. & Mayfield, R.D. (2012) Gene coexpression networks in human brain identify epigenetic modifications in alcohol dependence. *J Neurosci*, 32, 1884-1897.

Pontieri, F.E., Tanda, G. & Di Chiara, G. (1995) Intravenous cocaine, morphine, and amphetamine preferentially increase extracellular dopamine in the "shell" as compared with the "core" of the rat nucleus accumbens. *Proc Natl Acad Sci U S A*, 92, 12304-12308.

Poo, M.M. (2001) Neurotrophins as synaptic modulators. *Nat Rev Neurosci*, 2, 24-32.

Poon, M.M., Choi, S.H., Jamieson, C.A., Geschwind, D.H. & Martin, K.C. (2006) Identification of process-localized mRNAs from cultured rodent hippocampal neurons. *J Neurosci*, 26, 13390-13399.

Proctor, W.R., Poelchen, W., Bowers, B.J., Wehner, J.M., Messing, R.O. & Dunwiddie, T.V. (2003) Ethanol differentially enhances hippocampal GABA A receptor-mediated responses in protein kinase C gamma (PKC gamma) and PKC epsilon null mice. *J Pharmacol Exp Ther*, 305, 264-270.

Qiang, M., Denny, A.D. & Ticku, M.K. (2007) Chronic intermittent ethanol treatment selectively alters N-methyl-D-aspartate receptor subunit surface expression in cultured cortical neurons. *Mol Pharmacol*, 72, 95-102.

Qiao, X., Hefti, F., Knusel, B. & Noebels, J.L. (1996) Selective failure of brain-derived neurotrophic factor mRNA expression in the cerebellum of stargazer, a mutant mouse with ataxia. *J Neurosci*, 16, 640-648.

Quadros, I.M., Souza-Formigoni, M.L., Fornari, R.V., Nobrega, J.N. & Oliveira, M.G. (2003) Is behavioral sensitization to ethanol associated with contextual conditioning in mice? *Behav Pharmacol*, 14, 129-136.

Quertemont, E., Green, H.L. & Grant, K.A. (2003) Brain ethanol concentrations and ethanol discrimination in rats: effects of dose and time. *Psychopharmacology (Berl)*, 168, 262-270.

Ramos, A. (2008) Animal models of anxiety: do I need multiple tests? *Trends Pharmacol Sci*, 29, 493-498.

Rao, A. & Steward, O. (1991) Evidence that protein constituents of postsynaptic membrane specializations are locally synthesized: analysis of proteins synthesized within synaptosomes. *J Neurosci*, 11, 2881-2895.

Rao, A. & Steward, O. (1993) Evaluation of RNAs present in synaptodendrosomes: dendritic, glial, and neuronal cell body contribution. *J Neurochem*, 61, 835-844.

Rasmussen, D.D., Boldt, B.M., Bryant, C.A., Mitton, D.R., Larsen, S.A. & Wilkinson, C.W. (2000) Chronic daily ethanol and withdrawal: 1. Long-term changes in the hypothalamo-pituitary-adrenal axis. *Alcohol Clin Exp Res*, 24, 1836-1849.

Richardson, H.N., Lee, S.Y., O'Dell, L.E., Koob, G.F. & Rivier, C.L. (2008) Alcohol self-administration acutely stimulates the hypothalamic-pituitary-adrenal axis, but alcohol dependence leads to a dampened neuroendocrine state. *Eur J Neurosci*, 28, 1641-1653.

Righi, M., Tongiorgi, E. & Cattaneo, A. (2000) Brain-derived neurotrophic factor (BDNF) induces dendritic targeting of BDNF and tyrosine kinase B mRNAs in hippocampal neurons through a phosphatidylinositol-3 kinase-dependent pathway. *J Neurosci*, 20, 3165-3174.

Rimondini, R., Arlinde, C., Sommer, W. & Heilig, M. (2002) Long-lasting increase in voluntary ethanol consumption and transcriptional regulation in the rat brain after intermittent exposure to alcohol. *FASEB J*, 16, 27-35.

Roberts, A.J., Lessov, C.N. & Phillips, T.J. (1995) Critical role for glucocorticoid receptors in stress- and ethanol-induced locomotor sensitization. *J Pharmacol Exp Ther*, 275, 790-797.

Robinson, T.E. & Berridge, K.C. (1993) The neural basis of drug craving: an incentive-sensitization theory of addiction. *Brain Res Brain Res Rev*, 18, 247-291.

Robinson, T.E. & Kolb, B. (1997) Persistent structural modifications in nucleus accumbens and prefrontal cortex neurons produced by previous experience with amphetamine. *J Neurosci*, 17, 8491-8497.

Robinson, T.E. & Kolb, B. (1999) Alterations in the morphology of dendrites and dendritic spines in the nucleus accumbens and prefrontal cortex following repeated treatment with amphetamine or cocaine. *Eur J Neurosci*, 11, 1598-1604.

Rodd, Z.A., Kimpel, M.W., Edenberg, H.J., Bell, R.L., Strother, W.N., McClintick, J.N., Carr, L.G., Liang, T. & McBride, W.J. (2008) Differential gene expression in the nucleus accumbens with ethanol self-administration in inbred alcohol-preferring rats. *Pharmacol Biochem Behav*, 89, 481-498.

Rook, M.S., Lu, M. & Kosik, K.S. (2000) CaMKIIalpha 3' untranslated region-directed mRNA translocation in living neurons: visualization by GFP linkage. *J Neurosci*, 20, 6385-6393.

Rossetti, Z.L., Hmaidan, Y., Diana, M. & Gessa, G.L. (1993) Lack of tolerance to ethanol-induced dopamine release in the rat ventral striatum. *Eur J Pharmacol*, 231, 203-207.

Roux, P.P. & Barker, P.A. (2002) Neurotrophin signaling through the p75 neurotrophin receptor. *Prog Neurobiol*, 67, 203-233.

Russo, S.J., Dietz, D.M., Dumitriu, D., Morrison, J.H., Malenka, R.C. & Nestler, E.J. (2010) The addicted synapse: mechanisms of synaptic and structural plasticity in nucleus accumbens. *Trends Neurosci*, 33, 267-276.

Russo, S.J., Mazei-Robison, M.S., Ables, J.L. & Nestler, E.J. (2009) Neurotrophic factors and structural plasticity in addiction. *Neuropharmacology*, 56 Suppl 1, 73-82.

Saito, M., Szakall, I., Toth, R., Kovacs, K.M., Oros, M., Prasad, V.V., Blumenberg, M. & Vadasz, C. (2004) Mouse striatal transcriptome analysis: effects of oral self-administration of alcohol. *Alcohol*, 32, 223-241.

Sarthy, P.V., Fu, M. & Huang, J. (1989) Subcellular localization of an intermediate filament protein and its mRNA in glial cells. *Mol Cell Biol*, 9, 4556-4559.

Sax, K.W. & Strakowski, S.M. (2001) Behavioral sensitization in humans. *J Addict Dis*, 20, 55-65.

Schenk, S. & Davidson, E.S. (1998) Stimulant preexposure sensitizes rats and humans to the rewarding effects of cocaine. *NIDA Res Monogr*, 169, 56-82.

Schratt, G.M., Tuebing, F., Nigh, E.A., Kane, C.G., Sabatini, M.E., Kiebler, M. & Greenberg, M.E. (2006) A brain-specific microRNA regulates dendritic spine development. *Nature*, 439, 283-289.

Schroff, K.C., Cowen, M.S., Koch, S. & Spanagel, R. (2004) Strain-specific responses of inbred mice to ethanol following food shortage. *Addict Biol*, 9, 265-271.

Schuckit, M.A. (1994) Low level of response to alcohol as a predictor of future alcoholism. *Am J Psychiatry*, 151, 184-189.

Schwartz, R.D., Jackson, J.A., Weigert, D., Skolnick, P. & Paul, S.M. (1985) Characterization of barbiturate-stimulated chloride efflux from rat brain synaptoneurosomes. *J Neurosci*, 5, 2963-2970.

Shimizu, Y., Akiyama, K., Kodama, M., Ishihara, T., Hamamura, T. & Kuroda, S. (1997) Alterations of calmodulin and its mRNA in rat brain after acute and chronic administration of methamphetamine. *Brain Res*, 765, 247-258.

Shin, S., Stewart, R., Ferri, C.P., Kim, J.M., Shin, I.S., Kim, S.W., Yang, S.J. & Yoon, J.S. (2010) An investigation of associations between alcohol use disorder and polymorphisms on ALDH2, BDNF, 5-HTTLPR, and MTHFR genes in older Korean men. *Int J Geriatr Psychiatry*, 25, 441-448.

Shuster, L., Webster, G.W. & Yu, G. (1975) Increased running response to morphine in morphine-pretreated mice. *J Pharmacol Exp Ther*, 192, 64-67.

Simsek-Duran, F. & Lonart, G. (2008) The role of RIM1alpha in BDNF-enhanced glutamate release. *Neuropharmacology*, 55, 27-34.

Smith, A.W., Nealey, K.A., Wright, J.W. & Walker, B.M. (2011) Plasticity associated with escalated operant ethanol self-administration during acute withdrawal in ethanol-dependent rats requires intact matrix metalloproteinase systems. *Neurobiol Learn Mem*, 96, 199-206.

Smyth, G.K. (2004) Linear models and empirical bayes methods for assessing differential expression in microarray experiments. *Stat Appl Genet Mol Biol*, 3, Article3.

Sotelo, J.R., Canclini, L., Kun, A., Sotelo-Silveira, J.R., Calliari, A., Cal, K., Bresque, M., Dipaolo, A., Farias, J. & Mercer, J.A. (2014) Glia to axon RNA transfer. *Dev Neurobiol*, 74, 292-302.

Spanagel, R. (2009) Alcoholism: a systems approach from molecular physiology to addictive behavior. *Physiol Rev*, 89, 649-705.

St Johnston, D. (1995) The Intracellular Localization of Messenger RNAs. *Cell*, 81, 161-170.

Steward, O. (1983) Alterations in polyribosomes associated with dendritic spines during the reinnervation of the dentate gyrus of the adult rat. *J Neurosci*, 3, 177-188.

Steward, O. & Banker, G.A. (1992) Getting the message from the gene to the synapse: sorting and intracellular transport of RNA in neurons. *Trends Neurosci*, 15, 180-186.

Steward, O. & Levy, W.B. (1982) Preferential localization of polyribosomes under the base of dendritic spines in granule cells of the dentate gyrus. *J Neurosci*, 2, 284-291.

Steward, O. & Reeves, T.M. (1988) Protein-synthetic machinery beneath postsynaptic sites on CNS neurons: association between polyribosomes and other organelles at the synaptic site. *J Neurosci*, 8, 176-184.

Steward, O. & Schuman, E.M. (2001) Protein synthesis at synaptic sites on dendrites. *Annu Rev Neurosci*, 24, 299-325.

Steward, O., Wallace, C.S., Lyford, G.L. & Worley, P.F. (1998) Synaptic activation causes the mRNA for the IEG Arc to localize selectively near activated postsynaptic sites on dendrites. *Neuron*, 21, 741-751.

Steward, O. & Worley, P.F. (2001) Selective targeting of newly synthesized Arc mRNA to active synapses requires NMDA receptor activation. *Neuron*, 30, 227-240.

Strakowski, S.M., Sax, K.W., Setters, M.J. & Keck, P.E., Jr. (1996) Enhanced response to repeated d-amphetamine challenge: evidence for behavioral sensitization in humans. *Biol Psychiatry*, 40, 872-880.

Striplin, C.D. & Kalivas, P.W. (1993) Robustness of G protein changes in cocaine sensitization shown with immunoblotting. *Synapse*, 14, 10-15.

Stuber, G.D., Evans, S.B., Higgins, M.S., Pu, Y. & Figlewicz, D.P. (2002) Food restriction modulates amphetamine-conditioned place preference and nucleus accumbens dopamine release in the rat. *Synapse*, 46, 83-90.

Szabo, G. & Hoffman, P.L. (1995) Brain-derived neurotrophic factor, neurotrophin-3 and neurotrophin-4/5 maintain functional tolerance to ethanol. *Eur J Pharmacol*, 287, 35-41.

Szapacs, M.E., Mathews, T.A., Tessarollo, L., Ernest Lyons, W., Mamounas, L.A. & Andrews, A.M. (2004) Exploring the relationship between serotonin and brain-derived neurotrophic factor: analysis of BDNF protein and extraneuronal 5-HT in mice with reduced serotonin transporter or BDNF expression. *J Neurosci Methods*, 140, 81-92.

Szumlinski, K.K., Lominac, K.D., Oleson, E.B., Walker, J.K., Mason, A., Dehoff, M.H., Klugmann, M., Cagle, S., Welt, K., During, M., Worley, P.F., Middaugh, L.D. & Kalivas, P.W. (2005) Homer2 is necessary for EtOH-induced neuroplasticity. *J Neurosci*, 25, 7054-7061.

Tabakoff, B., Cornell, N. & Hoffman, P.L. (1986) Alcohol tolerance. *Ann Emerg Med*, 15, 1005-1012.

Tabakoff, B. & Ritzmann, R.F. (1979) Acute tolerance in inbred and selected lines of mice. *Drug Alcohol Depend*, 4, 87-90.

Takei, N., Inamura, N., Kawamura, M., Namba, H., Hara, K., Yonezawa, K. & Nawa, H. (2004) Brain-derived neurotrophic factor induces mammalian target of rapamycin-dependent local activation of translation machinery and protein synthesis in neuronal dendrites. *J Neurosci*, 24, 9760-9769.

Tanaka, T., Saito, H. & Matsuki, N. (1997) Inhibition of GABAA synaptic responses by brain-derived neurotrophic factor (BDNF) in rat hippocampus. *J Neurosci*, 17, 2959-2966.

Tasker, J.G., Di, S. & Malcher-Lopes, R. (2006) Minireview: rapid glucocorticoid signaling via membrane-associated receptors. *Endocrinology*, 147, 5549-5556.

Team, R.D.C. (2011) R: A Language and Environment for Statistical Computing. R Foundation for Statistical Computing, Saturday, January 1, 2011, Vienna, Austria.

Thiele, T.E., Crabbe, J.C. & Boehm, S.L., 2nd (2014) "Drinking in the Dark" (DID): A Simple Mouse Model of Binge-Like Alcohol Intake. *Curr Protoc Neurosci*, 68, 9 49 41-49 49 12.

Tiedge, H. & Brosius, J. (1996) Translational machinery in dendrites of hippocampal neurons in culture. *J Neurosci*, 16, 7171-7181.

Timmusk, T., Palm, K., Metsis, M., Reintam, T., Paalme, V., Saarma, M. & Persson, H. (1993) Multiple promoters direct tissue-specific expression of the rat BDNF gene. *Neuron*, 10, 475-489.

Tinsley, F.C., Taicher, G.Z. & Heiman, M.L. (2004) Evaluation of a quantitative magnetic resonance method for mouse whole body composition analysis. *Obes Res*, 12, 150-160.

Tongiorgi, E., Armellin, M., Giulianini, P.G., Bregola, G., Zucchini, S., Paradiso, B., Steward, O., Cattaneo, A. & Simonato, M. (2004) Brain-derived neurotrophic factor mRNA and protein are targeted to discrete dendritic laminas by events that trigger epileptogenesis. *J Neurosci*, 24, 6842-6852.

Tongiorgi, E., Righi, M. & Cattaneo, A. (1997) Activity-dependent dendritic targeting of BDNF and TrkB mRNAs in hippocampal neurons. *J Neurosci*, 17, 9492-9505.

Tordoff, M.G. (2007) Taste solution preferences of C57BL/6J and 129X1/SvJ mice: influence of age, sex, and diet. *Chem Senses*, 32, 655-671.

Tordoff, M.G. & Bachmanov, A.A. (2002) Influence of test duration on the sensitivity of the two-bottle choice test. *Chem Senses*, 27, 759-768.

Trapnell, C., Williams, B.A., Pertea, G., Mortazavi, A., Kwan, G., van Baren, M.J., Salzberg, S.L., Wold, B.J. & Pachter, L. (2010) Transcript assembly and quantification by RNA-Seq reveals unannotated transcripts and isoform switching during cell differentiation. *Nat Biotechnol*, 28, 511-515.

Treadwell, J.A. & Singh, S.M. (2004) Microarray analysis of mouse brain gene expression following acute ethanol treatment. *Neurochem Res*, 29, 357-369.

Trimmer, P.A., Phillips, L.L. & Steward, O. (1991) Combination of in situ hybridization and immunocytochemistry to detect messenger RNAs in identified CNS neurons and glia in tissue culture. *J Histochem Cytochem*, 39, 891-898.

Trujillo, K.A. & Akil, H. (1995) Excitatory amino acids and drugs of abuse: a role for N-methyl-D-aspartate receptors in drug tolerance, sensitization and physical dependence. *Drug Alcohol Depend*, 38, 139-154.

Tsai, G. & Coyle, J.T. (1998) The role of glutamatergic neurotransmission in the pathophysiology of alcoholism. *Annu Rev Med*, 49, 173-184.

Tsien, J.Z., Huerta, P.T. & Tonegawa, S. (1996) The essential role of hippocampal CA1 NMDA receptor-dependent synaptic plasticity in spatial memory. *Cell*, 87, 1327-1338.

Tusher, V.G., Tibshirani, R. & Chu, G. (2001) Significance analysis of microarrays applied to the ionizing radiation response. *Proc Natl Acad Sci U S A*, 98, 5116-5121.

Twiss, J.L. & Fainzilber, M. (2009) Ribosomes in axons--scrounging from the neighbors? ***Trends Cell Biol*****, 19, 236-243.**

Uhl, G.R., Liu, Q.R., Walther, D., Hess, J. & Naiman, D. (2001) Polysubstance abuse-vulnerability genes: genome scans for association, using 1,004 subjects and 1,494 single-nucleotide polymorphisms. ***Am J Hum Genet*****, 69, 1290-1300.**

Ujike, H., Takaki, M., Kodama, M. & Kuroda, S. (2002) Gene expression related to synaptogenesis, neuritogenesis, and MAP kinase in behavioral sensitization to psychostimulants. ***Ann N Y Acad Sci*****, 965, 55-67.**

Unpublished-Data.

Vanderschuren, L.J. & Kalivas, P.W. (2000) Alterations in dopaminergic and glutamatergic transmission in the induction and expression of behavioral sensitization: a critical review of preclinical studies. ***Psychopharmacology (Berl)*****, 151, 99-120.**

Villasana, L.E., Klann, E. & Tejada-Simon, M.V. (2006) Rapid isolation of synaptoneurosomes and postsynaptic densities from adult mouse hippocampus. ***J Neurosci Methods*****, 158, 30-36.**

Wallace, C.S., Lyford, G.L., Worley, P.F. & Steward, O. (1998) Differential intracellular sorting of immediate early gene mRNAs depends on signals in the mRNA sequence. ***J Neurosci*****, 18, 26-35.**

Wallgren, H. & Barry, H., III (1970) ***Actions of alcohol*****. Elsevier, New York.**

Walter, N.A., McWeeney, S.K., Peters, S.T., Belknap, J.K., Hitzemann, R. & Buck, K.J. (2007) SNPs matter: impact on detection of differential expression. ***Nat Methods*****, 4, 679-680.**

Wand, G.S. & Dobs, A.S. (1991) Alterations in the hypothalamic-pituitary-adrenal axis in actively drinking alcoholics. ***J Clin Endocrinol Metab*****, 72, 1290-1295.**

Wang, Y.T. & Salter, M.W. (1994) Regulation of NMDA receptors by tyrosine kinases and phosphatases. ***Nature*****, 369, 233-235.**

Wang, Z., Gerstein, M. & Snyder, M. (2009) RNA-Seq: a revolutionary tool for transcriptomics. *Nat Rev Genet*, 10, 57-63.

Waterhouse, E.G. & Xu, B. (2009) New insights into the role of brain-derived neurotrophic factor in synaptic plasticity. *Mol Cell Neurosci*, 42, 81-89.

Webster, M.K., Goya, L., Ge, Y., Maiyar, A.C. & Firestone, G.L. (1993) Characterization of sgk, a novel member of the serine/threonine protein kinase gene family which is transcriptionally induced by glucocorticoids and serum. *Mol Cell Biol*, 13, 2031-2040.

Wells, D.G. (2006) RNA-binding proteins: a lesson in repression. *J Neurosci*, 26, 7135-7138.

Wetmore, C., Olson, L. & Bean, A.J. (1994) Regulation of brain-derived neurotrophic factor (BDNF) expression and release from hippocampal neurons is mediated by non-NMDA type glutamate receptors. *J Neurosci*, 14, 1688-1700.

White, F.J. & Kalivas, P.W. (1998) Neuroadaptations involved in amphetamine and cocaine addiction. *Drug Alcohol Depend*, 51, 141-153.

White, F.J. & Wang, R.Y. (1984) Electrophysiological evidence for A10 dopamine autoreceptor subsensitivity following chronic D-amphetamine treatment. *Brain Res*, 309, 283-292.

Whittaker, V.P., Michaelson, I.A. & Kirkland, R.J. (1964) The separation of synaptic vesicles from nerve-ending particles ('synaptosomes'). *Biochem J*, 90, 293-303.

Wilhelm, J.E. & Vale, R.D. (1993) RNA on the move: the mRNA localization pathway. *J Cell Biol*, 123, 269-274.

Wilke, N., Sganga, M., Barhite, S. & Miles, M.F. (1994) Effects of alcohol on gene expression in neural cells. *EXS*, 71, 49-59.

Williams, C., Mehrian Shai, R., Wu, Y., Hsu, Y.H., Sitzer, T., Spann, B., McCleary, C., Mo, Y. & Miller, C.A. (2009) Transcriptome analysis of

synaptoneurosomes identifies neuroplasticity genes overexpressed in incipient Alzheimer's disease. *PLoS One*, 4, e4936.

Wise, R.A. (1982) *Common neural basis for brain stimulation reward, drug reward, and food reward. In: The neural basis of feeding and reward*. Hoebel BG, Novin D, eds, Brunswick, ME.

Wise, R.A. (2004) Dopamine, learning and motivation. *Nat Rev Neurosci*, 5, 483-494.

Wise, R.A. & Bozarth, M.A. (1987) A psychomotor stimulant theory of addiction. *Psychol Rev*, 94, 469-492.

Wise, R.A. & Rompre, P.P. (1989) Brain dopamine and reward. *Annu Rev Psychol*, 40, 191-225.

Wolen, A.R., Phillips, C.A., Langston, M.A., Putman, A.H., Vorster, P.J., Bruce, N.A., York, T.P., Williams, R.W. & Miles, M.F. (2012) Genetic dissection of acute ethanol responsive gene networks in prefrontal cortex: functional and mechanistic implications. *PLoS One*, 7, e33575.

Wolstenholme, J.T., Warner, J.A., Capparuccini, M.I., Archer, K.J., Shelton, K.L. & Miles, M.F. (2011) Genomic analysis of individual differences in ethanol drinking: evidence for non-genetic factors in C57BL/6 mice. *PLoS One*, 6, e21100.

Woo, N.H., Teng, H.K., Siao, C.J., Chiaruttini, C., Pang, P.T., Milner, T.A., Hempstead, B.L. & Lu, B. (2005) Activation of p75NTR by proBDNF facilitates hippocampal long-term depression. *Nat Neurosci*, 8, 1069-1077.

Wright, J.W. & Harding, J.W. (2009) Contributions of matrix metalloproteinases to neural plasticity, habituation, associative learning and drug addiction. *Neural Plast*, 2009, 579382.

Xu, F., Plummer, M.R., Len, G.W., Nakazawa, T., Yamamoto, T., Black, I.B. & Wu, K. (2006) Brain-derived neurotrophic factor rapidly increases NMDA receptor channel activity through Fyn-mediated phosphorylation. *Brain Res*, 1121, 22-34.

Xu, Y., Ehringer, M., Yang, F. & Sikela, J.M. (2001) Comparison of global brain gene expression profiles between inbred long-sleep and inbred short-sleep mice by high-density gene array hybridization. *Alcohol Clin Exp Res*, 25, 810-818.

Yaka, R., He, D.Y., Phamluong, K. & Ron, D. (2003a) Pituitary adenylate cyclase-activating polypeptide (PACAP(1-38)) enhances N-methyl-D-aspartate receptor function and brain-derived neurotrophic factor expression via RACK1. *J Biol Chem*, 278, 9630-9638.

Yaka, R., Tang, K.C., Camarini, R., Janak, P.H. & Ron, D. (2003b) Fyn kinase and NR2B-containing NMDA receptors regulate acute ethanol sensitivity but not ethanol intake or conditioned reward. *Alcohol Clin Exp Res*, 27, 1736-1742.

Yaka, R., Thornton, C., Vagts, A.J., Phamluong, K., Bonci, A. & Ron, D. (2002) NMDA receptor function is regulated by the inhibitory scaffolding protein, RACK1. *Proc Natl Acad Sci U S A*, 99, 5710-5715.

Zalewska-Kaszubska, J., Gorska, D., Dyr, W. & Czarnecka, E. (2008) Effect of chronic acamprosate treatment on voluntary alcohol intake and beta-endorphin plasma levels in rats selectively bred for high alcohol preference. *Neurosci Lett*, 431, 221-225.

Zapata, A., Gonzales, R.A. & Shippenberg, T.S. (2006) Repeated ethanol intoxication induces behavioral sensitization in the absence of a sensitized accumbens dopamine response in C57BL/6J and DBA/2J mice. *Neuropsychopharmacology*, 31, 396-405.

Zhang, J.H., Panicker, L.M., Seigneur, E.M., Lin, L., House, C.D., Morgan, W., Chen, W.C., Mehta, H., Haj-Ali, M., Yu, Z.X. & Simonds, W.F. (2010) Cytoplasmic polyadenylation element binding protein is a conserved target of tumor suppressor HRPT2/CDC73. *Cell Death Differ*, 17, 1551-1565.

Zhao, S., Fung-Leung, W.P., Bittner, A., Ngo, K. & Liu, X. (2014) Comparison of RNA-Seq and microarray in transcriptome profiling of activated T cells. *PLoS One*, 9, e78644.

Zhen, J., Reith, M.E. & Carr, K.D. (2006) Chronic food restriction and dopamine transporter function in rat striatum. *Brain Res*, 1082, 98-101.

Zhou, F.C., Anthony, B., Dunn, K.W., Lindquist, W.B., Xu, Z.C. & Deng, P. (2007) Chronic alcohol drinking alters neuronal dendritic spines in the brain reward center nucleus accumbens. *Brain Res*, 1134, 148-161.

Zhou, S. (2014) Comparison of RNA-Seq and microarray in transcriptome profiling of activated T cells. *PLoS One*, 9, e78644.

Zhou, Z., Yuan, Q., Mash, D.C. & Goldman, D. (2011) Substance-specific and shared transcription and epigenetic changes in the human hippocampus chronically exposed to cocaine and alcohol. *Proc Natl Acad Sci U S A*, 108, 6626-6631.

Vita

Megan Anne O'Brien was born on May 20, 1983 in St. Paul, Minnesota. She graduated from Memorial High School, Eau Claire, Wisconsin in 2001. She earned her Bachelor of Science in Biochemistry/Molecular Biology from University of Wisconsin – Eau Claire, Eau Claire, Wisconsin in 2006 where she performed research under the direction of Dr. Julie Anderson. She subsequently earned her Master of Science degree in Forensic Science from Arcadia University in 2008 where she performed research and acted as a mentor at The Forensic Mentors Institute. In 2008, she entered the doctoral program at Virginia Commonwealth University and in the Spring of 2009, joined the laboratory of Dr. Michael F. Miles. Upon acceptance of this dissertation, she will be awarded a Doctorate of Philosophy in Pharmacology and Toxicology. While attending graduate school she has received multiple honors including a Student Merit Award from the Research Society on Alcoholism, Best Student Paper from the Virginia Academy of Sciences, C.C. Clayton Award for Outstanding Scholarly Achievement, Anthony Ambrose Award for Best Graduate Student, and Phi Kappa Phi Nominee Award for Outstanding Scholarly Achievement. During the course of her graduate student career she was supported by a Ruth L. Kirschstein National Research Service Award for Individual Predoctoral Fellows (F31AA021035) from the National Institute of Alcohol Abuse and Alcoholism.